THE UNIVERSITY
of EDINBURGH

COMPLEX INTERNAL REPRESENTATIONS IN SENSORIMOTOR DECISION MAKING: A BAYESIAN INVESTIGATION

LUIGI ACERBI

Doctor of Philosophy

Doctoral Training Centre for Computational Neuroscience
Institute of Perception, Action and Behaviour
School of Informatics
University of Edinburgh

2014

Luigi Acerbi:
Complex internal representations in sensorimotor decision making: A Bayesian investigation
Doctor of Philosophy, 2014

SUPERVISORS:
Prof. Sethu Vijayakumar, Ph.D., FRSE
Prof. Daniel M. Wolpert, D.Phil., FRS, FMedSci

ABSTRACT

The past twenty years have seen a successful formalization of the idea that perception is a form of probabilistic inference. Bayesian Decision Theory (BDT) provides a neat mathematical framework for describing how an ideal observer and actor should interpret incoming sensory stimuli and act in the face of uncertainty. The predictions of BDT, however, crucially depend on the observer's internal models, represented in the Bayesian framework by priors, likelihoods, and the loss function. Arguably, only in the simplest scenarios (e.g., with a few Gaussian variables) we can expect a real observer's internal representations to perfectly match the true statistics of the task at hand, and to conform to exact Bayesian computations, but how humans systematically deviate from BDT in more complex cases is yet to be understood.

In this thesis we theoretically and experimentally investigate how people represent and perform probabilistic inference with complex (beyond Gaussian) one-dimensional distributions of stimuli in the context of sensorimotor decision making. The goal is to reconstruct the observers' internal representations and details of their decision-making process from the behavioural data – by employing Bayesian inference to uncover properties of a system, the ideal observer, that is believed to perform Bayesian inference itself. This "inverse problem" is not unique: in principle, distinct Bayesian observer models can produce very similar behaviours. We circumvented this issue by means of experimental constraints and independent validation of the results.

To understand how people represent complex distributions of stimuli in the specific domain of time perception, we conducted a series of psychophysical experiments where participants were asked to reproduce the time interval between a mouse click and a flash, drawn from a session-dependent distribution of intervals. We found that participants could learn smooth approximations of the non-Gaussian experimental distributions, but seemed to have trouble with learning some complex statistical features such as bimodality.

To investigate whether this difficulty arose from learning complex distributions or computing with them, we conducted a target estimation experiment in which "priors" where explicitly displayed on screen and therefore did not need to be learnt. Lack of difference in performance between the Gaussian and bimodal conditions in this task suggests that acquiring a bimodal prior, rather than computing with it, is the major difficulty. Model comparison on a large number of Bayesian observer models, representing different assumptions about the noise sources and details of the decision

process, revealed a further source of variability in decision making that was modelled as a "stochastic posterior".

Finally, prompted by a secondary finding of the previous experiment, we tested the effect of decision uncertainty on the capacity of the participants to correct for added perturbations in the visual feedback in a centre of mass estimation task. Participants almost completely compensated for the injected error in low uncertainty trials, but only partially so in the high uncertainty ones, even when allowed sufficient time to adjust their response. Surprisingly, though, their overall performance was not significantly affected. This finding is consistent with the behaviour of a Bayesian observer with an additional term in the loss function that represents "effort" – a component of optimal control usually thought to be negligible in sensorimotor estimation tasks.

Together, these studies provide new insight into the capacity and limitations people have in learning and performing probabilistic inference with distributions beyond Gaussian. This work also introduces several tools and techniques that can help in the systematic exploration of suboptimal behaviour. Developing a language to describe suboptimality, mismatching representations and approximate inference, as opposed to optimality and exact inference, is a fundamental step to link behavioural studies to actual neural computations.

LAY SUMMARY

A successful unifying hypothesis in neuroscience is that the nervous system attempts to choose a 'statistically optimal' course of action by accounting for sensory uncertainty and previous experience while serving the goals of the task at hand. Such optimal behaviour requires an ideal observer to record the pattern of past events and build an accurate internal model of the environment. Arguably, the performance of a real observer will match that of an ideal observer only in the simplest scenarios (e.g., those following simple statistical regularities) as we would not expect the brain to be able to recall and assess arbitrarily complex patterns of past events. However, we have yet to ascertain which statistical features of the environment induce suboptimal behaviour, and why.

In this thesis, we investigate people's performance in perceptual and motor tasks in the presence of events whose patterns feature varying levels of regularity and complexity. The goal is to understand what people learn about these patterns, and how the learnt patterns are employed in people's decision making process. We start by asking how people represent complex patterns of stimuli in the specific case of time perception. We conducted a series of psychophysical experiments where participants were asked to reproduce the time interval between a mouse click and a flash, drawn from a session-dependent pattern of intervals. We found that participants could learn, through practice, generic statistical features of the presented patterns, but had trouble with some specific aspects of those. In fact, in a separate psychophysical study, we found evidence that remembering the patterns of past events constitutes more of a challenge to decision making than manipulating the present complex statistical information. Finally, we asked whether a major source of suboptimality can be identified in the mental or physical effort required by the nervous system to correct for mistakes. We found that people are 'optimally lazy'; that is, they correct just enough to preserve their average performance in the task.

Together, these studies provide new insight into the human capacity for, and limitations in, learning and making statistically optimal decisions when dealing with prior events with complex patterns. This work also introduces several tools and techniques that can help in the systematic exploration of suboptimal behaviour. Developing a language to describe suboptimality, mismatching representations, and approximations – as opposed to optimality – is a fundamental step to link behavioural studies to actual neural computations in the brain.

PREFACE

ACKNOWLEDGEMENTS

Here we are.

I would like to thank my first supervisor, Sethu Vijayakumar, for giving me the freedom to pursue my research interests, for providing timely guidance and insight, and above all for reminding me to always be clear about the bigger picture, and resist the charm of mathematical minutiae. I am grateful to my second supervisor, Daniel Wolpert, for the many helpful Skype calls (recently, Google hangouts), for backing my several working visits to his lab during the course of my PhD, and for imbuing me with an understanding of the intricate psychophysical process whereby a tentative draft of a manuscript is transmuted into a scientific paper. I also thank Sae Franklin and James Ingram for their invaluable practical and technical support during my lab visits in Cambridge, and Peggy Seriès for introducing me to the wonders of the Bayesian brain.

The work presented in Chapter 3 received constructive feedback from Michael S. Landy and two anonymous reviewers. At various stages of its development, the study reported in Chapter 4 has benefited from helpful suggestions from Jeff Beck, Sophie Denève, Jan Drugowitsch, Wei Ji Ma, Paul R. Schrater, Angela J. Yu, and one or two anonymous reviewers.

I would like to thank several other people and fellow travellers who have directly or indirectly contributed to this thesis, by virtue of stimulating discussions or reciprocal encouragement: Paolo Puggioni, Lukas Solanka, and the rest of the DTC09 crew; then Matteo Colombo, Megan Peters, David Reichert, and Michael Schartner. I also thank the friends of a lifetime, old and new, who kept my stay in Scotland between bearable and amazing.

I am grateful to my family beyond words.

And, finally, I thank Maryam Babaei for carefully reading this thesis, fixing commas, typos, and Italianisms, for her thoughtful comments, and above all for her unwavering support for almost the full extent of my PhD. Thank you.

The work reported in Chapters 3, 4 and 5 is the result of my collaboration with Prof. Sethu Vijayakumar (University of Edinburgh, Edinburgh, UK) and Prof. Daniel Wolpert (University of Cambridge, Cambridge, UK).

- Chapter 3 is largely based on a paper published in *PLoS Computational Biology* (Acerbi et al., 2012), with minor changes and added content. This project was developed in Edinburgh (2011–2012).
- The work reported in Chapter 4 was also published in *PLoS Computational Biology* (Acerbi et al., 2014b). The experimental part of this project was conducted in Cambridge in autumn 2012. The chapter is mostly based on the published paper, with some added material.
- Chapter 5 is based on a manuscript in preparation. The experimental part of this project was also conducted in Cambridge, in autumn 2013. The chapter is an extended and modified version of the manuscript.

For all projects, I designed the experiments consulting with my thesis advisors. I set up and ran the experiments, with the exception of the 'sensorimotor noise estimation' experiment reported in Section 4.3.2, whose data were helpfully collected in my stead by Dr. Sae Franklin, in Cambridge. For all studies, I wrote a first draft of the manuscripts, which were edited with the help of Prof. Daniel Wolpert, and critically revised by all authors.

While writing this thesis, motivated by a recurrent question in my PhD, I conducted a preliminary study of the theoretical identifiability of Bayesian models of perception. This project was a collaboration between myself, Prof. Sethu Vijayakumar and Prof. Wei Ji Ma (New York University, New York, USA), and its results have been published in Acerbi et al. (2014a). Methods and goals of this side project share several commonalities with this thesis (see e. g., Section 6.2.2).

DECLARATION

I declare that this thesis was composed by myself, that the work contained herein is my own except where explicitly stated otherwise in the text, and that this work has not been submitted for any other degree or professional qualification except as specified.

Edinburgh, 2014

Luigi Acerbi, December 1, 2014

A Luisella e Emilio

CONTENTS

LIST OF FIGURES

LIST OF TABLES

ABBREVIATIONS

e.g.	for example
i.e.	that is
etc.	et cetera – and so forth
i.i.d.	independent and identically distributed
cdf	cumulative density function
pdf	probability density function
2AFC	Two-Alternative Forced Choice
AIC	Akaike Information Criterion
ANOVA	Analysis of Variance
BBH	Bayesian Brain Hypothesis
BDT	Bayesian Decision Theory
BIC	Bayesian Information Criterion
BLS	Bayesian Least Squares
BMS	Bayesian Model Selection
CRT	Cathode Ray Tube
DIC	Deviance Information Criterion
fMRI	functional Magnetic Resonance Imaging
GDIC	Group Deviance Information Criterion
JND	Just Noticeable Difference
KDE	Kernel Density Estimation
KL	Kullback-Leibler (divergence)
KR	Knowledge of Results
LCD	Liquid-Crystal Display

MAP Maximum a Posteriori

MCMC Markov Chain Monte Carlo

ML Maximum Likelihood

MLE Maximum Likelihood Estimation

rm-ANOVA repeated measures Analysis of Variance

RMSE Root Mean Squared Error

SD Standard Deviation

SDT Statistical Decision Theory

SE Standard Error

SEM Standard Error of the Mean

1

INTRODUCTION

> "And of course, the brain is not responsible for any of the sensations at all. [...] Thus, the brain, which is naturally cold, tempers the heat and seething of the heart."
>
> — Aristotle, *Parts of Animals*, trans. A. L. Peck

A powerful unifying idea in neuroscience is the hypothesis that the brain is intrinsically a probabilistic inference machine.[1] According to this hypothesis, the brain builds statistical models of relevant variables in its environment, keeps track of the uncertainty associated with sensory measurements, and updates its beliefs by combining new data with previous information according to the laws of probability, as expressed by *Bayes' theorem*. Bayesian probability is a take on probability theory which interprets probabilities as degrees of belief. Hence, the notion that the brain encodes and computes with beliefs as probability distributions has been named the *Bayesian brain hypothesis* (BBH; see Knill and Richards, 1996; Knill and Pouget, 2004; Doya et al., 2007; Whiteley, 2008; and also Friston, 2012 for an historical, personal perspective).

Bayes' theorem

Bayesian brain hypothesis

In this thesis, we both test and exploit the BBH by performing what has recently been dubbed *cognitive tomography* (Houlsby et al., 2013). We devise psychophysical experiments to probe the way in which human observers process sensorimotor information in a number on nontrivial tasks. The noisy pattern of subjects' behavioural data contains echoes of their mental representations and thought processes. We use the powerful machinery of mathematical modelling and machine learning as an instrument to reconstruct the complex internal representations inside our participants' heads. Some skepticism is imperative – can we really read human minds just from observed actions? Indeed, needless to say, our enterprise faces a long list of theoretical and practical pitfalls to navigate. Thus, as I commence the task of reporting how we did it and what we found, I ask the reader to expect some necessary lengthy technical passages. But first, a formal introduction.

cognitive tomography

1 *Pace* Aristotle, whose unconventional view of the brain as a cooling system was odd for a natural philosopher even at his times – but he had interesting arguments for it (Gross, 1995).

1.1 THE BAYESIAN BRAIN HYPOTHESIS

The BBH is not a specific statement, but rather a family of hypotheses with differing strengths, which can be roughly related to David Marr's three levels of analysis: computational, algorithmic and implementational (Marr, 1982; see also Colombo and Seriès, 2012 for a slightly different presentation). The less controversial form of BBH, and the most amenable to experiment, lies at Marr's computational level, and states that the brain produces behaviour that conforms, to various extents, to Bayesian inference, for example by correctly accounting for noise in the sensory and motor systems, or by accumulating and exploiting information about the statistics of stimuli in the environment (Knill and Richards, 1996; Kersten et al., 2004). This position corresponds to the idea that Bayesian theory provides a *normative framework* for describing the goals of the perceptual and motor systems – such as inferring hidden causes for the current sensations, and reacting accordingly – at an abstract level. The idea of *perception as unconscious inference* has a long history; the process of combining prior information with currently available sensory evidence has already been stated clearly in Helmholtz (1925), and seeds of this hypothesis can be traced back at least to writings of the early Arab physicist and polymath Ibn al-Haytham (Alhazen), about a thousand years ago.[2] The BBH, however, is usually interpreted as a stronger assertion that holds in-between Marr's computational and algorithmic levels, and casts Bayesian theory as a *process model* of computations in the brain (Maloney and Mamassian, 2009). This means that there is a direct, one-to-one mapping between elements of the theory, such as distinct probability distributions, and representations thereof in the brain, although details are left undefined. Finally, in recent years there has been the even bolder proposal that the brain's architecture implements probabilistic inference directly in the cortex (Lee and Mumford, 2003), meaning that the BBH spans across all of Marr's levels, from computational to implementational. There have been a few suggestions for specific neuronal mechanisms that may support Bayesian computations (sometimes called the *Bayesian coding hypothesis*; Knill and Pouget, 2004; Doya et al., 2007).

normative framework

process model

Bayesian coding hypothesis

In this thesis, we adopt an intermediate stance on the BBH, which we consider a good empirical description of human performance in several situations, and a powerful conceptual framework for clarifying and testing ideas about sensorimotor behaviour (Geisler, 2011; O'Reilly et al., 2012; Colombo and Seriès, 2012). Sympathizing with a pragmatic view of Bayesian reverse-engineering that tries to bridge Marr's

2 Helmholtz writes, unequivocally: "Previous experiences act in conjuction with present sensations to produce a perceptual image". Alhazen's writing is not much more ambiguous: "...familiar visible objects are perceived by sight through defining features and through previous knowledge..." (see Helmholtz, 1925; Ma et al., 2014).

levels (Zednik and Jäkel, 2014), we entertain the working hypothesis of BDT as a process model of perception and action (Maloney and Mamassian, 2009), but we remain agnostic about the level of implementation (see Chapter 6 for further discussion). Yet, even at the behavioural level there are still several outstanding open questions, and the field is mature for a more critical examination of the details of the BBH.

1.1.1 *Why Bayes? Optimal and probabilistic inference*

Why would the brain want to be Bayesian in the first place? The rationale is that the nervous system had to evolve means to cope with noisy, uncertain and ambiguous data, – and (Bayesian) probability theory is the best, *statistically optimal* fashion to deal with them. A seminal theorem discovered by Cox (1946, 1961) states that, under a few reasonable assumptions, such as agreement with basic axioms of propositional logic, probability theory is the only coherent way to attach single-valued real numbers to beliefs and to update them upon arrival of new evidence (through Bayes' theorem). Any other system of rules different from probability theory would lead to inconsistencies. In De Finetti's (1937) interpretation of probability, such incoherence would mean that an agent could be systematically tricked into losing bets by another agent with a better understanding of probability (the so-called *Dutch-book* argument). The 'opponents' would be Nature itself at the beginning of the game, and then other biological agents as the arms race for a probabilistic understanding of the world has begun (Geisler and Diehl, 2002, 2003). Since in the case of biological machines survival is at stake, an evolutionary perspective suggests that a nervous system ought to develop techniques to deal with probability very well, if not optimally, at least for immediate, low-level properties of the world involving perception and action. Whether higher-level cognitive functions ought to be included in this argument is less clear – the key point is whether selective pressures had enough time to perfect the probabilistic machinery for abstract thought. On the other hand, if the brain, and specifically the neo-cortex, implements a generic algorithm to perform hierarchical Bayesian computations, cognition may be probabilistic too (Lee and Mumford, 2003; Griffiths et al., 2008, 2010; Tenenbaum et al., 2011).

statistically optimal

Dutch-book

This line of reasoning brings us to expose a fine distinction within the BBH. In most cases, exact Bayesian computations are extremely demanding in terms of computational resources (space, that is memory, and time) and, therefore, for any problem of a sufficiently high complexity – as almost anything faced by the visual system, for example – we cannot expect the brain to reach the optimal solution within an ecologically-relevant time scale, but it will have to resort to approximations (Tsotsos, 2001; Beck et al., 2012). In fact, any Bayesian system will start behaving suboptimally

for sufficiently hard problems. With respect to the BBH, it is then typically understood that computations in the brain are optimal (fully Bayesian) for ecologically-relevant, simple sensorimotor tasks, and become gradually suboptimal for less relevant or more complex settings, although the boundary between the two regimes is unknown, and there may be several stages of increasing approximation. However, even in the case of suboptimal behaviour, we would still expect a Bayesian brain to be *probabilistic*, i. e. to qualitatively take into account probabilities, albeit not necessarily in the quantitatively correct form (Ma, 2012).

probabilistic

1.1.2 *Probability theory is only half of the story*

Probability theory provides us with almost no constraints on how to assign probabilities (they should be non-negative and should add up to one) and with a rule for belief updating (Bayes' theorem), but this is only part of the story. Two fundamental elements are missing: how to assign probabilities in the first place (*a priori*), and how to convert a probability distribution over states of the world, or possible outcomes of action, into a unified percept or motor command.

The problem of assigning a priori probabilities is, in fact, a thorny theoretical and empirical issue with roots in the foundations of probability and the philosophy of science (Jaynes, 2003). The practical solution when dealing with probabilities of behavioural stimuli consists of assuming that a biological agent's prior expectations should match the statistics of its environment (Seriès and Seitz, 2013). This approach may be justified for low-level sensory stimuli out of different considerations, such as *efficient coding* (Barlow, 1961; Olshausen and Field, 1997) and optimality (Ma, 2012), but the problem is shifted to a matter of defining what should be considered as the 'statistics of the environment' (e. g., under which timescales and further assumptions about random processes). These definitions are always somewhat arbitrary, as a biological agent may well have good reasons to hold probabilistic beliefs that do not fully match the statistics of the environment, especially in the artificial setting of a psychophysical experiment (Feldman, 2013). Moreover, even if we assume that the 'statistics of the environment' are well defined in a given context, we must ask whether (and how) an observer is able to acquire and represent such statistics, especially when they take a nontrivial form. This means that, as a further layer of complication, the observer could be *subjectively* Bayes-optimal – that is, optimal according to his or her internal representation of the world – without meeting the externally imposed criteria for optimality, as we will also see next. Clearly, telling whether an observer is behaving suboptimally because of non-Bayesian computations or because of Bayesian computations with wrong assumptions (Ma, 2012; Beck et al., 2012) con-

efficient coding

subjective optimality

stitutes a serious challenge, and, for certain cases, it may well be impossible to make the distinction, even in theory.

Another order of problems is represented by the question of how the brain chooses a single percept or action from a world of probability distributions. This problem of 'estimation' or 'action selection' is addressed with the help of an additional axiom independent from probability theory per se. It is clear why we need to choose a single course of action, as we learn from childhood that our limbs can be in one place at a time. It may be less clear why our brain needs to choose a single percept, but we take it as an empirical constraint of consistency. Healthy humans always experience unified percepts; even in ambiguous cases, such as bistable illusions, the brain keeps switching between alternative hypotheses (Leopold and Logothetis, 1999); we do not *see* a probability distribution over possible percepts, whatever that would look like. There are several plausible ways to transform a probability distribution into a so-called *point estimate*. For example, the brain may adopt a policy of *probability matching*, by drawing a random sample from the probability distribution that represents the current belief (Vulkan, 2000; Wozny et al., 2010). Alternatively, the brain may choose the estimate with maximal probability among the possible choices. This strategy looks more sensible, but still does not take into account the disparity of the consequences of our actions. Suppose that your visual system and memory tell you that there is 60%, maybe even a good 70%, chance that the mushrooms you found in the woods are safe to eat. You might want to reconsider your options and not simply carry on with the 'most likely' scenario according to your beliefs. A more principled approach, in analogy with variational methods from physics, would involve choosing an estimate that extremizes a functional of the probability distribution under consideration. In other words, a 'rational' decision maker may want to adopt a policy that statistically maximizes his or her average gains (or minimizes his or her average losses), according to some provided definition of gain or loss. This is achieved through a mathematical object called the *loss function*. In the example considered above, the loss function would encode a little loss for the option of throwing away the mushrooms, and a severe loss for the prospect of being hospitalized with mushroom poisoning. This approach is formalized by *Bayesian Decision Theory* (BDT), which is essentially Bayesian probability theory with the addition of a rule for transforming a probability distribution into a single choice (Berger, 1985; Maloney, 2002; Körding and Wolpert, 2006). Note that the passage from belief to choice is less stringent and less fundamental than Bayes' theorem per se (see for example Chapter 13 in Jaynes, 2003), as it is not a logical necessity for a biological system to minimize its *average* losses. Other factors may influence the observer's choices, such as the *variability* of the losses, or a willingness to minimize the maximal losses (*minimax strategy*); some of these devia-

point estimate
probability matching
loss function
Bayesian Decision Theory
minimax strategy

tions may be accounted for by variants of BDT. Moreover, even for standard BDT, the shape of the loss function itself is not determined by the theory, but needs to be fixed by additional considerations (although, in simple cases, a large class of loss functions produces very similar, if not identical, predictions). These theoretical issues aside, BDT or minor variations thereof have been empirically shown to account extremely well for human behaviour in a large variety of simple sensorimotor tasks, and BDT is assumed to be part of BBH (Yuille and Bülthoff, 1996; Körding and Wolpert, 2006).

1.1.3 *Bayesian computations in complex scenarios*

A large number of studies on sensorimotor decision making have been concerned with scenarios that included only *simple* probability distributions, mostly Gaussian. Due to specific properties and symmetries of Gaussian distributions, these cases do not reveal the extent to which humans perform Bayesian computations (Körding and Wolpert, 2004b). On the other hand, studies that examined perceptual and motor performance in more complex scenarios have yielded mixed results. Reported human performance spans from near-optimal to largely suboptimal, suggesting that there are limits to the human capacity of learning or handling complex distributions optimally. An investigation to find the point at which BDT stops being an accurate model of human behaviour may shed light on the approximations being used. The conditions for such a turning point are yet to be determined.

In terms of methodology, it is common practice to model psychophysical data by fitting the parameters of a single or a small number of Bayesian models via a point estimate, such as the *maximum likelihood estimate* (MLE). The goodness of fit is, then, compared via some statistical method, and the most supported model and its parameters are taken as a somewhat faithful description of subjects' behaviour. This approach is potentially problematic because Bayesian models may be *non-identifiable*; that is, multiple distinct models (or model parameters) may give very similar predictions (Mamassian and Landy, 2010). By using only a handful of *ad-hoc* models, and by resorting to a point estimate, researchers may miss the fact that several other models and parameter sets may be able to explain the data at least as well. This is not necessarily a problem if the goal is merely to show that a given Bayesian observer model can explain the data better than other models. However, potential issues arise if such estimated models and parameters are used to draw specific conclusions about subjects' hidden features, such as their internal representations, unless further validations are provided (Acerbi et al., 2014a).

maximum likelihood estimate

non-identifiable

For these reasons, in this thesis we perform a systematic study of human performance in sensorimotor decision-making tasks with *complex* (beyond Gaussian) distri-

butions. We extensively use Bayesian inference to estimate properties of the observers over a vast class of possible models (van den Berg et al., 2014). Our approach allows us to test suboptimal observers and variants of BDT, and we pay particular attention to the problem of model degeneracy (or non-identifiability). Among the properties of the observers that we work to reconstruct, we infer the subjects' internal representations of the distributions of stimuli in a semi-parametric way, with few assumptions on the underlying shape. In the following section, we review the Bayesian framework, an essential component of our modelling and analyses.

1.2 A PRIMER ON BAYESIAN DECISION THEORY

BDT is a *normative* or *prescriptive* theory that formalizes how rational agents ought to make *optimal* decisions – under the assumption that it is rational to minimize the average losses. Given the pivotal role of the Bayesian framework in this thesis, we provide here a brief introduction to the subject, which is also useful for establishing the mathematical notation used in the rest of the thesis. In the following section we describe Bayes' theorem and decision rules in BDT, concluding with a brief discussion on the degeneracy of BDT. The interested reader is referred to Berger (1985) for a more comprehensive introduction to statistical decision theory, and to Maloney (2002); Körding and Wolpert (2006) for its application to the study of perception and sensorimotor behaviour.

1.2.1 *Bayes' theorem*

inverse probability

Derived from the basic axioms of probability, Bayes' theorem (or rule) is a simple equation that represents the solution of the *inverse probability* problem – how to compute (*infer*) the probability of a given hypothesis s, such as an unknown state of the world, after observing some data (observation x). In the following we assume that both x and s are one-dimensional real variables, but the description applies also to multi-dimensional and discrete variables. Calculation of Bayes' rule takes two objects as inputs:

prior

- The *prior probability (density)*, or simply *prior*, of any hypothesis or state of the world, $p_{prior}(s)$. As the name suggests, this is the probability assigned to any hypothesis or state of affairs *before* observing the data.

sampling probability

- The *conditional probability (density)* of obtaining measurement or observation x given an hypothesis s, $p_{meas}(x|s)$, also called the *sampling probability (density)*. This is typically understood as the probability that a given state of the world

generates, or 'causes', the observed data, but it is not necessarily a causal relationship. When considered as a function of s (and not of x), as in Bayes' theorem, this mathematical object is called the *likelihood* and represents the support for the hypothesis given the observation.[3]

likelihood

A note on normalization: the prior is a probability distribution in s and therefore $\int p_{prior}(s)ds = 1$. However, Bayesian probability also admits *improper priors* that are not integrable, as we will see below. Secondly, $\int p_{meas}(x|s)\,dx = 1$, since $p_{meas}(x|s)$ is a probability distibution in x, but the likelihood, $p_{meas}(x|s)$ as a function of s, is generally not normalized.

improper priors

Bayes' theorem involves the calculation of the two following objects:

- The *posterior probability (density)* (or simply *posterior*), $p_{post}(s|x)$, represents the updated probability of the hypothesis *after* observing the data. This is the quantity we want to calculate.

posterior

- The *marginal likelihood* (or *evidence*), $Z \equiv p(x) = \int p_{prior}(s)p_{meas}(x|s)\,ds$, which typically serves the only purpose of a normalization constant for the posterior. When comparing different models, the marginal likelihood may be used as a Bayesian measure of support for each model (see Appendix A).

marginal likelihood

All these elements combine as follows to give Bayes' theorem:

$$p_{post}(s|x) = \frac{p_{meas}(x|s)\,p_{prior}(s)}{\int p_{prior}(s')p_{meas}(x|s')\,ds'}. \tag{1.1}$$

When the hypothesis space is large and complicated the calculation of the marginal likelihood may be computationally expensive. In this case, the posterior distribution may be evaluated by drawing samples from the unnormalized posterior via Markov Chain Monte Carlo (MCMC) methods. Simple analytical solutions can be found when *conjugate priors* are used that combine with the likelihood in a closed form which is in the same class of distributions as the prior.

conjugate priors

Let us consider the simple case of a Gaussian prior $p_{prior}(s) = \mathcal{N}\left(s\,\middle|\,\mu_{prior}, \sigma^2_{prior}\right)$, where $\mathcal{N}(x|\mu,\sigma^2)$ is a Gaussian distribution with mean μ and variance σ^2. For the measurement distribution we assume that the noise is again normally distributed

3 For the sake of clarity, some authors use a different notation to specify when they refer to the sampling probability density (a probability distribution of x) or to the likelihood (a function of s). In our case the context should be sufficient to avoid confusion.

and centered on the true value of the hypothesis: $p_{meas}(x|s) = \mathcal{N}(x|s, \sigma^2_{meas})$. The posterior takes therefore the form:

$$\begin{aligned} p_{post}(s|x) &= \frac{\mathcal{N}\left(s \middle| \mu_{prior}, \sigma^2_{prior}\right) \mathcal{N}(x|s, \sigma^2_{meas})}{\int \mathcal{N}\left(s' \middle| \mu_{prior}, \sigma^2_{prior}\right) \mathcal{N}(x|s', \sigma^2_{meas})\, ds'} \\ &= \mathcal{N}\left(s \middle| \frac{\mu_{prior}\sigma^2_{meas} + x\sigma^2_{prior}}{\sigma^2_{meas} + \sigma^2_{prior}}, \frac{\sigma^2_{meas}\sigma^2_{prior}}{\sigma^2_{meas} + \sigma^2_{prior}}\right), \end{aligned} \tag{1.2}$$

which is again a Gaussian distribution, since Gaussian distributions are conjugate priors of Gaussian likelihoods. Note that the posterior distribution has a mean that is linear in x, namely a weighted average of the mean of the prior and the mean of the likelihood (the observation), with relative weights equal to the *precisions* (inverse variances) of prior and likelihood. Moreover, the variance of the posterior is lower than either individual variance – the posterior has less uncertainty than the prior or the likelihood alone.

1.2.2 *Decision rules*

Bayes' theorem tells us how to update our beliefs so as to build a posterior distribution given an observation (Eq. 1.1), but it does not tell us what we should do with the posterior; this is the topic of *decision theory*.

decision theory

decision rule

A *decision rule* is a function that maps an observation onto a decision, which is typically interpreted as either an *action* or an *estimate*. Estimates are decisions about the value to give to a hidden variable, such as an unknown parameter (in which case the decision rule is also called an *estimator*). Decision theory aims to identify the optimal decision rule(s) according to some criteria. Since in this thesis we typically conflate the problem of estimation and action selection, we use for decisions the common notation of estimates, which is $\hat{s}$ for an estimate of s, or more in general for a decision related to state of the world s.

estimator

loss function

Optimality is defined with respect to a *loss function* $\mathcal{L}(\hat{s}, s)$, equivalently called *cost function*, a mathematical object that represents the loss or cost – a real number – for any specific decision, $\hat{s}$, when the world is in a given state of affairs, s. When the objective is to estimate the state of the world, the loss function encodes a penalty for the error between the estimate $\hat{s}$ and the supposed true value s, according to some measure of distance.

expected loss

In standard BDT, the decision rule is deterministic and corresponds to the choice that minimizes the *expected loss*, that is the loss averaged over all possible states of

the world, weighted by their (posterior) probability. The expected loss is a function of decision $\hat{s}$ for a given observation, x, and loss function $\mathcal{L}$:

$$\mathcal{E}\left[\hat{s}|x,\mathcal{L}\right] = \int p_{post}\left(s\,|x\right)\mathcal{L}\left(\hat{s},s\right)ds, \tag{1.3}$$

and the optimal decision for observation x corresponds to:

$$\begin{aligned} h^{opt}(x) &= \arg\min_{\hat{s}} \mathcal{E}\left[\hat{s}|x,\mathcal{L}\right] \\ &= \arg\min_{\hat{s}} \int p_{meas}\left(x\,|s\right)p_{prior}(s)\mathcal{L}\left(\hat{s},s\right)ds, \end{aligned} \tag{1.4}$$

where we have used the fact that, due to the argmin operation, the optimal decision is invariant to the rescaling of any of the components of the expected loss, so we can ignore normalization factors.

The theory does not impose any specific shape for the loss function, but typical requirements for a well-behaved loss function of an estimator are to be piecewise continuous and to be *veridical*, i.e. to have a global minimum for $\hat{s} = s$. A few loss functions are commonly chosen due to their mathematical properties, especially for allowing a closed-form solution to Eq. 1.4. *veridical*

▷ The *quadratic loss* function, $\mathcal{L}_{quad}\left(\hat{s},s\right) = \left(\hat{s}-s\right)^2$. The optimal decision that minimizes the expected quadratic loss is the *mean* of the posterior, as shown by the following calculation: *quadratic loss*

$$\begin{aligned} \frac{d}{d\hat{s}}\mathcal{E}\left[\hat{s}|x,\mathcal{L}_{quad}\right] = 0 \quad &\Longrightarrow \quad \int p_{post}\left(s\,|x\right)\frac{d}{d\hat{s}}\left(\hat{s}-s\right)^2 ds = 0 \\ &\Longrightarrow \quad 2\int p_{post}\left(s\,|x\right)\left(\hat{s}-s\right)ds = 0 \\ &\Longrightarrow \quad \hat{s} = \int s p_{post}\left(s\,|x\right)ds. \end{aligned} \tag{1.5}$$

This decision rule is sometimes called Bayesian least-squares, BLS, or MEAN. The mean of the posterior is a very popular decision rule among modellers, mostly because it is very easy to compute.

▷ The *zero-one loss* (or *delta loss*) that equally penalizes any choice different than the true value of s, $\mathcal{L}_{delta}\left(\hat{s},s\right) = -\delta\left(\hat{s}-s\right)$, where $\delta(x)$ is Dirac's delta function (Kronecker's delta is used instead for discrete variables). The optimal choice corresponds to the *mode* of the posterior, the point with maximal probability (*maximum a posteriori* or MAP decision rule). This is easy to show as the expected loss is identical to minus the posterior probability: *zero-one loss* *maximum a posteriori*

$$\mathcal{E}\left[\hat{s}|x,\mathcal{L}_{delta}\right] \;=\; -\int p_{post}\left(s\,|x\right)\delta\left(\hat{s}-s\right)ds \;=\; -p_{post}\left(\hat{s}\,|x\right). \tag{1.6}$$

MAP is another very established decision rule due to its conceptual simplicity.

absolute loss

▷ The *absolute loss*, $\mathcal{L}_{abs}(\hat{s}, s) = |\hat{s} - s|$, for which the optimal choice is the *median* of the posterior:

$$\begin{aligned} \frac{d}{d\hat{s}}\mathcal{E}\left[\hat{s}|x, \mathcal{L}_{abs}\right] = 0 \quad &\implies \quad \int p_{post}\left(s\,|x\right) \frac{d}{d\hat{s}}\,|\hat{s} - s|\, ds = 0 \\ &\implies \quad \int_{-\infty}^{\hat{s}} p_{post}\left(s\,|x\right) ds = \int_{\hat{s}}^{\infty} p_{post}\left(s\,|x\right) ds, \\ &\implies \quad P_{post}\left(\hat{s}|x\right) = 1 - P_{post}\left(\hat{s}|x\right) = \frac{1}{2}, \end{aligned} \tag{1.7}$$

robust estimator

where P_{post} is the cumulative density function of the posterior and the last equation is the definition of median. The median is a *robust* decision rule (or estimator) since it is not affected by the tails of the distribution, unlike the mean. Robust decision rules may be preferrable in many empirical situations since they tend to be less vulnerable to outlier observations. However, the median decision rule is not so common as its calculation is not straightforward.

inverted Gaussian loss

▷ The *inverted Gaussian loss*, $\mathcal{L}_{Gauss}(\hat{s}, s) = -\mathcal{N}\left(\hat{s}\,|s, \sigma_\ell^2\right)$, where σ_ℓ is the length scale or width of the loss. The inverted Gaussian loss leads to another robust estimator since the loss plateaus for values of the error a few times larger than σ_ℓ. Mathematically, the inverted Gaussian loss has the convenient property of allowing a continuous interpolation between the delta loss (for $\sigma_\ell \to 0$) and a quadratic loss (for $\sigma_\ell \gg \sigma_{post}$, where σ_{post} is a measure of length scale of the posterior, such as the standard deviation). The first point follows from the definition since $\lim_{\sigma_\ell \to 0} \mathcal{N}\left(\hat{s}\,|s, \sigma_\ell^2\right) = \delta\left(\hat{s} - s\right)$. For the second point, note that:

$$\begin{aligned} \mathcal{E}\left[\hat{s}|x, \mathcal{L}_{Gauss}\right]|_{\sigma_\ell \gg \sigma_{post}} &\propto \int p_{post}\left(s\,|x\right) \left[-e^{-\frac{(\hat{s}-s)^2}{2\sigma_\ell^2}}\right] ds \Bigg|_{\sigma_\ell \gg \sigma_{post}} \\ &\propto \int p_{post}\left(s\,|x\right) \left[-1 + \frac{(\hat{s}-s)^2}{2\sigma_\ell^2} + \ldots\right] ds \Bigg|_{\sigma_\ell \gg \sigma_{post}} \\ &\propto \int p_{post}\left(s\,|x\right) (\hat{s}-s)^2\, ds + \text{const}, \end{aligned} \tag{1.8}$$

where we have used the analytical expansion of the exponential and the last passage is almost exact when the length scale of the loss function is much larger than the scale of the posterior. Constant factors in the expected loss do not affect the decision, so Eq. 1.8 is equivalent to the expected quadratic loss. Another mathematical property is that, if the posterior is Gaussian (or a mixture of Gaussians), the inverted Gaussian loss allows for a closed-form expression for the expected loss, which can be numerically minimized with relative ease

(see Chapter 4). Although not as widespread as the MEAN and MAP decision rules, the inverted Gaussian loss is an appealing choice when a robust decision rule is needed.

These loss functions are only some textbook examples – an agent may have specific reasons for making decisions according to other, more complex losses.

Finally, in some cases, the loss is not evaluated on the decision per se, but on the *outcome* or *result* of the decision, which is another random variable. This is typically the case in action selection problems (as opposed to estimation), since the consequences of action are rarely certain, e. g. due to motor noise. The extension of the expected loss, Eq. 1.3, for considering this occurrence is straightforward:

outcome

$$\mathcal{E}\left[\hat{s}|x,\mathcal{L}\right] = \int p_{post}\left(s\,|x\right) p_{out}\left(r\,|\hat{s}\right) \mathcal{L}\left(r,s\right) ds\, dr, \tag{1.9}$$

where $p_{out}\left(r\,|\hat{s}\right)$ is the probability of outcome r given decision $\hat{s}$ and note that the expectation is taken on both the unknown state of the world s and the unknown outcome r.

1.2.3 *Degeneracy of BDT*

An inspection of Eq. 1.4 shows that there is an underlying degeneracy to BDT. Multiple combinations of priors, likelihoods and loss functions may lead to the same decision rule, as we illustrate in this section.

As mentioned before, decision rules are insensitive to proper linear transformations of the loss function (addition or multiplication by a constant):

$$\begin{aligned} s^{opt}(x) &= \arg\min_{\hat{s}} \int p_{meas}\left(x\,|s\right) p_{prior}(s) \left[\alpha\mathcal{L}\left(\hat{s},s\right) + \beta\right] ds, \qquad \text{with } \alpha > 0 \\ &= \arg\min_{\hat{s}} \left\{\alpha \int p_{meas}\left(x\,|s\right) p_{prior}(s)\mathcal{L}\left(\hat{s},s\right) ds + \text{const}\right\}, \\ &= \arg\min_{\hat{s}} \int p_{meas}\left(x\,|s\right) p_{prior}(s)\mathcal{L}\left(\hat{s},s\right) ds, \end{aligned} \tag{1.10}$$

but this does not constitute an issue as we can always fix these degrees of freedom by imposing some constraints (Körding and Wolpert, 2004b).

Another manifest form of degeneracy is that the decision rule is invariant to a simultaneous multiplication and division of the prior and loss function by any function of s:

$$\begin{aligned} s^{opt}(x) &= \arg\min_{\hat{s}} \int p_{meas}\left(x\,|s\right) p_{prior}(s) \mathcal{L}\left(\hat{s}, s\right) ds, \\ &= \arg\min_{\hat{s}} \int p_{meas}\left(x\,|s\right) \left[p_{prior}(s) \cdot f(s)\right] \left[\frac{\mathcal{L}\left(\hat{s}, s\right)}{f(s)}\right] ds, \\ &= \arg\min_{\hat{s}} \int p_{meas}\left(x\,|s\right) \widetilde{p}_{prior}(s) \widetilde{\mathcal{L}}\left(\hat{s}, s\right) ds, \end{aligned} \tag{1.11}$$

which means that there is at least an uncountable number of pairs of priors and loss functions that yield the same decision rule. An example of this kind is depicted in Figure 1.1. A similar argument extends to any combination of components obtained by multiplying the original prior, likelihood and loss function respectively by functions $f_1(s)$, $f_2(s)$, and $f_3(s)$ such that, for any s, $f_1(s) \cdot f_2(s) \cdot f_3(s) = \text{const}$.

A more specific form of degeneracy happens in the case of symmetric, unimodal posteriors – this is, for example, the case with Gaussian priors and Gaussian likelihoods, since the posterior is always Gaussian (Eq. 1.2). In this case, for the large class of symmetric loss functions that are non-decreasing in the absolute value of the error $|\hat{s} - s|$, the optimal choice is simply the maximum of the posterior (which is also the median and the mean).

We presented a brief list of cases of degeneracy, but depending on the specific shapes of the elements that appear in the expected loss, other degeneracies may emerge. Moreover, in addition to *exact* mathematical degeneracies, there is an even larger class of practical degeneracies that lead to empirically indistinguishable decision rules under the conditions of noise and amount of data collected in a typical experiment.

There is another aspect of BDT that is worth mentioning, as it is related to the same richness of the framework that leads to a redundancy of solutions. For any measurement distribution, loss function, and decision rule (with some additional assumptions[4]), there is always a prior able to induce that decision rule, a result that is known as *complete class theorem* (see Berger, 1985; Jaynes, 2003).

complete class theorem

inverse problem

All the remarks in this section point to the fact that the *inverse problem* of inferring the elements of BDT (prior, likelihood, or loss function) from a decision rule, or from a noisy estimate thereof such as a series of responses obtained in an experiment, is mathematically ill-posed. However, this does not mean that the enterprise is impossible, since additional constraints, such as reasonable assumptions on the shape of the probability distributions and losses, and independent validations, such as exper-

4 Namely, the decision rule needs to be *admissible*, which means there are no better decision rules for that loss and measurement distribution – ignoring the prior.

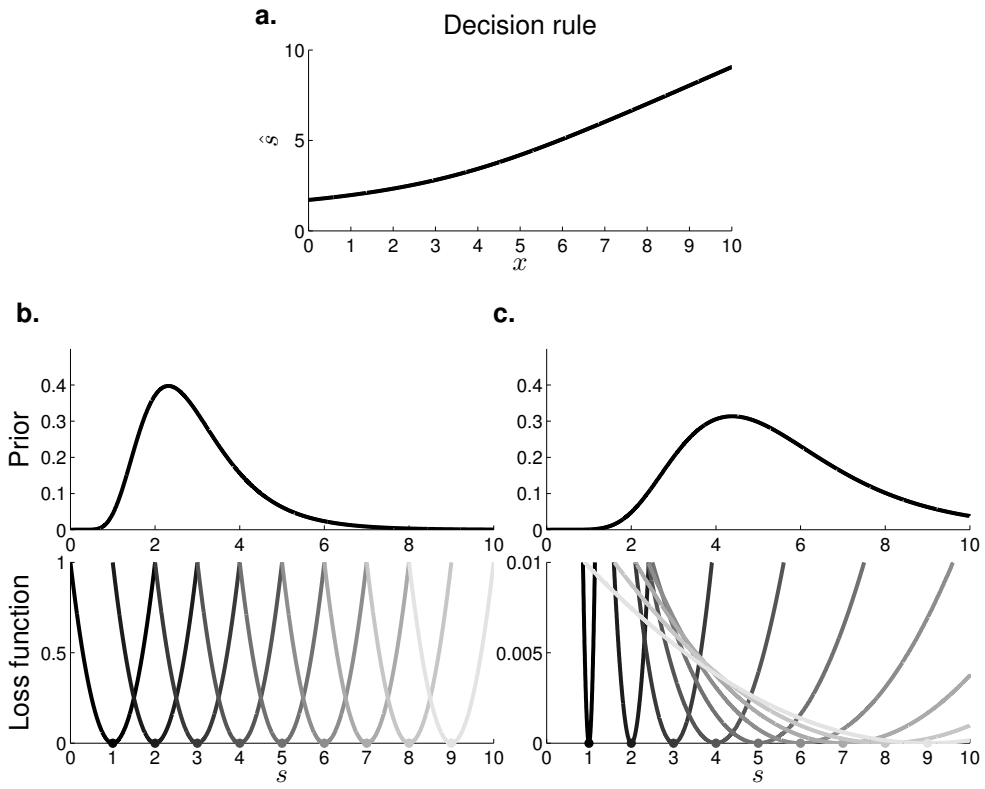

Figure 1.1: **An example of degeneracy of BDT.** A given decision rule does not identify a unique pair of prior and loss function. **a:** A decision rule that maps an observation x to a decision $\hat{s}$ (all axes are in arbitrary units). This decision rule is compatible with prior-loss pairs illustrated in panels **b** and **c**, and by an uncountable number of other prior-loss pairs. For this example we have assumed a Gaussian likelihood centered on the observation and with unit variance, but this kind of degeneracy holds for any likelihood. **b:** *Top*, a log-normal prior. *Bottom*, a quadratic loss function $\mathcal{L}(\hat{s}, s) = (\hat{s} - s)^2$. Each shaded line represents a slice of the loss function for a fixed value of s, indicated by a dot. **c:** *Top:* A log-normal prior multiplied by $1 + s^4$. *Bottom:* A loss function of the form $\mathcal{L}(\hat{s}, s) = (\hat{s} - s)^2/(1 + s^4)$.

iments that test multiple combinations of elements (Maloney and Mamassian, 2009), may allow us to uniquely identify a restricted and well-defined set of solutions. This topic will be a major recurrent theme in the thesis.

1.3 OVERVIEW OF THE THESIS

According to the BBH, humans – at least in their sensorimotor endeavours – behave as Bayesian observers and actors, by building internal representations of the statistics of the task at hand, and computing with them according to the prescriptions of BDT. On the other hand, when the statistical context reaches a certain level of complexity, we can realistically expect to measure deviations from Bayes-optimal behaviour,

due to failures and approximations in both the representations and the computations. The goal of this thesis is to develop tools and investigate how human observers represent and compute with complex distributions of stimuli in a variety of sensorimotor settings; to describe the aspects in which human behaviour deviates from the predictions of standard BDT; and to understand what this entails for the BBH and for human sensorimotor decision making in general. Ours is going to be a truly Bayesian investigation, as we unleash the full machinery of Bayesian inference so as to analyze the behaviour of a system, the ideal observer, that is believed to perform Bayesian inference itself.

1.3.1 *Content*

In this introductory chapter we have presented the motivations and goals for our work, and laid the bases of the methods that we use extensively in the thesis.

In Chapter 2 we analyze in depth the structure and elements of Bayesian models of perception and action, while reviewing the relevant literature from the vantage point of a modeller. In particular, we are interested in ways to model the observers' internal representations and the decision-making process itself.

In Chapter 3 we explore whether BDT is a good descriptive model of human behaviour in a time interval reproduction task that uses complex (non-Gaussian) distributions of durations and distinct experimentally-imposed error costs. At the same time, we use the Bayesian machinery to infer the internal representations of durations that subjects are able to learn. We find agreement with the experimental distributions for low-level statistical moments, but striking mismatches for complex features, such as bimodality.

To shed light on the origin of the discrepancies observed in the previous experiment, in Chapter 4 we examine how people perform probabilistic inference in a target estimation task that does not require observers to memorize complex statistics, but only to compute with them. We test subjects on a large variety of distributions, and with the help of an extensive factorial model comparison we are able to identify several sources of suboptimality in their behaviour which suggest a simple stochastic extension of BDT. Crucially, however, we do not observe any substantial difference in performance between Gaussian and bimodal distributions, suggesting that the difficulty that arose in the previous chapter was due to an issue with learning a complex prior, and not computing with it.

Prompted by a secondary finding of the previous experiment, in Chapter 5 we investigate within a centre of mass estimation experiment the effects that decision uncertainty may have on subjects' capability or willingness to correct for mistakes. Con-

firming the existence of a systematic bias in subjects' responses, we assess whether the observed effect could constitute a relevant deviation from BDT and a potential source of suboptimality.

Finally, in Chapter 6 we critically review our findings, the techniques we have used, and discuss how they represent a first step towards developing a common language for describing and analyzing suboptimality. A deep understanding of approximate representations and computations is needed, if one day we want to connect behavioural models of decision making with actual neural implementations, in the ultimate goal of bridging all levels of Marr's hierarchy.

2

BAYESIAN MODELLING OF PERCEPTION AND ACTION

> "We have now arrived within introductory range of that very meek-spirited creature known to modern science as the "*Observer*". It is a permanent obstacle in the path of our search for external reality that we can never entirely get rid of this individual. [...] All sciences deal only with a *standard* observer, unless the contrary is explicitly stated; and psychology is no exception to this rule."
>
> — John W. Dunne, *An Experiment With Time*

In this chapter, we review how Bayesian models have been succesfully used to characterize human behaviour in perception and action. Among all possible sensorimotor endeavours, we restrict our focus to a class of tasks with a simple, stereotyped structure that requires the subject to explicitly or implicitly estimate the value of a single perceptual variable of interest, such as the duration of a time interval (magnitude estimation; Jazayeri and Shadlen, 2010) or the position of a target for subsequent reaching (motor planning; Trommershäuser et al., 2003a). We generically refer to these types of psychophysical tasks as *sensorimotor estimation* tasks.[1] Formally, these tasks can be described by a simple statistical model, with only a few variables (i.e. nodes in a graphical model) whose general structure is assumed to be known by the observer. The simplicity of the experimental layout and of its mathematical description allows for an easy manipulation of the factors involved in the sensorimotor decision-making process. We especially focus on work that examines the role of the internal representation of the *statistical context* of the task, which is the essential component of any probabilistic computation. Here, we use the phrase 'statistical context of the task' somewhat loosely to refer to (a) the statistics of stimuli appearing in the task (or in the natural environment, under analogous conditions), (b) the statistics of sensory errors, and (c) the statistics of reward. These three components approximately correspond, in the internal model of the observer (and actor), to (a) priors, (b) likelihoods and (c) loss function (and motor errors that stochastically affect reward).

sensorimotor estimation

statistical context

1 We include under this definition also psychophysical tasks that are more commonly known as *discrimination tasks*, in which the observer is asked to judge whether a given stimulus is 'greater than' another stimulus along a relevant dimension (e.g., brighter, longer, more to the right). The rationale is that, broadly speaking, a discrimination task at the core still involves an estimation, but the observer reports differences between percepts as opposed to absolute values. Discrimination tasks are traditionally preferred in perceptual studies since some response biases are eliminated.

In the majority of cases, an observer (and actor) behaves optimally if and only if his or her internal representation of the statistics of the task match the true ones (Ma, 2012). The question that has driven the field for a long time – *are people Bayes optimal in task X?* – corresponds to asking whether people correctly perform probabilistic inference *and* their (implicit or explicit) internal representations match the objective statistics of the task at hand. The Bayesian framework allows modellers to ask also other quantitative questions about people's performance. For example, researchers have sought to determine under what conditions – that is, under which internal model of the task – the observed human behaviour could be considered *subjectively-optimal*. Finally, objective (and subjective) optimality is a useful gold standard, but, as we mentioned in the previous chapter, it may be an excessively strong – or even ill-defined – assumption for more complex tasks . Some studies extend or tweak the standard Bayesian framework to better characterize subjects' deviations from (supposed) optimal behaviour. Ma (2012) define as 'probabilistic' the behaviour of observers that take into account uncertainty in the task, though not necessarily in the optimal way. We note that 'probabilistic' may be easily mistaken for 'stochastic' (i.e. randomly variable), whereas here it has a completely different meaning – for example, a 'probabilistic' observer may be deterministic in his or her choices. To avoid confusion, we coin the word *Bayes-sensible* to indicate a performance that is sensitive to manipulations of uncertainty in the task in a qualitatively reasonable, but not necessarily Bayes-optimal, way.

subjectively-optimal

Bayes-sensible

There are several review articles and commentaries that present an introduction to the field of Bayesian psychophysics from various angles (for example, Geisler and Kersten, 2002; Mamassian et al., 2002; Geisler, 2003; Ernst and Bülthoff, 2004; Kersten et al., 2004; Yuille and Kersten, 2006; Vilares and Kording, 2011; Colombo and Seriès, 2012; Friston, 2012; Pouget et al., 2013; Seriès and Seitz, 2013; Feldman, 2014; Ma and Jazayeri, 2014 for phenomena in perception, with the usual bias towards vision; Körding and Wolpert, 2006; Wolpert, 2007; Bays and Wolpert, 2007; Trommershäuser et al., 2008a,b; Trommershäuser, 2009b; Maloney and Zhang, 2010; Orbán and Wolpert, 2011; Berniker and Kording, 2011; Wolpert and Landy, 2012 focused on action and motor planning). In their overview, these articles necessarily omit the more nitty-gritty details of Bayesian modelling. In view of the topics of this thesis, here we adopt, instead, the complementary and somewhat idiosyncratic perspective of a modeller (see Knill and Richards, 1996; Maloney, 2002; Ernst, 2006; Doya et al., 2007; Simoncelli, 2009; Ma, 2010, 2012; Ma et al., 2014), focusing on the role of (complex) internal representations. As mentioned in the introductory chapter, a self-aware approach to Bayesian modelling is necessary in the face of possible pitfalls and critiques

that might arise (Jones and Love, 2011; Bowers and Davis, 2012; Marcus and Davis, 2013).

standard Bayesian observer

We begin our survey of Bayesian models by introducing what we call the *standard Bayesian observer model* of sensorimotor estimation (Section 2.1). This model, or rather family of models, describes the structure of the typical Bayesian observer in a typical psychophysical experiment, which applies to a large number of basic perceptual and decision-making tasks with at most minor variations. The standard model is a simplified idealization that gives us a common framework to examine and compare features of different studies and modelling approaches. Following the historical development of the field, we start our review in Section 2.2 with studies that look at internal representations of sensory noise (*likelihoods*). Sensory likelihoods and noise distributions have been the main subject of study of sensory cue integration, so we will review work in the area that takes a Bayesian perspective. In Section 2.3 we proceed with an overview of studies that look at internal representations of the statistics of stimuli (roughly, *priors*). Prior expectations about the stimuli are acquired from the statistics of the environment, from the statistics of the experiment itself, or a combination of both. These studies ask a variety of questions, in particular whether and how subjects' sensorimotor behaviour matches the statistics of the stimuli (either the natural statistics, or those of the experiment). Finally, in Section 2.4, we review work on how human observers integrate considerations of cost and reward, usually through an externally imposed *loss function*, in their estimation process or in motor planning. In case of decisions that translate to a motor output, subjects need to take into account the variability of their actions in their computation of losses, possibly building an internal representation of motor uncertainty. Each section in this chapter closes with a brief summary under the heading *In this thesis*, which helps the reader connect the material of the section with the rest of the thesis.

likelihoods

priors

loss function

In this thesis

2.1 THE STANDARD BAYESIAN OBSERVER

The standard Bayesian observer model of sensorimotor estimation, or simply, from now on, the standard Bayesian observer, represents a unified mathematical description of a class of models that applies very generally to human observers performing a basic psychophysical task. The idea of describing perceptual tasks within a single statistical framework that involves a few random variables is an old one in psychophysics (Thurstone, 1927); for example, *signal detection theory* has been widely applied to detection and discrimination tasks (Green and Swets, 1988; Ma, 2010).

2.1.1 *The structure of the standard Bayesian observer*

The standard Bayesian observer is fully defined by two formal structures, depicted in Figure 2.1. The first structure is the *generative model* of the task that describes all relevant variables in the task and their *objective* statistical relationships (Figure 2.1a). The second structure is the *internal model* of the task, that is how the observer internally represents the task and its *subjective* statistical relationships (Figure 2.1b).[2] Almost all objective elements of the generative model have a subjective counterpart in the internal model. To distinguish between objective elements of the worlds and subjective representations thereof we adopt the notational convention in Table 2.1.

generative model

internal model

	Objective	Subjective
Distributions	$p(\cdot)$	$q(\cdot)$
Parameters	θ	$\tilde{\theta}$
Variables	y	y
Loss function	$(\mathcal{L}_{exp})$	$\mathcal{L}$

Table 2.1: **Notation for elements of the generative and internal models.** We consistently denote true, objective distributions with $p(\cdot)$ and their internal, subjective counterparts with $q(\cdot)$. Model parameters are typically denoted with a Greek letter in the objective generative model and with the same Greek letter with a tilde for the corresponding subjective parameter of the internal model. To avoid clutter, we do not explicitly distinguish between external and internal variables, as there is no risk of ambiguity (if a variable appears within a subjective distribution, it should be interpreted as an internal variable). Finally, some tasks impose an objective reward/penalty structure encoded by the experimental loss function, $\mathcal{L}_{exp}$, but in many cases the loss function $\mathcal{L}$ is intrinsically a subjective construct of the decision-making process.

The variables and distributions that appear in the standard Bayesian observer are:

- The *stimulus* $\boldsymbol{s}$. In a sensorimotor estimation task, the stimulus corresponds to the state of the world that the observer is asked to infer. The stimulus variable $\boldsymbol{s}$ encodes all relevant quantitative aspects of the stimulus (such as position, magnitude, direction of motion, etc.) and may be randomly drawn from an experimental stimulus distribution $p_{exp}(\boldsymbol{s})$ under the control of the experimenter. The physical stimulus $\boldsymbol{s}$ in each trial is known to the experimenter but not directly available to the observer. The observer has or develops a prior expectation for the stimulus, represented by the prior distribution over stimuli, $q_{prior}(\boldsymbol{s})$.[3]

stimulus

2 The internal model is still a (subjective) generative model, but to avoid confusion we use the term 'generative model' only for the objective statistical structure of the task.

3 Since priors do not live in a vacuum, it would be more correct to write $q_{prior}(\boldsymbol{s}|\boldsymbol{C})$, where $\boldsymbol{C}$ represents the *context*, i.e. all the information available to the observer, including, for example, the recent history of

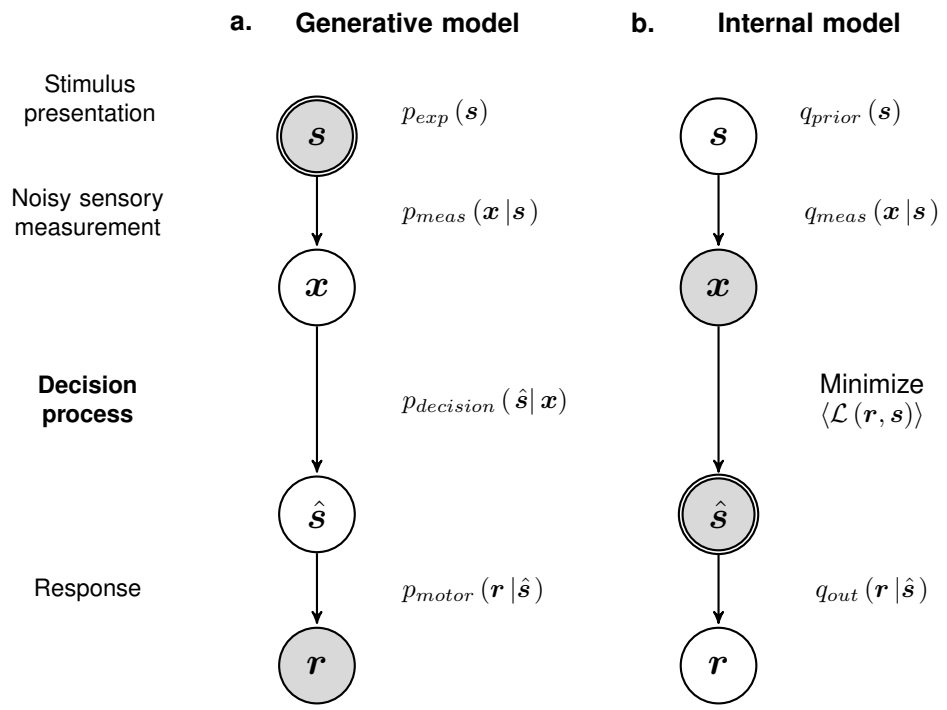

Figure 2.1: **Standard Bayesian observer model of sensorimotor estimation.** This figure outlines the graphical representation of the standard Bayesian model of a simple sensorimotor task, as seen from the outside (**a.** generative model) and from the subjective point of view of the observer (**b.** internal model). The nodes represent the variables involved in the task, which, in general, can be multidimensional (white nodes for hidden variables, shaded nodes for known variables, double-contour nodes for *chosen* variables; see below). Arrows indicate the influence of one node on another, expressed in mathematical terms by conditional probability distributions (described in the text). **a: Generative model.** This graph represents the objective generative model of the data as observed by the experimenter. In a given trial, a stimulus s, chosen by the experimenter, is presented to the observer. The observer (and actor) decides for action $\hat{s}$ after experiencing noisy sensory measurement x. The chosen action, further perturbed by motor noise, yields observed response r. The shaded nodes denote experimentally accessible variables (s and r). **b: Internal model.** This graph represents the observer's internal representation of the generative model of the data. The observer receives noisy sensory measurement x and has to infer the best estimate or action $\hat{s}$, considering all the possible values of the other hidden variables (s and r). Shaded nodes denote variables accessible to the observer (x and $\hat{s}$). In particular, $\hat{s}$ is under the observer's choice (by default, according to the Bayesian rule of minimization of the expected loss). Note that no element of the internal model is directly accessible to the experimenter: all the decision-making process is represented in the generative model (panel **a**) by the decision probability $p_{decision}(\hat{s}|x)$.

We use a different notation for the experimental distribution and the prior since

past trials. The notation $q_{prior}(s|C)$ also reminds us that priors are nothing but posteriors conditioned on the contextually available information – according to the usual machinery of Bayesian belief updating. Keeping this in mind, we resort to the less cumbersome notation.

the relationship between the two can be a complex one (Seriès and Seitz, 2013; Feldman, 2013). In general, s is a vector and may contain information about multiple stimulus dimensions, but our focus in this thesis will be mainy limited to one-dimensional stimuli.

▷ The *internal measurement* x. It is a common assumption that the stimuli are corrupted by sensory noise according to sensory measurement (or *sampling*) distribution $p_{meas}(x|s)$. The x's live in an internal (abstract) sensory measurement space which, in first approximation, can be thought of as an internal representation of the stimulus space. In each trial, x is available to the observer but not to the experimenter. The distribution $q_{meas}(x|s)$ is the observer's representation of the sensory noise distribution (as a function of s, it corresponds to the internal sensory likelihood). Usually, p_{meas} and q_{meas} are assumed to belong to the same parametric family of distributions (e. g., Gaussian), but with possibly mismatching sensory noise parameters, such as different standard deviations σ and $\tilde{\sigma}$. Formally, $p_{meas}(x|s)$ is always used as a conditional distribution (s is fixed, x varies; see Figure 2.1a) and $q_{meas}(x|s)$ as a likelihood in the decision-making process (x is fixed, s varies; see Figure 2.1b), but the actual naming convention in the field is quite loose, with the term 'likelihood' applied to both. *internal measurement*

▷ The *decision* $\hat{s}$. The decision corresponds to the course of action chosen by the observer after the measurement x, a step that can generally be stochastic (see below). The *decision probability (density)*, $p_{decision}(\hat{s}|x)$, fully encodes the observer's decision-making process which is detailed in Figure 2.1b. If the decision takes the form of a deterministic function of the measurement, as it is for example according to standard BDT (see Section 1.2.2), then the decision probability collapses to a delta function (see below, Section 2.1.2). The decision variable is not directly accessible to the experimenter. In the internal model, the decision variable is chosen by the observer according to some decision rule, such as minimization of the expected loss for a certain (subjective) loss function $\mathcal{L}(r, s)$. *decision* *decision probability*

▷ The *response* r. In each trial, the response r includes all relevant behavioural variables measured by the experimenter. The actual response may differ from the planned decision $\hat{s}$ due to motor noise (or other sources of outcome variability, that we either ignore or clump into the motor term), according to the *probability distribution of motor errors*, $p_{motor}(r|\hat{s})$, sometimes improperly called *motor likelihood*. The observer's estimate of motor uncertainty is encoded in the subjective motor error distribution $q_{motor}(r|\hat{s})$ (the subjective motor likelihood). Clearly r is not accessible to the observer at the moment of decision. *response* *motor error distribution*

2.1.2 *The response probability and optimal decision*

response probability

Following the generative model in Figure 2.1a, the *response probability (density)*, when given stimulus $\boldsymbol{s}$, can be computed as:

$$\Pr(\boldsymbol{r}|\boldsymbol{s}) = \int p_{motor}(\boldsymbol{r}|\hat{\boldsymbol{s}})\, p_{decision}(\hat{\boldsymbol{s}}|\boldsymbol{x})\, p_{meas}(\boldsymbol{x}|\boldsymbol{s})\; d\boldsymbol{x}\, d\hat{\boldsymbol{s}}, \tag{2.1}$$

which is integrated over the unobserved variables $\boldsymbol{x}$ and $\hat{\boldsymbol{s}}$. The sensory and motor noise distributions, respectively $p_{meas}(\boldsymbol{x}|\boldsymbol{s})$ and $p_{motor}(\boldsymbol{r}|\hat{\boldsymbol{s}})$, can, in principle, be experimentally assessed. The decision probability $p_{decision}(\hat{\boldsymbol{s}}|\boldsymbol{x})$ depends on the strategy adopted by the observer. The standard Bayesian observer is assumed to be following Bayesian Decision Theory (BDT; see Section 1.2.2), according to the internal model depicted in Figure 2.1b. When the decision is a deterministic function of the measurement, $\boldsymbol{s}^*(\boldsymbol{x})$, such as in BDT, the decision probability collapses to a delta function: $p_{decision}(\hat{\boldsymbol{s}}|\boldsymbol{x}) = \delta(\hat{\boldsymbol{s}} - \boldsymbol{s}^*(\boldsymbol{x}))$, and the expression of the response probability simplifies to:

$$\Pr(\boldsymbol{r}|\boldsymbol{s}) = \int p_{motor}(\boldsymbol{r}|\boldsymbol{s}^*(\boldsymbol{x}))\, p_{meas}(\boldsymbol{x}|\boldsymbol{s})\; d\boldsymbol{x}. \tag{2.2}$$

The observer computes the optimal decision $\boldsymbol{s}^*$ by minimizing the expected loss according to his or her internal model of the task (see Figure 2.1b). The loss function $\mathcal{L}(\boldsymbol{r}, \boldsymbol{s})$ encodes the subjective cost of giving response $\boldsymbol{r}$ when the real stimulus is $\boldsymbol{s}$. Some sensorimotor tasks comprehend an explicit cost function (e. g., expressed with a numerical score or with a financial reward for the participants), but in most other cases the loss function is only mildly constrained by the task goals (see Section 2.4).

The optimal decision that minimizes the expected loss for a generic loss function takes the form (see also Eq. 1.9):

$$\boldsymbol{s}^*(\boldsymbol{x}; \mathcal{L}) = \arg\min_{\hat{\boldsymbol{s}}} \int q_{motor}(\boldsymbol{r}|\hat{\boldsymbol{s}})\, q_{meas}(\boldsymbol{x}|\boldsymbol{s})\, q_{prior}(\boldsymbol{s})\, \mathcal{L}(\boldsymbol{r}, \boldsymbol{s})\; d\boldsymbol{s}\, d\boldsymbol{r}. \tag{2.3}$$

observer and actor

A model that contains Eq. 2.3 may be referred to as an *observer and actor* model, since the decision process takes into account the consequences of action. Conversely, an observer, non-actor model would compute the expected loss directly on the decision, avoiding an integration:

$$\boldsymbol{s}^*(\boldsymbol{x}; \mathcal{L}) = \arg\min_{\hat{\boldsymbol{s}}} \int q_{meas}(\boldsymbol{x}|\boldsymbol{s})\, q_{prior}(\boldsymbol{s})\, \mathcal{L}(\hat{\boldsymbol{s}}, \boldsymbol{s})\; d\boldsymbol{s}. \tag{2.4}$$

Even though an observer, non-actor model is suboptimal if the true statistics of the task include a stochastic outcome (e. g., due to motor noise), there are experimental

conditions in which differences between Eqs. 2.3 and 2.4 become empirically negligible. We only specify whether or not an observer model is also an actor when it is relevant. Generally, the computation of the optimal decision, Eqs. 2.3 or 2.4, involves a marginalization over several unobserved variables, followed by a minimization, but for certain classes of posterior distributions (e.g., Gaussian or mixture of Gaussians) and loss functions (e.g., quadratic), the optimal solution, or at least the expected loss, may afford an analytical expression.

We have seen in this section that the standard model is defined by several mathematical objects: (a) the sensory measurement distribution and internal likelihood, $p_{meas}(\boldsymbol{x}|\boldsymbol{s})$ and $q_{meas}(\boldsymbol{x}|\boldsymbol{s})$; (b) the prior $q_{prior}(\boldsymbol{s})$; and (c) the loss function $\mathcal{L}(\boldsymbol{r},\boldsymbol{s})$, plus possibly the objective and subjective motor error distributions, $p_{motor}(\boldsymbol{r}|\hat{\boldsymbol{s}})$ and $q_{motor}(\boldsymbol{r}|\hat{\boldsymbol{s}})$, for an observer and actor model. To understand the inner workings of Bayesian observer models, and how they have been used to capture several different aspects of sensorimotor behaviour, we separately analyze relevant examples of each object class in each of the following sections.

2.1.3 *In this thesis*

Since all psychophysical experiments analyzed in this thesis involve some version of sensorimotor estimation, the standard Bayesian observer is the main building block of all our modelling endeavours.

- ▷ In Chapter 3, we will develop a family of standard Bayesian observers and actors for a time interval reproduction task. The models differ in terms of the choice of priors, likelihoods and loss functions, but are otherwise standard.
- ▷ In Chapter 4 we will build a large class of observer models based on minor variants of the standard Bayesian observer. In particular, we will describe several models that depart slightly from BDT by having a suboptimal stochastic element in the decision-making process (that is, $p_{decision}(\hat{\boldsymbol{s}}|\boldsymbol{x})$ is not a delta function).
- ▷ Finally, in Chapter 5 we will construct a standard observer and actor model for a centre-of-mass estimation task in which participants' behaviour can be explained with a non-trivial loss function.

All of the observer (and actor) models developed in this thesis are described by the graphical model in Figure 2.1, and they closely follow the definitions and equations presented in this section. The only minor difference is that in all the models we will introduce, the task-relevant dimension of the stimuli is only one (i.e., duration or

horizontal position), so we will drop the 'bold' vector notation on the variables: the stimulus becomes s, the measurement x, etc.

2.2 SENSORY NOISE DISTRIBUTIONS AND LIKELIHOODS

In this section we briefly review the role of sensory noise distributions and their subjective counterparts, the internal sensory likelihoods, in the Bayesian modelling of perception.

2.2.1 *Sensory measurement distributions*

Internal measurements of proximal sensory stimuli are noisy due to several reasons, such as physical stochasticity in the stimulus (e.g., molecular motion in chemical sensing, photon absorption of light quanta), signal transduction and transmission noise, and neuronal variability; see Faisal et al. (2008) for a review. Moreover, internal sensory measurements may be ambiguous due to an intrinsic *ill-posedness* of the sensory mapping, whereby a high-dimensional stimulus $\boldsymbol{s}$ passes through an intermediate, lower-dimensional representation $\boldsymbol{x}$ that affords multiple interpretations (the typical example is vision, in which the three-dimensional world is mapped to a two-dimensional image on the retina; Poggio et al., 1985). In ideal observer theory, all such details of the sensory processing are summarized by the objective sensory measurement (or sampling) distribution, $p_{meas}(\boldsymbol{x}|\boldsymbol{s})$. In the following paragraphs we present various classes of sensory noise distributions and discuss how they can be experimentally measured.

ill-posedness

Gaussian measurement noise

The simplest and most common form of sensory noise distribution is (multivariate) normal, which in the one-dimensional case yields:

$$p_{meas}(x|s) = \mathcal{N}(x|s, \sigma^2_{sens}), \tag{2.5}$$

where σ_{sens}, the standard deviation (SD) of the sensory noise, does not depend on the stimulus value; that is, the noise is *homoscedastic*. A rationale for Eq. 2.5, aside from experimental validation, stems from the assumption that several small perturbations contribute independently to the sensory noise, summing up to a normal distribution according to the central limit theorem, or variants thereof. Eq. 2.5 is also a reasonable choice, due to maximum-entropy considerations, if we do not have any information about the noise process but we can recover its mean and variance (Jaynes, 2003).

homoscedastic noise

Normally-distributed sensory measurements are the default assumption in signal detection theory (Green and Swets, 1988).

Gaussian measurement noise with stimulus-dependent variance

An important generalization of Eq. 2.5 is given by the case in which the sensory variance depends on the stimulus value:

$$p_{meas}(x|s) = \mathcal{N}\left(x \,\middle|\, s, \sigma^2_{sens}(s)\right). \tag{2.6}$$

In this case, we say that the noise is *stimulus-dependent* (formally, *heteroscedastic*), in the sense that sensory variability changes along with the task-relevant dimension of the stimulus, as opposed to depending on task-irrelevant properties of the stimulus (such as blur or contrast). *heteroscedastic noise*

Eq. 2.6 is relevant, for example, in *magnitude estimation* tasks, in which the variable of interest is a non-negative stimulus magnitude, such as duration, speed, or light intensity. In these cases, the empirical *Weber-Fechner's law* states that the sensory noise is (approximately) proportional to the stimulus value, $\sigma_{sens}(s) \approx W \cdot s$, where W is *Weber's fraction*. Since Weber-Fechner's law makes the noise distribution scale-invariant, it is also known as the *scalar property* of noise in the time perception literature (Gibbon, 1977). The 'pure' scalar property predicts that Weber's fraction is constant across *all* scales, which has been experimentally disproved (Lewis and Miall, 2009); nevertheless, the law may still hold as a good approximation for certain ranges. A variant of Weber-Fechner's law that corrects for deviations at lower levels of the noise includes a lower bound on the noise, such as $\sigma^2_{sens}(s) = \sigma_0^2 + W^2 s^2$ (Getty, 1975). *Weber-Fechner's law*

The key difference between Eqs. 2.5 and 2.6 is that the former expression retains a Gaussian shape as a likelihood (function of s), whereas the latter does not (see Section 2.2.2). A non-Gaussian likelihood constitutes a moderate to severe complication to Bayesian computations, so sometimes it is convenient to change the representation of the stimulus: $s \longrightarrow g(s)$, where $g(s)$ is an appropriately chosen *sensory transform*, such that the noise distribution in the transformed space is approximately Gaussian with constant variance. For example, it is a common modelling choice to use logarithmic coordinates for the stimulus in order to account for Weber-Fechner's law or variants, with mappings such as $g(s) = \log s$ (Jürgens and Becker, 2006; Battaglia et al., 2011; Petzschner and Glasauer, 2011) or $g(s) = \log(1 + \beta \cdot s)$, with β a constant (Knill, 1998a; Stocker and Simoncelli, 2006b). We now show the general rule for choosing $g(s)$, of which we give an informal proof (Acerbi et al., 2014a). *sensory transform*

Proposition 2.1. *Assume that the measurement noise distribution is Gaussian and heteroscedastic with variance $\sigma^2_{sens}(s)$ (see Eq. 2.6). If the noise magnitude is low compared*

to the magnitude of the stimulus, $\sigma_{sens}(s) \ll s$, and $\sigma_{sens}(s)$ changes slowly as a function of s, the following sensory transform:

$$g(s) = \int_{-\infty}^{s} \frac{1}{\sigma_{sens}(s')} ds' \; + \; const, \tag{2.7}$$

constructed so that $g(s)$ is continuous, maps the stimulus scale to a space in which the measurement noise is approximately Gaussian with constant variance (homoscedastic).

Proof. Note that $\frac{dg}{ds}(s) = \frac{1}{\sigma_{sens}(s)}$ by construction. We can write:

$$\begin{aligned} g(x) &= g(s + \sigma_{sens}(s) \cdot \eta) \\ &\approx g(s) + \frac{dg}{ds}(s) \cdot \sigma_{sens}(s) \cdot \eta \\ &= g(s) + \eta, \end{aligned} \tag{2.8}$$

where η is a normally distributed random variable with zero mean and unit variance. The second passage of Eq. 2.8 uses a first-order Taylor expansion, assuming that the noise magnitude is small compared to the magnitude of the stimulus, and changes slowly as a function of s.[4] Under these assumptions, the last passage shows that the measurement variable in the transformed space is approximately Gaussian with mean $g(s)$ and unit variance. □

For example, it is easy to show that for Weber-Fechner's law, $\sigma_{sens}(s) = W \cdot s$, the solution of Eq. 2.7 takes the well-known logarithmic form $g(s) \propto \log s$. In general, the transformation to a different stimulus scale can be seen as a mere mathematical trick performed by the modeller to simplify calculations, but in some cases it has been argued that it corresponds to the actual encoding of stimulus values in the brain, such as for the proposed logarithmic representation of number (Dehaene et al., 2008). However, as Proposition 2.1 shows, it may be hard to discriminate between linear representations with magnitude-dependent precision and nonlinear (e.g., logarithmic) representations with a fixed precision. Statements about the real scale of internal representations remain controversial when based only on psychophysical data (Dehaene, 2001; Cantlon et al., 2009).

Generic measurement noise

Finally, there are scenarios in which the measurement distribution is utterly non-Gaussian, usually because of a complex relationship between the stimulus variable (e.g., surface slant) and the modelled measurement variables (e.g., texture size and shape). This is not uncommon in vision, due to operators such as projection, rotation

4 This can be formalized as a series of requirements on the higher-order derivatives of $g(s)$.

and scaling (Poggio et al., 1985; Bülthoff and Yuille, 1991). Finding the expression for the measurement distributions as a function of the experimental variables can become a considerable exercise in trigonometry; see, for example, Knill (1998a) for a derivation of texture properties from surface slant and tilt, and Schrater and Kersten (2000) for a computation of depth from different sets of visual cues.

Psychophysical measures of sensory noise

For many psychophysical tasks, the noise at a given value of the stimulus can be empirically estimated through a classic measurement of discrimination performance, the *threshold* of the psychometric function (Thurstone, 1927; Green and Swets, 1988; Wichmann and Hill, 2001; Kuss et al., 2005). The typical experimental procedure consists of a *two-alternative forced choice* task (2AFC): in each trial, two stimuli s_1 and s_2 are simultaneously or sequentially presented to the observer and the task consists of reporting whether a one-dimensional stimulus property of one given stimulus (such as intensity, duration or length) is greater than the same property of the other, e. g. $s_1 \overset{?}{>} s_2$.[5] If we assume that the observer estimates each stimulus independently, the probability of responding '$s_1 > s_2$' in a 2AFC task is given by:

threshold

2AFC

$$\begin{aligned}\Pr\left('s_1 > s_2'|s_1, s_2\right) &= \int_{s^*(x_1)>s^*(x_2)} p_{meas}\left(x_1\,|s_1\right) p_{meas}\left(x_2\,|s_2\right) dx_1 dx_2 \\ &\approx \int_{-\infty}^{\infty} p_{meas}\left(x_1\,|s_1\right) \left\{ \int_{-\infty}^{x_1} p_{meas}\left(x_2\,|s_2\right) dx_2 \right\} dx_1,\end{aligned} \tag{2.9}$$

where the domain of integration of the first integral is for $s^*(x_1) > s^*(x_2)$, $s^*(x)$ being the optimal estimate for the stimulus given internal measurement x. The second passage follows if the optimal estimate, $s^*(x)$, is approximately equal to the sensed noisy measurement x, which is true in the absence of biases to the decision-making process (a flat prior, a well-behaved and symmetric loss function, and with the reasonable assumption that the internal likelihood peaks at the measurement). If the noise distribution is Gaussian with constant noise (Eq. 2.5), Eq. 2.9 reduces to a simple sigmoidal form:

$$\Pr\left(s_1 > s_2|s_1, s_2\right) = \frac{1}{2}\left[1 + \operatorname{erf}\left(\frac{1}{\sqrt{2}} \cdot \frac{s_1 - s_2}{\sqrt{2}\sigma_{sens}}\right)\right]. \tag{2.10}$$

The noise σ_{sens} can be recovered by fitting the psychometric curve, but traditionally it was taken as the threshold value, $s_1 - s_2$, at which discrimination probability is $\sim 76\%$ (the value of a cumulative Gaussian $\frac{1}{\sqrt{2}}$ of a SD from the mean). The actual psychometric function usually includes a lapse term to allow for occasional mistakes

5 When the stimuli are presented sequentially, the layout is also called *two-intervals forced choice* (2IFC).

and improve the robustness of the inference (Wichmann and Hill, 2001). Recent computational developments have allowed researchers to look into subtle issues of reconstructing psychometric curves, such as non-stationarity (Fründ et al., 2011), recency and order effects (Raviv et al., 2012), erroneous estimates of the lapse rate (Prins, 2012), and systematic response biases caused by task-irrelevant stimulus attributes (Jogan and Stocker, 2014).

2.2.2 *Internal sensory likelihoods*

The subjective likelihood, $q_{meas}(\boldsymbol{x}|\boldsymbol{s})$, appears in the inverse problem of recovering stimulus $\boldsymbol{s}$ given measurement $\boldsymbol{x}$ (Eq. 2.3). The likelihood formally encodes the observer's internal representation of the uncertainty associated with a sensory measurement (roughly, its 'error bars'). The representation and availability of sensory uncertainty has been receiving increasing attention in the recent years (see Orbán and Wolpert, 2011; Bach and Dolan, 2012 for reviews). Many observer models simply assume that $q_{meas}(\boldsymbol{x}|\boldsymbol{s}) \equiv p_{meas}(\boldsymbol{x}|\boldsymbol{s})$, but here we review studies that explicitly ask whether the observer's internal representation is equal to the actual measurement distribution: $q_{meas}(\boldsymbol{x}|\boldsymbol{s}) \stackrel{?}{=} p_{meas}(\boldsymbol{x}|\boldsymbol{s})$, a prerequisite of optimal behaviour. There are essentially two ways to probe the internal representation of noise: either by requiring the observer to *explicitly* evaluate his or her confidence in a perceptual judgment (e.g., Barthelmé and Mamassian, 2009, 2010), or by tracking how the observer's *implicit* belief about measurement noise alters his or her behaviour. In this thesis we deal with the latter approach.

Note that, according to BDT, the sensory likelihood will generally interact with the prior and loss function to implicitly drive a sensorimotor decision (Eq. 2.3). However, since we will extensively describe priors and loss functions in the following sections, here we consider studies whose main focus is strictly on sensory likelihoods. Arguably, a field that has been deeply involved with the Bayesian examination of sensory likelihoods, their shape and interactions (with a minimal contribution of other elements of BDT) is *sensory cue integration* (Ernst and Bülthoff, 2004; Trommershauser et al., 2011; Fetsch et al., 2013). A 'cue' is informally understood as any signal that carries information on the state of some property of the environment, both within and across the senses (Fetsch et al., 2013). The leading question in most of these studies is whether (and how) human observers combine distinct, redundant cues about external sensory stimuli in a statistically optimal fashion, according to the principles of Bayesian inference (which correspond to maximum-likelihood estimation when the prior is absent and the loss function is assumed to be a zero-one loss).

sensory cue integration

The recurrent expression 'optimal cue integration' means that the observer combines cues *as if* he or she had a correct internal representation of the likelihoods associated with each cue.[6] Note that, even if the brain performs Bayesian computations, the likelihood needs not have a separate representation from the stimulus itself: stimulus uncertainty could be automatically encoded in the response patterns of populations of neurons (Ernst and Banks, 2002; Ma et al., 2006).

Gaussian likelihoods and linear cue integration

We start by revising the idealized cue-combination experiment in the case of two independent cues. The typical experimental methodology is called *perturbation analysis* (Young et al., 1993). The observer is presented with two slightly discrepant sensory cues s_1, s_2 (e.g., stereo and texture, or visual and tactile feedback), and the task requires him or her to estimate the value of an underlying stimulus s (e.g., the slant of a surface, or the height of a bar). It is easy to show that in the case of Gaussian likelihoods and measurement distributions, the observer's estimate s^* is distributed as another Gaussian variable with mean and variance given by:

perturbation analysis

$$\mathbb{E}[s^*] = \frac{s_1\tilde{\sigma}^2_{sens2} + s_2\tilde{\sigma}^2_{sens1}}{\tilde{\sigma}^2_{sens1} + \tilde{\sigma}^2_{sens2}} \tag{2.11}$$

$$\mathrm{Var}[s^*] = \frac{\sigma^2_{sens1}\tilde{\sigma}^4_{sens2} + \sigma^2_{sens2}\tilde{\sigma}^4_{sens1}}{\left(\tilde{\sigma}^2_{sens1} + \tilde{\sigma}^2_{sens2}\right)^2} \overset{\tilde{\sigma}^2_{sens\#} \equiv \sigma^2_{sens\#}}{\Longrightarrow} \frac{\tilde{\sigma}^2_{sens1}\tilde{\sigma}^2_{sens2}}{\tilde{\sigma}^2_{sens1} + \tilde{\sigma}^2_{sens2}}, \tag{2.12}$$

where $\sigma^2_{sens\#}$ denotes the measurement variance and $\tilde{\sigma}^2_{sens\#}$ is the likelihood variance, for cues $\# = 1, 2$. Note that: (a) the mean estimate is a weighted linear combination of the sensory cues s_1, s_2, with weights proportional to their relative reliabilities, respectively $\frac{\tilde{\sigma}^2_{sens2}}{\tilde{\sigma}^2_{sens1}+\tilde{\sigma}^2_{sens2}}$ and $\frac{\tilde{\sigma}^2_{sens1}}{\tilde{\sigma}^2_{sens1}+\tilde{\sigma}^2_{sens2}}$; and (b) if $\tilde{\sigma}^2_{sens\#} \equiv \sigma^2_{sens\#}$ for both cues, the variance of the estimate is smaller than the variance of each individual cue, and incidentally corresponds to the variance of the posterior.[7] A strong case for optimal cue combination can be made only if *both* the mean and the variance of the combined estimate match Eqs. 2.11 and 2.12, with $\tilde{\sigma}^2_{sens\#} = \sigma^2_{sens\#}$. Otherwise, for example, the mean estimate alone could match Eq. 2.11 via a suboptimal probabilistic cue-switching strategy, whereby the observer chooses one cue, ignoring the other, with probability proportional to its reliability (Ghahramani et al., 1997; Landy and Kojima, 2001).

Early studies showed evidence supporting the idea that human observers take into account cue reliability when computing cue weights, such as in depth estimation from texture and stereo (Young et al., 1993), target estimation from audio and visual

6 Modulo non-identifiable features; for example, with Gaussian likelihoods, optimal behaviour depends only on the ratio of the variances.

7 It is *not* true in general that the variance of the estimate equals the variance of the posterior.

cues (Ghahramani et al., 1997), edge localization from texture information (Landy and Kojima, 2001) and spatial localization from visual and auditory signals (Battaglia et al., 2003). Reduction of the combined variance of the estimate was found in judging hand position from visual and proprioceptive feedback (van Beers et al., 1996), or depth from texture and motion (Jacobs, 1999). Strong empirical support for near-optimal cue integration, however, comes from studies that simultaneously analyzed the mean and variance of the combined estimates under conditions with different noise levels (e.g., added blur to visual feedback), finding a good match with predictions from individual variances (see Ernst and Bülthoff, 2004 for a review). Examples include tasks such as length estimation from visual and haptic information (Ernst and Banks, 2002; Gepshtein and Banks, 2003), target localization from visual and audio signals (Alais and Burr, 2004), and shape information from realistic (non-virtual) visual and haptic cues (Helbig and Ernst, 2007).

To sum up, there is considerable evidence that human observers perform near-optimal linear cue-integration in several perceptual tasks, suggesting that the nervous system has a method to quickly evaluate the sensory noise – and consequently adjust the width of the likelihood – associated with each cue. Although there have been various proposals, details of such a mechanism are unknown to date, as they were over a decade ago (Jacobs, 2002).

Non-Gaussian likelihoods and nonlinear cue integration

In the studies considered in the previous paragraphs, the likelihoods were (approximately) Gaussian, and a weighted linear combination of the cues was the optimal solution. Even though cue reliability changed among different experimental conditions, this information could have been provided by ancillary cues, such as blur or viewing angle (Landy et al., 1995; but see Barthelmé and Mamassian, 2010). A different case arises when cue uncertainty depends on the stimulus value itself (see Eq. 2.6), which yields a non-Gaussian likelihood and therefore a nonlinear optimal combination. In practice, if the discrepancy between the cues is not too large, the solution can still be linearized around the stimulus – but, crucially, the weights would not be constant, changing across different stimulus magnitudes (Yuille and Bülthoff, 1996; Knill and Saunders, 2003). This scenario is arguably more complex than linear cue combination and it is unclear, a priori, whether human observers would have such a flexible internal representation of sensory noise.

Knill (1998b) develops an ideal observer model for discriminating surface orientation from texture that includes several non-Gaussian likelihoods. Qualitatively, human observers behave like the ideal observer (Knill, 1998a), although their performance is typically suboptimal. Saunders and Knill (2001) show that human observers

nonlinearly combine stereo and skew-symmetry cues to estimate the slant and tilt of a planar figure, in broad agreement with a Bayesian observer model. Knill and Saunders (2003) perform a tighter test of whether humans adopt an internal likelihood of stereo and texture information from slant that correctly matches the slant-dependent measurement noise. Their results show a reasonable quantitative agreement at the individual level, with possibly some degree of suboptimality.[8] In another study, near-optimal cue combination was found for slant judgement from texture and disparity cues, under a variety of slants and viewing distances (Hillis et al., 2004).[9] In a different domain, Drewing and Ernst (2006) show that cue weights qualitatively follow the change predicted by individual cue reliabilities in a curvature discrimination task from haptic cues of force and position, whose noise changes as a function of curvature. In the case of duration estimation, for which the noise follows the scalar property, recent work supports close-to-optimal integration of audio-visual 'filled' intervals (Hartcher-O'Brien et al., 2014).

All these studies provide evidence that human observers' likelihoods take into account stimulus-dependency (heteroscedasticity) of noise, with possibily some amount of suboptimality. It is unclear whether humans follow a fully nonlinear integration strategy or rather a locally-linear approximation, as in most tested models.

Non-Gaussian likelihoods from mixture models

Another natural way of obtaining a non-Gaussian likelihood is when the measurement noise is believed to emerge from a mixture of different sources, so that the noise distribution itself is non-Gaussian. The combination of multiple distributions with different variances may yield a distribution that is *heavier-tailed* than a Gaussian. Heavy tailed distributions are associated with 'robust' estimation, since, as likelihoods, they are implicitly more tolerant to outliers in the presence of a big discrepancy between cues. For example, mixture models have been succesfully used in slant perception to represent likelihoods that encode multiple hypotheses about the world, such as properties of textures (texture can be isotropic or homogeneneous; Knill, 2003) and property of shapes (figures may be circles or generic ellipses; Knill, 2007). Other studies showed that psychophysical data were well described by observer models with heavy-tailed likelihoods, such as in a slant discrimination task with disparity and

heavy-tailed likelihoods

8 The authors conclude that, on average, stereo cues appear to be over-weighted with respect to texture information, according to the psychophysical data. However, this discrepancy may emerge since the model used in the study computes 'optimal' cue weights based on a locally-linear approximation of the optimal, nonlinear solution – but the approximation may be poor, since the noise exhibits large changes as a function of slant (Knill and Saunders, 2003, Figure 5).

9 The locally-linear approximation in this study seems to hold due to a moderate variation of texture noise as a function of slant (compare Figure 4 in Hillis et al., 2004 with Figure 5 in Knill and Saunders, 2003).

texture cues (Girshick and Banks, 2009) and in an audio-visual target estimation task (Natarajan et al., 2009).

These studies provide some evidence that human performance shows qualitative effects of robust cue integration in the presence of large discrepancies between cues. However, we do not know whether such behaviour was 'optimal', because the heavy-tailed noise distributions were postulated and not measured separately (Girshick and Banks, 2009 did measure single-cue reliabilities, but assuming a single-Gaussian model). More generally, it is unclear whether statements of optimality with non-Gaussian likelihoods can be proved at all, beyond qualitative agreement, since changes in higher-order moments of the sampling noise distribution may have large effects on the predicted optimal behaviour, but such fine details of noise distributions are difficult to measure experimentally (Rosas and Wichmann, 2011). Also, 'robust' cue integration (or segregation) in the presence of highly discrepant cues is probably better described within a *causal* (or *structural*) *inference* framework in which the observer needs also to infer the causal structure of the task, that is, infer whether the perceived sensory cues are caused by a single event or by distinct, unrelated events (Körding and Tenenbaum, 2007; Körding et al., 2007; Hospedales et al., 2007; Sato et al., 2007; Natarajan et al., 2009). A discussion of causal inference models is beyond the scope of this chapter.

causal inference

Near-optimal internal models of sensory noise

There are a few studies that show that human performance at cue combination can be far from optimal, suggesting that observers may have a wrong internal model of cue reliability. Some effects of suboptimality may be due to the presence of correlation between cues which are not accounted for by basic observer models (Oruç et al., 2003). Then, there are cases in which human observers simply seem to behave suboptimally, such as in a slant discrimination task from texture and haptic cues (Rosas et al., 2005) or from texture and motion cues (Rosas et al., 2007). Another study found evidence for probabilistic cue switching, as opposed to cue integration, in a sensorimotor pointing task that required observers to combine visual and proprioceptive force information (Serwe et al., 2009).[10]

Nevertheless, almost all cue integration studies agree that humans take sensory uncertainty into account when combining different cues, and we have seen a remarkable number of studies that show that humans perform close to optimally in a variety of simple perceptual tasks. Overall, this large body of work provides evidence that internal sensory likelihoods are typically well-correlated with the corresponding sensory

10 Although a later study found a performance closer to optimal with a moderately different setup (Serwe et al., 2011).

noise distributions, possibly due to a continuous process of inter-sensory and intra-sensory calibration, so that the simplifying assumption of $q_{meas}(\boldsymbol{x}|\boldsymbol{s}) \approx p_{meas}(\boldsymbol{x}|\boldsymbol{s})$ may be acceptable, at least as a first approximation, when dealing with natural sensorimotor tasks.

2.2.3 *In this thesis*

Sensory noise needs to be accurately modelled – even when it is not the main subject of enquiry – because any assumption about measurement distributions and likelihoods will affect the inferences about the other elements of decision-making.

- ▷ In Chapter 3 we will verify whether the sensory noise distributions (and associated likelihoods) in a time interval reproduction task follow the scalar property, or are instead more likely to have constant variance. In order to validate our modelling, we will use the psychophysical methods described in Section 2.2.1 to independently measure subjects' sensory noise (Weber's fraction) in a 2AFC task, checking whether there is a good correlation between the independent estimate and the model-recovered parameters.
- ▷ In Chapter 4 we will introduce a target estimation task that maps to a simple model of probabilistic inference wherein observers need to integrate a 'cue' with a visually provided 'prior'. Given the somewhat artificial nature of the sensorimotor task, we will not assume that observers know the true values of the reliability of the cue, so $q_{meas}(\boldsymbol{x}|\boldsymbol{s}) \not\equiv p_{meas}(\boldsymbol{x}|\boldsymbol{s})$ as per many of the studies seen in Section 2.2.2, and, in fact, we will report consistent mismatches. We will also separately assess additional sensory noise that observers may have in judging the cue position, which is used in a sub-class of models. We will see that sensory noise in estimating the position of the cue does not play a major role in determining observers' suboptimality in the task.
- ▷ Finally, the centre-of-mass estimation task in Chapter 5 requires the observer to estimate a ratio between the areas of two disks, for which we assume Weber-Fechner noise that we model in logarithmic space, as per the method described in Section 2.2.1. Given the perceptual nature of the task, and in order to reduce model complexity, here we will assume that $q_{meas}(\boldsymbol{x}|\boldsymbol{s}) \equiv p_{meas}(\boldsymbol{x}|\boldsymbol{s})$.

2.3 PRIORS

Priors are probably the most distinctive element of the Bayesian approach – so much so that in the absence of a prior, Bayesian estimation becomes ML estimation and BDT falls back to *statistical* decision theory (Maloney and Zhang, 2010). Priors can be described as belonging to two broad categories (Seriès and Seitz, 2013): *contextual* priors are acquired and apply in a limited context, such as the experimental session; *structural* priors are learnt from the environment on a longer timescale and apply in a more general setting – they may even be built-in in the perceptual system (such as chicken's innate prior that light comes from above; Hershberger, 1970).

contextual and structural priors

2.3.1 *Priors and empirical distributions*

In the standard Bayesian observer, the prior represents the subjective expectation about the value of a stimulus $\boldsymbol{s}$ in a given context, expectation that manifests itself in measurable perceptual and decision-making biases. The objective counterpart of a prior is the *empirical distribution* – just as the internal likelihood has a parallel in the objective measurement distribution – although the relationship between prior and empirical distribution needs some explaining, as it depends on the category of prior.

empirical distribution

For a contextual prior developed in the course of an experiment, the empirical distribution corresponds to the experimental probability of the stimulus (which may change in time, depending on the stochastic process generating the stimulus). In the simplest case, the statistics of the stimuli in the experiment are kept constant, with i.i.d. stimuli $\sim p_{exp}(\boldsymbol{s})$; that is, the empirical distribution is *stationary*. Structural priors, instead, have been shaped on a much longer timescale by the statistics of the environment. Therefore, the empirical distribution to look at, assuming (and ensuring) that there is no learning in the course of the experiment, is not the distribution of stimuli in the experiment, but the 'ecological prior' given by the natural statistics of the stimulus for the dimension under consideration (e.g., speed, orientation).

stationarity

The statement that, in the case of optimal decision-making, the prior *ought to* match the (stationary) empirical distribution presents subtle issues (Feldman, 2013). First, the distinction between contextual and structural prior is somewhat arbitrary, especially because structural priors can be quickly overridden (Adams et al., 2004; Sotiropoulos et al., 2011). Second, in the case of structural priors, even assuming that we can overcome the practical difficulties in collecting data about natural statistics of the stimuli, it is not always clear what exactly constitutes the reference class of stimuli to take into account. Finally, other assumptions about the generative process of the stimulus, such as stationarity, are likely to be violated in the environment and, there-

fore, by human observers (Raviv et al., 2012; Kwon and Knill, 2013). In other words, we should not necessarily expect a naïve match between the observer's prior and the empirical distribution (Feldman, 2013). Nonetheless, the Bayesian framework can be used to investigate the relationship between the empirical distribution – acquired in the experiment, from the environment, or both – and the observer's prior. In this analysis, we define *'optimality'*, in quotation marks, as the case in which the observer's prior seems to match the chosen empirical distribution – the quotes remind us of the caveats of such a definition.

'optimality'

2.3.2 *Learning contextual priors*

In this section we briefly review how human sensorimotor behaviour in sensorimotor estimation tasks is affected by statistical features of the experimental distribution of stimuli. The basic psychophysical experiment has the following stereotyped form: in each trial, the observer is exposed to a random stimulus s drawn from a stationary experimental distribution $p_{exp}(s)$, such as a Gaussian distribution with given mean and variance (in almost all cases, the stimulus space under consideration is one-dimensional). In different conditions, usually mixed within the experiment, sensory noise is manipulated – e.g., by adding blur or altering contrast – to affect the width of the measurement distribution, and, therefore, of the likelihood. Alternatively, the noise distribution is kept fixed, but observers perform on multiple experimental distributions $p^{(1)}_{exp}(s), p^{(2)}_{exp}(s), \ldots$ in different (blocks of) sessions. Subjects are trained on hundrends or thousands of trials per condition, usually till performance plateaues, to ensure that prior expectations are adapted to the statistics of the experiment.

Gaussian contextual priors

We start by reviewing whether human observers are sensitive to the low-order moments (mean and variance) of a distribution of stimuli. The mathematics of the standard Bayesian observer in the case of a Gaussian prior with Gaussian likelihood and measurement distribution is remarkably similar to that of the cue combination case (Eqs. 2.11 and 2.12). Assuming any symmetric, veridical loss function, the estimate s^* is distributed as another Gaussian variable with mean and variance given by:

$$\mathbb{E}\left[s^*\right] = \frac{s\tilde{\sigma}^2_{prior} + \tilde{\mu}_{prior}\tilde{\sigma}^2_{sens}}{\tilde{\sigma}^2_{sens} + \tilde{\sigma}^2_{prior}} \tag{2.13}$$

$$\mathrm{Var}\left[s^*\right] = \frac{\sigma^2_{sens}\tilde{\sigma}^4_{prior}}{\left(\tilde{\sigma}^2_{sens} + \tilde{\sigma}^2_{prior}\right)^2} \tag{2.14}$$

where $\tilde{\mu}_{prior}$ and $\tilde{\sigma}^2_{prior}$ denote respectively the (subjective) mean and variance of the prior. Comparing Eqs. 2.13 and 2.14 with their counterparts, Eqs. 2.11 and 2.12, we can see that the prior effectively acts as a second cue. Incidentally, this means that the considerations we made in Section 2.2.2 with respect to Gaussian likelihoods hold for the case of Gaussian priors as well. In particular, Bayesian biases are characterized by a response that is the average of the mean of the prior and the location of the current stimulus, weighted by their relative reliabilities (Eq. 2.13). Also, due to the mathematical equivalence between a prior and an extra cue, sometimes prior information can be modelled as a 'cue from memory' (e. g., Brouwer and Knill, 2007, 2009). This duality shows that the distinction between priors and likelihoods is somewhat arbitrary.

slope and bias

The main observables of interest here are the *slope* and *bias* (i.e., constant error) exhibited by the mean response as a function of the stimulus, which should be a linear function (Eq. 2.13). As per the cue combination case, a test of 'optimality' needs to independently measure the sensory noise for each experimental manipulation, to verify that the weights given to prior and cue respect the actual statistics of the task. Unlike cue combination experiments, the compliance of the variance of the estimate with Eq. 2.14 is rarely checked, because other sources of variability, such as motor noise, confound the measurement.

Körding and Wolpert (2004a) showed in a seminal work that humans behave in qualitative agreement with the predictions of Bayesian integration in sensorimotor learning. In their task, subjects had to perform a reaching movement to a fixed target, receiving a visual cue about hand position only at a point halfway through the movement. Unbeknownst to the participants, the visual cue was displaced to the right with respect to the true hand position, with the amount of displacement drawn from a Gaussian distribution, $p_{exp}(s)$, with $\mu_{exp} = 1$ cm and $\sigma_{exp} = 0.5$ cm. Also, the visual cue was provided with different levels of added noise ($\sim$ blur). Crucially, participants received performance feedback (true movement endpoint position) only in trials with no added noise, preventing them from adjusting their endpoint with a hill-climbing strategy in the noisy conditions. Körding and Wolpert (2004a) report that subjects, after 1000 training trials, fully compensated for the average displacement in the absence of the visual cue ($\sigma_{meas} = \infty$), by pointing 1 cm to the *left* of the target. Moreover, when the cue was present, participants' corrections were in-between the displacement suggested by the cue and the mean displacement, qualitatively weighted by cue reliability. Notably, this work does not show that human observers were 'optimal' in the task, since the amount of sensory noise associated with the different levels of blur was not independently measured. Nevertheless, it was the first study to clearly show

that participants combined prior information acquired during the experiment and available sensory feedback in a statistically sensible fashion.

Tassinari et al. (2006) importantly extended the above result to a rapid pointing task in which they also measured each observer's sensory and motor noise in separate experiments. These independent estimates allowed the authors not only to test whether subjects were 'optimal' in the task, but also to identify additional sources of suboptimality in subjects' performance. The study concludes that participants reliably learnt the variance of the experimental distribution and behaved in a statistically sensible way, but they were hindered by other sources of variability (see Chapter 4).

Other studies that manipulated the experimental distribution showed that human observers sensibly adapt to changes in the mean and variance of the distribution of stimuli, namely by changing the slope and bias of their responses in the correct direction. For example, participants gave less weight to the prior mean when the experimental distribution was broader: in a force estimation task (Körding et al., 2004b), in a sensorimotor timing task (Miyazaki et al., 2005), and in a toy coin-catching task (Berniker et al., 2010). Similarly, human participants rapidly adapted their biases towards the mean of each different experimental distribution, as seen in a temporal order judgment task (Miyazaki et al., 2006), in a time interval reproduction task (Jazayeri and Shadlen, 2010; Cicchini et al., 2012), or in a distance estimation task (Petzschner and Glasauer, 2011). As per the analogous cue-integration case, when the error follows Weber-Fechner's law the 'optimal' solution does not take a linear form, Eq. 2.13, anymore, and the weight given to the sensory cue decreases with the magnitude of the stimulus (Jazayeri and Shadlen, 2010; Petzschner and Glasauer, 2011). We will explore this case more in detail in Chapter 3.

This large body of work shows overwhelming evidence that humans adapt to the low-order statistics (mean and variance) of experimental distributions of stimuli in a variety of sensorimotor estimation tasks, in broad agreement with the predictions of Bayesian integration.[11] Moreover, the simple framework provided by the standard Bayesian model is able to elegantly explain phenomena normally observed in psychophysical research, such as (a) the *central tendency* or *regression to the mean*, the fact that responses are biased towards the mean of the experimental distribution; and (b) the *range effect*, the fact that the biases depend on the width of the stimulus distribution (Petzschner, 2013). However, almost all the studies we presented up to now only trained participants either on Gaussians, or on uniform distributions that were treated as Gaussians in the analysis, leaving the open question of how humans would react to more complex distributions.

central tendency

range effect

11 We cannot be more precise because here, unlike in the cue combination field, requirements of full 'optimality' are rarely thoroughly checked, with a few notable exceptions (e. g., Tassinari et al., 2006).

Complex contextual priors

In this section we examine a few examples of how humans perform in the presence of experimental distributions that present more complex statistical features, such as non-zero higher order moments (skewness, kurtosis) and multiple modes. We focus on the complexity of the *shape* of stationary, one-dimensional distributions. Other forms of complexity, such as multiple dimensions or spatio-temporal correlations between trials are beyond the scope of this brief review.

Körding and Wolpert (2004a,c) trained participants in the reaching task described in the previous section using also a bimodal and a trimodal distribution. In order for people to learn such distributions, performance feedback was provided on every trial, all trials had no added sensory noise, and the number of trials was doubled (2000 training trials and 2000 test trials). Even so, subjects showed only qualitative learning in the case of the trimodal distribution (Körding and Wolpert, 2004c). Subjects' biases were consistent with the learning of the bimodal distribution, although individual performance showed a large amount of variability (Körding and Wolpert, 2004a).

Chalk et al. (2010) investigated whether human observers can implicitly learn a bimodal distribution of motion directions. Motion stimuli were tested at different levels of contrast (corresponding to different amounts of sensory noise), with one of the levels being near-threshold. After the estimation, participants also had to report whether a stimulus was present in the trial (detection task); occasionally a trial had no moving stimuli. Chalk and colleagues found that participants' responses were biased, on average, towards the most presented directions of motion, in a way consistent with Bayesian integration; a model comparison rejected other possible strategies that did not combine a prior with noisy sensory stimuli. Moreover, participants occasionally 'hallucinated' stimulus motion in the trials with no stimuli, reporting a false positive in the detection task. Interestingly, the distribution of responses, conditioned on a false positive detection, qualitatively reproduced the experimental distribution, suggesting that participants were 'hallucinating' from the prior. The authors fit the estimation data with a Bayesian observer model equipped with a parametric prior, finding a qualitative match between the parameters of the reconstructed priors and the experimental distribution. This study presents evidence that human observers can approximately learn bimodal distribution relatively quickly (the entire experiment lasted 1700 trials, but biases emerged already "within few minutes of task-performance"; Chalk et al., 2010).

More recently, Gekas et al. (2013) used a variant of the above-described motion estimation task to test whether participants could learn two experimental distributions at once, with distinct distributions implicitly identified by different stimulus colours. The distributions were uniform and bimodal in one experiment, bimodal

and trimodal in another. The findings were mixed: observers learnt an aggregate distribution in the former case (ignoring colour), and developed distinct biases in the latter, but hardly learnt the true underlying distributions. Interestingly, a similar question was addressed in a distance production-reproduction experiment that exposed participants to two distinct experimental distributions, identified by arbitrary symbolic cues (Petzschner et al., 2012). This study found that participants could learn the two distinct distributions. A major difference between the two studies is the fact that Petzschner and colleagues used uniform distributions with different means, as opposed to complex multimodal distributions.[12]

These studies provide preliminary evidence that participants are affected by higher-order statistical features of the context, but whether human observers develop Bayes-sensible biases, and the speed of this process, seems to change wildly across experiments and individuals, without an obvious pattern. Clearly, it could always be the case that participants did not experience enough trials to learn such complex features. To understand the complexity of prior expectations, we examine, in the following section, the shape of structural priors, that possibly had a lifetime to develop.

2.3.3 *Structural priors*

It has been proposed that several systematic biases of human perception and action, including a number of different illusions, can be explained as a process of probabilistic inference, whereby noisy sensory information is combined with an ecological prior that is 'optimally' adapted to the statistics of the environment (see Geisler and Kersten, 2002; Feldman, 2013 for a critical analysis). Contrarily to the case of contextual priors, which can be more or less directly manipulated via the statistics of stimuli in the experiment, structural priors are not under the direct control of the experimenter. To solve this issue, researchers adopt one or more of the following techniques when choosing how to model structural priors: (a) priors are postulated, possibly in a parametric form with a few free parameters that are fit from the data; (b) priors are expressed in some semi-parametric or non-parametric form and (almost) entirely recovered from the data; (c) priors are reconstructed by the statistics of the environment. Method (c) is the approach with the strongest predictive appeal, as (a) and (b) alone may feel somewhat circular and 'post hoc' (Bowers and Davis, 2012; Marcus and Davis, 2013). However, in many cases measuring the natural statistics of

12 Another relevant factor is that the cue distinguishing the two distributions was explicit (a text specifying 'short' or 'long') for Petzschner et al. (2012) and only implicit (stimulus colour) in Gekas et al. (2013). In particular, even though humans have been shown to implicitly learn arbitrary correlations between cues after extensive training (Ernst, 2007), there is evidence that colour may be a 'bad' cue for categorization (Gorea and Sagi, 2000; Seydell et al., 2010; Howard et al., 2013), except when related to stimuli that are naturally associated with colour, such as light sources (Kerrigan and Adams, 2013).

stimuli represents a major technical challenge. In such situations, methods (a) and (b) can still provide useful insights, especially if they are able to predict a novel illusion or unify several unexplained phenomena (Colombo and Hartmann, 2014).

As a 'textbook' example, Girshick et al. (2011) measured the statistics of orientations of line segments from a large database of natural images and had human participants perform an orientation discrimination experiment. A Bayesian observer model that incorporated a non-parametric prior was fit to the individual psychophysical data, finding that the shape of each subject's prior qualitatively matched the natural statistics of orientations. In the rest of this section we will examine in detail a well-known case study that has prompted the development of several modelling techniques.

A case study: the slow-speed prior in motion perception

slow-speed prior

A paradigmatic example of structural prior is provided by the *slow-speed prior*, which has been proposed as a unifying explanation for a variety of visual illusions in motion perception (Weiss et al., 2002; see Geisler and Kersten, 2002; Seriès and Seitz, 2013 for a commentary). Weiss and colleagues built an observer model with a Gaussian likelihood (based on a simple model of pixel intensity noise) and a Gaussian prior on speed centered on zero. The specific shape of the prior was chosen for mathematical convenience, but the model was, nonetheless, able to qualitatively explain a wide range of classical effects in motion perception (Weiss et al., 2002). The model has been subsequently improved with a more realistic, nonlinear dependence of the likelihood on contrast (Hürlimann et al., 2002). Interestingly, a Gaussian prior for slow speeds has been recently proposed to explain also several tactile illusions, such as length contraction and the 'cutaneous rabbit' (Goldreich, 2007; Goldreich and Tong, 2013).

Further support for the slow-speed prior in visual motion perception was given by Stocker and Simoncelli (2006b), who non-parametrically inferred the shape of the speed prior (and the sensory noise) from psychophysical data. The likelihood, assumed to be equal to the objective noise distribution, was Gaussian with noise that depended separately on speed and contrast. The noise dependence on speed was accounted for via a transformed sensory mapping in logarithmic space (see Section 2.2.1) while the dependence on contrast was given a neurally-inspired functional form. Through some approximations, the authors derived an expression for the expected bias and slope of a psychometric curve of speed discrimination, as a function of reference stimulus speed and various model parameters, including the profile of the prior and of the sensory noise. The model fit showed that participants consistently had prior expectations for slow speeds, which were heavier-tailed (i.e. changing more slowly and eliciting milder biases) than a standard Gaussian, approximately follow-

ing a power law (Stocker and Simoncelli, 2005, 2006b). This work provides further evidence for the slow-speed prior by showing that observers' behaviour is consistent with such an hypothesis, even when, save smoothness, no specific assumption for the shape of the prior is made a priori. Moreover, it provides a framework in which further quantitative questions can be asked. For example, Hedges et al. (2011) augmented the observer model with a structural inference component to explain the perceptual coherence of superimposed moving gratings. Another study combined the model of Stocker and Simoncelli (2006b) with an existing 'ratio model' of speed perception in order to account for some complex dependency of perceived speed on the contrast and temporal frequency of the stimuli (Sotiropoulos et al., 2014).

Another take on the slow-speed prior is given by Zhang et al. (2013b). Zhang and colleagues argued that a prior for slow-speeds would only hold for stimuli near the fovea, whereas the periphery of the visual field is exposed to faster motions which are expected to be biased towards centrifugal directions (i.e., away from the fovea). Participants performed in a direction of motion discrimination task with stimuli presented at the periphery of vision; the amount of sensory noise was varied by manipulating stimulus duration (as opposed to the manipulation of contrast in the previous studies). Additionally, sensory noise in each experimental condition was assessed via a separate experiment. Observers' data agreed with the hypothesis, showing, for example, that uncertain stimuli in the periphery of vision, albeit physically stationary, were perceived in centrifugal motion. The priors non-parametrically reconstructed from individual datasets showed that almost all probability mass was given to centrifugal speeds, with a small bump to centripetal speeds (possibly an artifact).

Contextual changes to structural priors

Recent work has shown that structural priors can be over-ridden by the context, suggesting that the distinction between structural and contextual priors is somewhat arbitrary (Seriès and Seitz, 2013). For example, humans have a natural expectation that light comes from above (precisely, from above-left), which has been found to bias shape perception, quick visual search, and reflectance judgments (Mamassian and Goutcher, 2001; Mamassian and Landy, 2001; Adams, 2007; Stone et al., 2009). However, Adams et al. (2004) showed that human observers, unlike chickens (Hershberger, 1970), can easily learn a new direction for a light source, transferring this implicit knowledge to another laboratory task. Moreover, it has been shown that human observers can learn multiple priors associated with different light colours (Kerrigan and Adams, 2013). Morgenstern et al. (2011) observed that the light prior is also easily over-ridden by other sensory cues. Through a simple Bayesian observer model they inferred the ratio between the weight given to the prior and the weight given

to lightning cues of different strength, finding that the prior accounts for very weak lightning information. Even the slow-speed prior is susceptible to change: after exposure to fast-moving gratings over the course of multiple sessions, people gradually changed their expectations about motion speed, which manifested in a differently biased perception of ambiguously moving stimuli (Sotiropoulos et al., 2011).

The difference between structural and contextual priors can be understood by considering the open problem of how observers choose what prior to adopt in a given context, which can be formalized within the framework of model selection (the *competitive priors* of Yuille and Bülthoff, 1996) and hierarchical Bayesian inference (Lloyd and Leslie, 2013). A structural prior can be modelled as an 'a priori' prior, a weak prior compatible with a large variety of contexts, but that is easily over-ridden in the presence of cues that suggest the usage of more specific priors.

competitive priors

2.3.4 *Inferring individual priors*

As we have seen in the previous sections, we often do not know the empirical distribution of stimuli (for structural priors) and even when we know it because it is imposed experimentally (for contextual priors), we cannot be sure that observers have learnt it fully. Nonetheless, assuming that human observers approximately behave as Bayesian observers, we can reverse-engineer the decision-making model and infer the priors compatible with subjects' behaviour from individual datasets – with all the caveats about model non-identifiability that we have discussed previously (see Section 1.2.3). In a Bayesian observer model, the prior $q_{prior}(s)$ is represented either in a parametric form or in a so-called non-parametric (or semi-parametric) form; in this context, 'non-parametric' usually means that there are so many parameters (e.g., dozens) that the prior can assume any reasonable shape.[13] This is both an advantage and a drawback of the non-parametric approach, since the expressive power comes at the risk of overfitting the data.

Common parametric models include, obviously, the Gaussian distribution (e.g, Berniker et al., 2010; Sotiropoulos et al., 2011; Petzschner and Glasauer, 2011; Cicchini et al., 2012) and the Von Mises distributions (the equivalent of Gaussian distributions for circular statistics; see e.g. Morgenstern et al., 2011), and mixtures of a few Gaussian (Huszár et al., 2010; Houlsby et al., 2013) or Von Mises distributions (Mamassian and Landy, 2001; Chalk et al., 2010; Gekas et al., 2013).[14] Other parametric forms are

13 This is not exactly the meaning of non-parametric in Bayesian statistics, which implies a model whose complexity (number of effective parameters) also adapts to the data (Gershman and Blei, 2012; Gelman et al., 2013).

14 Note that a mixture of three or more Gaussian (or Von Mises) distributions could be already considered a non-parametric prior, since it can approximate a large number of target distributions.

usually inspired by results from a non-parametric approach, such as a power-law for the slow-speed prior (Hedges et al., 2011) or a skewed Gaussian for the centrifugal prior (Zhang et al., 2013b).

Non-parametric priors are typically inferred from the data via two types of techniques. The first class of methods directly computes the values of the (log) prior from the data by exploiting some specific assumption. For example, Körding and Wolpert (2004a) assume that that the mean of the posterior coincides with the true stimulus (which is true only on average); Stocker and Simoncelli (2006b) and Sotiropoulos et al. (2014) additionally assume that likelihood width is narrow so that the log prior can be linearized around the measurement; and Paninski (2006) proposes to extract the prior from the constraints imposed by the data via dynamic programming, where degeneracies are solved via a chosen regularizer (essentially, an hyperprior on smoothness). In the second family of methods, priors are modelled by specifying the value of the (log) prior over a pre-defined grid, each value of the prior being a free parameter of the model (Stone et al., 2009; Girshick et al., 2011; Zhang et al., 2013b). If the grid is coarse, values of the prior at intermediate grid points may be obtained via interpolation, such as with splines (Girshick et al., 2011) or Gaussian processes (Zhang et al., 2013b).

With a few exceptions, such as Zhang et al. (2013b), where the full posterior probability of the parameters is computed, the priors are typically recovered by maximizing the likelihood of the data under the model. Likelihood maximization is at risk of overfitting, especially for non-parametric priors; this risk is partially alleviated by including additional constraints in the inference (such as smoothness, see Stone et al., 2009).

2.3.5 *In this thesis*

In this thesis, prior expectations, understood as internal representations of experimental distributions, play a key role. The main unknowns under study are the flexibility and accuracy of such priors beyond the Gaussian case.

- ▷ In Chapter 3 we will explore the complexity of internal representations of experimental statistics of stimuli in the domain of sensorimotor timing. To go beyond the Gaussian case, we will train observers on different types of distributions: uniform, skewed, and bimodal, for which human performance is still not understood, as we have seen in Section 2.3.2. For computational reasons, we will first model individual priors in a fixed parametric form; once we have identified the best model components describing an observer, we will subsequently non-parametrically infer the shape of his or her prior, extending methodologies

briefly mentioned in Section 2.3.4. The non-parametric form will allow us to compare properties of the inferred priors and of the experimental distribution, including higher-order moments.

- In Chapter 4 we will work towards understanding the source of the difficulty humans have in performing probabilistic inference with complex distributions, as seen in Section 2.3.2. Specifically, we will have subjects perform inference with visually displayed 'priors' belonging to different classes of distributions (Gaussian, unimodal, bimodal). We will test observer models that incorporate several different approximations and even a noisy estimate of these 'priors'. Finally, we will also non-parametrically reconstruct the group prior corresponding to each experimental distribution, as a means of characterizing systematic biases in how priors are subjectively treated in the task.
- In Chapter 5 we exploit complex prior expectations as a tool to modulate target uncertainty, in order to reveal unexpected biases in subjects' performance. Namely, we construct a trimodal distribution of endpoint positions whose central mode is 'easy' to target (low uncertainty, due to a delta function) and the side modes are 'hard' (high uncertainty, due to broader distributions), looking for a difference in behaviour.

2.4 LOSS FUNCTIONS AND MOTOR ERROR DISTRIBUTIONS

Priors and likelihoods, examined in the previous sections, combine in the inference process to yield the posterior distribution. A decision rule is, then, needed to specify how the observer chooses a course of action, ideally to minimize his or her average losses (see Section 1.2.2). In this section we review how the explicit and implicit structure of rewards of the task, reflected in the loss function and in the internal representation of motor errors, affects sensorimotor decision making. For the sake of simplicity, we will often use the term 'observer' in place of the more correct but cumbersome 'observer and actor'.

2.4.1 *Loss functions in sensorimotor estimation*

In a sensorimotor estimation task, the reward or loss associated with a decision depends on the cost or loss (negative utility) entailed by the outcome of the decision, encoded by the loss function, and on the probability of the outcomes associated with each decision, represented by the motor error distribution. In the case of purely perceptual tasks, the outcome (motor) variability is often neglected.

Loss functions share some common conceptual properties with priors, even if they are different mathematical objects. First, we can adapt the classification used for priors (see Section 2.3) and loosely divide loss functions into *contextual*, which depend on the task at hand, such as the scores on different regions of a dartboard or monetary prizes associated with correct perceptual classifications, and *structural*, which depend on previous experience and general properties of the sensorimotor systems. Second, loss functions are *subjective* constructs, even more so than priors. For example, in many cases there is no clear objective counterpart for the loss function, and even when a quantitative goal of a sensorimotor task can be identified, it can be argued that the way in which different rewards are subjectively weighted (the negative utility of each outcome) is unknown.[15]

Similarly to what we have seen with prior expectations, an experimenter can either impose a loss function on the task, by providing explicit feedback on losses and rewards (also called *knowledge of results*) or leave it underconstrained, in which case the observer will use whatever loss he or she deems appropriate given the generic task goals. Leaving the loss function experimentally undefined may seem unwise, but there are many situations in which knowledge of results needs to be withheld in order to avoid spurious influences on participants' behaviour. For example, a study of structural priors typically does not provide performance feedback, otherwise participants could start to adapt to the experimental distribution of stimuli. In many sensorimotor estimation tasks, the lack of an explicit loss function is somewhat mitigated by the following facts:

knowledge of results

- In a purely perceptual task (no motor error), if the posterior is Gaussian (e.g., due to a Gaussian prior combined with a Gaussian likelihood), the optimal estimate corresponds to the mean of the posterior for any symmetric, veridical loss function.
- In a sensorimotor task, if the posterior *and* the motor error distribution are Gaussian, the optimal estimate corresponds to the mean of the posterior for the inverted Gaussian loss, the quadratic loss and the delta loss (the last two being limiting cases of the first).

These results show that, under common assumptions, optimal behaviour in a sensorimotor estimation task does not depend heavily on the details of the loss function. On the other hand, when these assumptions fail (e.g., the posterior is strongly skewed or bimodal, or the loss function is not symmetric), determining the shape of the loss function becomes relevant.

15 This arbitrariness led Jaynes, a strong supporter of the Bayesian approach, to state that "from a fundamental standpoint loss functions are less firmly grounded than prior probabilities" (Jaynes, 2003, Chapter 13).

2.4.2 *Contextual loss functions*

decision making under risk

Decision making in the presence of a well-defined loss function and knowledge of the underlying probabilities is called *decision making under risk*. A large body of work has investigated whether human observers are able to 'optimally' integrate knowledge of their sensorimotor uncertainty with an externally imposed (contextual) loss function so as to maximize gains or, equivalently, minimize losses. Humans suffer from well-known non-normative biases in cognitive decision making under risk (Kahneman and Tversky, 1979), but, as we have seen in the previous sections, sensorimotor decisions may elicit behaviours that are surprisingly close to statistical optimality (although these, as usual, depend on how we define and test for optimality; Jarvstad et al., 2014). In this section we will briefly review several studies of motor planning and perceptual decision making in the presence of an external loss function.

Motor planning under risk

experimental loss function

The typical experimental layout for looking at motor planning under risk imposes an arbitrary reward/penalty structure – the *experimental loss function*, $\mathcal{L}_{exp}(\boldsymbol{r}, \boldsymbol{s})$ – onto the response space (see Trommershäuser et al., 2008a,b for a review). The reward/penalty configuration is usually explicitly shown to the observer in each trial, and may change from trial to trial or in different blocks. The ideal observer should choose the optimal action (e.g., aiming point) by taking into account the motor variability of the subsequent movement, in order to maximize the chance of a high-scoring response. In terms of losses, the equation for the subjectively optimal action is:

$$\boldsymbol{s}^*(\boldsymbol{x}; \mathcal{L}) = \arg\min_{\hat{\boldsymbol{s}}} \int q_{motor}(\boldsymbol{r}|\hat{\boldsymbol{s}})\, \mathcal{L}(\boldsymbol{r}, \boldsymbol{s})\, d\boldsymbol{r}, \tag{2.15}$$

which is Eq. 2.3 without priors and sensory noise. As usual, Eq. 2.15 is objectively 'optimal' if the internal elements of decision making match their objective counterparts, that is $q_{motor}(\boldsymbol{r}|\hat{\boldsymbol{s}}) \equiv p_{motor}(\boldsymbol{r}|\hat{\boldsymbol{s}})$ and $\mathcal{L}(\boldsymbol{r}, \boldsymbol{s}) \equiv \mathcal{L}_{exp}(\boldsymbol{r}, \boldsymbol{s})$. Formally, since there are no priors involved, the framework Eq. 2.15 belongs to is statistical decision theory (SDT) rather than BDT, but it is merely a matter of naming conventions.

In a seminal work, Trommershäuser et al. (2003a) analyzed the performance of human observers in a rapid pointing task. The target was a green circle on a screen (worth 100 points), which was adjacent to or partially overlapped by one or two red 'penalty' circles (worth 0, -100 or -500 points). The subjects' motor error distribution was separately measured, allowing the computation of the optimal aiming point for each observer in each configuration, according to SDT. The study found

that the observers' average endpoint was close to the 'optimal' position in a first experiment (only one penalty circle), whereas it was mostly suboptimal in a second experiment (with two penalty circles). However, the authors argue that the suboptimality was likely due to a small rightward response bias and not (entirely) to errors in motor planning. Interestingly, after training on practice configurations, participants were able to immediately adapt to new configurations, showing no trace of feedback-driven learning after each trial ('hill-climbing'), nor changes in their motor variability. Trommershäuser et al. (2003a,b) provided a flexible experimental framework to investigate the applicability of SDT to human sensorimotor decision-making, spawning a series of follow-up studies.

One line of work examined how humans adapt to changes in the probabilities involved in the task, and in the way in which probabilistic information is conveyed (see Trommershäuser, 2009a for a review). Trommershäuser et al. (2005), unbeknownst to the participants, added different amounts of noise to the movement endpoint position (and to its visual feedback), effectively altering the subjects' motor variability in the task. The study found that participants adjusted to the increased variability, shifting the aiming point in accordance to the task-relevant noise in a near-optimal way. Maloney et al. (2007) introduced stochasticity in the loss function by including targets that had 50% chance of rewarding zero points instead of the usual reward or penalty. Participants were explicitly informed of this element and, as it is usual with numerically provided probabilistic information (Kahneman and Tversky, 1979), their performance fell remarkably short of optimal. Conversely, Seydell et al. (2008), using a slightly different one-dimensional layout, introduced stochasticity in the loss function by having the penalty regions ('defenders') randomly jump to a nearby position after movement completion. An ideal observer had to take into account the statistics of the jumps in addition to his or her own motor uncertainty. Participants trained on the task for several sessions, reaching a good performance level in both symmetric and asymmetric conditions, with occasional suboptimal choices. Importantly, in a second experiment participants rapidly adjusted their pointing behaviour when the losses associated with each 'defender' were explictly switched after five sessions of training, suggesting that they had learnt an internal representation of the task and not a mere stimulus-action contingency. A recent work directly compared cognitive ('economic') decision-making with an equivalent motor decision-making task, by seeing how observers selected between alternative choices with different probabilities and rewards (*lotteries*) in the two cases (Wu et al., 2009). Results were similar across tasks, but participants were generally risk-seeking in the motor task and risk-averse in the economic task, an effect that was explained by a different weighting of probabilities in the two conditions (whose reason is unclear).

lotteries

Other studies investigated the limits humans may have in performing optimal computations of expected gain. Wu et al. (2006) tested participants on more complex, asymmetrical configurations, finding that participants were moderately suboptimal with these. The authors argue that previously found optimality was likely due to the fact that participants exploited symmetries in the configurations to simplify the computation of optimal behaviour. In another study, Trommershäuser et al. (2006b) used simple configurations but delayed the onset of the penalty circle, finding that participants achieved a reasonably good performance as long as the full reward/penalty region was available near the time of movement onset, suggesting that humans can quickly perform computations of optimal behaviour (at least in simple cases). In line with this finding, Trommershäuser et al. (2006a) showed that humans, given a choice between two different configurations, can rapidly point to the one which would yield a higher expected gain (with some decision noise). Finally, note that the label of 'optimality' is not very robust as it depends on the statistical methods used to assess it. A recent study in motor planning demonstrates that small changes in experimental layout can have major effects on the statistical attribution of 'optimality' (Jarvstad et al., 2014).

Perceptual decision making under risk

Arguably, the motor system has to adapt to ever-changing task demands, which may explain why an arbitrary reward/loss structure can be so easily integrated during action. It is unclear if perception would afford the same amount of flexibility.

Some studies suggest that perceptual decision-making under risk is similar to motor planning under risk. For example, Landy et al. (2007) asked observers to estimate the mean orientation of a large number of line segments whose individual orientations were randomly drawn from a Von Mises distribution with a given trial-dependent (or block-dependent) concentration parameter ($\sim$ inverse variance). For small variance, all bars were oriented roughly in the same direction and uncertainty was low; for high variance, the bars were scattered in several directions and the difficulty in averaging them resulted in high uncertainty. Observers had to place a 'net', which contained both a reward and a penalty region, to enclose the estimated mean direction. The study found that participants were quite sensible (if not optimal) in positioning the net when different levels of sensory noise were presented in separate blocks. Performance level dropped when different levels of noise were interleaved in the same block, and became generally suboptimal, with a large intersubject variability, when noise was changing continuously from trial to trial. Another study found near-optimal behaviour in an 'offset' discrimination task with an asymmetric payoff matrix (Whiteley and Sahani, 2008). Crucially, participants only received blocked per-

formance feedback, preventing a 'hill-climbing' strategy, suggesting that observers were integrating their internal representations of sensory uncertainty and reward (however, the study did not perform a stronger test with multiple levels of noise).

A limitation that is unique to perception is that sensory estimates are performed continuously – within a relatively short time window, we always perceive a unique state of the world. Ideally, decision making under risk in an observer and actor model should take into account both the full perceptual posterior, the loss function and the motor error distribution (Eq. 2.3). However, the perceptual posterior may be relatively short-lived, occasionally 'collapsing' into a single percept after a perceptual estimate has been implicitly or explicitly performed. This phenomenon has been hypothesized by Stocker and Simoncelli (2008) to explain observed biases in a motion discrimination and estimation task, and a similar effect of categorical perception that leads to suboptimal behaviour was recently reported by Fleming et al. (2013).

2.4.3 *Structural loss functions*

Structural loss functions can be thought as 'natural' costs associated with certain generic endeavours. From the point of view of the modeller, structural loss function, similarly to structural priors, are: (a) postulated from first principles, (b) chosen for mathematical convenience, or (c) inferred from the data given a parametric or non-parametric form. For example, the field of motor control has been characterized by several attempts at defining a structural loss function of (arm) movement, such as integrated squared jerk (Hogan, 1984), integrated squared torque change (Uno et al., 1989), endpoint variance under signal-dependent noise (Harris and Wolpert, 1998), or other forms of biomechanical constraints (see Trommershäuser et al., 2008b). In general, the aim of these efforts is not necessarily to find the 'true' loss function, which, if it exists at all, may have a very complex shape, but rather to find a simple approximation that is able to account for a large amount of human data in a variety of domains.

Studies in perception have traditionally assumed simple structural loss functions that correspond to basic statistical features of the posterior distribution of the stimulus, such as the mode of the posterior (zero-one loss) or the mean (quadratic loss); see Section 1.2.2 and Yuille and Bülthoff (1996). Note that, as we remarked before, the detailed shape of a loss function is relevant only when the posterior is non-Gaussian. For example, an inverted Gaussian loss has been used within a model of bistable perception which would join modes in the posterior if they were near enough, but preserve them when they were far away (van Ee et al., 2003). More complex structural

loss functions are found in *continuous* perceptual decision-making (Drugowitsch et al., 2012).

The typical structural loss function of sensorimotor tasks is assumed to be quadratic in endpoint error (Harris and Wolpert, 1998). However, Körding and Wolpert (2004b) had human participants aim at a target with a virtual pea-shooter whose distribution of shots was asymmetric and bimodal, with variable separation between peaks. By looking at how subjects placed the pea-shooter with respect to the target, the authors could infer the subjective loss associated with each error. The non-parametrically reconstructed loss function was quadratic for small errors and nearly-linear for larger errors. Parametrically, this corresponded to either a power-law with power less than two (~ 1.7) or an inverted Gaussian loss, suggesting that human sensorimotor behaviour is better described by a robust, sub-quadratic loss function.

effort

Besides task demands (e.g., hitting the target), another important structural component of the loss function is represented by *effort*, which generally represents energy consumption and other psychophysical resources (Todorov and Jordan, 2002). Körding et al. (2004a) borrows from economics a general technique to infer loss functions by estimating the observers' indifference curves, i.e. actions that are assumed to be equally (un)desirable. There, the method is applied to infer the cost associated with producing a force of a certain intensity for a given time, finding a non-trivial interaction between force and duration, that is, nonetheless, quite consistent between subjects. O'Sullivan et al. (2009) explicitly measured the weight of effort (produced force) in the loss function against the weight of task error in a force production experiment that allowed to disambiguate between the two components. Interestingly, the effort term was found to be approximately seven times more important than the variability term, suggesting that effort may still significantly affect behaviour in task-oriented movements.

2.4.4 *Motor error distribution*

In the standard Bayesian model, motor error distributions represent variability in enacting the movement due to neuromuscular noise (van Beers et al., 2004) and noise in motor preparation (Churchland et al., 2006). Abstract motor planning (e. g., which target to hit) is assumed to be noiseless in BDT and corresponds to Eq. 2.3 (but see Section 2.4.5). Sensory noise in motor planning, which in some cases may have a primary role in determining motor variation (Osborne et al., 2005), is here either negligible or explicitly modelled through the sensory measurement distribution (Section 2.2.1).

The shape of the distribution of motor errors typically depends on the movement trajectory and details of the motor plan (Todorov, 2004), but in most sensorimotor estimation task it can be well approximated with a Gaussian:

$$p_{motor}\left(\boldsymbol{r}\,|\hat{\boldsymbol{s}}\right) = \mathcal{N}\left(\boldsymbol{r}\,|\hat{\boldsymbol{s}}, \boldsymbol{\Sigma}_{motor}(\hat{\boldsymbol{s}})\right), \tag{2.16}$$

where $\boldsymbol{\Sigma}_{motor}(\hat{\boldsymbol{s}})$ is the *motor error covariance matrix*, which generally depends on the value of the estimate (e.g., the estimated target position). In the simplest case, the noise is constant and either one-dimensional or isotropic (the covariance matrix is diagonal), with variance σ^2_{motor}. Isotropic noise is found, for example, in many pointing tasks whose target plane is approximately at a constant distance from the observer (e.g., Trommershäuser et al., 2003a,b; Tassinari et al., 2006). Note, however, that the covariance matrix may have a complex, anisotropic dependence on position (e.g., van Beers et al., 2004; Gepshtein et al., 2007). For one-dimensional tasks, another common form of motor variability is proportional to the estimate, $\sigma_{motor}(\hat{s}) \propto \hat{s}$, due to signal-dependent noise (Harris and Wolpert, 1998) or to scalar noise in motor timing (Gibbon, 1977). An interesting hypothesis is that the magnitude of motor noise in different movements is influenced by the statistics of natural movements (Howard et al., 2009a).

motor error covariance matrix

Internal representations of motor uncertainty

Just as we did for the sensory measurement distributions in Section 2.2.2, we can ask whether human observers have an accurate internal representation, $q_{motor}\left(\boldsymbol{r}\,|\hat{\boldsymbol{s}}\right)$, of their own motor variability. Assuming a Gaussian representation for the internal motor variability, as per Eq. 2.16 but with subjective motor covariance $\tilde{\boldsymbol{\Sigma}}_{motor}(\hat{\boldsymbol{s}})$, the question is: $\tilde{\boldsymbol{\Sigma}}_{motor}(\hat{\boldsymbol{s}}) \stackrel{?}{=} \boldsymbol{\Sigma}_{motor}(\hat{\boldsymbol{s}})$. A sufficient condition for testing this equality is the verification of the observer's near-optimal behaviour, according to SDT, in a sensorimotor task whose expected gain crucially depends on the observer's estimate of his or her motor uncertainty.[16] We have seen from previous work that human observers near-optimally represent simple spatial motor noise distributions (constant, isotropic Gaussians, see e. g. Trommershäuser et al., 2003a) and quickly update their internal representations of such noise given visual feedback (Trommershäuser et al., 2005). Here we report a few examples from other domains (i.e., time), with more complex shapes of motor noise or with different types of tasks.

16 This is a *sufficient* condition because, even if we observe suboptimal performance, it could still be that the observer has a correct internal representation of his or her motor variability, but does not correctly represent or integrate other features of the task. Also, note that it is sufficient modulo issues of non-degeneracy.

Gepshtein et al. (2007) tested whether human observers know the covariance of their endpoint variability in a reaching task that required them to rapidly aim at targets placed on a touch screen at various distances and directions from a central starting point. By placing penalty regions at various positions around the target, the authors could test whether subjects took into account the full two-dimensional shape of their motor errors, which depended on target position (endpoint distributions were elongated in movement direction, and larger for larger movements). Participants sensibly accounted for the anisotropy of their noise distributions, and most of them performed near-optimally, suggesting that human observers had a rather precise representation of their own motor uncertainty. Hudson et al. (2010) investigated observers' capability to adapt their internal representation of motor uncertainty to added anisotropic noise. Subjects' reaching movements were randomly perturbed in the horizontal direction, leaving the vertical direction unaffected. Participants, instead, adjusted their pointing behaviour almost perfectly as if the added noise was equal in all directions, suggesting that observers were adopting an isotropic internal model of motor uncertainty. Recently, Zhang et al. (2013a) studied human observers' knowledge of their own motor uncertainty. In the first part of the experiment, observers were as usual required to reach to target/penalty configurations; in the second part, they were asked to choose which one of two configurations would yield a higher average gain, given their movement precision. Their choice preferences showed that participants ignored anisotropy of their motor errors, and only half of the subjects had an accurate internal model of the amount of motor noise.

In the temporal domain, Mamassian (2008) reported that participants consistently performed suboptimally in a time reproduction task with a fixed target duration (500 ms), in which penalties were assigned for either undershoots or overshoots, depending on the condition. Observers shifted their timing reponses away from the penalty regions, but not as much as they should have, according to their timing variability. Also, contrarily to the spatial case (Trommershäuser et al., 2005), participants did not change their response strategies at all when additional Gaussian noise ($\sigma_{extra} = 50$ ms) was injected to their responses. Mamassian (2008) summarizes this behaviour as 'overconfident' since participants behaved as if they underestimated the amount of their motor noise, or the amount of their losses. On the other hand, in the same year, Hudson et al. (2008) reported that participants performed near-optimally in a temporal production task with a similar structure (temporal target at 650 ms, penalty regions before or after the target, added Gaussian noise with $\sigma_{extra} = 25$ ms). However, we note that the alleged near-optimality may be due to a constrained form of analysis, i.e. the authors performed a model comparison in which the 'optimal' observer model fit the data significantly better, in terms of marginal likelihood, than a

few suboptimal models, but it is not clear how close the participants' internal representations of motor uncertainty were to their true noise.[17]

Finally, an alternative way to test subjects' internal representations of motor uncertainty that does not involve arbitrary loss functions is represented by paradigms that introduce a trade-off between sensory uncertainty and motor uncertainty. In these tasks, participants need to perform a motor act (e.g., hit a target, catch a virtual ball) designed so that motor variability increases over time (because less time is available to plan and perform the movement) and, conversely, sensory variability decreases over time (because more sensory information becomes available). The ideal observer needs to choose the optimal movement time by accounting for the temporal profile of both sensory and motor uncertainty so that the probability of hitting the target is maximized. Several studies show that people have a sensible internal representation of their sensory and motor uncertainty over time (e.g., Battaglia and Schrater, 2007; Faisal and Wolpert, 2009).

In conclusion, there is evidence that human observers build and update internal representations of their own motor uncertainty and adjust their behaviour accordingly in a Bayes-sensible way, although such representations may systematically deviate from the true noise distributions in important aspects (e.g., underestimation of the magnitude of noise, lack of anisotropy).

2.4.5 *Decision noise*

Decision making in the standard observer model, according to Bayesian or statistical decision theory, is *deterministic*: the decision, be it an estimate or a planned action, is a fixed function of the available information (Eqs. 2.3, 2.4 and 2.15). Noise is either 'upstream' sensory noise (before the decision), modelled by $p_{meas}(\boldsymbol{x}|\boldsymbol{s})$, or 'downstream' motor noise (after the decision), represented by $p_{motor}(\boldsymbol{r}|\hat{\boldsymbol{s}})$; see Figure 2.1a. This situation is rather unrealistic, as it presumes that the observer is able to flawlessly choose the course of action that minimizes the expected loss without *decision noise*. Note that the expression 'decision noise' in the literature loosely refers to any form of added noise (e.g., Weiss et al., 2002; Knill and Saunders, 2003; Hillis et al., 2004). Here by decision noise we mean stochasticity that emerges during the decision-making process, specifically during the computation and minimization of the expected loss (Paninski,

decision noise

17 Model comparison rejected a pair of observer models in which the parameters of the internal representation of motor uncertainty (constant noise and Weber's fraction) were free to vary, but the validity of this result is somewhat unclear given that improper priors with unknown bounds were used for the model parameters, a choice that may have catastrophic effects on model comparison (Gelman et al., 2013). The suspicion that the free-parameter models may have been exceedingly penalized by the usage of improper priors is supported by the fact that the reported model evidence is strikingly lower than that of any other suboptimal model in Hudson et al. (2008).

2006; Trommershäuser et al., 2006a; Stone et al., 2009). Therefore, we expect the decision noise to be a function of the elements of decision making, and, in particular, to depend on the posterior distribution.

For example, a realistic assumption that has received relatively little attention in models of sensorimotor decision making is that the observer's evaluation of the expected loss is likely to be noisy. Direct signatures of variability in estimation of the expected loss have been found in motor planning tasks in which the observer had to quickly choose the most rewarding target between two presented configurations (Trommershäuser et al., 2006a; Jarvstad et al., 2014). This form of noise would predict stochastic deviations from optimal behaviour when the difference in expected loss between alternative choices is small, and near-optimal behaviour for large differences in expected loss. Instead, various other stochastic heuristics have been used to model choice variability.

Probability matching and sampling

probability matching

A stochastic decision rule that has been used sometimes in perception consists of *probability matching*, whereby a random estimate is drawn from the posterior distribution. Probability matching is a well-known phenomenon in psychology, according to which observers, asked to predict the outcome of a binary event, answer randomly and proportionally to the frequencies of the outcomes, instead of taking the optimal strategy of choosing the most probable outcome (see Vulkan, 2000 for a review). Probability matching, as well as any stochastic decision rule, is suboptimal for how task goals are defined in our framework, but there are settings in which it might be a convenient strategy, such as foraging and some competitive games. For example, recent work has suggested that probability matching may be a strategy of looking for patterns (Gaissmaier and Schooler, 2008), and that it may be due to internal beliefs about the generative model of the task (Green et al., 2010).

posterior-matching

In perception, probability matching on the posterior, or simply *posterior-matching*, has been used to model observers' choices in multistable perception, such as that of convex/concave line drawings (Mamassian and Landy, 1998) or of bulging/indented ridges (Mamassian and Landy, 2001). Mamassian and Landy (1998) call it a 'non-committing' decision rule and argue that, in the absence of an obvious goal, "it is not inappropriate for the observers' judgement to reflect the computed posterior probability". Probability matching has also been used to model observers' behaviour in causal inference of multisensory perception (Wozny et al., 2010) and in an auditory categorization task (Gifford et al., 2014). A more general hypothesis is that the brain approximates the posterior distribution by drawing a number κ of samples from it (Fiser et al., 2010) – posterior-matching is simply the case for $\kappa = 1$. In perception,

sampling models of decision making have been used in multistable perception (Sundareswara and Schrater, 2008; Moreno-Bote et al., 2011) and in a distance estimation task (Battaglia et al., 2011). *sampling*

2.4.6 *In this thesis*

This thesis focusses on internal representations and how they are manipulated during the decision-making process. In our modelling we explore the applicability of different loss functions and decision rules.

- In Chapter 3 we will examine whether participants integrate the experimentally provided performance feedback – which is related to the loss function – in a time interval reproduction task. In particular, we will use two different shapes of feedback, one that relates to a standard, symmetric loss function, and one that entails a skewed, asymmetrical loss, to see whether observers adapt to arbitrary losses as seen in Section 2.4.2. In a secondary analysis, we will also infer the exponent of the loss function, testing whether there is a significant deviation from the quadratic assumption. Regarding the shape of the motor error, described in Section 2.4.4, we will verify whether our observers are best described by a constant motor error or by one that grows with the duration of the interval, as per the scalar property.
- In Chapter 4 we will explore several variants of the decision-making process in a target estimation task. In particular, we will compare classical observer models that follow deterministic BDT against observer models that incorporate decision noise (posterior-matching, sampling, and others), as briefly described in Section 2.4.5. We will provide a simple stochastic decision rule that approximates different sources of noise in decision making.
- In Chapter 5, we will show that observers' behaviour in a centre-of-mass estimation task, in which they are allowed to compensate for their mistakes, may require us to take into account an effort term in the loss function, as suggested by studies reported in Section 2.4.3, to explain the observed lack of correction in trials with higher perceptual uncertainty.

3

COMPLEX INTERNAL REPRESENTATIONS IN SENSORIMOTOR TIMING

> "With regard to time, our *feeling* of duration or of the lapse of time is notoriously an unsafe guide as to the time that has elapsed by the clock. [...] But in so far as time consists in an *order* of before and after, there is no need to make such a distinction; the time-order which events seem to have is, so far as we can see, the same as the time-order which they do have. At any rate no reason can be given for supposing that the two orders are not the same."
>
> — Bertrand Russel, *The Problems of Phylosophy*

In this chapter we study the nature of internal representations built by human observers in a sensorimotor timing task in which we varied both the distributions of time intervals, from uniform to highly skewed or bimodal, and the error mapping that determined the performance feedback. This work was originally published in *PLoS Computational Biology* (Acerbi et al., 2012).

3.1 TEMPORAL CONTEXT BIASES INTERVAL TIMING

Human time perception is notoriously riddled with biases and illusions of both temporal *duration* and, perhaps more surprisingly, subjective *order* of events (Eagleman, 2008). Virtually any manipulation of stimulus properties and task layout systematically alters the perception of time: for example, larger stimuli (brighter, bigger, more numerous) and novel or unpredictable stimuli are judged to last longer (Xuan et al., 2007; Pariyadath and Eagleman, 2007), saccades compress spatio-temporal judgements (Morrone et al., 2005), flickering frequency alters perceived duration (Kanai et al., 2006), and repeated exposure to a specific inter-stimulus lag alters subjective temporal order (Fujisaki et al., 2004; Miyazaki et al., 2006; Stetson et al., 2006). Moreover, temporal judgments are particularly susceptible to the central tendency and range effects common to other psychophysical magnitudes (Hollingworth, 1910; Fraisse, 1984). Various explanations have been proposed for some of these phenomena, such as a common metric for space, time, and number (Walsh, 2003) or the hypothesis that subjective duration depends on energy expenditure for encoding a stimulus (Eagleman and Pariyadath, 2009).

Here we focus specifically on biases that emerge from the statistics of previously experienced durations, in the simplified case in which the only variable that changes from trial to trial is target duration.[1] This layout allows us to see how the perception of a target duration s is affected by the *temporal context*, i.e. the experimental distribution of durations, $p_{exp}(s)$. Moreover, note that (a) the sensing of time intervals is inherently noisy (Buhusi and Meck, 2005; Lewis and Miall, 2009); and (b) the ability to estimate sensorimotor time intervals in the subsecond range and to react accordingly is fundamental in many behaviourally relevant circumstances (Mauk and Buonomano, 2004), such as dodging a blow or assessing causality ('was it me producing that noise?'). Therefore, it is typically advantageous to enhance time estimates with previous knowledge of the temporal context, and we may expect the nervous system to be reasonably good at that.

temporal context

As we have seen in Section 2.3, Bayesian integration has been successfully applied to describe the behaviour of human observers when combining contextual prior information with noisy sensory measurements. It has been shown in various timing experiments that humans can take into account relevant temporal statistics of a task in a Bayes-sensible fashion, if not quite optimal, such as in sensorimotor coincidence timing (Miyazaki et al., 2005), tactile simultaneity judgements (Miyazaki et al., 2006), planning movement duration (Hudson et al., 2008), time interval estimation (Jazayeri and Shadlen, 2010; Ahrens and Sahani, 2011; Cicchini et al., 2012), and multisensory integration of duration (Shi et al., 2013b; Hartcher-O'Brien et al., 2014); see Shi et al. (2013a) for a review.

The work by Jazayeri and Shadlen (2010) represents a seminal study in the field, by showing a striking example of Bayesian integration in a time interval reproduction task (Jones and Mcauley, 2005 had performed a similar study, although without giving a Bayesian interpretation). In different blocks of trials, participants were trained on three distinct experimental distributions of stimuli, which were uniform over three partially overlapping ranges ('short', 'intermediate' and 'long'). Participants received positive perfomance feedback when their reproduced duration was within a small window of the physical duration. The authors showed that a standard Bayesian observer model whose sensorimotor noise followed the scalar property and with a quadratic loss function ('Bayes least square') was able to quantitatively capture the main features of human data, such as the regression to the mean (biases towards the mean of the current experimental distribution of stimuli) and the range effect (the biases were stronger at longer intervals due to the greater sensory uncertainty). The study left several open questions. First, the subjects' sensorimotor noise proper-

1 Depending on the experimental design, the target duration may be the duration of a stimulus ('filled' interval) or the interval between two brief stimuli (inter-stimulus or 'empty' interval).

ties were not independently measured, leaving unknown whether participants were 'optimal' at the task or merely sensible. Second, in their analysis the authors simply assumed that subjects had fully acquired uniform priors identical to the experimental distributions. Under this assumption, they rejected the hypothesis that subjects were following a MAP strategy (a zero-one loss function, similar to the provided feedback). However, this result feels inconclusive due to the degeneracy of Bayesian models (see Section 1.2.3). For example, it can be equally argued that subjects were using a MAP strategy, although with a different prior, such as a smoothed approximation of the uniform distribution. Mamassian and Landy (2010) present a similar argument regarding the scalar property, which could be explained instead via a constant noise model and an asymmetric loss function. Finally, it is unclear how human observers would behave in the presence of more complex distributions of duration.

In a recent experiment, Ryan (2011) tested different groups of participants on various distributions of duration in a time interval reproduction task, with visual and auditory stimuli. Distributions were uniform over the range, skewed and bimodal ('V'-shaped). Results must be judged with caution given that the experiment lasted only 120 trials. Nonetheless, in the different conditions, participants started developing distinct biases that could have been partially consistent with a Bayesian interpretation (the study did not involve any modelling). However, responses did not show 'attraction' to the extremes of the bimodal, 'V'-shaped distribution, contrarily to the quick biases that were reported in a motion estimation task (Chalk et al., 2010).

In general, as a realistic working hypothesis, we can expect the observers to acquire, after training, an internal representation of the statistics of the temporal intervals which is an approximation of the true, objective experimental distribution. It can be argued that this approximation in most cases would be 'similar enough' to the true distribution, so that, in practice, the distinction between subjective and objective distribution is an unnecessary complication. This is not exact though, first of all because it is unknown whether the similarity assumption would hold for complex temporal distributions, such as skewed and bimodal, and secondly because the specific form of the approximation can lead to observable differences in behaviour even for simple cases (see Figure 3.1).

We propose that understanding how humans learn and approximate temporal statistics in a given context can help explain a number of observed temporal biases. In view of the variety of adaptation phenomena observed especially in the temporal domain (e. g., temporal recalibration, Fujisaki et al., 2004; Stetson et al., 2006), and of several examples of the failure of 'optimal' multisensory integration of 'empty' intervals (Burr et al., 2009; Shi et al., 2010; Hartcher-O'Brien and Alais, 2011), it is worthwhile to ask whether people are able to acquire an internal representation of

complex distributions of inter-stimulus intervals in the first place, and what are their limitations.

As seen in Chapter 2, Bayesian Decision Theory (BDT) provides a neat and successful framework for representing the internal beliefs of an ideal observer in terms of a (subjective) prior distribution. We, therefore, adopted the standard Bayesian observer (see Section 2.1) as a framework to infer the subjects' acquired beliefs about the experimental distributions. Since the behaviour of a Bayesian observer depends crucially not only on the prior, but also on the likelihoods and the loss function, with an underlying degeneracy, we need to properly model and validate these elements as well.

3.1.1 *Summary*

In this chapter we analyze the timing responses of human observers for progressively more complex temporal distributions of durations in a motor-sensory time interval reproduction task with explicit performance feedback.

We carried out a full Bayesian model comparison analysis among a discrete set of candidate likelihoods, priors and loss functions in order to find the observer model most supported by the data, characterizing the behaviour of each individual subject across multiple conditions. Having inferred the form of the likelihoods and loss functions for each subject, we could then perform a non-parametric reconstruction (see Section 2.3.4) of what the subjects' prior distributions would look like under the assumptions of our framework, and we compared them with the experimental distributions. The inferred priors suggest that people learn smoothed approximations of the experimental distributions which take into account not only mean and variance but also higher-order statistics, although some complex features (kurtosis, bimodality) seem to deviate systematically from those of the experimental distributions.

3.2 METHODS

3.2.1 *Experimental procedures*

Participants

Twenty-five subjects (17 male and 8 female; age range 19–34 years) including the first author participated in the study. Except for the first author all participants were naïve to the purpose of the study. All participants were right-handed, with normal or corrected-to-normal vision and reported no neurological disorder. Participants were

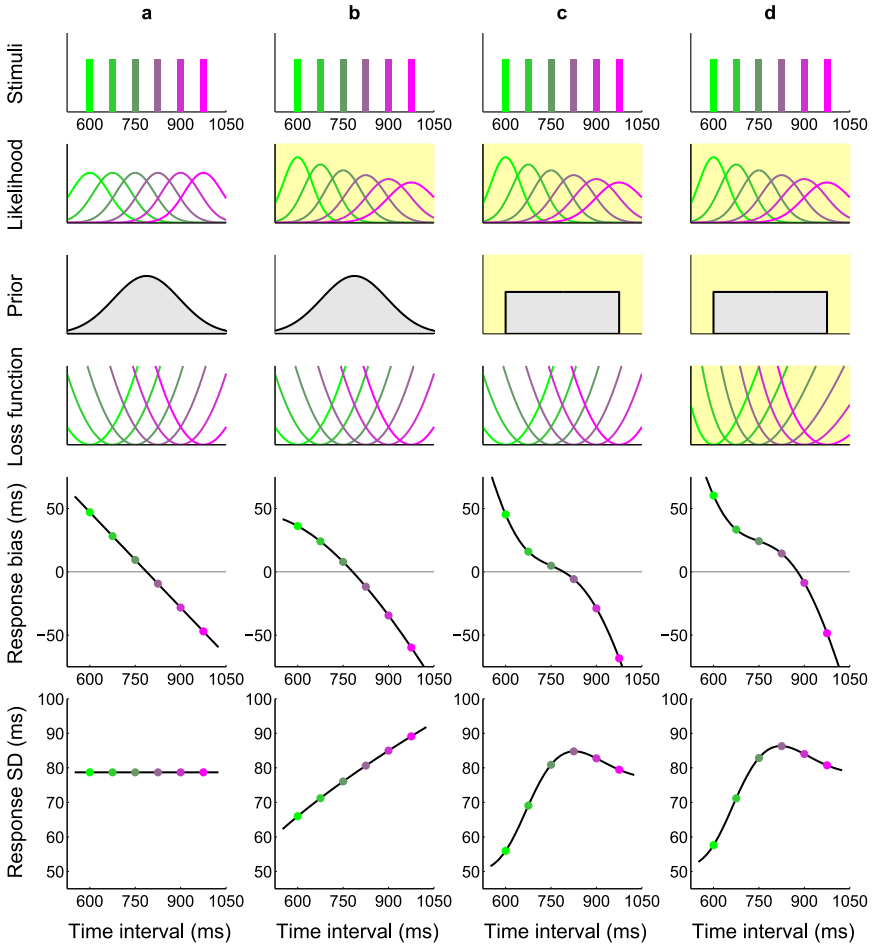

Figure 3.1: **Comparison of response profiles for different ideal observers in the timing task.** The responses of four different ideal observers (*columns* **a-d**) to a discrete set of possible stimuli durations are shown (*top row*); for visualization purpose, each stimulus duration in this plot is associated with a specific colour. The behaviour crucially depends on the combination of the modelled observer's temporal sensorimotor noise (likelihood), prior expectations and loss function (*rows* 2-4); see Figure 3.2 bottom for a description of the observer model. For instance, the observer's sensorimotor variability could be constant across all time intervals (column **a**) or grow linearly in the interval, according to the 'scalar' property of interval timing (column **b-d**). An observer could be approximating the true, discrete distribution of intervals as a Gaussian (columns **a-b**) or with a uniform distribution (columns **c-d**). Moreover, the observer could be minimizing a typical quadratic loss function (columns **a-c**) or a skewed cost imposed through an external source of feedback (column **d**). Yellow shading highlights the changes of each model (column) from model (**a**). All changes to the observer's model components considerably affect the statistics of the predicted responses, summarized by response bias, i.e. average difference between the response and true stimulus duration, and SD (*bottom two rows*). For instance, all models predict a central tendency in the response (that is, a bias that shifts responses approximately towards the center of the interval range), but bias profiles show characteristic differences between models.

compensated for their time and an additional monetary prize was awarded to the three best naïve performers (lowest mean squared error). The University of Edinburgh School of Informatics ethics committee approved the experimental procedures and all subjects gave informed consent.

Materials and stimuli

Participants sat in a dimly lit room, $\sim$ 50 cm in front of a Dell M782p CRT monitor (160 Hz refresh rate, 640×480 resolution). Participants rested their hand on a high-performance mouse which was fixed to a table and hidden from sight under a cover. The mouse button was sampled at 1 kHz (with a 13 ± 1 ms latency). Participants wore ear-enclosing headphones (Sennheiser EH2270) playing white noise at a moderate volume, thereby masking any experimental noise. Stimuli were generated by a custom-written program in MATLAB (Mathworks, U.S.A.) using the Psychophysics Toolbox extensions (Brainard, 1997; Pelli, 1997; Kleiner et al., 2007). All timings were calibrated and verified with an oscilloscope.

Behavioural task

Each trial started with the appearance of a grey fixation cross at the center of the screen (27 pixels, 1.5° diameter); see Figure 3.2 (top) for a depiction of the task. Participants were required to then click on the mouse button at a time of their choice and this led to a visual flash being displayed on the screen after a delay of s ms, the *target interval*, which could vary from trial to trial. The flash consisted of a circular yellow dot (1.5° diameter and 1.5° above the fixation cross) which appeared on the screen for 18.5 ms (3 frames). The target interval s was defined from the start of the button press to the first frame of the flash, and was drawn from a block-dependent distribution $p_{exp}(s)$. Participants were then required to reproduce the target interval by pressing and holding the mouse button for the same duration. The duration of button press (r ms, the *response*) was recorded on each trial. Participants were required to wait at least 250 ms after the flash before starting the interval reproduction, otherwise the trial was discarded and re-presented later.

target interval

response

After the button release, 450–850 ms later (uniform distribution), feedback of the performance was displayed for 62 ms. This consisted of a rectangular box (height 2.5°, width 20°) in the lower part of the screen with a central vertical line representing zero error and a dotted line representing the reproduction error on that trial (see Figure 3.2, top right). The horizontal position of the error line relative to the zero-error line was computed via an *error mapping* as either $f_{Sk}(r,s) = \kappa \cdot \frac{r-s}{r}$ (Skewed feedback) or $f_{St}(r,s) = \kappa \cdot \frac{r-s}{787.5}$ (Standard feedback), depending on the experimental condition, with $\kappa = 400$ pixels (22.2°). Therefore, for a response r that was shorter than the

error mapping

target interval s the error line was displayed to the left of the zero-error line, and the converse for a response longer than the target interval. The fixation cross disappeared 500–750 ms after the error feedback, followed by a blank screen for another 500–750 ms and the reappearance of the fixation cross signalled the start of a new trial.

We provided performance feedback (also known as 'knowledge of results', or KR) on a trial-by-trial basis, so as to constrain the loss function, speed up learning and allow the subjects to adjust their behaviour; our results therefore provide an upper bound on human performance (Salmoni et al., 1984; Blackwell and Newell, 1996). The 'artificial' response-dependent asymmetry in the Skewed mapping was chosen to test whether participants would integrate the provided feedback error into their decision process, as opposed to other possibly more natural forms of error, such as the Standard error $f_{St} \propto r - s$ or the Fractional error $f_{Fr} \propto \frac{r-s}{s}$ (see later).

Experiments

Each experiment consisted of a number of blocks, each comprising of several sessions. In different experimental blocks we varied both the statistical distribution of the intervals, $p_{exp}(s)$, and the shape of the error mapping, $f(r, s)$. Details of the experimental layout for each block are reported in Table 3.1. The participants were divided into experimental groups as follows:

- *Experiment 1:* This experiment represented a basic test for the experimental paradigm and modelling framework with simple uniform distributions over different ranges. *Statistics:* Short Uniform and Long Uniform blocks with Skewed feedback (4 participants, including the first author).

- *Experiment 2:* This experiment compared subjects' responses in a uniform condition vs a non-uniform one, over the same range of intervals. *Statistics:* Medium Uniform and Medium Peaked blocks with Skewed feedback (6 participants, including the first author).

- *Experiment 3:* This experiment verified the effect of feedback on subjects' responses by imposing a different error mapping. *Statistics:* Medium Uniform block with Standard feedback (6 participants, including the first author).

- *Experiment 4:* This experiment tested subjects with a more extreme non-uniform distribution. *Statistics:* Medium High-Peaked block with Standard feedback (3 participants).

- *Experiment 5:* This experiment verified the limits of subjects' capability of learning with bimodal distributions of intervals. *Statistics:* Medium Bimodal with

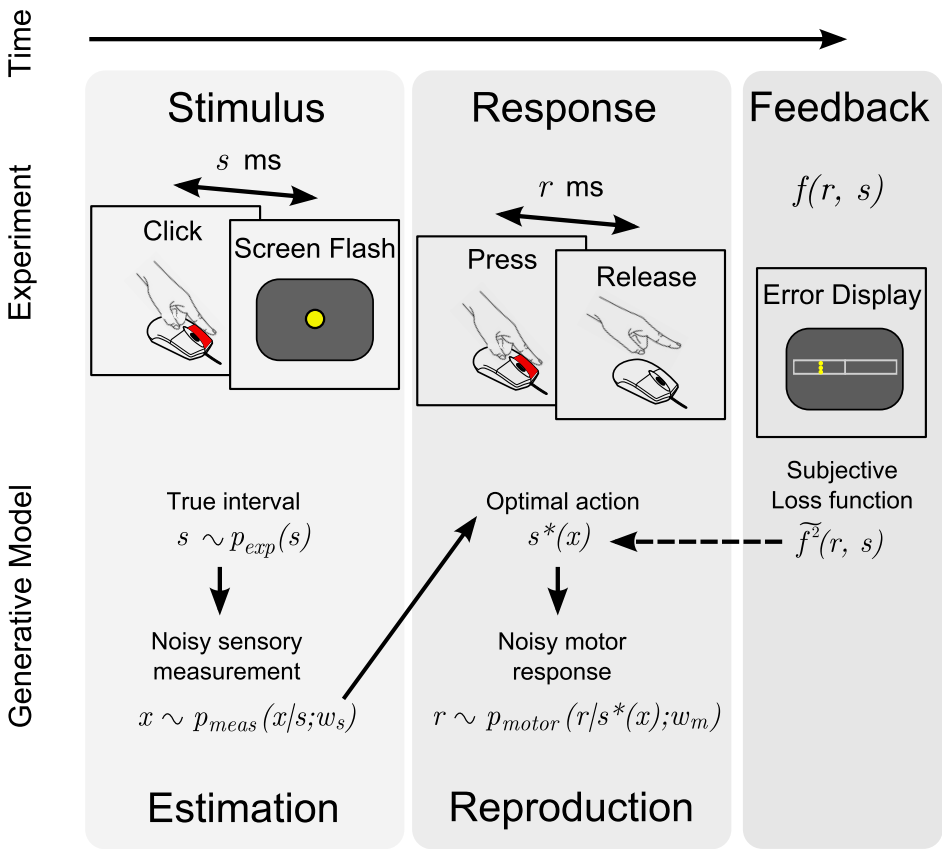

Figure 3.2: **Time interval reproduction task and generative model.** *Top:* Outline of a trial. Participants clicked on a mouse button and a yellow dot was flashed s ms later at the center of the screen, with s drawn from a block-dependent distribution (estimation phase). The subject then pressed the mouse button for a matching duration of r ms (reproduction phase). Performance feedback was then displayed according to an error mapping $f(r,s)$. *Bottom:* Generative model for the time interval reproduction task. The interval s is drawn from the experimental distribution $p_{exp}(s)$. The stimulus induces in the observer the noisy sensory measurement x with conditional probability density $p_{meas}(x|s;w_s)$ (the sensory measurement distribution), with w_s a sensory variability parameter. The action subsequently taken by the ideal observer is assumed to be the 'optimal' action $s^*(x)$ that minimizes the subjectively expected loss (Eq. 3.1). The subjectively expected loss depends on terms such as the prior $q_{prior}(s)$ and the loss function (squared subjective error mapping $\widetilde{f}(r,s)$), which do not necessarily match their objective counterparts. The chosen action is then corrupted by motor noise, producing the observed response r according to the motor error distribution $p_{motor}(r|s^*;w_m)$, where w_m is a motor variability parameter.

Standard feedback (4 participants) and Wide Bimodal with Standard feedback (4 participants).

The order of the blocks for Exps. 1 and 2 were randomized across subjects. Each block consisted of three to six sessions, terminating when the participant's performance had

stabilized (fractional change in mean squared timing error between sessions less than 0.08). For Exp. 5 we required participants to perform a minimum of five sessions.

Exp.	Subjects	Interval range	Distribution	Peak probability	Feedback
1	$n = 4$	Short	Uniform	–	Skewed
		Long	Uniform	–	
2	$n = 6$	Medium	Uniform	–	Skewed
		Medium	Peaked	7/12	
3	$n = 6$	Medium	Uniform	–	Standard
4	$n = 3$	Medium	High-Peaked	19/24	Standard
5 a	$n = 4$	Medium	Bimodal	1/3 and 1/3	Standard
5 b	$n = 4$	Wide	Wide-Bimodal	See text	Standard

Table 3.1: **Summary of experimental layout for all experiments.** Each line represents an experimental block, grouped by experiment; subjects in Exps. 1 and 2 took part in two blocks, whereas in Exp. 5 two distinct groups of subjects took part in each block. For each block, the table reports number of subjects (n), interval ranges, type of distribution, probability of the 'peak' (i.e. most likely) intervals and shape of performance feedback. Tested ranges were Short (450–825 ms), Medium (600–975 ms), Long (750–1125 ms) and Wide (450–1125 ms), each covered by 6 intervals (10 for the Wide block) separated by 75 ms steps. Distributions of intervals were Uniform (1/6 probability per interval), Peaked/High-peaked (the 'peak' interval at 675 ms appeared with higher probability than non-peak stimuli, which were equiprobable), Bimodal (intervals at 600 and 975 ms appeared with higher probability) and Wide-Bimodal (intervals at 450–600 ms and 975–1125 ms appeared with higher probability). The Skewed feedback takes the form $\propto \frac{r-s}{r}$ whereas the Standard feedback $\propto r - s$, where r is the reproduced duration and s is the target interval in a trial.

Each session consisted of around 500 trials and was broken up into runs of 84–96 trials. Within each run the number of each interval type was set to reflect the underlying distribution exactly and the order of the presentations was then randomized. However, for the High-Peaked session we ensured that each less likely interval was always preceded by 3–5 'peak' intervals. Subjects could take short breaks between runs.

Sensorimotor measurements sessions

All participants of Exps. 1 and 2 additionally took part in a side sensory and motor measurement session. In these sessions all stimuli and materials were identical to the ones presented in the main experiment. The design of these sessions itself was chosen to be as similar as possible to the main experiment, but focussing only on the sensory (estimation) or motor (reproduction) part of the task.

In the sensory noise measurement session subjects performed a 2AFC time interval discrimination task ($\sim$ 320 trials). Each trial, subjects clicked on a mouse button and a dot flashed on screen after a given duration (s_1 ms). Subjects clicked again on the mouse button, and a second dot flashed on screen after s_2 ms. At the end of each trial subjects had to specify which interval was longer, with correct responses followed by a positive feedback tone. Intervals s_1 and s_2 were adaptively chosen from the range 300–1275 ms on a trial by trial basis in order to approximately maximize the expected gain in information about the sensory variability of the subject in that range (we adapted the algorithm described in Kontsevich and Tyler, 1999).

In the motor noise measurement session, each trial subjects had to produce a given block-dependent interval by holding the mouse button. Subjects received visual feedback of their performance through the Skewed error mapping (as in Exps. 1 and 2). For each block the target interval was always the same (500, 750 or 1000 ms) and the subjects were instructed about it. Subjects performed on the three intervals twice, in a randomized order, for a total of six blocks (30 trials per block, the first five trials of each block were discarded).

3.2.2 *Data analysis*

We examined the last two sessions of each block of the main experiment, when performance had plateaued so as to exclude any learning period of the experiment. We analysed all trials for the uniform distributions and Wide Bimodal block. For the non-uniform distributions, we picked a random subset of the frequently-sampled intervals such that all intervals contributed equally in the model comparison (results were mostly independent of the chosen random subset), with the exception of the Wide Bimodal block for which we would have had too few data points per interval. For each subject we analyzed about 1000 trials for the Uniform or Wide Bimodal blocks, $\sim$ 500 for the Peaked or Medium Bimodal block and $\sim$ 200 trials for the High-Peaked block. We discarded trials with time-stamp errors (e.g. multiple or non-detected clicks) and trials whose response durations fell outside a block-dependent allowed window of 225–1237 ms (Short), 300–1462 ms (Medium), 375–1687 ms (Long) and 225–1687 ms (Wide), giving 124 discarded trials out of a total of $\sim$ 30000 trials ($\sim$ 0.4%). Note that 93% of the discarded trials had responses of less than 150 ms, which we attribute to accidental mouse presses.

In our data analysis we use all non-discarded data points, but for the sake of visualization we represent a dataset with two important summary statistics: the *response bias* (average difference between the response and target stimulus) and standard deviation (SD) of the responses, for each stimulus interval (see Figure 3.1, bottom rows).

response bias

For all analyses the criterion for statistical significance was $p < 0.05$.

3.2.3 *Observer models*

We modelled the subjects' performance with a family of standard Bayesian ideal observer (and actor) models which incorporated both the perception (time interval estimation) and action (reproduction) components of the task; see Figure 3.2 (bottom) for a depiction of the generative model of the data.

Standard Bayesian observer

According to the standard Bayesian observer of sensorimotor estimation (Section 2.1), we assume that on a given trial a time interval s is drawn from a probability distribution $p_{exp}(s)$ (the experimental distribution) and the observer makes an internal measurement x that is corrupted by sensory noise according to the sensory measurement distribution $p_{meas}\left(x\,|s;w_s\right)$, where w_s is a parameter that determines the sensory (estimation) variability. Subjects then reproduce the interval with a motor command of duration $\hat{s}$. This command is corrupted by motor noise, producing the response duration r – the observed reproduction time interval – with conditional probability density $p_{motor}\left(r\,|\hat{s};w_m\right)$ (the *motor error distribution*), with w_m a motor (reproduction) variability parameter. Subjects receive an error specified by a mapping $f(r,s)$ and we assume they try to minimize a (quadratic) loss based on this error.

In our model we assume that subjects develop an internal estimate of both the experimental distribution and error mapping (the feedback associated with a response r to stimulus s), which leads to the construction of a (subjective) prior, $q_{prior}(s)$, and subjective error mapping $\widetilde{f}(r,s)$; the latter is then squared to obtain the loss function. This allows the prior and subjective error mapping to deviate from their objective counterparts, respectively $p_{exp}(s)$ and $f(r,s)$.

Following BDT (see Eq. 2.3), the 'optimal' action $s^*(x)$ is calculated as the action $\hat{s}$ that minimizes the subjectively expected loss:

$$s^*(x) = \arg\min_{\hat{s}} \int p_{meas}\left(x\,|s;w_s\right) q_{prior}(s) p_{motor}\left(r\,|\hat{s};w_m\right) \widetilde{f}^2(r,s)\,ds\,dr, \tag{3.1}$$

where the integral on the right hand side is proportional to the subjectively expected loss. Combining Eq. 3.1 with the generative model of Figure 3.2 (bottom) we computed the distribution of responses of an ideal observer for a target time interval s, integrating over the hidden internal measurement x, which was not directly accessible in our experiment.

Therefore, the reproduction time r of an ideal observer, given the target interval s, is distributed according to (see Eq. 2.2):

$$\Pr(r|s;w_s,w_m) = \int p_{meas}(x|s;w_s)\, p_{motor}(r|s^*(x);w_m)\, dx. \tag{3.2}$$

Eqs. 3.1 and 3.2 are the key equations that allow us to simulate our task. Eq. 3.1 represents the internal model and deterministic decision process adopted by the subject, whereas Eq. 3.2 represents probabilistically the objective generative process of the data. Note that the experimental distribution $p_{exp}(s)$ and objective error mapping $f(r,s)$ do not appear in any equation: the distribution of responses of the ideal observers only depends on their internal representations of prior and loss function. To limit model complexity, in the majority of our analyses we assume that the internal representations of the sensory and motor error distributions that appear in the internal model (Eq. 3.1) match the objective ones that appear in the generative model (Eq. 3.2).

Bayesian observer model components

The family of Bayesian ideal observer models described by Eqs. 3.1 and 3.2 is characterized by a number of independent *model factors* or components whose specific choices can be factorially combined to give rise to a large model space (see Figure 3.3). This methodology of building and subsequently testing models via independent components has been recently named *factorial model comparison* (van den Berg et al., 2014). Model factors are introduced in the following list.

model factors

factorial model comparison

i. The sensory measurement distribution is Gaussian:

$$p_{meas}(x|s;w_s) = \mathcal{N}\left(x|s,\sigma^2_{meas}(s)\right), \tag{3.3}$$

whose noise can be either *constant* or *scalar*:

$$\sigma^2_{meas}(s) = \begin{cases} (w_s \cdot 787.5)^2 & \text{(constant)} \\ (w_s s)^2 & \text{(scalar).} \end{cases} \tag{3.4}$$

For the scalar case, w_s simply specifies the coefficient of proportionality of the SD with respect to the mean, whereas in the constant case it specifies the proportion of noise with respect to a fixed interval (787.5 ms, average of all experimental durations).

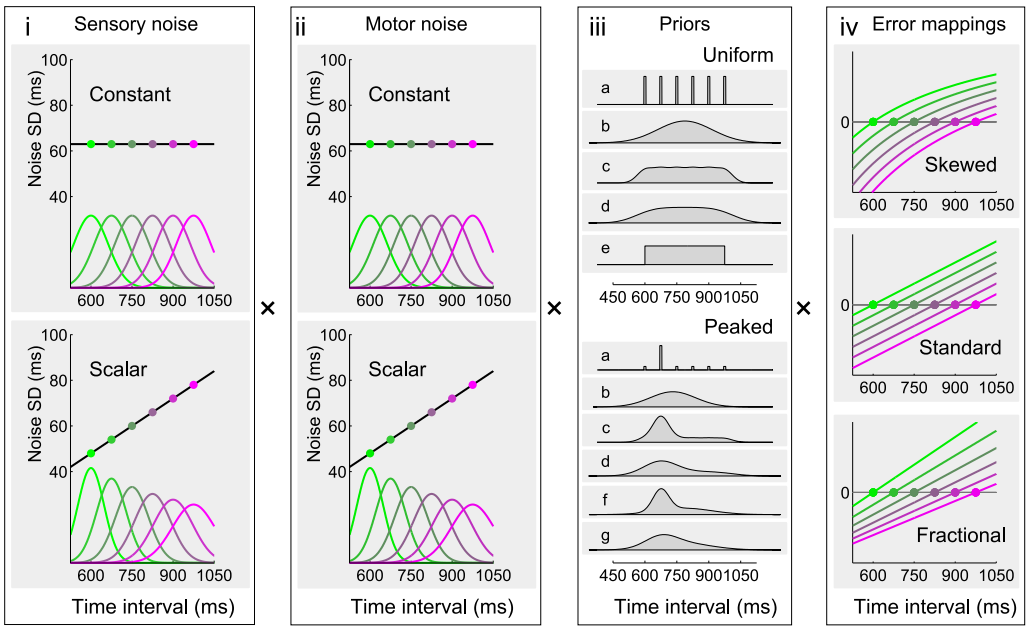

Figure 3.3: **Bayesian observer and actor model components.** Candidate (**i**) sensory and (**ii**) motor error distributions, independently chosen for the sensory and motor noise components of the model. The noise distributions are Gaussians with either constant or 'scalar' (i.e. homogeneous linear) variability. The amount of variability for the sensory (resp. motor) component is scaled by parameter w_s (resp. w_m). **iii**) Candidate priors for the Medium Uniform (top) and Medium Peaked (bottom) blocks. The candidate priors for the Short Uniform (resp. Long Uniform) blocks are identical to those of the Medium Uniform block, shifted by 150 ms in the negative (resp. positive) direction. See Section 3.2.3 for a description of the priors. **iv**) Candidate subjective error maps. The graphs show the error as a function of the response duration, for different discrete stimuli (drawn in different colours). From top to bottom: Skewed error $\widetilde{f}_{Sk}(r,s) \propto \frac{r-s}{r}$; Standard error $\widetilde{f}_{St}(r,s) \propto r-s$; and Fractional error $\widetilde{f}_{Fr}(r,s) \propto \frac{r-s}{s}$. The scale is irrelevant, as the model is invariant to rescaling of the error map. The squared subjective error map defines the loss function (as per Eq. 3.1).

ii. Analogously, the motor error distribution is Gaussian:

$$p_{motor}\left(r \,|s^*(x); w_m\right), \tag{3.5}$$

whose noise can be either *constant* or *scalar*:

$$\sigma^2_{motor}(\hat{s}) = \begin{cases} (w_m \cdot 787.5)^2 & \text{(constant)} \\ (w_m \hat{s})^2 & \text{(scalar).} \end{cases} \tag{3.6}$$

iii. The approximation scheme for the prior, $q_{prior}(s)$, can be:

a) the true, discrete distribution;

b) a single Gaussian with same mean and variance as the true distribution;

c) a mixture of six (ten for the Wide range) 'narrow' Gaussians (37.5 ms SD) centered on the true discrete intervals, with mixing weights equal to the relative probability of the true intervals;

d) as (c) but with 'broad' Gaussians (75 ms SD);

e) a continuous uniform distribution from the shortest to the longest interval.

f–g) For Exps. 2 and 4 we also considered a mixture of two Gaussians with mixing weights π and $1-\pi$, with π equal to the proportion of 'peak' intervals that emerge from the uniform background distribution ($\pi = 0$ for the Uniform block, $\pi = 0.5$ for the Peaked block and $\pi = 0.75$ for the High-Peaked block). The first Gaussian is centered on the peak (675 ms) and with a small (f: 37.5 ms) or large (g: 75 ms) SD, the second Gaussian is centered on the mean of the Medium range (787.5 ms) and with SD equal to that of the discrete Uniform distribution (128.7 ms). Therefore, for the Medium Uniform block approximation schemes (f) and (g) reduce to a single Gaussian. Analogously, for Exp. 5 we considered a mixture of three Gaussians with mixing weights π, π and $1-2\pi$, with π equal to the total frequency of one of the two 'peaks' emerging from the uniform background distribution ($\pi = 1/4$ for the Medium Bimodal block and $\pi = 9/28$ for the Wide Bimodal block). The first two Gaussians are centered on the peaks (Medium: 600 ms and 975 ms; Wide: 525 ms and 1050 ms) and with a small (f: Medium: 37.5 ms; Wide: 61.2 ms) or large (g: twice the small) SD. The third Gaussian is centered on the mean of the range (787.5 ms) and with SD equal to that of the discrete Uniform distribution over the range (Medium: 128.7 ms; Wide: 251.6 ms).

The values of SDs that appear in the mixture of Gaussians in (c), (d), (f) and (g) (narrow 37.5 ms, broad 75 ms) were chosen since 75 ms is the gap between time intervals in all experimental distributions. For the Wide Bimodal block, 61.2 ms is the SD of the sample for three intervals separated by 75 ms.

iv. The (subjective) loss function is assumed to be the square of the subjective error mapping: $\mathcal{L}(r,s) = \widetilde{f}^2(r,s)$. The subjective error mapping can be:

$$\widetilde{f}(r,s) = \begin{cases} \frac{r-s}{r} & \text{(Skewed)} \\ r-s & \text{(Standard)} \\ \frac{r-s}{s} & \text{(Fractional).} \end{cases} \tag{3.7}$$

Note that the Fractional error was not used as feedback in the experiments, but we included it as a possibility for the Bayesian observer as it might represent

an appropriate error signal if time has a logarithmic representation in the brain (Gibbon, 1981). In fact, the logarithmic squared loss yields:

$$(\log r - \log s)^2 = \left(\log \frac{r}{s}\right)^2 = \left(\log\left[1 + \frac{r-s}{s}\right]\right)^2 \approx \left(\frac{r-s}{s}\right)^2 \quad \text{for} \quad \left|\frac{r-s}{s}\right| \ll 1.$$

The pseudo-quadratic form for the loss is chosen mostly for computational reasons. We extend the analysis to a non-quadratic loss function in Section 3.3.2.

Note that, to avoid overfitting, priors and loss functions do not have continuous parameters in our preliminary analysis. Instead, we considered a finite number of parameter-free models of loss function, prior and shape of likelihoods, leaving only two continuous parameters for characterizing the sensory and motor variability (w_s and w_m).

3.2.4 *Model comparison and non-parametric analysis*

Bayesian model comparison

For each participant we assumed that the sensory and motor noise, the approximation scheme for the priors, and the loss function were shared across different experimental blocks. For each observer model M and each subject's dataset $\mathcal{D}$ (that is all blocks within an experiment) we calculated the posterior probability of the model given the data, $\Pr(M|\mathcal{D}) \propto \Pr(\mathcal{D}|M)$, assuming a flat prior over the models (see Appendix A for a recap of Bayesian model comparison). The *marginal likelihood* is given by:

marginal likelihood

$$\Pr(\mathcal{D}|M) = \int \Pr(\mathcal{D}|w_s, w_m, M) \Pr(w_s, w_m|M)\, dw_s\, dw_m, \tag{3.8}$$

where $\Pr(w_s, w_m|M)$ is the prior over the parameters and $\Pr(\mathcal{D}|w_s, w_m, M)$ is the likelihood of the data given a specific model and value of the parameters. We assumed the same prior over parameters for all models, with independence between parameters, $\Pr(w_s, w_m|M) = \Pr(w_s)\Pr(w_m)$. For both parameters we used a broad Beta prior, $\sim \text{Beta}(1.3, 2.6)$, chosen to weakly favour the range 0.03–0.3 in agreement with a vast literature on human timing errors (Lewis and Miall, 2009). The likelihood of the data was computed according to our observer model, Eq. 3.2, assuming independence across trials:

$$\Pr(\mathcal{D}|w_s, w_m, M) = \prod_{i=1}^{N} \Pr\left(r^{(i)} \middle| s^{(i)}; w_s, w_m\right), \tag{3.9}$$

with N the total number of test trials and $s^{(i)}, r^{(i)}$ respectively the target interval and response in the i-th test trial. The calculation of $\Pr(r|s; w_s, w_m)$ in Eq. 3.2 requires a computation of the optimal action s^*, that is, the action $\hat{s}$ that minimizes the expected loss (Eq. 3.1). The minimization was performed analytically for the Standard and Fractional loss function and numerically for the Skewed loss function (function `fminbnd` in MATLAB; we assumed that s^* always fell in the range 20–2000 ms; the results were checked against analytical results obtained through a Taylor-expansion approximation of the loss function that holds for $|\frac{r-s}{s}| \ll 1$).

We computed the marginal likelihood through Eqs. 3.8 and 3.9 both with a full numerical integration and using a Laplace approximation, with essentially identical results. For each dataset, given the posterior distribution over parameters and models, we computed the posterior predictive mean and SD for both the bias and the SD of the response of each stimulus (see Section A.2 in the Appendix). The integration for the posterior predictive checks was performed both over parameters and over models, but typically only one of the models contributed significantly to the integral.

Non-parametric reconstruction of the priors

To examine the subjects' priors using a non-parametric approach, for each subject we took the most supported (i) sensory and (ii) motor noise and (iv) loss function, as inferred from the model comparison. We then allowed the priors to vary independently over a broad class of smooth, continuous distributions. For each block, the log prior was specified by the values of ten (14 for the Wide range) control points at 75 ms steps over the ranges: Short 300–1025 ms, Medium 450–1175 ms, Long 600–1325 ms and Wide 300–1325 ms. The control points were centered on the interval range of the block but extended outside the range to allow for tails or shifts. The non-parametric prior $q_{prior}(s)$ was calculated by interpolating the values of the prior in log space with a Gaussian process (Rasmussen and Williams, 2006) with squared exponential covariance function with fixed scale ($\sigma_y = 1$ in log space, $\ell = 75$ ms) and a small nonzero noise term to favour conditioning. The Gaussian processes were used only as a smooth interpolating method and not as an active part of the inference.[2] In order to infer the prior for each subject and block, we sampled from the posterior distribution of priors $\propto \Pr(\mathcal{D}|q_{prior}, M)$ using a slice sampling MCMC algorithm (Neal, 2003). We ran ten parallel chains (3000 burn-in samples, 1500 saved samples per chain) obtaining a total of 15000 sampled priors per subject and block. Convergence of sampling method was checked both by visual inspection and by comparing the average moments of the priors obtained from each chain against the others for the same subject and block. Differences between the means were empirically negligible

2 The same technique has been used later by Zhang et al. (2013b).

(maximum difference < 1 ms). For each sampled prior we calculated the first four central moments (mean, SD, skewness and excess kurtosis) and computed the mean and SD of the moments across the sample sets of individual subjects and over the sample set of all subjects.

3.3 RESULTS

We first present a description of the results of Exps. 1 and 2, and then report a series of analyses on those two main experiments combined, including a number of investigations regarding the role of sensorimotor noise. Exps. 3, 4 and 5 test specific aspects of the model and of subjects' behaviour with more complex distributions, and are presented thereafter.

3.3.1 *Experiments 1 and 2*

Exp. 1: Uniform distributions over different ranges

In the first experiment the distribution of time intervals consisted of a set of six equally spaced discrete times with equal probability according to either a Short Uniform (450–825 ms) or Long Uniform (750–1125 ms) distribution. The feedback followed a Skewed error mapping $f_{Sk} \propto \frac{r-s}{r}$.

We examined the mean bias in the response (mean reproduction interval minus actual interval, $\bar{r} - s$, also termed 'constant error' in the psychophysical literature), as a function of the actual interval (Figure 3.4 top). Subjects' responses showed a regression to the mean consistent with a Bayesian process that integrates the prior with sensory evidence (see Chapter 2). That is, little bias was seen for intervals that matched the mean of the prior (637.5 ms for Short Uniform, red points, and 937.5 ms for Long Uniform, green points). However, at other intervals a bias was seen towards the mean interval of that experimental block, with subjects reporting intervals longer than the mean as shorter than they really were and conversely intervals shorter than the mean as being longer than they really were. Moreover, this bias increased almost linearly with the difference between the mean interval and the actual interval. Qualitatively, this bias profile is consistent with most reasonable hypotheses for the prior, likelihoods and loss functions of an ideal Bayesian observer (even though details may differ). The SD of the response (Figure 3.4 bottom) showed a roughly linear increase with interval duration, in agreement with the scalar property of interval timing (Gibbon, 1977; Rakitin et al., 1998).

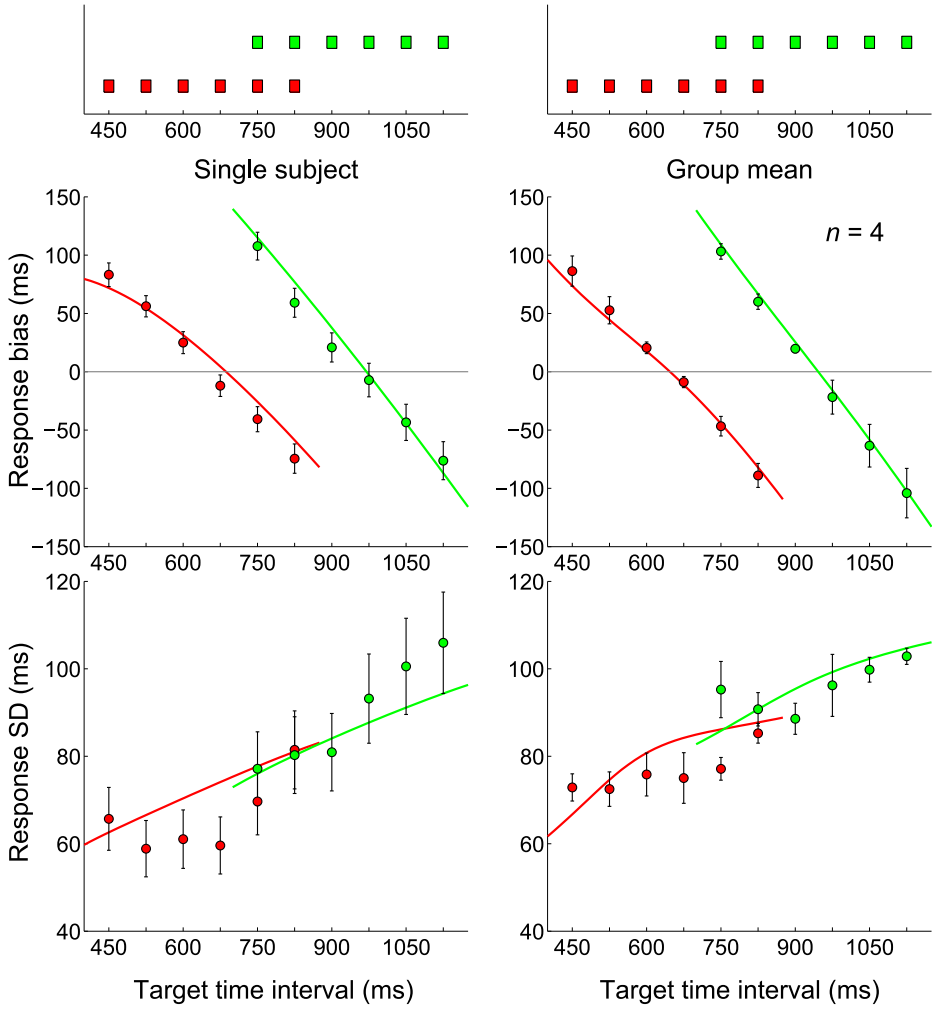

Figure 3.4: **Exp. 1: Short Uniform and Long Uniform blocks.** *Very top:* Experimental distributions for Short Uniform (red) and Long Uniform (green) blocks, repeated on top of both columns. *Left column:* Mean response bias (average difference between the response and true interval duration, top) and SD of the response (bottom) for a representative subject in both blocks (red: Short Uniform; green: Long Uniform). Error bars denote SEM (standard error of the mean). Continuous lines represent the Bayesian model 'fit' obtained averaging the predictions of the most supported models (Bayesian model averaging). *Right column:* Mean response bias (top) and SD of the response (bottom) across subjects in both blocks (mean ± SE across subjects). Continuous lines represent the Bayesian model 'fit' obtained averaging the predictions of the most supported models across subjects.

These results qualitatively suggest that the temporal context influences subjects' performance in the motor-sensory timing task in a way which may be compatible with a Bayesian interpretation, and in agreement with previous work which considered purely sensory intervals and uniform distributions (Jones and Mcauley, 2005; Jazayeri and Shadlen, 2010; Cicchini et al., 2012). To quantitatively verify the hypothesis that a Bayesian model would be able to describe the data, for each participant we

computed the support for each model based on the psychophysical data, that is the model marginal likelihood $\Pr(\mathcal{D}|M)$, which is proportional to the posterior probability of the model (see Section 3.2.3). We then calculated the Bayesian model average for the mean bias and SD of the response, shown by the continuous lines in Figure 3.4. Note that the Bayesian model 'fits' are obtained by integrating the model predictions over the posterior of all models and parameters (model averaging), with no parameter fitting. In general, the mean biases fits show a good quantitative match with the group averages ($R^2 \geq 0.95$ for both blocks); the SDs are typically more erratic and we found mainly a qualitative agreement, as observed in previous work (see e. g., Figure S3 in Jazayeri and Shadlen, 2010).

Exp. 2: Uniform and Peaked distributions on the same range

As in the first experiment, six different equally-spaced intervals were used, with two different distributions. However, in this experiment both blocks had the same range of intervals (Medium: 600–975 ms). In one block (Medium Peaked) one of the intervals (termed the 'peak') occurred more frequently than the other 5 intervals, that were equiprobable. That is, the 675 ms interval occurred with $p = 7/12$ with the other 5 intervals occurring each with $p = 1/12$. In the other block (Medium Uniform) the 6 intervals were equiprobable. The feedback gain for both blocks was again the Skewed error map $f_{Sk} \propto \frac{r-s}{r}$.

Examination of the responses showed a central tendency as encountered in the previous experiment (Figure 3.5 top). However, despite the identical range of intervals in both blocks, subjects were sensitive to the relative probability of the intervals (Ryan, 2011). In particular, the responses in the Peaked block (light blue points) appeared to be generally shifted towards shorter durations and this shift was interval dependent (see Figure 3.6). This behaviour is qualitatively consistent with a simple Bayesian inference process, according to which the responses are 'attracted' towards the regions of the prior distribution with greatest probability mass. Intuitively, the average ('global') shift of responses can be thought of as arising from the shift in the distribution mean, from the Uniform distribution (mean 787.5 ms) to the Peaked distribution (mean 731.3 ms); whereas interval-dependent ('local') effects are a superimposed modulation by the probability mass assignments of the distribution. This is only a simplified picture, as the biases depend on a non-linear inference process, which is also influenced by other details of the Bayesian model (such as the loss function), but the qualitative outcome is likely to be similar in many relevant cases.

The SD of the responses showed a significant decrease in variability around the peak for the Peaked condition (Figure 3.5 bottom; paired t-test $t_{(5)} = 3.95$, $p < 0.05$). This effect could be simply due to practice as subjects received feedback more often

at peak intervals, however the local modulation of bias previously described (Figure 3.6) suggests a Bayesian interpretation. In fact, because of the local 'attraction' effect, interval durations close to the peak would elicit responses that map even closer to it, therefore compressing the perceptual variability, an example of bias-variance trade-off (Jazayeri and Shadlen, 2010).

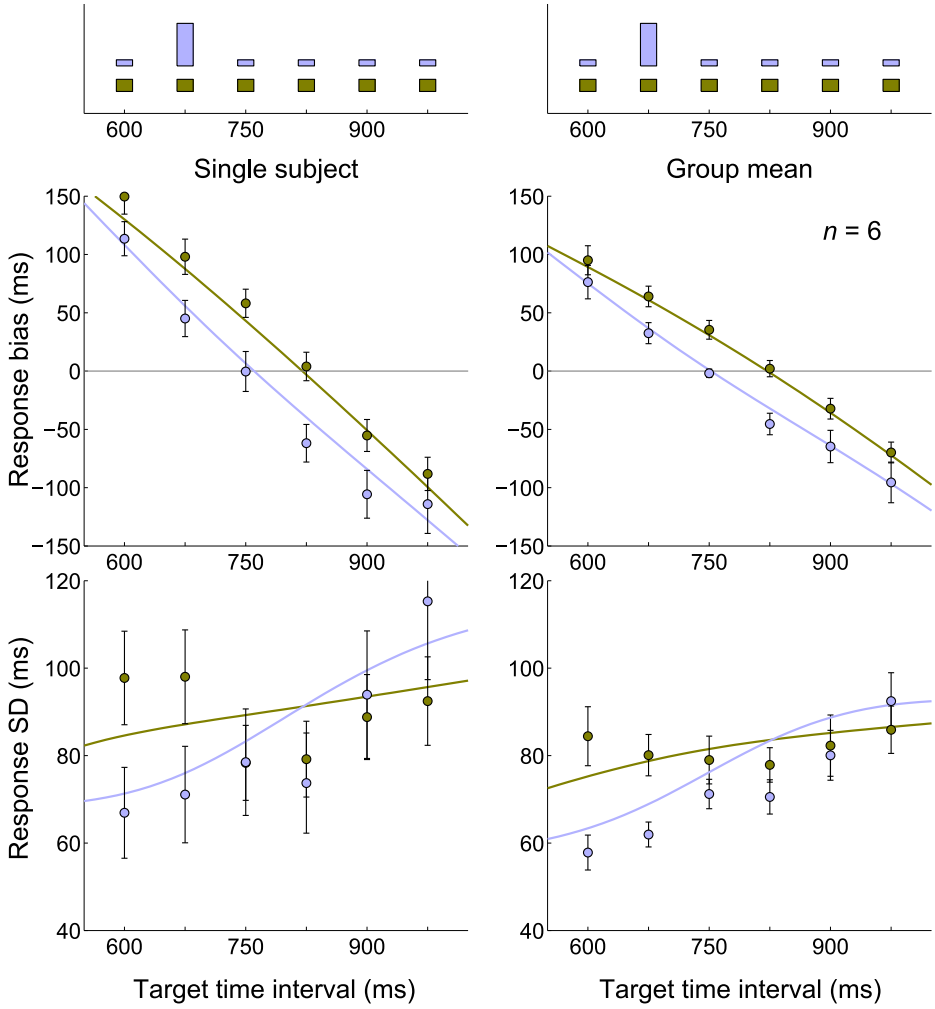

Figure 3.5: **Exp. 2: Medium Uniform and Medium Peaked blocks.** *Very top:* Experimental distributions for Medium Uniform (light brown) and Medium Peaked (light blue) blocks, repeated on top of both columns. *Left column:* Mean response bias (top) and SD of the response (bottom) for a representative subject in both blocks (light blue: Medium Uniform; light brown: Medium Peaked). Error bars denote SEM. Continuous lines represent the Bayesian model fit. *Right column:* Mean response bias (top) and SD of the response (bottom) across subjects in both blocks (mean ± SE across subjects). Continuous lines represent the Bayesian model fit averaged across subjects.

The results of the second experiment show that people take into account the different nature of the two experimental distributions, in agreement with previous work that found differential effects in temporal reproduction for skewed vs uniform dis-

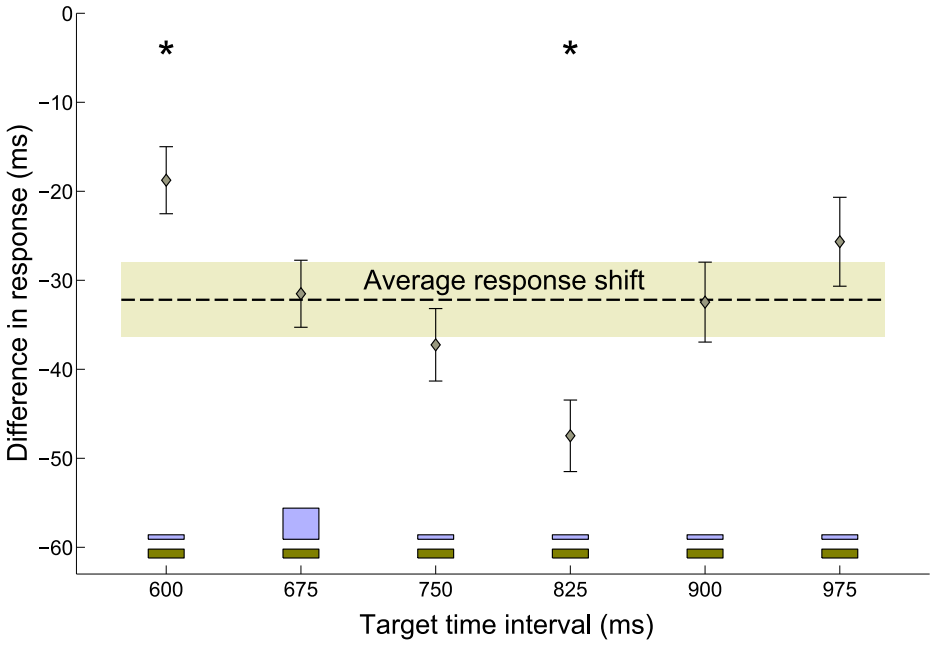

Figure 3.6: **Exp. 2: Difference in response between Medium Peaked and Medium Uniform blocks.** Difference in response between the Medium Peaked and the Medium Uniform conditions as a function of the actual interval, averaged across subjects (± 1 SEM). The experimental distributions (light brown: Medium Uniform; light blue: Medium Peaked) are plotted for reference at bottom of the figure. The dashed black line represents the average response shift (difference in response between blocks, averaged across all subjects and stimuli), with the shaded area denoting ± 1 SEM. The average response shift is significantly different from zero (-32.2 ± 7.9 ms; paired t-test $t_{(5)} = 4.86$, $p < 0.01$), meaning that the two conditions elicited consistently different performance. Additionally, the responses were subject to a 'local' (i.e. interval-dependent) modulation superimposed to the average shift, that is, intervals close to the peak of the distribution (675 ms) were attracted towards it, in addition to the average shift, while intervals far away from the peak were less affected. (*) The response shift at 600 ms and 825 ms is significantly different from the average response shift; $p < 0.01$.

tributions of temporal intervals on a wider, suprasecond range (Ryan, 2011). The performance of the subjects in the two blocks is consistent with a Bayesian 'attraction' in the response towards the intervals with higher prior probability mass. Moreover, although the average negative shift in the response observed in the Peaked condition versus the Uniform one might be compatible with a temporal recalibration (Stetson et al., 2006; Heron et al., 2009) or binding (Haggard et al., 2002) effect that shortens the perceived duration between action and sensory consequences, the specific interval-dependent bias modulation (Figure 3.6) and the reduction in variability around the peak (Figure 3.5 bottom) suggest there may instead be in this case a Bayesian explanation (see also Discussion, Section 3.4). As before, we computed the Bayesian model

fit (or 'posterior prediction') via model averaging, finding again a good quantitative agreement with the group mean biases ($R^2 \geq 0.95$ for both blocks) and a qualitative agreeement for the SDs.

3.3.2 *Analysis of the first two experiments*

We present now a series of analyses of the first two experiments. First, we applied the machinery of Bayesian model comparison to infer the most likely model components, which we subsequently fixed in order to non-parametrically reconstruct the subjects' priors. Then, we tested additional hypotheses about subjects' behaviour by building a few extensions of the model.

Factorial model comparison

For each participant of Exps. 1 and 2 we calculated the posterior probability of each model component (by summing over models with the same components). Table 3.2 reports the most supported (i) sensory and (ii) motor noise models, (iii) priors and (iv) loss function.

The model comparison confirmed that the best noise models were represented by the 'scalar' variability, which had relevant support for both the sensory component (7 subjects out of 10) and the motor component (8 subjects out of 10). This result is consistent with previous work in both the sensory and motor domain (Mates, 1994; Rakitin et al., 1998; Hudson et al., 2008; Jazayeri and Shadlen, 2010). The most supported subjective error map was the Skewed error (7 subjects out of 10), which matched the feedback we provided experimentally. The priors most supported by the data were typically smooth, peaked versions of the experimental distributions. In particular, according to the model comparison, almost all subjects (9 out of 10) approximated the discrete uniform distributions in the Uniform blocks with normal distributions (same mean and variance as the true distribution; Figure 3.3 iii top, b). However, in Exp. 2 most people (5 out of 6) seemed to approximate the experimental distribution in the Peaked block not with a standard Gaussian, but with a skewed variant of a normal distribution (Figure 3.3 iii bottom, d, f and g), suggesting that their responses were influenced by higher order moments of the true distribution and not just the mean and variance (see Discussion).

For Exp. 2 we also relaxed some constraints on the priors, allowing the model selection to pick a Medium Uniform prior for the Medium Peaked block and vice versa. Nevertheless, the model comparison showed that the most supported models were still the ones in which the priors matched the block distribution, supporting our

Subject	Sensory noise		Motor noise		Prior		Loss function	
	Experiment 1							
LA	Sc	(1.000)	Sc	(1.000)	b	(1.000)	Sk	(1.000)
JW	Sc	(0.967)	Sc	(1.000)	b	(0.960)	St	(1.000)
TL	Cn	(1.000)	Sc	(1.000)	b	(1.000)	Sk	(1.000)
DB	Sc	(1.000)	Sc	(0.974)	e	(0.997)	St	(1.000)
	Experiment 2							
LA	Sc	(1.000)	Sc	(0.997)	g	(1.000)	Sk	(1.000)
AC	Cn	(1.000)	Sc	(1.000)	f	(0.978)	St	(1.000)
AP	Cn	(1.000)	Sc	(0.981)	b	(1.000)	Sk	(1.000)
HH	Sc	(0.997)	Sc	(0.997)	g	(0.998)	Sk	(0.875)
JB	Sc	(0.998)	Cn	(0.996)	f	(0.997)	Sk	(1.000)
TZ	Sc	(1.000)	Cn	(1.000)	d	(0.976)	Sk	(1.000)
	Experiment 3							
LA	Cn	(0.910)	Sc	(0.990)	b	(1.000)	St	(0.993)
NY	Sc	(0.988)	Sc	(0.780)	b	(1.000)	Fr	(1.000)
JL	Sc	(0.528)	Sc	(1.000)	b	(0.999)	St	(1.000)
RD	Cn	(1.000)	Sc	(0.996)	b	(0.998)	Fr	(1.000)
PD	Sc	(0.758)	Cn	(1.000)	b	(0.999)	St	(1.000)
JE	Cn	(0.896)	Sc	(0.912)	b	(1.000)	St	(1.000)
	Experiment 4							
RR	Cn	(0.986)	Sc	(0.950)	a	(0.998)	St	(−)
DD	Cn	(0.726)	Cn	(0.641)	f	(0.511)	St	(−)
					g	(0.486)		
NG	Cn	(0.980)	Sc	(0.973)	b	(0.503)	St	(−)
					g	(0.458)		

Table 3.2: **Bayesian model comparison: most supported observer model components for Exps. 1–4.** Most supported observer model components (posterior probability), for each subject, according to the Bayesian model comparison. A posterior probability $p > 0.95$ should be considered suggestive evidence, and $p > 0.99$ significant (posterior probability $p > 0.9995$ is written as 1.000, with a slight abuse of notation). The sensory and motor noise models can either be constant (Cn) or scalar (Sc); the subjective priors (a-g) are described in the Methods (Section 3.2.3); the loss function can be Skewed (Sk), Standard (St) or Fractional (Fr) (see also Figure 3.3). Note the switch in preferred loss function from Exps. 1 and 2 (which received Skewed feedback) to Exp. 3 (which received Standard feedback). In Exp. 4 the loss function was fixed to Standard to constrain the model selection.

previous findings that subjects' responses were consistent with the temporal context and changed when switching from one block to another (as visible in Figure 3.5).

Non-parametric reconstruction of the priors

To study in detail the internal representations, we relaxed the constraint on the priors. Rather than choosing from a fixed set of candidate priors (Figure 3.3 iii), we allowed the prior to vary over a much wider class of smooth, continuous distributions. We assumed that the noise models and loss function emerging from the model comparison were a good description of the subjects' decision making and sensorimotor processing in the task. We therefore fixed these components of the observer's model and inferred non-parametrically, on an individual basis, the shape of the priors most compatible with the measured responses (Figure 3.7; see Section 3.2.3 for details).

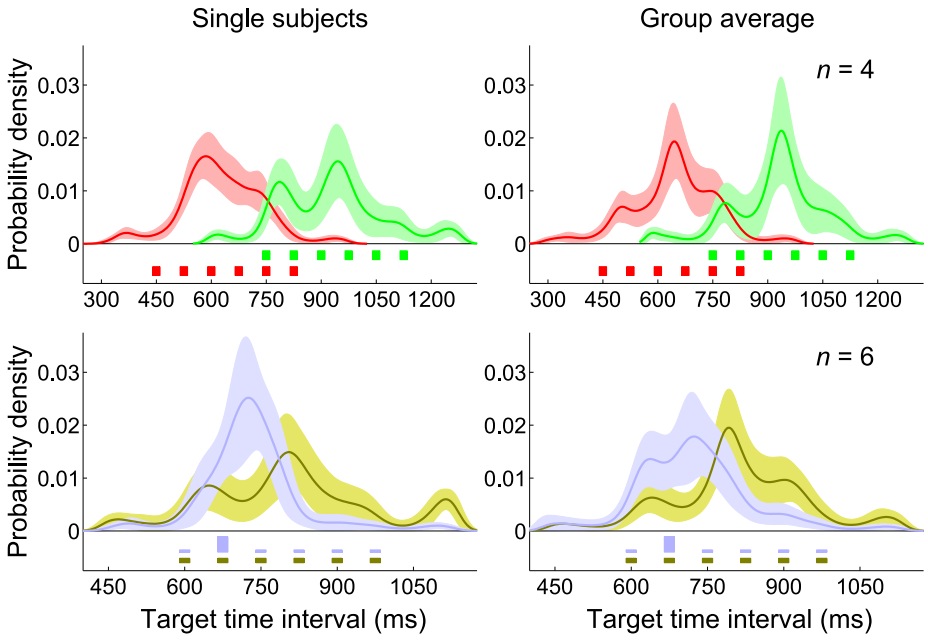

Figure 3.7: **Non-parametrically inferred priors (Exps. 1 and 2).** *Top row:* Short Uniform (red) and Long Uniform (green) blocks. *Bottom row:* Medium Uniform (light brown) and Medium Peaked (light blue) blocks. *Left column:* Non-parametrically inferred priors for representative participants. *Right column:* Average inferred priors. Shaded regions are ± 1 SD For comparison, the discrete experimental distributions are plotted under the inferred priors.

Examination of the recovered priors shows that the subjective distributions were significantly different from zero only over the range corresponding to the experimental distribution, with only occasional tails stretching outside the interval range (e. g., Figure 3.7 bottom left). This suggests that in general people were able to localize the stimulus range in the blocks. The priors did not typically take a bell-like shape, but

rather we observed a more or less pronounced peak at the mean of the true distribution, with the remaining probability mass spread over the rest of the range. Interestingly, the group averages for the Uniform priors over the Short, Medium and Long ranges (Figure 3.7 top right, both, and bottom right, light brown) exhibit very similar, roughly symmetrical shapes, shifted over the appropriate stimulus range. Conversely, the Peaked prior (Figure 3.7 bottom right, light blue) had a distinct, skewed shape.

To compare the inferred priors with the true distribution, we calculated their distribution moments (Table 3.3). We found that the first three moments of the inferred priors (in the table reported as mean, SD and skewness) were statistically indistinguishable from those of the true distributions for all experimental conditions (Hotelling's multivariate one-sample T^2 test considering the joint distribution of mean, SD and skewness against the true values: $p > 0.45$ for all blocks). This result is consistent with the previously stated hypothesis that participants had developed an internal representation which included higher order moments and not just the mean and variance of the experimental distribution. However, when including the fourth moment (kurtosis) in the analysis, we observed a statistically significant deviation of the recovered priors with respect to the true distributions (Hotelling's T^2 test with the joint distribution of the first four moments: $p < 10^{-4}$ for all blocks); in particular, the inferred priors seem to have more pronounced peaks and/or heavier tails. Our analysis therefore showed that, according to the inferred priors, people generally acquired internal representations that were smooth, heavy-tailed approximations to the experimental distributions of intervals, in agreement up to the first three moments.

The deviation of the fourth moment deserves an investigation. First, the heightened kurtosis is not an artifact due to the averaging process across subjects or the sampling process within subjects, as we averaged the moments computed for each sampled distribution (see Section 3.2.3) rather than computing the moments of the average distribution. In other words, all recovered priors are (on average) heavy tailed, it's not just the mean prior that it is 'accidentally' heavy tailed as a mixture of light-tailed distributions. So this result could mean that the subjects' internal representations are actually heavy-tailed, for instance to allow for unexpected stimuli (Feldman, 2013). However, there could be a simpler explanation that the presence of outliers arise from occasional trivial mistakes of the participants. We consider this hypothesis in the next section.

Bayesian observer model with lapse

The reconstructed priors show a systematic increase (and variability) in the inferred kurtosis which may be an artifact due to outliers. To verify whether this is the case,

	Short Uniform		Long Uniform	
	Objective	Subjective	Objective	Subjective
Mean (ms)	637.5	644.2 ± 12.8	937.5	929.9 ± 19.6
SD (ms)	128.1	117.4 ± 13.3	128.1	131.2 ± 16.9
Skewness	0	−0.17 ± 0.24	0	−0.12 ± 0.41
Ex. Kurtosis	−1.27	0.86 ± 1.24	−1.27	0.82 ± 0.98
	Medium Uniform		Medium Peaked	
	Objective	Subjective	Objective	Subjective
Mean (ms)	787.5	805.7 ± 27.4	731.3	724.1 ± 24.0
SD (ms)	128.1	130.4 ± 23.5	106.6	110.13 ± 18.5
Skewness	0	−0.16 ± 0.41	1.14	0.78 ± 0.42
Ex. Kurtosis	−1.27	0.80 ± 1.44	0.09	2.20 ± 2.39

Table 3.3: **Main statistics of the experimental distributions and non-parametrically inferred priors (Exps. 1 and 2; Skewed feedback).** Comparison between the main statistics of the 'objective' experimental distributions and the 'subjective' priors non-parametrically inferred from the data. The subjective moments are computed by averaging the moments of sampled priors pooled from all subjects (±1 SD); see Figure 3.7, right column and Methods for details. In statistics, the excess kurtosis is defined as kurtosis −3, such that the excess kurtosis of a normal distribution is zero. Heavy tailed distributions have a positive excess kurtosis.

we considered a straightforward extension of our model which added the possibility of occasional mistakes.

We extended the Bayesian observer model described by Eqs. 3.1 and 3.2 by introducing for each subject in Exps. 1 and 2 a third continuous parameter, the *lapse rate* λ (Wichmann and Hill, 2001; Kuss et al., 2005). For each trial, the observer has some probability λ of ignoring the current stimulus and responding with uniform probability over the range of allowed responses – a very simple model of outliers due to mistakes. The response probability with lapse is:

lapse rate

$$\Pr_{\text{lapse}}(r|s; w_s, w_m, \lambda) = \lambda \frac{1}{L} + (1-\lambda) \Pr(r|s; w_s, w_m), \tag{3.10}$$

where L is the allowed response window duration (which is block-dependent, see Data Analysis in Section 3.2.1). By using Eq. 3.10 in Eq. 3.9 we computed the marginal likelihood of models with lapse. We took a Beta(1, 9) prior for λ that mildly favours small values of the lapse parameter (Kuss et al., 2005). As before, we extracted the most supported model components and subsequently inferred the subjective priors.

The excess kurtosis for the observers with lapse, computed by averaging the moments of sampled priors pooled from all subjects, was (mean ±1 SD): 0.85 ± 1.30

(Short Uniform), 0.70 ± 1.01 (Long Uniform); 0.91 ± 1.57 (Medium Uniform), 1.87 ± 1.84 (Medium Peaked); as opposed to a true excess kurtosis of -1.27 (Uniform blocks) and 0.09 (Peaked block). The average moments of the reconstructed priors did not differ significantly from the ones computed with the basic model without lapse (see Table 3.3), and in particular the kurtosis was similar, being in general systematically higher than the true distribution kurtosis, and still quite variable.

In terms of marginal likelihood, generally the models with lapse performed better than the original models, but with no qualitative difference in the preferred model components. Crucially, the kurtosis of the recovered priors was still in disagreement with the true value, ruling out the possibility that the heightened kurtosis had been caused by trivial outliers. We will consider other possibilities in the Discussion, Section 3.4.

Non-quadratic loss function

Our basic model assumed a quadratic (or pseudo-quadratic) loss function that was obtained by squaring the subjective error map $\widetilde{f}(r,s)$. The exponent 2 allowed a semi-analytical solution of Eq. 3.1, which made tractable the problems of: (a) computing the marginal likelihood for a relatively large class of models; and (b) non-parametrically inferring the subjects' priors. However, previous work has shown that people in sensorimotor tasks may be instead following a subquadratic loss function (Körding and Wolpert, 2004b).

For the sake of completeness, we explored an extended model with non-quadratic loss functions. For computational reasons we could not perform a full Bayesian model comparison, but we considered only the 'best' observer model per subject. For each subject we chose the most supported model components for the sensory and motor noise and the shape of the subjective error mapping (Standard, Skewed or Fractional), whereas for the prior we took the mean non-parametrically inferred prior (separately for each subject). The exponent of the loss function was now free to vary, so that the equation for the optimal action reads:

$$s^*(x) = \arg\min_{\hat{s}} \int p_{meas}\left(x\,|s;w_s\right) q_{prior}(s)\, p_{motor}\left(r\,|\hat{s};w_m\right) \left|\widetilde{f}(r,s)\right|^{\nu} ds\, dr, \qquad (3.11)$$

where $\nu > 0$ is a continuous free parameter representing the exponent of the loss function. Eq. 3.11 was solved numerically (functions `fminbnd` and `trapz` in MATLAB) for various values of x and then linearly interpolated. Through Eqs. 3.2 and 3.9 we computed for each subject the posterior probability of the exponent $\Pr\left(\nu\,|\mathcal{D}\right) \propto \Pr\left(\mathcal{D}\,|\nu\right) \Pr\left(\nu\right)$, where we assumed an (improper) uniform prior on ν.

Results are shown in Figure 3.8 as a box plot for each subject's inferred ν. Taking the median of the posterior distribution as the inferred value for ν, the exponent averaged across subjects (excluding one outlier) is 1.88 ± 0.06 which is marginally lower than 2 (t-test $t_{(8)} = -2.04$, $p = 0.08$).[3] This result is in qualitative agreement with Körding and Wolpert (2004b) which found that subjects were following a subquadratic loss function (with exponent 1.72 ± 0.03 for a power law). Our average inferred exponent is however higher, and only marginally lower than 2, but this might be due to the fact that the subjects' priors have been inferred under the assumption of a quadratic loss function, and therefore priors may be already 'fitting' some features of the data that were due instead to a subquadratic loss function.

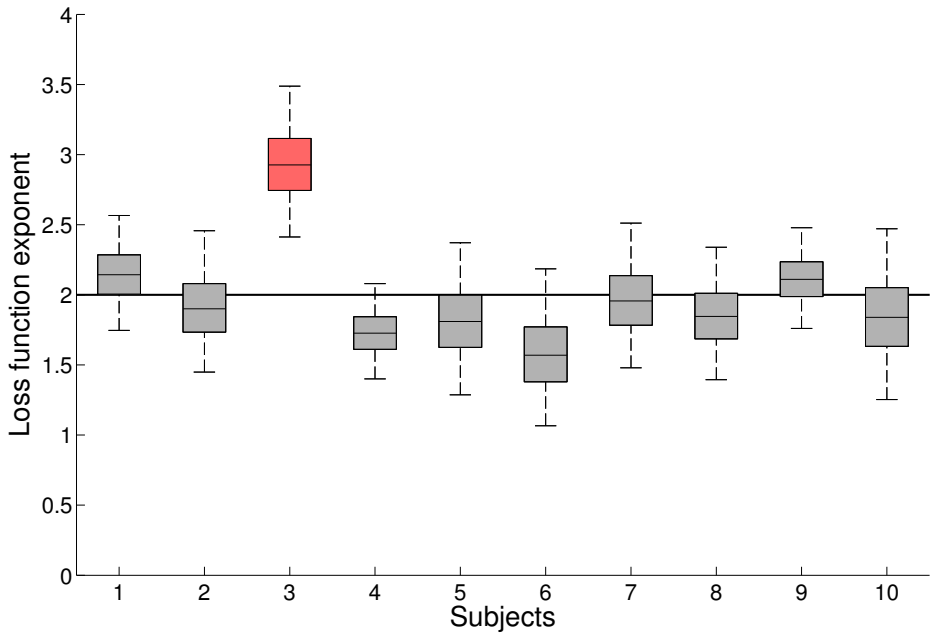

Figure 3.8: **Non-quadratic loss function.** Inferred exponents ν of the loss function for subjects in Exps. 1 (ss 1–4) and 2 (ss 5–10). The box plots have lines at the lower quartile, median, and upper quartile values; whiskers cover 95% confidence interval. Excluding one outlier (s3, in red), the average inferred exponent is marginally lower than 2 ($p < 0.07$).

In conclusion, although we found some support for a slightly subquadratic loss function, our analysis did not find significant evidence to reject the quadratic exponent in the loss, suggesting that $\nu \approx 2$ represents a viable approximation which we keep using in the rest of the work.

3 Taking the mean of the posterior instead of the median renders analogous results.

3.3.3 *Analysis of sensorimotor noise*

A complete study of Bayesian behaviour requires an accurate analysis of the properties of sensorimotor noise of the observers (see Sections 2.2 and 2.4.4). In this section we describe a set of additional experiments and analyses which tested various hypotheses about our subjects' sensorimotor noise.

Measuring sensory and motor noise

The sensory (estimation) and motor (reproduction) noise distributions in our observer model are represented by normal distributions whose SD (either constant or 'scalar', Figure 3.3 i and ii) is governed by the two parameters w_s, w_m. Here we examine whether the parameter values w_s, w_m inferred from the data correspond to direct measures of sensory and motor variability.

For each subject in Exps. 1 and 2 we computed the posterior distribution of w_s, w_m as a weighted average over all models, and took the mean of the posterior as the 'model-inferred' sensory and motor variability for that subject. We examined whether the model-inferred values corresponded to direct measures of sensory and motor variability (w'_s, w'_m) obtained in separate experiments. We directly estimated each subject's sensory variability in a 2AFC time interval discrimination task, and analogously we directly estimated the subjects' motor variability in a time interval 'production' task (see Experimental procedures, Section 3.2.1, for details). For each subject we built simple ideal observer models of the discrimination and production tasks in which the sensory and motor variability could either be constant or scalar (according to the results of the model comparison in the main experiment). We computed the posterior distributions of the sensory and motor noise parameters, and took the mean of these posteriors as the 'directly-measured' noise parameters (w'_s, w'_m).

The comparison between the model-inferred values and the directly-measured ones is shown in Figure 3.9 for the sensory (left) and motor (right) noise parameters. For sensory variability, we found that w'_s had a good correlation ($R^2 = 0.77$) with w_s, and the group means were in good agreement ($\overline{w_s} = 0.157 \pm 0.002$, $\overline{w'_s} = 0.166 \pm 0.009$). For the motor variability, the group means were quantitatively similar, even though in slight statistical disagreement ($\overline{w_m} = 0.072 \pm 0.001$, $\overline{w'_m} = 0.078 \pm 0.001$), but we did not find a correlation between w'_m and w_m (see Discussion).

These results suggest that the model parameters for the noise properties extracted from the full model were in agreement with independent measures of these noise properties in isolation. Interestingly, independent measurements of the sensory noise had predictive power on the subjects' performance even at the individual level, due to the good correlation with the sensory model parameter. The lack of correlation

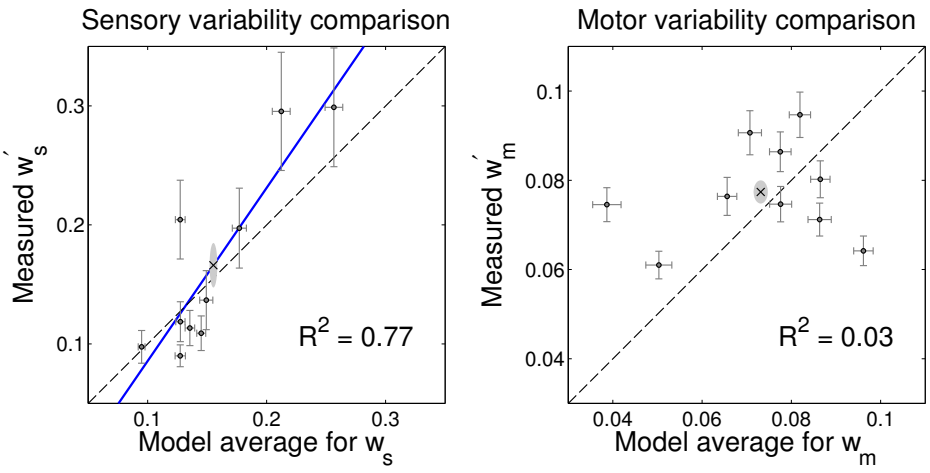

Figure 3.9: **Comparison of sensory and motor noise parameters (main experiment vs direct measurements).** For each participant of Exps. 1 and 2 ($n = 10$) we directly measured the sensory (w'_s) and motor (w'_m) variabilities. For each subject we also calculated the model-averaged parameters w_s and w_m that appear in our Bayesian ideal observer model. The parameters are compared in the figure, (w_s, w'_s) to the left and (w_m, w'_m) to the right. Each dot is a participant's parameter mean ± 1 SD. The group means are plotted as crosses (shaded area 95% confidence interval). The continuous line is a linear fit.

for the motor noise parameter at the individual level may have been due to other noise factors, not contemplated in the model, that influenced the variance of the produced response (e. g. noise in the decision making process, non-Gaussian likelihoods, deviations from the exact scalar property, etc.).

Internal knowledge of sensory variability

Our modelling framework allowed us to ask whether subjects 'knew' their own sensory variability in the task (see Section 2.2.2). We extended our original model by introducing a distinction between the objective sensory variability w_s and the subjective estimate the Bayesian observer had of its value, $\widetilde{w}_s$. The computation of the optimal action was modified accordingly:

$$s^*(x) = \arg\min_{\hat{s}} \int p_{meas}\left(x \,|s; \widetilde{w}_s\right) q_{prior}(s) p_{motor}\left(r \,|\hat{s}; w_m\right) \widetilde{f}^2(r,s)\, ds\, dr, \qquad (3.12)$$

which is almost identical to Eq. 3.1, but note that the expected loss depends now on the subjective value $\widetilde{w}_s$ instead of w_s. The other equations of the model remained unchanged as they depend on the objective sensory noise.

We performed a full Bayesian model comparison with the extended model, where all components (likelihoods, prior, loss function) were free to vary as per the basic model comparison, the only difference being the presence of three continuous pa-

rameters ($w_s, w_m, \widetilde{w}_s$) and Eq. 3.12. Results of the model comparison showed that the extended models performed comparably or slightly worse than the original models in terms of marginal likelihood (average difference in log marginal likelihood: -5.3 ± 2.9; paired t-test $t_{(9)} = -1.83$, $p = 0.10$), meaning that the additional parameter did not provide any significant advantage for explaining the data. This result suggests that most subjects had a reasonably accurate estimate of their own sensory variability.

Note that an analogous study for the motor variability is not feasible with our dataset as the problem becomes in this case under-constrained (see Section 2.4.4). In fact, if we separate the objective motor variability w_m from its subjective estimate $\widetilde{w}_m$, some observer models do not even depend on $\widetilde{w}_m$ (e. g., an observer with constant motor likelihood and Standard loss function), and others show only a weak dependence. In order to meaningfully test whether people 'knew' their own motor variability a much stronger asymmetry in the loss function is needed, along with some other experimental manipulations (see for instance Hudson et al., 2008).

3.3.4 *Experiments 3, 4 and 5*

We performed a series of additional experiments that ask specific questions about subjects' behaviour with a different loss function and with more complex distributions.

Exp. 3: Effect of the shape of feedback on the loss function

In our ideal observer model we compared three candidate loss functions: Skewed, Standard and Fractional (Figure 3.3 iv). The results of the model comparison in the first two experiments with Skewed feedback showed that there was a good match between experimentally provided feedback and subjective error metric. However, we could not rule out the possibility, albeit unlikely, that participants were ignoring the experimental feedback and following an internal error signal that just happened to be similar in shape to the Skewed error. We, therefore, performed an additional experiment to verify that subjects behaviour is driven by the feedback provided.

We again used a Medium Uniform block but now with Standard error $f(r, s) \propto r - s$ as feedback (see Figure 3.10). The model comparison for this group showed that the responses of 4 subjects out of 6 were best explained with a Standard loss function. Moreover, no subject appeared to be using the Skewed loss function (Table 3.2). These results confirm that most people correctly integrate knowledge of results with sensory information in order to minimize the average (squared) error, or an empirically similar metric. Furthermore, all inferred individual priors showed a remarkable

agreement with a smoothed approximation of the experimental distribution of intervals (Figure 3.11 top), suggesting that the Standard error feedback may be easier to use for learning. As in the previous experiments, the average moments of the inferred priors (up to skewness) were statistically indistinguishable from those of the true distribution, with a significant difference in the kurtosis (Table 3.4 left; Hotelling's T^2 test, first three moments: $p > 0.95$; first four moments: $p < 10^{-7}$).

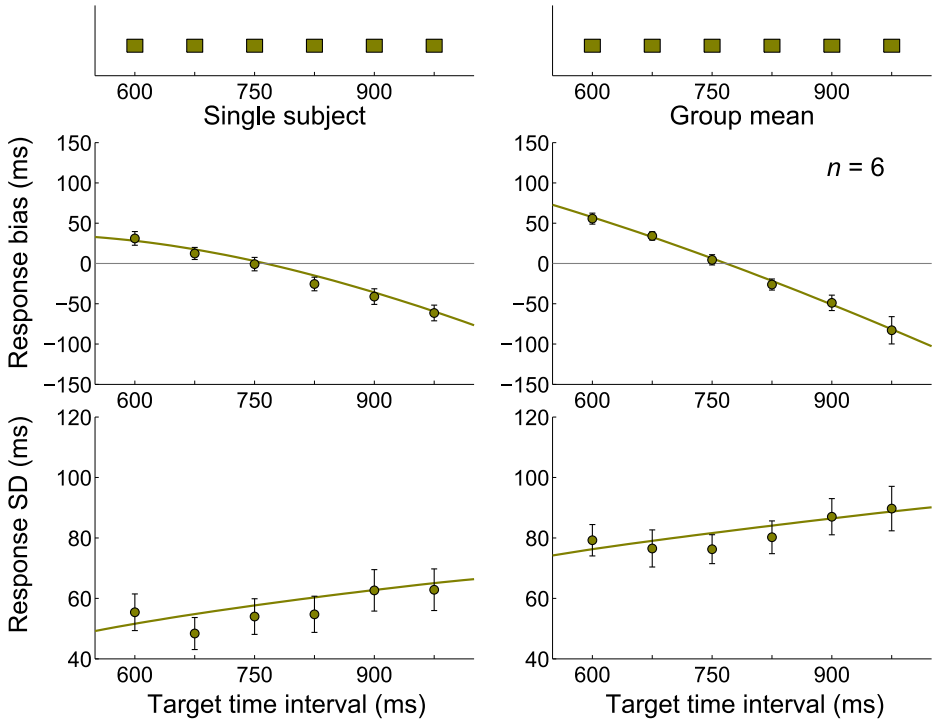

Figure 3.10: **Exp. 3: Medium Uniform block with Standard feedback.** *Very top:* Experimental distribution for Medium Uniform block, repeated on top of both columns. *Left column:* Mean response bias (top) and SD of the response (bottom) for a representative subject. Error bars denote SEM. Continuous lines represent the Bayesian model fit. *Right column:* Mean response bias (top) and SD of the response (bottom) across subjects (mean ± SEM across subjects). Continuous lines represent the Bayesian model fit averaged across subjects.

Exp. 4: High-Peaked distribution

In the Peaked block we did not observe any significant divergence from the Bayesian prediction. However, the ratio of presentations of 'peak' intervals (675 ms) to the others was low (1.4) and possibly not enough to induce other forms of temporal adaptation (Heron et al., 2009, 2012). To examine whether we might see deviations from Bayesian integration for larger ratios we therefore tested another group of subjects on a more extreme variant of the Peaked distribution in which the peak stimulus had a probability of $p \approx 0.8$ and therefore a ratio of about 4.0. We provided feedback

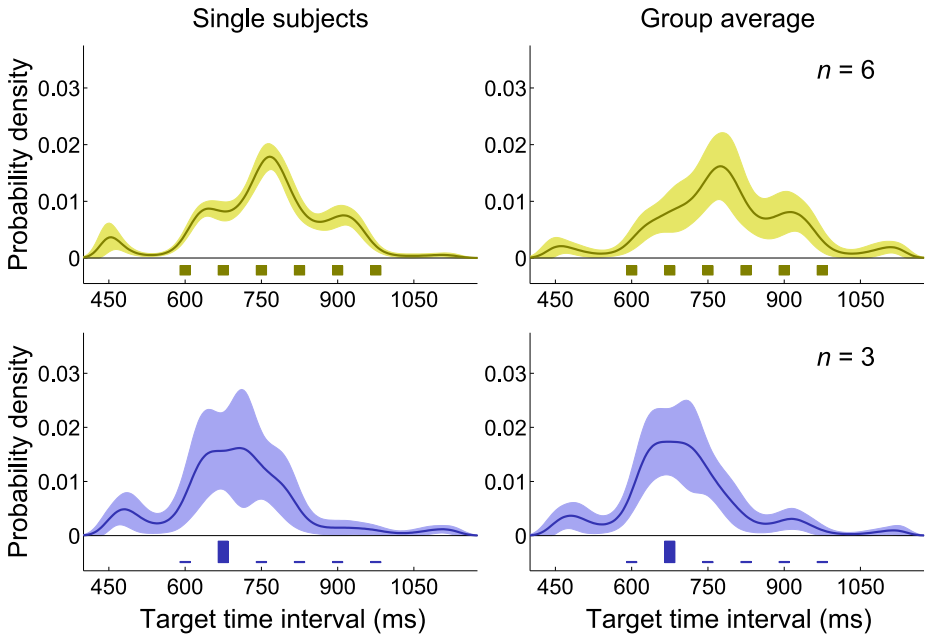

Figure 3.11: **Non-parametrically inferred priors (Exps. 3 and 4).** *Top row:* Medium Uniform (light brown) block. *Bottom row:* Medium High-Peaked (dark blue) block. *Left column:* Non-parametrically inferred priors for representative participants. *Right column:* Average inferred priors. Shaded regions are ± 1 SD For comparison, the discrete experimental distributions are plotted under the inferred priors.

	Medium Uniform		Medium High-Peaked	
	Objective	Subjective	Objective	Subjective
Mean (ms)	787.5	782.6 ± 18.7	703.1	702.0 ± 17.9
SD (ms)	128.1	131.7 ± 13.6	80.5	119.5 ± 17.9
Skewness	0	0.03 ± 0.30	2.25	0.67 ± 0.37
Ex. Kurtosis	−1.27	0.42 ± 0.53	−0.86	1.66 ± 1.32

Table 3.4: **Main statistics of the experimental distributions and non-parametrically inferred priors (Exps. 3 and 4; Standard feedback).** Comparison between the main statistics of the 'objective' experimental distributions and the 'subjective' priors non-parametrically inferred from the data. The subjective moments are computed by averaging the moments of sampled priors pooled from all subjects (±1 SD); see Figure 3.11, right column and Section 3.2.3 for details.

through the Standard error mapping, as the previous experiment had showed that subjects can follow it at least as well as the Skewed mapping.

Due to the large peak interval presentation frequency we had fewer test data points in the model fitting. Therefore, we constrained the model comparison by only considering the Standard loss in order to prevent the emergence of spurious model components capturing random patterns in the data. We found that the recovered internal priors were in good qualitative agreement with the true distribution, with statistically indistinguishable means (Figure 3.11 bottom, and Table 3.4; one sample two-tailed t-test $p > 0.90$). When variance and higher moments were included in the analysis, though, the distributions were significantly different (Hotelling's T^2 test, mean and variance: $p < 0.05$; first three moments: $p < 0.01$; first four moments: $p < 10^{-7}$) suggesting that the distribution may have been 'too peaked' to be learnt exactly; see Discussion. Nevertheless, the observed biases of the responses were well explained by the standard Bayesian models (group mean: $R^2 = 0.95$), and the SDs were in qualitative agreement with the data (Figure 3.12).

Exp. 5: Bimodal distributions

Our previous experiments show that people are able to learn good approximation of flat or unimodal distributions of intervals relatively quickly (a few sessions), under the guidance of corrective feedback. Previous work in sensorimotor learning (Körding and Wolpert, 2004a) and motion perception (Chalk et al., 2010) has shown that people can learn bimodal distributions (see Section 2.3.2). Whether the same is attainable for temporal distributions is unclear; a recent study of time interval reproduction (Ryan, 2011) obtained less definite results with a bimodal 'V-shaped' distribution, although

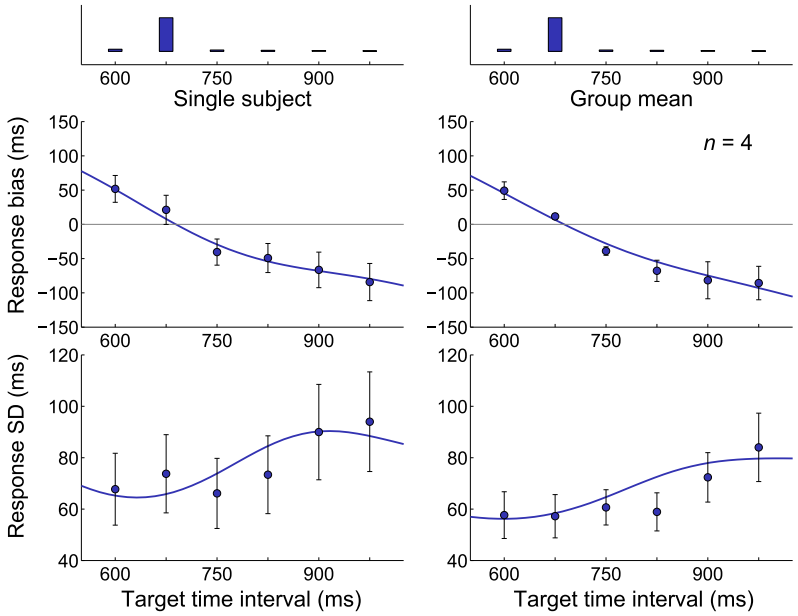

Figure 3.12: **Exp. 4: Medium High-Peaked block.** *Very top:* Experimental distribution for Medium High-Peaked block, repeated on top of both columns. *Left column:* Mean response bias (top) and SD of the response (bottom) for a representative subject. Error bars denote SEM. Continuous lines represent the Bayesian model fit. *Right column:* Mean response bias (top) and SD of the response (bottom) across subjects (mean ± SEM across subjects). Continuous lines represent the Bayesian model fit averaged across subjects.

training might have been too short, as subjects were exposed only to 120 trials in total and without performance feedback.

To examine whether subjects could easily learn bimodality of a temporal distribution with the help of feedback we tested two new groups of subjects on bimodal distributions of intervals on a Medium range (600–975 ms, as before) and on a Wide range (450–1125 ms), providing in both cases Standard feedback. In the Medium Bimodal block the intervals at 600 and 975 ms had each probability $p = 4/12$, whereas the other four middle intervals (675, 750, 825, 900 ms) had each probability $p = 1/12$. In the Wide Bimodal block the six 'extremal' intervals (450, 525, 600 ms and 975, 1050, 1125 ms) had each probability $p = 4/28$ whereas the middle intervals had probability $p = 1/28$. Note that in both cases extremal intervals were four times as frequent as middle intervals.

In the Medium Bimodal block, subjects' responses exhibited a typical central tendency effect (Figure 3.13 top left) which suggests that people did not match the bimodality of the underlying distribution. To constrain the model comparison we inferred the subjects' priors under the assumption of scalar sensory and motor noise models and Standard loss function, as found by our previous analyses. As before, we

first used a discrete set of priors (see Modelling, Section 3.2.3) that we used to compute the model fit to the data and then we performed a non-parametric inference. The non-parametrically inferred priors for the Medium Bimodal distribution (Figure 3.13 top right) suggest that on average subjects developed an internal representation that differed from those seen in previous experiments and, as before, we found a good agreement between moments of the experimental distribution and moments of the inferred priors up to skewness (Table 3.5 left). However, results of the Bayesian model comparison among a discrete class of flat, unimodal or bimodal priors do not support the hypothesis that subjects actually learnt the bimodality of the experimental distribution. Part of the problem may have been that in the Medium Bimodal distribution the two modes were relatively close, and due to sensory and motor uncertainty subjects could not gather enough evidence that the experimental distribution was not unimodal (but see Discussion, Section 3.4). We repeated the experiment therefore on a wider range with a different group of subjects.

The pattern of subjects' responses in the Wide Bimodal block shows a characteristic 'S-shaped' bias profile (Figure 3.13 top right) which is compatible with either a flat or a slightly bimodal prior. The non-parametrically inferred priors for the Wide Bimodal distribution (Figure 3.13 bottom right) again suggest that on average subjects acquired, albeit possibly with less accuracy (Table 3.4 right), some broad features of the experimental distribution; however, individual datasets are quite noisy and again we did not find strong evidence for learning of bimodality.

Our results with bimodal distributions confirm our previous finding that people seem to be able to learn broad features of experimental distributions of intervals (mean, variance, skewness) with relative ease (a few sessions of training with feedback). However, more complex features (kurtosis, bimodality) seem to be much harder to learn (see Discussion, Section 3.4).

	Medium Bimodal		Wide Bimodal	
	Objective	Subjective	Objective	Subjective
Mean (ms)	787.5	794.5 ± 34.2	787.5	822.1 ± 70.7
SD (ms)	160.6	155.7 ± 37.2	251.6	219.2 ± 29.3
Skewness	0	−0.33 ± 0.39	0	−0.22 ± 0.57
Ex. Kurtosis	−1.72	−0.08 ± 0.90	−1.64	−0.40 ± 0.51

Table 3.5: **Main statistics of the experimental distributions and non-parametrically inferred priors for bimodal distributions (Exp. 5; Standard feedback).** Comparison between the main statistics of the 'objective' experimental distributions and the 'subjective' priors non-parametrically inferred from the data. The subjective moments are computed by averaging the moments of sampled priors pooled from all subjects (±1 SD); see Figure 3.13, bottom and Methods for details.

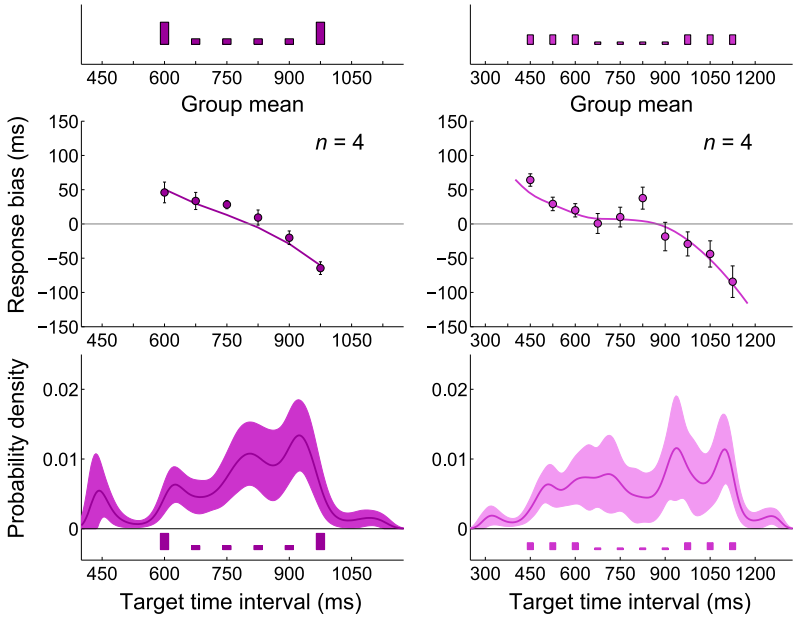

Figure 3.13: **Exp. 5: Medium Bimodal and Wide Bimodal blocks, mean bias and non-parametrically inferred priors.** *Very top:* Experimental distributions for Medium Bimodal (dark purple, left) and Wide Bimodal (light purple, right) blocks. *Top:* Mean response bias across subjects (mean ± SEM across subjects) for the Medium Bimodal (left) and Wide Bimodal (right) blocks. Continuous lines represent the Bayesian model 'fit' averaged across subjects. *Bottom:* Average inferred priors for the Medium Bimodal (left) and Wide Bimodal (right) blocks. Shaded regions are ±1 SD. For comparison, the experimental distributions are plotted again under the inferred priors.

3.4 DISCUSSION

Our main finding is that humans, with the help of corrective feedback, are able to learn various statistical features of both simple (uniform, symmetric) and complex (peaked, asymmetric or bimodal) distributions of time intervals. In our experiments, the inferred internal representations were smooth, heavy tailed approximations of the experimental distributions, in agreement typically up to third-order moments. Moreover, our results suggest that people take into account the shape of the provided feedback and integrate it with knowledge of the statistics of the task in order to perform their actions.

The statistics of the responses of our subjects in the Uniform blocks were consistent with results from previous work; in particular, we found biases towards the mean of the range of intervals (central tendency; Hollingworth, 1910; Jones and Mcauley, 2005; Jazayeri and Shadlen, 2010; Cicchini et al., 2012) and the variability of the responses grew roughly linearly in the sample interval duration (scalar property; Lewis and Miall, 2009; Jazayeri and Shadlen, 2010). The responses in the Peaked and High-Peaked blocks showed analogous biases, but they were directed towards the mean of the distribution rather than the mean of the range of intervals (the two means overlap in the Uniform case) (Ryan, 2011). We also observed a significant reduction in variability at the peak. These results show that subjects considered the temporal statistics of the context in their decision-making processes. We found a similar regression to the mean for a 'narrow' bimodal distribution (Medium Bimodal), in qualitative agreement with previous work that found a simple central tendency with a 'V-shaped' temporal distribution (Ryan, 2011; although with very limited training, no feedback and a suprasecond range). However, for a bimodal distribution on a wider range we observed 'S-shaped' biases which seem compatible with a nonlinear decision making process (Körding and Wolpert, 2004a). More refined conclusions needed the support of a formal framework.

3.4.1 *Validation of the Bayesian model*

Our modelling approach consisted of building a family of Bayesian observer and actor models, which provided us with a mathematical structure in which to ask specific questions about our subjects (Battaglia et al., 2011), going beyond mere statements about Bayesian optimality. In particular, we were interested in (1) whether people would be able to learn nontrivial temporal distributions of intervals and what approximations they might use, and (2) how their responses would be affected by performance feedback, which is related to the implicit loss function of the task. Our

observer model resembled the Bayesian Least Squares (BLS) observer described in Jazayeri and Shadlen (2010), but it explicitly included an action component as part of the internal model. Moreover, to answer (1) we allowed the prior to differ from the experimental distribution, and to study (2) we considered additional shapes for the loss function in addition to the Standard squared loss $\propto (r-s)^2$.

The factorial model comparison (van den Berg et al., 2014) gave us specific answers for the most likely components describing each of our subjects, and a first validation came from the success of the most supported Bayesian observer and actor models in capturing the statistics of the subjects' responses in the task. However, goodness of fit per se is not necessarily an indicator that the components found by the model comparison reflected true findings about the subjects, rather than 'overfitting' arbitrary statistical relationships in the data. This is of particular relevance for Bayesian models, because of the underlying degeneracy among model components (Mamassian and Landy, 2010).

Our approach consisted in considering a large, 'reasonable' set of observer models that we could link to objective features of the experiment. This does not solve the degeneracy problem per se but it prevents the model comparison from finding arbitrary solutions. In particular, the set of experiments was designed in order to provide evidence that each element of the model mapped on to an experimentally verifiable counterpart; crucially, we found that a change in a component of the experimental setup (e. g., experimental distribution and feedback) correctly induced a switch in the corresponding inferred component of the model (prior and loss function). We also avoided overfitting by limiting our basic models to only two continuous noise parameters, which were then computed through model averaging and further validated by independent direct measures.

To further validate our methods, we directly measured the subject's noise parameters (sensory and motor noise, w'_s and w'_m) in separate tasks and compared them with the model parameters w_s, w_m inferred from the main experiments (see Section 3.3.3). The rationale is that, in an idealized situation, we would be able to measure some features of the subjects with an objective, independent procedure and the same features would be predictive of the individual performances in related tasks (Tassinari et al., 2006). The measured parameters were highly predictive of the group behaviour, and reasonably predictive at the individual level for the sensory parameter, confirming that the model parameters were overall correctly representing objective 'noise properties' of the subjects.

Overall, our modelling techniques were therefore validated by (a) goodness of fit, (b) consistency between inferred model components and experimental manipulations,

and (c) consistency between the model parameters and independent measurements of the same quantities.

3.4.2 *Comparison between inferred priors and experimental distributions*

Given the validation of the results of the model comparison, we performed a non-parametric inference of the priors acquired by participants during the task. Other recent works have inferred the shape of subjective 'natural' perceptual priors non-parametrically, such as in visual orientation perception (Girshick et al., 2011) and speed perception (Stocker and Simoncelli, 2006b; Zhang et al., 2013b), but studies that focussed on experimentally acquired priors mostly recovered them under parametric models (see Section 2.3.4). The non-parametric method allowed us to study quantitatively the accuracy of the subjects in learning the experimental distributions, comparing summary statistics such as the moments of the distributions up to fourth order. Note that the significance and reliability of the recovered priors is based on the correctness of our assumptions regarding the observer and actor model; unconstrained priors might capture all sorts of statistical details, one of the typical objections to Bayesian modelling (Jones and Love, 2011; Bowers and Davis, 2012). By being fully Bayesian we reduced the possibility for overfitting, although for reasons of computational tractability we had to divide the model selection stage from the prior reconstruction process.

The internal representations inferred from the data show a good agreement with the central moments of the true distributions typically up to third order (mean, variance and skewness). Subjects however manifested some difficulties in learning variance and skewness when the provided distribution was extremely peaked, with a width less than the subjects' perceptual variability. This discrepancy observed in the High-Peaked block may have arisen because (a) the experimental distribution's standard deviation was equal or lower in magnitude compared to the perceptual variability of the subjects (experimental distribution SD: 80.5 ms; subject's average sensory SD at the mean of the distribution: 96.1 ± 12.1 ms; mean $\pm$ SD across subjects) and (b) due to the shape of the distribution, subjects had much less practice with intervals away from the peak. Another explanation is that subjects' representation of relative frequencies of different time intervals was systematically distorted, with overestimation of small relative frequencies and underestimation of large relative frequencies (see Zhang and Maloney, 2012 for a critical review), but note that this would arguably produce a change in the mean of the distribution as well, which we did not observe.

Moreover, the recovered priors in all blocks had systematically heavier tails (higher kurtosis) than the true distributions. It must be noted that the kurtosis, being the fourth-order central moment, is highly sensitive to random fluctuations in the data and its error is positively skewed (outliers will tendentially *increase* the observed kurtosis). Therefore, there might be a bias in our reconstruction method that would favour more kurtotic distributions. By exploring an extended model that included lapses we ruled out that this particular result was due to trivial outliers in our datasets. However, our results are compatible with more sophisticated lapse models and with other reasons for the heavy tails we recovered, in particular (a) the noise distributions might be non-Gaussian, with heavier tails (Natarajan et al., 2009), and (b) the loss functions might follow a less-than-quadratic power law (Körding and Wolpert, 2004b). For the latter hypothesis we found some evidence, although inconclusive, by studying observer models with non-quadratic loss functions (Section 3.3.2). Experimentally, both (a) and (b) would imply that in our datasets there would be more outliers than we would expect from a Gaussian noise model with quadratic losses.

Our experiments with bimodal distributions show that, although people's responses were affected by the experimental distribution of intervals in a way which is clearly different from our previous experiments with uniform or peaked distributions, the inferred priors in general fail to capture bimodality and are consistent instead with a broad uniform or multimodal prior (where the peaks however do not necessarily fall at the right places). Note that the average sensory standard deviation for subjects in Exp. 5 was 87 ± 18 ms (Medium Bimodal; mean $\pm$ SD across subjects) and 106 ± 28 ms (Wide Bimodal), calculated at the center of the interval range. In other words, in both blocks, the centers of the peaks were well-separated in terms of perceptual discriminability (on average by at least four SDs). This suggests that most subjects did not simply fail to learn the bimodality of the distributions because they had problems distinguishing between the two peaks.

A formula for approximately-learnt priors

Our work provides substantial evidence that the assumption that observers' priors match the experimental distribution of stimuli is unlikely to hold for non-Gaussian distributions. It would be useful to have a formula for a 'generic' approximately-learnt prior, with a single parameter that can be tuned to govern the amount of approximation. For example, this would be useful to compute a realistic expectation about the behaviour of an observer even *before* running an experiment. A look at our recovered priors (both parametric and non-parametric) combined with theoretical considerations suggest a simple parametric description. Let $p_{exp}(s)$ be a non-Gaussian

empirical distribution with mean μ_{exp} and variance σ^2_{exp}. We propose the following 'generic' expression for an approximately-learnt prior:

$$\tilde{q}_{prior}(s) = (1 - \pi_{app}) \cdot p_{exp}(s) + \pi_{app} \cdot \mathcal{N}\left(s \,\middle|\, \mu_{exp}, \sigma^2_{exp}\right), \tag{3.13}$$

which is a mixture of the empirical distribution (possibly smoothed with a Gaussian kernel), and a Gaussian with mean and variance that match the moments of the true distribution, with mixture weight $0 \leq \pi_{app} \leq 1$. Eq. 3.13 represents a simple model according to which subjects have rapidly learnt mean and variance of the experimental distribution, but have only partially acquired its higher-order features.[4] In Figure 3.14 we fit Eq. 3.13 to our recovered group priors, finding that the approximation, albeit crude, represents the observers' priors considerably better than the experimental distributions. Realistic values of π_{app} in interval timing appear to be in the range 0.5–1. It is possible that the amount of learning is greater in other perceptual domains (see Chapter 6 for discussion).

3.4.3 *Temporal recalibration and feedback*

Lag adaptation is a robust phenomenon for which the perceived duration between two inter-sensory or motor-sensory events shortens after repeated exposure to a fixed lag between the two (Fujisaki et al., 2004; Stetson et al., 2006); see Vroomen and Keetels, 2010 for a review. Even though lag adaptation was initially presented as a 'global' recalibration effect affecting all intervals (e. g., Di Luca et al., 2009), recent work suggests that recalibration may be 'local' and affect only intervals in a neighborhood of the adapter lag (e. g., Roach et al., 2011; Rohde et al., 2014a). A recent study has shown that predictability of the visuo-motor delay is necessary to elicit temporal recalibration in a variety of behavioural measures, from spatio-temporal errors to shifts in the point of subjective simultaneity (Rohde et al., 2014b). What is clear from all these studies is that lag adaptation cannot be interpreted as a simple Bayesian effect in terms of prior expectations represented by the sample distribution of adaptation and test intervals, since its signature is a 'repulsion' from the adapter as opposed to the 'attraction' induced by a prior (Miyazaki et al., 2006; Stocker and Simoncelli, 2006a; Roach et al., 2011).[5]

Our experimental setup for the peaked blocks mimicked the distributions of intervals of typical lag adaptation experiments (Stetson et al., 2006; Heron et al., 2009),

4 By construction, $\tilde{q}_{prior}$ has the same mean and variance as p_{exp}, but other statistical features may deviate depending on π_{app}.

5 Note that temporal recalibration might be explained by a Bayesian model whose parameters are updated over time, for example via a Kalman filter (Burge et al., 2008) or via a structural inference process (Sato et al., 2007; Sato and Aihara, 2009; Acerbi and Vijayakumar, 2011).

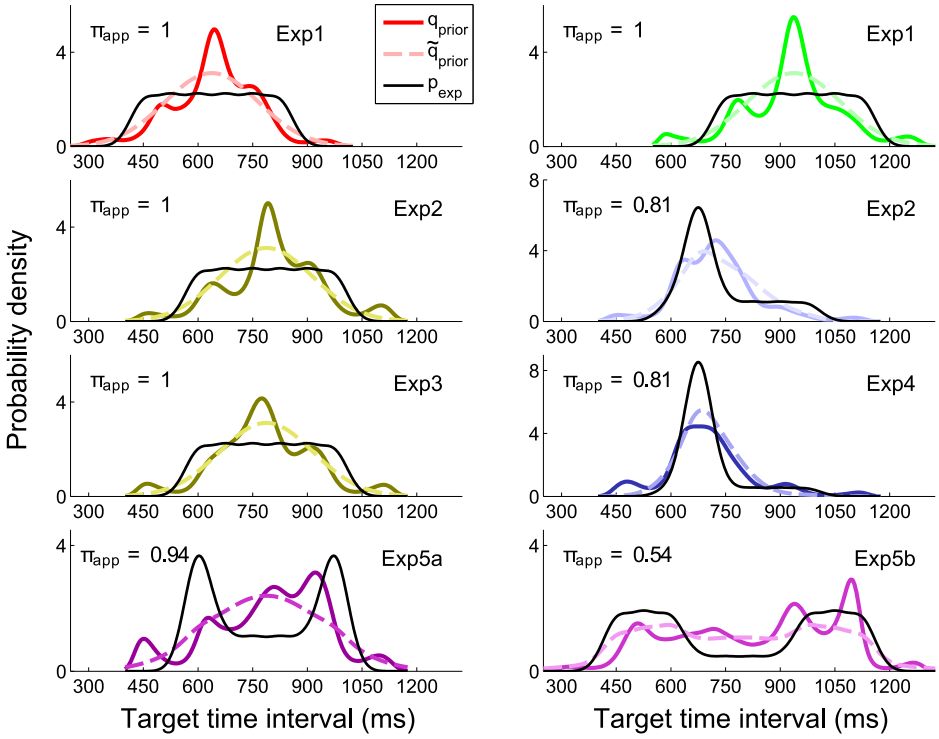

Figure 3.14: **Approximately-learnt priors.** Each panel shows the group mean inferred prior q_{prior} for an experimental condition (continuous coloured line), the best-fitting 'generic' approximate prior $\tilde{q}_{prior}$ (dashed coloured line) and the experimental distribution p_{exp} (black line). The experimental distributions were smoothed with a Gaussian kernel with $\sigma = 37.5$ ms. For each panel we also report the fitted value of π_{app} (see Eq. 3.13). Fits were obtained by minimizing the squared error between distributions (results were analoguous by minimizing the KL-divergence).

with the adapter interval set at 675 ms (the 'peak'). However, we did not detect any noticeable disagreement with the predictions of our Bayesian observer model and, in particular, there was no significant 'repulsion effect' from the peak, neither global nor local. Our results suggest that people are not subject to the effects of lag adaptation, or can easily compensate for them in the presence of corrective feedback.

Sensorimotor lag adaptation seems to belong to a more general class of phenomena of temporal recalibration which induce an adjustment of the produced (or estimated) timing of motor commands to meet the goals of the task at hand. In the case of experimentally induced actuator delays in a time-critical task, such as controlling a spaceship through a minefield in a videogame (Cunningham et al., 2001a) or driving a car in a simulated environment (Cunningham et al., 2001b), visual temporal information about delays provides an obvious, compelling reason to recalibrate the timing of actions (but see Rohde et al., 2014b for a critical analysis). However, feedback regarding timing performance need not be provided only in temporal ways. Previous studies have shown that people take into account performance feedback (knowledge of results) when the feedback about the timing of their motor response is provided in various ways, such as verbal or visual report in milliseconds (Blackwell and Newell, 1996; Franssen and Vandierendonck, 2002) or bars of variable length (Ryan and Robey, 2002). Interestingly, people tend to also follow 'erroneous' feedback (Ryan and Robey, 2002; Ryan et al., 2004; Ryan and Fritz, 2007). However, this can be explained by the fact that people's behaviour in a timing task is goal-oriented (e. g., minimizing feedback error), and therefore these experiments suggest that people are able to follow external, rather than erroneous, feedback. In fact, when participants are told that feedback might sometimes be incorrect, which corresponds to setting different expectations regarding the goal of the task, they adjust their timing estimates taking feedback less into account (Ryan et al., 2004). Ambiguity regarding the goal of a timing task with non-obvious consequences – as opposed to actions that have obvious sensorimotor consequences, such as catching a ball – can be reduced by imposing an explicit gain/loss function (Mamassian, 2008; Hudson et al., 2008), and it has been found that people can act according to an externally presented asymmetric cost, even though their timing behaviour is not necessarily 'optimal' (e. g., Mamassian, 2008; see Section 2.4.2).

Our work extends these previous findings by performing a model comparison with different types of symmetric and asymmetric loss functions and providing additional evidence that most people are able to correctly integrate an arbitrary external feedback in their decision process, while executing a sensorimotor timing task, so to minimize the feedback error.

3.4.4 *Bayesian sensorimotor timing*

There is growing evidence that many aspects of human sensorimotor timing can be understood in terms of Bayesian decision theory (Miyazaki et al., 2005; Hudson et al., 2008; Jazayeri and Shadlen, 2010; Cicchini et al., 2012); see Shi et al. (2013a) for a review. The mechanism through which people build time estimates, e.g. an 'internal clock', is still unclear (Grondin, 2010), but it has been proposed that observers may integrate both internal and external stochastic sources of temporal information in order to estimate the passage of time (Ahrens and Sahani, 2011; Hass and Herrmann, 2012).

Motivated by these results, in our work we assumed that people build an internal representation of the temporal distribution of intervals presented in the experiment. However, for all timing tasks in which more or less explicit knowledge of results is given to the subjects (e. g., ours, Jones and Mcauley, 2005; Jazayeri and Shadlen, 2010), an alternative explanation is that people simply learn a mapping from a duration measurement to a given reproduction time (strategy known as *table look-up*), with no need of learning of a probability distribution (Maloney and Mamassian, 2009). At the moment we cannot completely discard this possibility, but other timing studies have shown that people perform according to Bayesian integration even in the absence of feedback both for simple (Miyazaki et al., 2006; Cicchini et al., 2012) and possibly skewed distributions (Ryan, 2011), suggesting that people indeed take into account the temporal statistics of the task in a context-dependent way. Moreover, previous work in motor learning in the spatial domain has shown that people do not simply learn a mapping from a stimulus to a response, but adjust their performance according to the reliability of the sensory information (Körding and Wolpert, 2004a), a signature of probabilistic inference (Ma, 2012). Analogous findings have been obtained in multisensory integration (Ernst and Banks, 2002; Alais and Burr, 2004; Beierholm et al., 2009) and for visual judgements (an 'offset' discrimination task) under different externally imposed loss functions (Whiteley and Sahani, 2008), crucially in all cases without knowledge of results (see Chapter 2). All these findings together support the idea that sensorimotor learning follows Bayesian integration, also in the temporal domain. However, the full extent of probabilistic inference in sensorimotor timing needs further study, possibly involving transfer between different conditions in the absence of knowledge of results (Maloney and Mamassian, 2009).

Our results answer some of the questions raised by Jazayeri and Shadlen (2010), in particular about the general shape of the distributions internalized by the subjects and the influence of feedback on the responses. An avenue for further work is related to the detailed profile of the likelihoods and possible departures from the scalar

property (Lewis and Miall, 2009; Zarco et al., 2009; Laje et al., 2011), especially in the case of complex experimental distributions. It is reasonable to hypothesize that strongly non-uniform samples of intervals might affect the shape of the likelihood itself, if only for the simple reason that people practice more on some given intervals. Cognitive, attentional and adaptation mechanisms might play various roles in the interaction between non-uniform priors and likelihoods, in particular without the mitigating effect of knowledge of results. A relatively less explored but important research direction involves extending the model to a biologically more realistic observer and actor model, examining the connections with network dynamics (Karmarkar and Buonomano, 2007; Buonomano and Laje, 2010) or population coding (Heron et al., 2012; Cai et al., 2012), bridging the gap between a normative description and mechanistic accounts of time perception. Another extension of the model would consider a non-stationary observer, whose response strategy changes from trial to trial (even after training), possibly in order to account for sequential effects of judgement which may be due to an iterative update of the prior (Stewart et al., 2005; Petzschner and Glasauer, 2011; Saunders and Vijayakumar, 2012; Raviv et al., 2012).

Finally, whereas our analysis suggests that subjects found it relatively easy to learn unimodal distributions of intervals, bimodal distributions seemed to represent a much harder challenge. The fact that subjects developed non-linear biases suggest that their behaviour was affected by the experimental distribution of intervals, but it is unclear whether they had a major problem in learning the bimodal statistics, or in performing correct probabilistic inference. In the next chapter, we will investigate what may be the sources of subjects' apparent suboptimal performance in the presence of complex distributions.

4

TARGET ESTIMATION WITH COMPLEX PROBABILISTIC INFORMATION

> "Queenie, Queenie who's got the ball?
> Are they short, or are they tall?
> Are they hairy, or are they bald?
> You don't know because you don't have the ball!"
>
> — *Queenie, Queenie, who's got the ball?*
> A common children's probabilistic inference game

In this chapter we explore the sources of suboptimality in sensorimotor probabilistic computations by means of a novel estimation task that requires observers to perform Bayesian inference with explicitly provided distributions, thereby removing the difficulty of learning a prior. This work was originally published in *PLoS Computational Biology* (Acerbi et al., 2014b).

4.1 PROBABILISTIC COMPUTATIONS IN SENSORIMOTOR DECISION MAKING

We have seen in Chapter 2 that a large body of work supports the idea that human sensorimotor decision making qualitatively conforms to the predictions of BDT in taking into account sensory uncertainty (Section 2.2), relevant statistics of the context and previous experience (Section 2.3), and implicit or explicit goals of the task at hand (Section 2.4). Agreement with the theory is striking in several 'simple' cases with mostly Gaussian statistics and linear operations on the variables of the task, but it is also easy to find numerous examples with slightly more complex settings in which deviations from optimal behaviour are observed (see Chapter 2). An analogous pattern appeared in our time interval reproduction experiments in Chapter 3. Subjects' behaviour qualitatively aligned with the predictions of BDT but their performance was generally far from optimal given the true experimental distributions of stimuli and subjects' sensorimotor noise. Observed performance was compatible with an approximate representation of the prior that failed to capture complex features of the experimental distribution (see Section 3.4).

Bayes-optimal decision making can be abstractly divided in two separate processes: acquisition and representation of the relevant statistics of the task (priors, likelihoods, loss functions) and probabilistic computations with such representations (inference

and action selection via minimization of the expected loss). In most psychophysical studies that look at human performance in the presence of complex statistics, however, there is a difficulty in separating any constraints and idiosyncrasies in performing Bayesian computations per se from any deficiencies in learning and recalling the correct prior. For example, we have described human performance under bimodal distributions of stimuli (see 'Complex contextual priors' in Section 2.3.2 and 'Exp. 5: Bimodal distributions' in Section 3.3.4). Here the normative prescription of Bayesian integration under a wide variety of assumptions would be that responses should be biased towards one peak of the distribution or the other, depending on the current sensory information. However, for such bimodal priors, the emergence of Bayesian biases can require thousands of trials (Körding and Wolpert, 2004a) or be apparent only on pooled data (Chalk et al., 2010), and often data show at best a complex pattern of biases which is only in partial agreement with the underlying distribution (Gekas et al., 2013 and our results, see Figure 3.13). It is unknown whether this mismatch is entirely due to the difficulty of learning statistical features of the bimodal distribution, or there are significant additional limitations in performing Bayesian computations even when the prior is fully learnt.

In order to tease out the sources of suboptimality in human probabilistic inference, we need either to ensure that observers perfectly know the prior, or design the task so that the need of learning the prior does not arise in the first place. Here we follow the latter path and investigate how human observers compute with probabilistic information that is provided on a trial-by-trial basis. Previous work in movement planning under risk suggests that humans are better decision makers with probabilities implicit in a sensorimotor task than with numerically communicated probabilities in a similar economic task (see Maloney et al., 2007; Trommershäuser et al., 2008a for a review). It is actually unclear whether this apparent gap is true or an artifact of methodological differences between fields (Maloney et al., 2007; Wu et al., 2009), as supported by recent work (Jarvstad et al., 2013, 2014). Nonetheless, we avoid numerical information and we choose to communicate probability distributions via a visual representation, motivated by work on movement planning under risk that suggests that humans can integrate visually provided costs so as to nearly maximize expected gain (see Section 2.4.2).

Only a few previous studies looked specifically at how human observers manipulate visually provided probabilistic information in a sensorimotor task. Tassinari et al. (2006) displayed prior information about the target position in a pointing task as a two-dimensional Gaussian cloud on the screen. The distribution remained fixed for the whole duration of the experiment, so the graphical representation likely served as a visual aid to consolidate the prior that was learnt with practice. Assuming that

subjects had a good representation of the experimental distibution (due to extensive training and visual feedback), the authors identified several additional sources of suboptimality in the observers' behaviour (Tassinari et al., 2006). A stronger test for Bayesian computations requires probability distributions to change every trial (Ma, 2012). Hudson et al. (2007) tested subjects in a rapid pointing task in which the target, a vertical bar, would appear only at midpoint during movement. Before movement, observers were graphically provided with probabilistic information about the target bar location among a number of possible locations (9 or 7 locations, depending on the experiment). Prior probability was conveyed via the density of bright pixels within each possible target location. Different subjects performed in two experiments with distinct sets of distributions that were randomly presented each trial. The 'location' experiment used five prior distributions that had a single peak with $p = 0.68$ on one of the five central locations and were equally low on the other eight locations ($p = 0.04$). In the 'scale' experiment, three distributions were used that had uniformly high probability in a central region of varying width (1, 3 or 5 bars) and low probability elsewhere. Given the complexity of the kinematics and dynamics of the pointing task, the authors could not build a full observer and actor model, but instead devised a number of necessary conditions for statistical optimality in the task. Their analyses could not reject optimality for the 'location' condition, that tested how subjects computed with probabilistic information about the mode of the distribution. However, they rejected optimality for the 'scale' condition which tested how people took into account information about the spread of the distribution. In another study, Seydell et al. (2008) showed that subjects could sensibly integrate visually provided probabilistic information about the future location of reward/penalty areas. Note that the authors described the task as having a stochastic loss function, but an equivalent formulation comprehends a deterministic loss function and probabilistic prior information about target configurations (see Section 2.4.2).

These studies suggest that we may use visually provided 'prior' information as an experimental means to investigate the extent to which human observers perform probabilistic inference on complex distributions, beyond simple Gaussians, and the algorithms and approximations they might adopt (see Section 2.4.5).

4.1.1 *Summary*

In this chapter we look systematically at how people integrate uncertain cues with trial-dependent 'priors' in a target estimation task. A 'prior' here is a complex visual cue providing explicit probabilistic information about the unknown target location. The priors were displayed as an array of potential targets distributed according to

various density classes – Gaussian, unimodal or bimodal. Our paradigm affords full control over the generative model of the task and separates the aspect of computing with a probability distribution from the problem of learning and recalling a prior.

We examined subjects' performance in manipulating probabilistic information as a function of the shape of the prior. Participants' behaviour in the task was in qualitative agreement with Bayesian integration, although quite variable and generally suboptimal, but the degree of suboptimality did not differ significantly across different classes of distributions or levels of reliability of the cue. In particular, performance was not greatly affected by complexity of the distribution per se – for instance, people's performance with bimodal priors was analogous to that with Gaussian priors, in contrast to previous learning experiments. This finding suggests that major deviations encountered in previous studies are likely to be primarily caused by the difficulty in learning complex statistical features rather than computing with them.

We systematically explored the sources of suboptimality and variability in subjects' responses in the target estimation task by employing a methodology that has been recently called *factorial model comparison* (van den Berg et al., 2014). Using this approach we generated a set of models by combining different sources of suboptimality, such as different approximations in decision making with different forms of sensory noise, in a factorial manner. Our model comparison was able to reject some common models of variability in decision making, such as probability matching with the posterior distribution (posterior-matching) or a sampling-average strategy consisting of averaging a number of samples from the posterior distribution. The observer model that best describes the data is a Bayesian observer with a slightly mismatched representation of the likelihoods, with sensory noise in the estimation of the parameters of the prior, that occasionally lapses, and most importantly has a stochastic representation of the posterior that may represent additional variability in the inference process or in action selection.

4.2 METHODS

4.2.1 *Experimental procedures*

Participants

Twenty-four subjects (10 male and 14 female; age range 18–33 years) participated in the study. All participants were naïve to the purpose of the study. All participants were right-handed according to the Edinburgh handedness inventory (Oldfield, 1971), with normal or corrected-to-normal vision and reported no neurological

disorder. Participants were compensated for their time. The Cambridge Psychology Research Ethics Committee approved the experimental procedures and all subjects gave informed consent.

Behavioural task

target line

Subjects were required to locate an unknown target given probabilistic information about its horizontal position s along a *target line* (Figure 4.1a–b). Information consisted of a visual representation of the a priori probability distribution of targets for that trial and a noisy cue about the actual target position (Figure 4.1b).

Subjects held the handle of a robotic manipulandum (vBOT, Howard et al., 2009b). The visual scene from a CRT monitor (Dell UltraScan P1110, 21-inch, 100 Hz refresh rate) was projected into the plane of the hand via a mirror (Figure 4.1a) that prevented the subjects from seeing their hand. The workspace origin, coordinates $[0, 0]$, was $\sim$ 35 cm from the torso of the subjects, with positive axes towards the right (x axis) and away from the subject (y axis). The workspace showed a home position (1.5 cm radius circle) at $[0, -15]$ cm and a cursor (1.25 cm radius circle) that tracked the hand position.

On each trial a hundred potential targets (0.1 cm radius dots) were shown around the target line at positions $[u_j, v_j]$, for $j = 1, \ldots, 100$, where the u_j formed a fixed discrete representation of the trial-dependent 'prior' distribution $p_{prior}(s)$, obtained through a regular sample of the cdf (see Figure 4.1d), and the v_j were small random offsets used to facilitate visualization, $v_j \sim \text{Uniform}(-0.3, 0.3)$ cm. The true target, unknown to the subject, was chosen by picking one of the potential targets at random with uniform probability. A cue (0.25 cm radius circle) was shown at position $[x_{cue}, -d_{cue}]$. The horizontal position x_{cue} provided a noisy measurement of the target position corrupted with Gaussian noise, with:

$$p_{meas}\left(x_{cue} \,|s, d_{cue}\right) = \mathcal{N}\left(x_{cue} \,|s, \sigma^2_{cue}(d_{cue})\right), \tag{4.1}$$

where σ_{cue} is the cue variability which was linearly related to the distance of the cue from the target line, d_{cue} (cues distant from the target line were noisier than cues close to it). In our setup, the noise level σ_{cue} could only either be low for 'short-distance' cues, $\sigma_{low} = 1.8$ cm ($d_{short} = 3.9$ cm), or high for 'long-distance' cues, $\sigma_{high} = 4.2$ cm ($d_{long} = 9.1$ cm). Both the prior distribution and cue remained on the screen for the duration of a trial. (See Figure 4.1c–d for the generative model of the task.)

After a 'go' beep, subjects were required to move the handle towards the target line, choosing an endpoint position such that the true target would be within the cursor radius. The manipulandum generated a spring force along the depth axis ($F_y = -5.0$

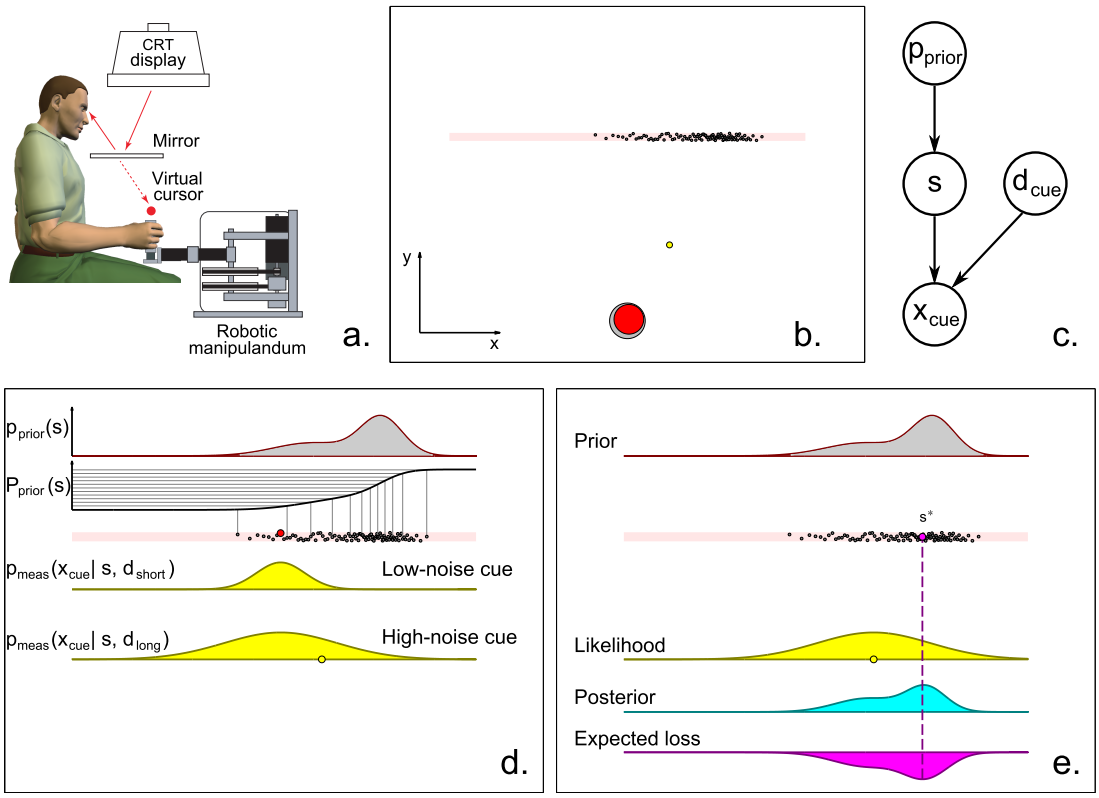

Figure 4.1: **Experimental procedure. a: Setup.** Subjects held the handle of a robotic manipulandum. The visual scene from a CRT monitor, including a cursor that tracked the hand position, was projected into the plane of the hand via a mirror. **b: Screen setup.** The screen showed a home position (grey circle), the cursor (red circle) here at the start of a trial, a line of potential targets (dots) and a visual cue (yellow dot). The task consisted in locating the true target among the array of potential targets, given the position of the noisy cue. The target line is shaded here for visualization purposes. **c: Generative model of the task.** On each trial the position of the hidden target s was drawn from a trial-dependent prior $p_{prior}(s)$, whose shape was chosen randomly from a session-dependent class of distributions. The vertical distance of the cue from the target line, d_{cue}, was either 'short' or 'long', with equal probability. The horizontal position of the cue, x_{cue}, depended on s and d_{cue}. The participants had to infer s given x_{cue}, d_{cue}, and the current prior p_{prior}. **d: Details of the generative model.** The potential targets constituted a discrete representation of $p_{prior}(s)$, built by taking equally spaced samples from the inverse of the cdf of the prior, $P_{prior}(s)$. The true target (red dot) was chosen uniformly at random from the potential targets, and the horizontal position of the cue (yellow dot) was drawn from a Gaussian distribution, $p_{meas}(x_{cue}|s, d_{cue})$, centered on the true target s and whose SD was proportional to the distance d_{cue} from the target line (either low-noise or high-noise cues). Here we show the location of the cue for a high-noise trial. **e: Components of Bayesian decision making.** A Bayesian observer combines the prior distribution with the likelihood to obtain a posterior distribution, which is then convolved with the loss function (here whether the target will be encircled by the cursor) and the observer picks the 'optimal' target location s^* (purple dot) that minimizes the expected loss (dashed line).

N/cm) for cursor positions past the target line, preventing subjects from overshooting. The horizontal endpoint position of the movement (velocity of the cursor less than 0.5 cm/s), after contact with the target line, was recorded as the subject's response r for that trial.

At the end of each trial, subjects received visual feedback on whether their cursor encircled (a 'success') or missed the true target (partial feedback). On full feedback trials, the position of the true target was also shown (0.25 cm radius yellow circle). Feedback remained on screen for 1 s. Potential targets, cues and feedback then disappeared. A new trial started 500 ms after the subject had returned to the home position.

For simplicity, all distances in the experiment are reported in terms of standardized screen units (window width of 1.0), with $x \in [-0.5, 0.5]$ and 0.01 screen units corresponding to 3 mm. In screen units, the cursor radius is 0.042 and the SD of noise for short and long distance cues is respectively $\sigma_{low} = 0.06$ and $\sigma_{high} = 0.14$.

To explain the task, subjects were told that the each dot represented a child standing in a line in a courtyard, seen from a bird's eye view. On each trial a random child was chosen and, while the subject was 'not looking', the child threw a yellow ball (the cue) directly ahead of them towards the opposite wall. Due to their poor throwing skills, the farther they threw the ball the more imprecise they were in terms of landing the ball straight in front of them. The subject's task was to identify the child who threw the ball, after seeing the landing point of the ball, by encircling him or her with the cursor. Subjects were told that the child throwing the ball could be any of the children, chosen randomly each trial with equal probability. Subjects were familiarized with the generative model of the task in a preliminary practice block in which they observed the yellow ball (the cue) being thrown by the 'children' at short and long distances.

Experimental sessions

training session

After the practice block (64 trials), all subjects performed a *training session* (576 trials) in which the 'prior' distributions of targets shown on the screen (the set of children) corresponded to Gaussian distributions with a standard deviation (SD) that varied between trials (σ_{prior} from 0.04 to 0.18 standardized screen units; Figure 4.2a). The actual position of the target (the 'child' who threw the ball) was revealed at the end of each trial and a displayed score kept track of the number of 'successes' in the session (full performance feedback). The use of Gaussian priors in the training session allowed us to assess whether our subjects could use explicit priors in our novel experimental setup in the same way in which they have been shown to learn Gaussian priors through extended implicit practice (see 'Gaussian contextual priors'

in Section 2.3.2). Note however that, in contrast with the previous studies, our subjects were required to compute each trial with a different Gaussian distribution.

After the training session, subjects were randomly divided in three groups ($n = 8$ each) to perform a *test session* (576–640 trials). Test sessions differed with respect to the class of prior distributions displayed during the session. For the 'Gaussian test' group, the distributions were the same eight Gaussian distributions used during training (Figure 4.2a). For the 'unimodal test' group, on each trial the prior was randomly chosen from eight unimodal distributions with fixed SD but with varying skewness and kurtosis (see below and Figure 4.2b). For the 'bimodal test' group, priors were chosen from eight (mostly) bimodal distributions with fixed SD but variable separation and weighting between peaks (see below and Figure 4.2c). During the test session, at the end of each trial subjects were informed whether they 'succeeded' or 'missed' the target but the target's actual location was not displayed. We provided only partial feedback in order to examine how subjects transferred their knowledge from the Gaussian training set to the priors in the test set (Maloney and Mamassian, 2009). Pilot studies had shown that partial feedback was enough to keep subjects motivated in the task but would not provide them with significant information that would alter their behaviour. The 'Gaussian test' group allowed us to verify that subjects' behaviour would not change after removal of full performance feedback. The 'unimodal test' and 'bimodal test' groups provided us with novel information on how subjects perform probabilistic inference with complex distributions. Moreover, non-Gaussian priors allowed us to evaluate several hypotheses about subjects' behaviour that are not testable with Gaussian distributions alone (Körding and Wolpert, 2004b).

test session

Sessions were divided in four runs. Subjects could take short breaks between runs and there was a mandatory 15 minutes break between the training and test sessions.

Prior distributions

Each session presented eight different types of priors and two cue noise levels (corresponding to either 'short' or 'long' cues), for a total of 16 different conditions (36–40 trials per condition). Trials from different conditions were presented in random order. Depending on the session and group, priors belonged to one of the following classes (see Figure 4.2):

- *Gaussian priors:* Eight Gaussian distributions with evenly spread SDs between 0.04 and 0.18 i.e. $\sigma_{prior} \in \{0.04, 0.06, \ldots, 0.18\}$ screen units.
- *Unimodal priors:* Eight unimodal priors with fixed SD $\sigma_{prior} = 0.11$ and variable skewness and kurtosis. With the exception of platykurtic prior 4, which is a mixture of 11 Gaussians, and prior 8, which is a single Gaussian, all other priors

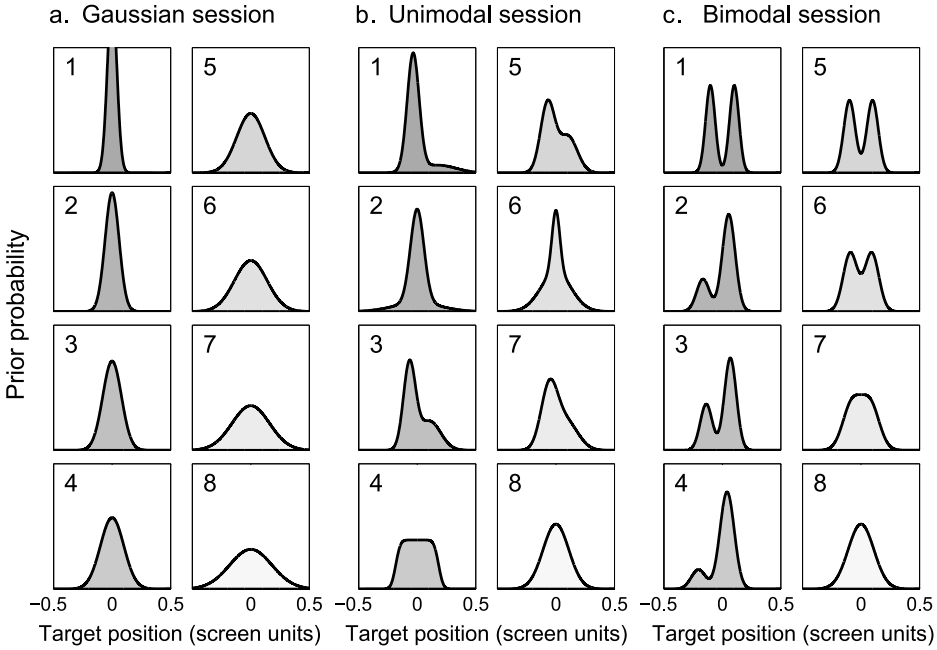

Figure 4.2: **Prior distributions.** Each panel shows the (unnormalized) probability density for a 'prior' distribution of targets, grouped by experimental session, with eight different priors per session. Within each session, priors are numbered in order of increasing differential entropy (i.e. increasing variance for Gaussian distributions). During the experiment, priors had a random location (mean drawn uniformly) and asymmetrical priors had probability $1/2$ of being 'flipped'. Target positions are shown in standardized screen units (from -0.5 to 0.5). **a: Gaussian priors.** These priors were used for the training session, common to all subjects, and in the Gaussian test session. SDs cover the range $\sigma_{prior} = 0.04$ to 0.18 screen units in equal increments. **b: Unimodal priors.** All unimodal priors have fixed SD $\sigma_{prior} = 0.11$ screen units but different skewness and kurtosis (see text for details). **c: Bimodal priors.** All priors in the bimodal session have fixed SD $\sigma_{prior} = 0.11$ screen units but different relative weights and separation between the peaks (see text).

were realized as mixtures of two Gaussians that locally maximize differential entropy for given values of the first four central moments. In the maximization we included a constraint on the SDs of the individual components so to prevent degenerate solutions ($0.02 \leq \sigma_i \leq 0.2$ screen units, for $i = 1, 2$). Skewness and excess kurtosis were chosen to represent various shapes of unimodal distributions, within the strict bounds that exist between skewness and kurtosis of a unimodal distribution (Teuscher and Guiard, 1995). The values of (skewness, kurtosis) for the eight distributions, in order of increasing differential entropy: 1: $(2, 5)$; 2: $(0, 5)$; 3: $(0.78, 0)$; 4: $(0, -1)$; 5: $(0.425, -0.5)$; 6: $(0, 1)$; 7: $(0.5, 0)$; 8: $(0, 0)$.

▷ *Bimodal priors:* Eight (mostly) bimodal priors with fixed SD $\sigma_{prior} = 0.11$ and variable separation and relative weight. The priors were realized as mixtures of two Gaussians with equal variance:

$$p_{prior}(s) = \pi\mathcal{N}\left(s\,|\mu_1, \sigma^2\right) + (1-\pi)\mathcal{N}\left(s\,|\mu_2, \sigma^2\right). \tag{4.2}$$

Separation was computed as $d' = \frac{\mu_1 - \mu_2}{\sigma}$, and relative weight was defined as $w = \frac{\pi}{1-\pi}$. The values of (separation, relative weight) for the eight distributions, in order of increasing differential entropy: 1: $(5,1)$; 2: $(4,3)$; 3: $(4,2)$; 4: $(4,5)$; 5: $(4,1)$; 6: $(3,1)$; 7: $(2,1)$; 8: $(0,-)$ (the last distribution is a single Gaussian).

For all priors, the mean μ_{prior} was randomly drawn from a uniform distribution whose bounds were chosen such that the extremes of the discrete representation would fall within the active screen window (the actual screen size was larger than the active window). Also, asymmetric priors had 50% probability of being flipped horizontally about the mean.

Measuring sensorimotor noise

We performed a separate sensorimotor estimation experiment to obtain an independent measure of subjects' sensorimotor variability. The sensorimotor variability includes subjects' noise in determining the location of the cue and projecting it back onto the target line as well as any motor noise in indicating that location. Ten subjects (3 male and 7 female; age range 21–33 years) that had taken part in the main experiment also participated in the control experiment.

The experimental setup had the same layout as the main experiment (see Figure 4.1), with the following differences: (a) no discrete distribution of targets was shown on screen, only a horizontal target line; (b) in all trials the target was drawn randomly from a uniform distribution whose range covered the width of the active screen window; (c) as usual, half of the trials featured short-distance cues and the other half long-distance cues, but both types of cues had no added noise. In each trial the target was always perfectly above the shown cue, with $s \equiv x_{cue}$.

Subjects performed a short practice session (64 trials) followed by a test session (288 trials). Full performance feedback was provided during both practice and test. Feedback consisted in a visual display of the true position of the target and an integer-valued score that was maximal (10 points) for a perfect 'hit' and decreased rapidly away from the target, according to the following equation:

$$\text{Score}(r,s) = \text{Round}\left(10 \cdot \exp\left\{-\frac{(r-s)^2}{2\sigma_{score}^2}\right\}\right)$$

where r is the response in the trial, s is the target position, σ_{score} is one-tenth of the cursor diameter ($8.3 \cdot 10^{-3}$ screen units or 2.5 mm) and Round(z) denotes the value of z rounded to the nearest integer.

4.2.2 *Data analysis*

Analysis of behavioural data

Data analysis was conducted in MATLAB 2010b (Mathworks, U.S.A.). To avoid edge artifacts in subjects' response due to the discretization of the displayed distribution, we discarded trials in which the cue position, x_{cue}, was outside the range of the discretized prior (2691 out of 28672 trials: 9.4%). We included these trials in the experimental session in order to preserve the probabilistic relationships between variables of the task.

For each trial, we recorded the response location r and the reaction time (RT) was defined as the interval between the 'go' beep and the start of the subject's movement. For each subject and session we computed a nonlinear kernel regression estimate of the average RT as a function of the SD of the posterior distribution, σ_{post}. We only considered a range of σ_{post} for which all subjects had a significant density of data points. Results did not change qualitatively for other measures of spread of the posterior, such as the exponential entropy (Campbell, 1966).

Optimality index and success probability

success probability

An objective measure of performance in each trial is the *success probability* $p_{success}(r)$, that is, the probability that the target would be within a cursor radius' distance from the given response (final position of the cursor) under the generative model of the task. We defined the *optimality index* (i.e. theoretical efficiency) for a trial as the success probability normalized by the maximal success probability $p^*_{success}$, that is the success probability of an optimal response. The optimality index allows us to study variations in subjects' performance which are not trivially induced by variations in the difficulty of the task.

optimality index

The success probability $p_{success}(r)$ in a given trial represents the probability of locating the correct target according to the generative model of the task (independent of the actual position of the target). For a trial with cue position x_{cue}, cue noise variance σ^2_{cue}, and prior distribution $p_{prior}(s)$, the success probability is defined as:

$$p_{success}(r) = \int_{r-\frac{\ell}{2}}^{r+\frac{\ell}{2}} \left[\frac{1}{\int ds'\, p_{prior}(s') \mathcal{N}\left(s' \,|x_{cue}, \sigma^2_{cue}\right)} p_{prior}(s) \mathcal{N}\left(s \,\middle|x_{cue}, \sigma^2_{cue}\right) \right] ds, \quad (4.3)$$

where the integrand is the posterior distribution according to the continuous generative model of the task and ℓ is the diameter of the cursor. Solving the integral in Eq. 4.3 for a generic mixture-of-Gaussians prior, $p_{prior}(s) = \sum_{i=1}^{m} \pi_i \mathcal{N}\left(s \,|\mu_i, \sigma_i^2\right)$, we obtain:

$$p_{success}(r) = \left(\sum_{i'=1}^{m} \gamma_{i'}\right)^{-1} \sum_{i=1}^{m} \frac{\gamma_i}{2} \left[\operatorname{erf}\left(\frac{r + \frac{\ell}{2} - \nu_i}{\sqrt{2}\tau_i}\right) - \operatorname{erf}\left(\frac{r - \frac{\ell}{2} - \nu_i}{\sqrt{2}\tau_i}\right)\right], \qquad (4.4)$$

where the symbols γ_i, ν_i and τ_i are defined in Eq. 4.8 (see below). The maximal success probability is simply computed as $p^*_{success} = \max_r p_{success}(r)$.

Note that in our case a metric based on the theoretical success probability is more appropriate than the observed fraction of successes for a given sample of trials (empirical efficiency), as the latter introduces additional error due to mere chance.[1]

The priors for the Gaussian, unimodal and bimodal sessions were chosen such that the average maximal success probability of each class was about the same ($\sim 51.5\%$) making the task challenging and of equal difficulty across the experiment.

Statistical analyses

All regressions in our analyses used a robust procedure, computed using Tukey's 'bisquare' weighting function (`robustfit` in MATLAB). Robust means for data visualization and computation of summary statistics were calculated as trimmed means, discarding 10% of values from each side of the sample. Statistical differences were assessed using repeated-measures ANOVA (rm-ANOVA) with Greenhouse-Geisser correction of the degrees of freedom in order to account for deviations from sphericity (Greenhouse and Geisser, 1959). A logit transform was applied to the optimality index measure before performing rm-ANOVA, in order to improve normality of the data (results were qualitatively similar for non-transformed data). Nonlinear kernel regression estimates to visualize mean data were computed with a Nadaraya-Watson estimator with rule-of-thumb bandwidth (Härdle et al., 2004). For all analyses the criterion for statistical significance was $p < 0.05$.

4.2.3 *Observer models*

Subjects' performance was modelled with a family of Bayesian ideal observers which incorporate various hypotheses about the decision-making process and internal representation of the task, with the aim of characterizing various possible sources of deviations from optimal behaviour (Tassinari et al., 2006); see Figure 4.1e for a depiction

1 The observed fraction of successes fluctuates around the true success probability with binomial statistics, and the error can be substantial for small sample size.

of the elements of decision making in a trial. All these observers are 'Bayesian' because they build a posterior distribution through Bayes' rule, but the operations they perform with the posterior can differ from the normative prescriptions of Bayesian Decision Theory (BDT).

Similarly to what we did in Chapter 3, we constructed a large model set with a factorial approach that consists in combining different independent model 'factors' that can take different 'levels' (van den Berg et al., 2014). The basic factors we considered in our first analysis are:

1. *Decision making* (3 levels): Bayesian Decision Theory ('BDT'), stochastic posterior ('SPK'), posterior probability matching ('PPM').
2. *Cue-estimation sensory noise* (2 levels): absent or present ('S').
3. *Noisy estimation of the prior* (2 levels): absent or present ('P').
4. *Lapse* (2 levels): absent or present ('L').

Observer models are identified by a model string, for example 'BDT-P-L' indicates an observer model that follows BDT with a noisy estimate of the prior and suffers from occasional lapses. Our basic model set comprises 24 observer models; we also considered several variants of these models that are described in the text. All main factors are explained in the following sections and summarized in Table 4.1. The term 'model component' is used through the text to indicate both factors and levels.

Decision making: Standard BDT observer ('BDT')

The 'decision-making' factor comprises model components with different assumptions about the decision process. We start describing the 'baseline' Bayesian observer model, BDT, that follows standard BDT. Suboptimality, in this case, emerges if the observer's internal estimates of the parameters of the task take different values from the true ones (see Chapter 2). As all subsequent models are variations of the BDT observer we describe this model in some detail.

On each trial the information available to the observer is comprised of the 'prior' distribution $p_{prior}(s)$, the cue position x_{cue}, and the distance d_{cue} of the cue from the target line, which is a proxy for cue variability, $\sigma_{cue} \equiv \sigma(d_{cue})$. The posterior distribution of target location, s, is computed by multiplying together the prior with the likelihood function. For the moment we assume the observer has perfect access to the displayed cue location and prior (i.e. $q_{prior}(s) \equiv p_{prior}(s)$), and knowledge that cue variability is normally distributed. However, we allow the observer's estimate of

Label	Model description	# parameters	Free parameters (θ_M)
BDT	Decision making: BDT	4	$\sigma_{motor}, \tilde{\sigma}_{low}, \left(\tilde{\sigma}_{high} \times 2\right)$
PPM	Decision making: Posterior probability matching	4	$\sigma_{motor}, \tilde{\sigma}_{low}, \left(\tilde{\sigma}_{high} \times 2\right)$
SPK	Decision making: Stochastic posterior	6	$\sigma_{motor}, \tilde{\sigma}_{low}, \left(\tilde{\sigma}_{high}, \kappa\right) \times 2$
PSA	Decision making: Posterior sampling average (*)	6	$\sigma_{motor}, \tilde{\sigma}_{low}, \left(\tilde{\sigma}_{high}, \kappa\right) \times 2$
S	Cue-estimation noise	+2	$+ \left(\Sigma_{cue} \times 2\right)$
P	Prior estimation noise	+2	$+ \left(\eta_{prior} \times 2\right)$
L	Lapse	+2	$+ \left(\lambda \times 2\right)$
MV	Gaussian approximation: mean/variance (*)	–	–
LA	Gaussian approximation: Laplace approximation (*)	–	–

Table 4.1: **Set of model factors.** Table of all major model factors, identified by a label and short description. An observer model is built by choosing a model level for decision making and then optionally adding other components. For each model component the number of free parameters is specified. A '$\times 2$' means that a parameter is specified independently for training and test sessions; otherwise parameters are shared across sessions. See main text for the meaning of the various parameters. (*) These additional components appear in the comparison of alternative models of decision making.

the variance of the likelihood ($\tilde{\sigma}^2_{low}$ and $\tilde{\sigma}^2_{high}$) to mismatch the actual variance (σ^2_{low} and σ^2_{high}). Therefore, the posterior is given by:

$$p_{post}(s) = p_{post}(s|x_{cue}, d_{cue}, p_{prior}) \propto p_{prior}(s)\mathcal{N}\left(x_{cue}\,|s, \tilde{\sigma}^2_{cue}\right). \tag{4.5}$$

In general, for any given trial, the choice the subject makes (desired pointing location for s) can be a probabilistic one, leading to a decision or 'target choice' distribution (see Section 2.1.2). However, for standard BDT, the choice is deterministic given the trial parameters, leading to a 'target choice' distribution that collapses to a delta function:

$$p_{target}\left(\hat{s}|x_{cue}, d_{cue}, p_{prior}\right) = \delta\left[\hat{s} - s^*(x_{cue}; d_{cue}, p_{prior})\right], \tag{4.6}$$

where $\hat{s}$ is the observer's decision and s^* is the 'optimal' target position that minimizes the observer's expected loss. The explicit task in our experiment is to place the target within the radius of the cursor, which is equivalent to a *boxcar loss function*[2] with a window size equal to the diameter of the cursor (the circle is large enough that the loss is still effectively 'boxcar' after considering the vertical jitter of the targets). For computational reasons, in our observer models we approximate the boxcar loss with an inverted Gaussian that best approximates the boxcar, with fixed SD $\sigma_\ell = 0.027$ screen units (see below and Section B.2.3 in the Appendix).

boxcar loss function

In our experiment all priors were mixtures of m (mainly 1 or 2) Gaussian distributions of the form $p_{prior}(s) = \sum_{i=1}^{m} \pi_i \mathcal{N}\left(s\,|\mu_i, \sigma_i^2\right)$, with $\sum_{i=1}^{m} \pi_i = 1$. It follows that the expected loss is a mixture of Gaussians itself, and the optimal target that minimizes the expected loss takes the form (see below, 'Computing the optimal target', for details):

$$s^*(x_{cue}) = s^*(x_{cue}; d_{cue}, p_{prior}) = \arg\min_{\hat{s}} \left\{ -\sum_{i=1}^{m} \gamma_i \mathcal{N}\left(\hat{s}\,|\nu_i, \tau_i^2 + \sigma_\ell^2\right) \right\}, \tag{4.7}$$

where we defined:

$$\gamma_i \equiv \pi_i \mathcal{N}\left(x_{cue}\,|\mu_i, \sigma_i^2 + \tilde{\sigma}^2_{cue}\right), \quad \nu_i \equiv \frac{\mu_i \tilde{\sigma}^2_{cue} + x_{cue}\sigma_i^2}{\sigma_i^2 + \tilde{\sigma}^2_{cue}}, \quad \tau_i^2 \equiv \frac{\sigma_i^2 \tilde{\sigma}^2_{cue}}{\sigma_i^2 + \tilde{\sigma}^2_{cue}}. \tag{4.8}$$

For a single-Gaussian prior ($m = 1$), $p_{prior} = \mathcal{N}\left(s\,|\mu_1, \sigma_1^2\right)$, and the posterior distribution is itself a Gaussian distribution with mean $\mu_{post} = \nu_1$ and variance $\sigma^2_{post} = \tau_1^2$, so that $s^*(x_{cue}) = \mu_{post}$.

2 Also called rectangular or 'square well' loss.

We assume that the subject's response is corrupted by motor noise, which we take to be normally distributed with SD σ_{motor}. By convolving the target choice distribution (Eq. 4.6) with motor noise we obtain the final response distribution:

$$\Pr\left(r \,|x_{cue}, d_{cue}, p_{prior}\right) = \mathcal{N}\left(r \,|s^*(x_{cue}), \sigma^2_{motor}\right). \tag{4.9}$$

The calculation of the expected loss in Eq. 4.7 does not explicitly take into account the consequences of motor variability, but this approximation has minimal effects on the inference (see Section 4.4.2).

The behaviour of observer model BDT is completely described by Eqs. 4.7, 4.8 and 4.9. This observer model is *subjectively* Bayes optimal; the subject applies BDT to his or her internal model of the task, which might be wrong. Specifically, the observer will be close to *objective* optimality only if his or her estimates for the likelihood parameters, $\tilde{\sigma}_{low}$ and $\tilde{\sigma}_{high}$, match the true likelihood parameters of the task (σ_{low} and σ_{high}). As extreme cases, if $\tilde{\sigma}_{low}, \tilde{\sigma}_{high} \longrightarrow 0$ the BDT observer will ignore the prior and only use the noiseless cues, whereas for $\tilde{\sigma}_{low}, \tilde{\sigma}_{high} \longrightarrow \infty$ the observer will use only probabilistic information contained in the priors.

Decision making: Noisy decision makers ('SPK' and 'PPM')

An alternative to BDT is a family of observer models in which the decision-making process is probabilistic, either because of noise in the inference or stochasticity in action selection. We model these various sources of variability without distinction as stochastic computations that involve the posterior distribution.

We start our analysis by considering a specific model, SPK (stochastic posterior, κ-power), in which the observer minimizes the expected loss (Eq. 4.7) under a noisy, approximate representation of the posterior distribution, as opposed to the deterministic, exact posterior of BDT (Figure 4.3a and 4.3d); later we will consider other variants of stochastic computations. As before, we allow the SD of the likelihoods, $\tilde{\sigma}_{low}$ and $\tilde{\sigma}_{high}$, to mismatch their true values. For mathematical and computational tractability, we do not directly simulate the noisy inference during the model comparison. Instead, we showed that different ways of introducing stochasticity in the inference process – either by adding noise to an explicit representation of the observer's posterior (Figure 4.3b and 4.3e), or by building a discrete approximation of the posterior via sampling (Figure 4.3c and 4.3f) – induce variability in the target choice that is well approximated by a power function of the posterior distribution itself; see Section B.1 in the Appendix for details.

We, therefore, use the power function approximation with power κ – hence the name of the model – to simulate the effects of a stochastic posterior on decision mak-

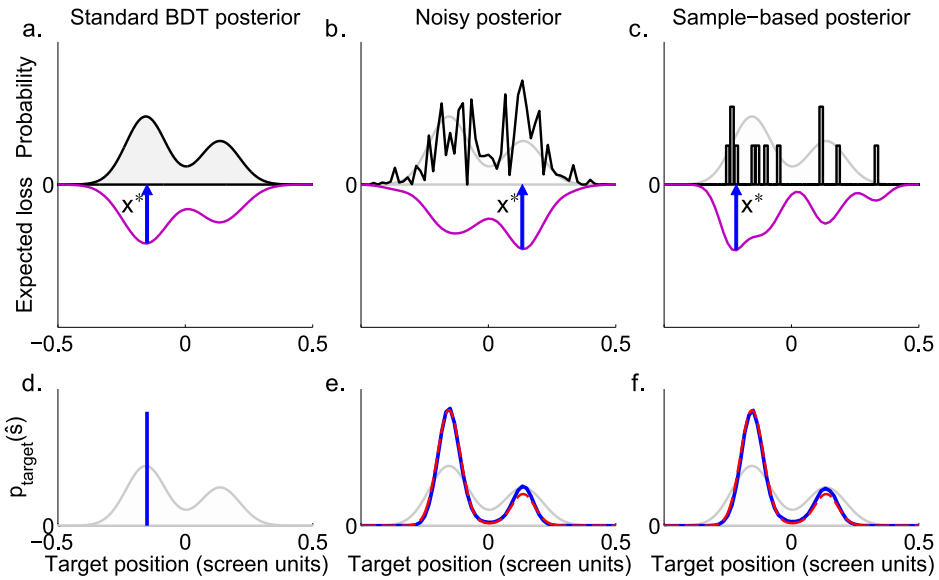

Figure 4.3: **Decision making with stochastic posterior distributions. a–c:** Each panel shows an example of how different models of stochasticity in the representation of the posterior distribution, and therefore in the computation of the expected loss, may affect decision making in a trial. In all cases, the observer chooses the subjectively optimal target s^* (blue arrow) that minimizes the expected loss (purple line; see Eq. 4.7) given his or her current representation of the posterior (black lines or bars). The original posterior distribution is showed in panels b–f for comparison (shaded line). **a:** Original posterior distribution. **b:** Noisy posterior: the original posterior is corrupted by random multiplicative or Poisson-like noise (in this example, the noise has caused the observer to aim for the wrong peak). **c:** Sample-based posterior: a discrete approximation of the posterior is built by drawing samples from the original posterior (grey bars; samples are binned for visualization purposes). **d–f:** Each panel shows how stochasticity in the posterior affects the distribution of target choices $p_{target}(\hat{s})$ (blue line). **d:** Without noise, the target choice distribution is a delta function peaked on the minimum of the expected loss, as per standard BDT. **e:** On each trial, the posterior is corrupted by different instances of noise, inducing a distribution of possible target choices $p_{target}(\hat{s})$ (blue line). In our task, this distribution of target choices is very well approximated by a power function of the posterior distribution, Eq. 4.10 (red dashed line); see Section B.1 in the Appendix for details. **f:** Similarly, the target choice distribution induced by sampling (blue line) is fit very well by a power function of the posterior (red dashed line). Note the extremely close resemblance of panels e and f (the exponent of the power function is the same).

ing, without committing to a specific interpretation. The target choice distribution in model SPK takes the form:

$$p_{target}(\hat{s}|x_{cue}, d_{cue}, p_{prior}) \propto \left[p_{post}(\hat{s})\right]^{\kappa}, \tag{4.10}$$

where the power exponent $\kappa \geq 0$ is a free parameter inversely related to the amount of variability. Eq. 4.10 is convolved with motor noise to give the response distribution.

The power function conveniently interpolates between a posterior-matching strategy (for $\kappa = 1$) and a maximum a posteriori (MAP) solution ($\kappa \to \infty$); see also Battaglia et al. (2011); Moreno-Bote et al. (2011).

We consider as a separate component the specific case in which the power exponent κ is fixed to 1, yielding a posterior probability matching observer, PPM, that takes action according to a single draw from the posterior distribution (see Section 2.4.5).

Observer models with cue-estimation sensory noise ('S')

We consider a family of observer models, S, in which we drop the assumption that the observer perfectly knows the horizontal position of the cue. We model sensory variability by adding Gaussian noise to the internal measurement of x_{cue}, which we label ξ_{cue}:

$$p\left(\xi_{cue}|x_{cue}, d_{cue}\right) = \mathcal{N}\left(\xi_{cue}\,\middle|\,x_{cue}, \Sigma^2(d_{cue})\right) \qquad \text{with } \Sigma^2(d_{cue}) \in \left\{\Sigma^2_{low}, \Sigma^2_{high}\right\}, \quad (4.11)$$

where Σ^2_{low}, Σ^2_{high} represent the variances of the estimates of the position of the cue, respectively for low-noise (short-distance) and high-noise (long-distance) cues. According to Weber's law, we assume that the measurement error is proportional to the distance from the target line d_{cue}, so that the ratio of Σ_{high} to Σ_{low} is equal to the ratio of d_{long} to d_{short}, and we need to specify only one of the two parameters (Σ_{high}). Given that both the cue variability and the observer's measurement variability are normally distributed, their combined variability will still appear to the observer as a Gaussian distribution with variance $\tilde{\sigma}^2_{cue} + \Sigma^2_{cue}$, assuming independence. Therefore, the observer's internal model of the task is formally identical to the description we gave before by replacing x_{cue} with ξ_{cue} in Eq. 4.5. Since the subject's internal measurement is not accessible during the experiment, the observed response probability is integrated over the hidden variable ξ_{cue} (see also Eq. 4.19 later). A model with cue-estimation sensory noise ('S') tends to the equivalent observer model without noise for $\Sigma_{cue} \to 0$.

Observer models with noisy estimation of the prior ('P')

We introduce a family of observer models, P, in which subjects have access only to noisy estimates of the parameters of the prior, p_{prior}. For this class of models we assume that estimation noise is structured along a task-relevant dimension.

Specifically, for Gaussian priors we assume that the observers take a noisy internal measurement of the SD of the prior, $\tilde{\sigma}_{prior}$, which according to Weber's law follows a log-normal distribution:

$$p(\tilde{\sigma}_{prior}|\sigma_{prior}) = \text{Log}\mathcal{N}\left(\tilde{\sigma}_{prior}\,\middle|\,\sigma_{prior}, \eta^2_{prior}\right), \tag{4.12}$$

where σ_{prior}, the true SD, is the log-scale parameter and $\eta_{prior} \geq 0$ is the shape parameter of the log-normally distributed measurement (respectively mean and SD in log space). We assume an analogous form of noise on the width of the platykurtic prior in the unimodal session. Conversely, we assume that for priors that are mixtures of two Gaussians the main source of error stems from assessing the relative importance of the two components. In this case we add log-normal noise to the weights of each component, which we assume to be estimated independently:

$$p(\tilde{\pi}_i|\pi_i) = \text{Log}\mathcal{N}\left(\tilde{\pi}_i\,\middle|\,\pi_i, \eta^2_{prior}\right) \qquad \text{for } i = 1, 2, \tag{4.13}$$

where π_i are the true mixing weights and η_{prior} is the noise parameter previously defined. Note that Eq. 4.13 is equivalent to adding normal noise with SD $\sqrt{2}\,\eta_{prior}$ to the log weights ratio in the 'natural' log odds space (Zhang and Maloney, 2012).

The internal measurements of $\tilde{\sigma}_{prior}$ (or $\tilde{\pi}_i$) are used by the observer in place of the true parameters of the priors in the inference process (e.g. Eq. 4.8). Since we cannot measure the internal measurements of the subjects, the actual response probabilities are computed by integrating over the unobserved values of $\tilde{\sigma}_{prior}$ or $\tilde{\pi}_i$ (see later). For $\eta_{prior} \to 0$ an observer model with prior noise ('P') tends to its corresponding version with no noise.

A different type of measurement noise on the prior density is represented by 'unstructured', pointwise noise, which can be shown to be indistinguishable from noise in the posterior under certain assumptions (see Section B.1.3 in the Appendix).

Observer models with lapse ('L')

It is possible that the response variability exhibited by the subjects could be simply explained by occasional lapses. Observer models with a lapse term are common in psychophysics to account for missed stimuli and additional variability in the data (Wichmann and Hill, 2001). According to these models, in each trial the observer has a typically small, fixed probability $0 \leq \lambda \leq 1$ (the *lapse rate*) of making a choice from a lapse probability distribution instead of the optimal target s^*. As a representative lapse distribution we choose the prior distribution (*prior-matching lapse*). The target

prior-matching lapse

choice for an observer with lapse has distribution:

$$p_{target}^{(lapse)}\left(\hat{s}|x_{cue}, d_{cue}, p_{prior}\right) = (1-\lambda)\cdot p_{target}\left(\hat{s}|x_{cue}, d_{cue}, p_{prior}\right) + \lambda \cdot p_{prior}(\hat{s}), \quad (4.14)$$

where the first term in the right hand side of the equation is the target choice distribution (either Eq. 4.6 or Eq. 4.10, depending on the decision-making factor), weighted by the probability of *not* making a lapse, $1-\lambda$. The second term is the lapse term, with probability λ, and it is clear that the observer model with lapse ('L') reduces to an observer with no lapse in the limit $\lambda \to 0$. Eq. 4.14 is then convolved with motor noise to provide the response distribution. We also tested a lapse model in which the lapse distribution was uniform over the range of the displayed prior distribution. Observer models with uniform lapse performed consistently worse than the prior-matching lapse model, so we only report the results of the latter.

Additional observer models for non-Gaussian priors

Finally, we considered a number of additional model components whose predictions differ from the previously described models only when the posterior distribution is non-Gaussian. These observer models represent different generalizations of how a noisy decision process could affect behaviour beyond the Gaussian case, and are subject to a separate model comparison (see 'Comparison of alternative models of decision making' in Section 4.3.3). When performing this second model comparison, we included in the analysis only trials in which the theoretical posterior distribution is considerably non-Gaussian (see below); this restriction immediately excludes the training sessions and the Gaussian group, in which all priors and posteriors are strictly Gaussian.

As new models, we introduce first an additional level for the decision-making factor, posterior-sampling average (PSA). This observer model chooses a target by taking the average of $\kappa \geq 1$ samples drawn from the posterior distribution (Battaglia et al., 2011). This strategy is equivalent to an observer with a sample-based posterior that applies a quadratic loss function when choosing the optimal target. For generality, with an interpolation method we allow κ to be a real number (see below). For Gaussian posteriors, model PSA is identical to SPK.

We also introduce a new model factor according to which subjects may use a single Gaussian to approximate the full posterior. The mean/variance model (MV) assumes that subjects approximate the posterior with a Gaussian with matching low-order moments (mean and variance). For observer models that act according to BDT, model MV is equivalent to the assumption of a quadratic loss function during target selection, whose optimal target choice equals the mean of the posterior. Alternatively,

a commonly used Gaussian approximation in Bayesian inference is the Laplace approximation (LA). In this case, the observer approximates the posterior with a single Gaussian centered on the mode of the posterior and whose variance depends on the local curvature at the mode (see Section A.3.2 in the Appendix). The main difference of the Laplace approximation from other models is that the posterior is usually narrower, since it takes into account only the main peak.

Computing the optimal target

According to Bayesian Decision Theory (BDT), the key quantity an observer needs to compute in order to make a decision is the (subjectively) expected loss for a given action. In our task, the action corresponds to a choice of a cursor position $\hat{s}$, and the expected loss takes the form:

$$\mathcal{E}[\hat{s}; p_{post}, \mathcal{L}] = \int p_{post}(s)\mathcal{L}(\hat{s}, s)\, ds, \tag{4.15}$$

where $p_{post}(s)$ is the subject's posterior distribution of target position, described by Eq. 4.5, and the loss associated with choosing position $\hat{s}$ when the target location is s is represented by loss function $\mathcal{L}(\hat{s}, s)$.

Our task has a clear 'hit or miss' structure that is represented by the (inverted) boxcar function:

$$\mathcal{L}_{box}(\hat{s}, s; \ell) = \begin{cases} -\frac{1}{\ell} & \text{for } |\hat{s} - s| < \frac{\ell}{2} \\ 0 & \text{otherwise,} \end{cases} \tag{4.16}$$

where $\hat{s} - s$ is the distance of the chosen response from the target, and ℓ is the size of the allowed window for locating the target (in the experiment, the cursor diameter). The boxcar loss allows for an analytical expression of the expected loss, but the optimal target still needs to be computed numerically. Therefore we make a smooth approximation to the boxcar loss represented by the inverted Gaussian loss:

$$\mathcal{L}_{Gauss}(\hat{s}, s; \sigma_\ell) = -\mathcal{N}\left(s \,|\hat{s}, \sigma_\ell^2\right), \tag{4.17}$$

where the parameter σ_ℓ governs the scale of smoothed detection window. The Gaussian loss approximates extremely well the predictions of the boxcar loss in our task, to the point that performance under the two forms of loss is empirically indistinguishable (see Section B.2.3 in the Appendix). However, computationally the Gaussian loss is preferrable as it allows much faster calculations of optimal behaviour.

For the decision process, BDT assumes that observers choose the 'optimal' target position s^* that minimizes the expected loss (compare with Eq. 2.4):

$$\begin{aligned} s^* &= \arg\min_{\hat{s}} \mathcal{E}[\hat{s}; p_{post}, \mathcal{L}_{Gauss}] \\ &= \arg\min_{\hat{s}} \left\{ -\sum_{i=1}^{m} \pi_i \int \mathcal{N}\left(s \,|\mu_i, \sigma_i^2\right) \mathcal{N}\left(s \,|x_{cue}, \tilde{\sigma}_{cue}^2(d_{cue})\right) \mathcal{N}\left(s \,|\hat{s}, \sigma_\ell^2\right) \, ds \right\}, \end{aligned} \tag{4.18}$$

where we have used Eqs. 4.5, 4.15 and 4.17. With some algebraic manipulations, Eq. 4.18 can be reformulated as Eq. 4.7. Given the form of the expected loss, the solution of Eq. 4.7 is equivalent to finding the maximum (mode) of a Gaussian mixture model. No analytical solution is known for more than one model component ($m > 1$), so we implemented a fast and accurate numerical solution adapting the algorithm in Carreira-Perpiñán (2000).

Computing the response probability

The probability of observing response r in a trial, $\Pr(r\,|\text{trial})$ (e.g., Eq. 4.9) is the key quantity for our probabilistic modelling of the task. For basic observer models, $\Pr(r\,|\text{trial})$ is obtained as the convolution between a Gaussian distribution (motor noise) and a target choice distribution in closed form (e. g., a power function of a mixture of Gaussians), such as in Eqs. 4.6, 4.10, and 4.14. Response probabilities are integrated over latent variables of model factor S (ξ_{cue}; see Eq. 4.11) and of model factor P ($\log\tilde{\sigma}_{prior}$ and $\log\frac{\tilde{\pi}_1}{\tilde{\pi}_2}$; see Eqs. 4.12 and 4.13). Integrations were performed analytically when possible or otherwise numerically (`trapz` in MATLAB or Gauss-Hermite quadrature method for non-analytical Gaussian integrals, see e. g. Press et al., 2007). For instance, the observed response probability for model factor S takes the shape:

$$\begin{aligned} \Pr\left(r \,|x_{cue}, d_{cue}, p_{prior}\right) = \int \left[\int \mathcal{N}\left(r \,|\hat{s}, \sigma_m^2\right) p_{target}\left(\hat{s}|\xi_{cue}, d_{cue}, p_{prior}\right) d\hat{s} \right] \\ \times \mathcal{N}\left(\xi_{cue} \,|x_{cue}, \Sigma_{cue}^2\right) d\xi_{cue}, \end{aligned} \tag{4.19}$$

where we are integrating over the hidden variables ξ_{cue} and $\hat{s}$. The target choice distribution p_{target} depends on the decision-making model component (such as Eqs. 4.6 and 4.10). Without loss of generality, we assumed that the observers are not aware of their internal variability. Predictions of model S do not change whether we assume that the observer is aware of his or her measurement error Σ_{cue}^2 or not; differences amount just to redefinitions of $\tilde{\sigma}_{cue}^2$.

For a Gaussian prior with mean μ_{prior} and variance σ^2_{prior}, the response probability has the following closed-form solution:

$$\Pr\left(r \left| x_{cue}, d_{cue}, \mu_{prior}, \sigma^2_{prior}\right.\right) = \mathcal{N}\left(r \left| \mu_{resp}, \sigma^2_{response}\right.\right), \tag{4.20}$$

with

$$\mu_{resp} \equiv \frac{\mu_{prior}\tilde{\sigma}^2_{cue} + x_{cue}\sigma^2_{prior}}{\sigma^2_{prior} + \tilde{\sigma}^2_{cue}}, \qquad \sigma^2_{resp} \equiv \sigma^2_m + \frac{1}{\kappa}\frac{\sigma^2_{prior}\tilde{\sigma}^2_{cue}}{\sigma^2_{prior} + \tilde{\sigma}^2_{cue}} + \left(\frac{\sigma^2_{prior}}{\sigma^2_{prior} + \tilde{\sigma}^2_{cue}}\right)^2 \Sigma^2_{cue}, \tag{4.21}$$

where κ is the noise parameter of the stochastic posterior in model component SPK ($\kappa = 1$ for PPM; $\kappa \sim \infty$ for BDT) and Σ_{cue} is the sensory noise in estimation of the cue position in model S ($\Sigma_{cue} = 0$ for observer models without cue-estimation noise). For observer models P with noise on the prior, Eq. 4.20 was numerically integrated over different values of the internal measurement (here corresponding to $\log \sigma_{prior}$) with a Gauss-Hermite quadrature method.

For non-Gaussian priors there is no closed form solution similar to Eq. 4.20 and the calculation of the response probability, depending on active model components, may require up to three nested numerical integrations. Therefore, for computational tractability, we occasionally restricted our analysis to a subset of observer models, as indicated in the Results section.

For model class PSA (posterior sampling average), the target choice distribution is the probability distribution of the average of κ samples drawn from the posterior distribution. For a posterior that is a mixture of Gaussians and integer κ, it is possible to obtain an explicit expression whose number of terms grows exponentially in κ (a Gaussian approximation applies for large values of κ due to the central limit theorem). Values of the distribution for non-integer κ were found by linear interpolation between adjacent integer values. For model class LA (Laplace approximation) we found the mode of the posterior numerically (Carreira-Perpiñán, 2000) and analytically evaluated the second derivative of the log posterior at the mode. The mean of the approximate Gaussian posterior is set to the mode and the variance to minus the inverse of the second derivative (see Eq. A.8).

For all models, when using the model-dependent response probability, $\Pr(r\,|\text{trial})$, in the model comparison, we added a small regularization term:

$$\Pr^{(reg)}(r|\text{trial}) = (1-\epsilon)\cdot\Pr(r\,|\text{trial}) + \epsilon, \tag{4.22}$$

with $\epsilon = 1.5 \cdot 10^{-6}$ (the value of the pdf of a normal distribution at 5 SDs from the mean). This change in probability is empirically negligible, but from the point of view of model comparison the regularization term introduces a lower bound $\log \epsilon$ on the log probability of a single trial, preventing single outliers from having unlimited weight on the log likelihood of a model, increasing therefore the robustness of the inference.

4.2.4 *Model comparison and non-parametric analysis*

Computing the posterior distribution of the parameters

For each observer model M and each subject's dataset $\mathcal{D}$ we evaluated the posterior distribution of parameters, $\Pr(\boldsymbol{\theta}_M | \mathcal{D}, M)$, where $\boldsymbol{\theta}_M$ is in general a vector of model-dependent parameters (see Table 4.1). Each subject's dataset $\mathcal{D}$ comprised of two sessions (training and test), for a total of about 1200 trials divided in 32 distinct conditions (8 priors $\times$ 2 noise levels $\times$ 2 sessions). In general, we assumed subjects shared the motor parameter σ_{motor} across sessions. We also assumed that from training to test sessions people would use the same high-noise to low-noise ratio between cue variability ($\tilde{\sigma}_{high}/\tilde{\sigma}_{low}$); so only one cue-noise parameter ($\tilde{\sigma}_{high}$) needed to be specified for the test session. Conversely, we assumed that the other noise-related parameters (κ, Σ_{high}, η_{prior}, λ), if present, could change freely between sessions, reasoning that additional response variability can be affected by the presence or absence of feedback, or as a result of the difference between training and test distributions. These assumptions were validated via a preliminary model comparison (see Section B.3.2 in the Appendix). Table 4.1 lists a summary of observer models and their free parameters.

We computed the posterior distribution of the parameters as $\Pr(\boldsymbol{\theta}_M | \mathcal{D}, M) \propto \Pr(\mathcal{D} | \boldsymbol{\theta}_M, M) \Pr(\boldsymbol{\theta}_M | M)$, where we assumed a factorized prior over parameters, $\Pr(\boldsymbol{\theta}_M | M) = \prod_i \Pr(\theta_i | M)$. Having obtained independent measures of typical sensorimotor noise parameters of the subjects in a sensorimotor estimation experiment, we took informative log-normal priors on parameters σ_{motor} and Σ_{high} (when present), with log-scale respectively $\log 3.4 \cdot 10^{-3}$ and $\log 7.7 \cdot 10^{-3}$ screen units and shape parameters 0.38 and 0.32 (see Section 4.3.2; results did not depend crucially on the shape of the priors). For the other parameters we took a non-informative uniform prior $\sim$ Uniform$[0, 1]$ (dimensionful parameters were measured in normalized screen units), with the exception of the η_{prior} and κ parameters. The η_{prior} parameter that regulates the noise in the prior could occasionally be quite large so we adopted a broader range $\sim$ Uniform$[0, 4]$ to avoid edge effects. A priori, the κ parameter that governs noise

in decision making could take any positive nonzero value (with higher probability mass on lower values), so we assumed a prior $\sim$ Uniform[0, 1] on $1/(\kappa+1)$, which is equivalent to a prior $\sim 1/(\kappa+1)^2$, for $\kappa \in [0, \infty)$. Formally, a value of κ less than one represents a performance more variable than posterior-matching (for $\kappa \to 0$ the posterior distribution tends to a uniform distribution). Results of the model comparison were essentially identical whether we allowed κ to be less than one or not. We took a prior $\sim 1/\kappa^2$ on the positive real line since it is integrable; an improper prior such as a noninformative prior $\sim 1/\kappa$ is not recommendable in a model comparison between models with non-common parameters (see Gelman et al., 2013 and Appendix A).

The posterior distribution of the parameters is proportional to the data likelihood, which was computed in logarithmic form as:

$$\log \Pr\left(\mathcal{D} \,|\boldsymbol{\theta}_M, M\right) = \sum_{i=1}^{N} \log \Pr^{(reg)}\left(r^{(i)}|\text{trial}_i\right), \tag{4.23}$$

where $\Pr^{(reg)}$ is the regularized probability of response given by Eq. 4.22, and trial_i represents all the relevant variables of the i-th trial. Eq. 4.23 assumes that the trials are independent and that subjects' parameters are fixed throughout each session (stationarity).

Sampling from the posterior distribution of the parameters

A convenient way to compute a probability distribution whose unnormalized pdf is known (Eq. 4.23) is by using a MCMC method (e. g., slice sampling; Neal, 2003). For each dataset and model, we ran three parallel chains with different starting points (10^3 to 10^4 burn-in samples, $2 \cdot 10^3$ to $5 \cdot 10^4$ saved samples per chain, depending on model complexity) obtaining a total of $6 \cdot 10^3$ to $1.5 \cdot 10^5$ sampled parameter vectors. Marginal pdfs of sampled chains were visually checked for convergence. We also searched for the global minimum of the (minus log) marginal likelihood by running a minimization algorithm (`fminsearch` in MATLAB) from several starting points (30 to 100 random locations). With this information we verified that, as far as we could tell, the chains were not stuck in a local minimum. Finally, we computed Gelman and Rubin's potential scale reduction statistic R for all parameters (Gelman and Rubin, 1992). Large values of R indicate convergence problems, whereas values close to 1 suggest convergence. Longer chains were run when suspicion of a convergence problem arose from any of these methods. In the end, the average R (across parameters, participants and models) was 1.003 and almost all values were < 1.1 suggesting good convergence.

Given the parameter samples, we computed the DIC score (deviance information criterion; Spiegelhalter et al., 2002) for each dataset and model. The DIC score is a

metric that combines a goodness of fit term and a penality for model complexity, similarly to other metrics adopted in model comparison, such as Akaike Information Criterion (AIC) and Bayesian Information Criterion (BIC), with the advantage that DIC takes into account an estimate of the effective complexity of the model and it is particularly easy to compute given MCMC output (see Section A.3.3 in the Appendix for details). DIC scores are meaningful only in a comparison, so we only report DIC scores differences between models (ΔDIC). Although a difference of 3–7 points is already suggested to be significant (Spiegelhalter et al., 2002), we follow a conservative stance, for which the difference in DIC scores needs to be 10 or more to be considered significant (e. g., Battaglia et al., 2011). In Section B.3.1 of the Appendix we report a set of model comparisons evaluated in terms of group DIC (GDIC). The assumption of GDIC is that all participants' datasets have been generated by the same observer model, and all subjects contribute equally to the evidence of each model.

Hierarchical Bayesian model selection

In the Results section, instead, we compared models according to a hierarchical Bayesian model selection method (BMS; Stephan et al., 2009) that treats both subjects and models as random factors, that is, multiple observer models may be present in the population. BMS uses an iterative algorithm based on variational inference to compute model evidence from individual subjects' marginal likelihoods (or approximations thereof, such as DIC, with the marginal likelihood being $\approx -\frac{1}{2}$ DIC). BMS is particularly appealing because it naturally deals with group heterogeneity and outliers. Moreover, the output of the algorithm has an immediate interpretation as the probability that a given model is responsible for generating the data of a randomly chosen subject. BMS also allows to easily compute the cumulative evidence for groups of models and we used this feature to compare distinct levels within factors (Stephan et al., 2009). As a Bayesian metric of significance we report the exceedance probability P^* of a model (or model level within a factor) being more likely than any other model (or level). We consider values of $P^* > 0.95$ to be significant. The BMS algorithm is typically initialized with a symmetric Dirichlet distribution that represents a prior over model probabilities with no preference for any specific model (Stephan et al., 2009). Since we are comparing a large number of models generated by the factorial method, we chose for the concentration parameter of the Dirichlet distribution a value $\alpha_0 = 0.25$ that corresponds to a weak prior belief that only a few observer models are actually present in the population ($\alpha_0 \to 0$ would correspond to the prior belief that only one model is true, similarly to GDIC, and $\alpha_0 = 1$ that any number of models are true). Results are qualitatively independent of the specific choice of α_0 for a large range of values.

When looking at alternative models of decision making in our second factorial model comparison, we excluded from the analysis 'uninteresting' trials in which the theoretical posterior distribution (Eq. 4.5 with the true values of σ_{low} and σ_{high}) was too close in shape to a Gaussian; since predictions of these models are identical for Gaussian posteriors, Gaussian trials constitute only a confound for the model comparison. A posterior distribution was considered 'too close' to a Gaussian if the Kullback-Leibler divergence between a Gaussian approximation with matching low-order moments and the full posterior was less than a threshold value of 0.02 nats (results were qualitatively independent of the chosen threshold). In general, this preprocessing step removed about 45–60% of trials from unimodal and bimodal sessions (clearly, Gaussian sessions were automatically excluded).

In Section B.3.1 of the Appendix we report instead a classical (frequentist) analysis of the group difference in DIC between models (GDIC), which assumes that all datasets have been generated by the same unknown observer model. In spite of different assumptions, BMS and GDIC agree on the most likely observer model, validating the robustness of our main findings. The two approaches exhibit differences with respect to model ranking because GDIC, as a 'fixed effect' method, does not account for group heterogeneity and outliers (Stephan et al., 2009; see Section B.3.1 in the Appendix for details). Finally, we assessed the impact of each factor on model performance by computing the average change in DIC associated with a given component.

Non-parametric reconstruction of the priors

We reconstructed the group priors as a means to visualize the subjects' common systematic biases under a specific observer model. Each group prior $q_{prior}(s)$ was 'non-parametrically' represented by a mixture of Gaussians with a large number of components ($m = 31$). The components' means were equally spaced on a grid that spanned the range of the discrete representation of the prior; SDs were equal to the grid spacing. The mixing weights $\{\pi_i\}_{i=1}^{m}$ were free to vary to define the shape of the prior (we enforced symmetric values on symmetric distributions, and the sum of the weigths to be one). The representation of the prior as a mixture of Gaussians allowed us to cover a large class of smooth distributions using the same framework as the rest of our study.

For this analysis we fixed subjects' parameters to the values inferred in our main model comparison for one of the most supported model, SPK-L (i.e. to the robust means of the posterior of the parameters). For each prior in each group (Gaussian, unimodal and bimodal test sessions), we simultaneously inferred the shape of the non-parametric prior that explained each subject's dataset, assuming the same distribution q_{prior} for all subjects. Specifically, we sampled from the posterior distribution

of the parameters of the group priors, $\Pr\left(q_{prior}\,|\mathcal{D}\right)$, with a flat prior over log values of the mixing weights $\{\pi_i\}_{i=1}^{m}$. We ran 5 parallel chains with a burn-in of 10^3 samples and $2\cdot 10^3$ samples per chain, for a total of 10^4 sampled vectors of mixing weights (see before for details on sampling). Each sampled vector of mixing weights corresponds to a prior $q_{prior}^{(j)}$, for $j = 1\ldots 10^4$. For each sampled prior we also computed the first four central moments (mean, variance, skewness and kurtosis) and calculated the posterior average of the moments.

4.3 RESULTS

We first describe the results of the experiment and subjects' performance in a model-free way (Section 4.3.1). We then briefly present the findings of the sensorimotor estimation session (Section 4.3.2). This section concludes with an extended presentation of the results of our model comparisons (Section 4.3.3).

4.3.1 *Human performance*

We first performed a model-free analysis of subjects' performance. Figure 4.4 shows three representative prior distributions and the pooled subjects' responses as a function of the cue position for low (red) and high (blue) noise cues. Note that pooled data are used here only for display and all subjects' datasets were analyzed individually. The cue positions and responses in Figure 4.4 are reported in a coordinate system relative to the mean of the prior (set as $\mu_{prior} = 0$). For all analyses we consider relative coordinates without loss of generality, having verified the assumption of translational invariance of our task (see Section B.2.1 in the Appendix).

Figure 4.4 shows that subjects' performance was affected by both details of the prior distribution and the cue. Also, subjects' mean performance (continuous lines in Figure 4.4) show deviations from the prediction of an optimal Bayesian observer (dashed lines), suggesting that subjects' behaviour may have been suboptimal.

Linear integration with Gaussian priors

We examined how subjects performed in the task under the well-studied case of Gaussian priors (see Section 2.3.2). Given a Gaussian prior with SD σ_{prior} and a noisy cue with horizontal position x_{cue} and known variability σ_{cue} (assuming Gaussian noise), the most likely target location can be computed through Bayes' theorem. In the rela-

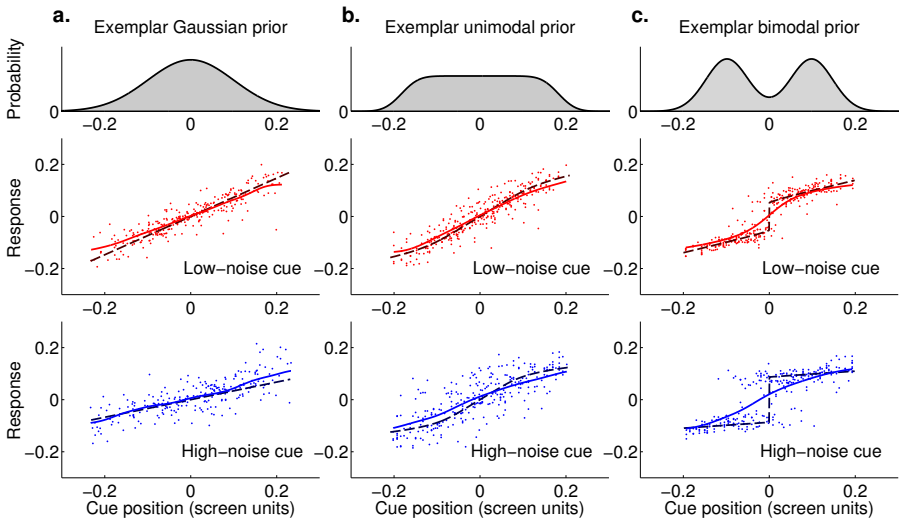

Figure 4.4: **Subjects' responses as a function of the position of the cue.** Each panel shows the pooled subjects' responses as a function of the position of the cue either for low-noise cues (red dots) or high-noise cues (blue dots). Each column corresponds to a representative prior distribution, shown at the top, for each different group (Gaussian, unimodal and bimodal). In the response plots, dashed lines correspond to the Bayes optimal strategy given the generative model of the task. The continuous lines are a kernel regression estimate of the mean response (see Data analysis, Section 4.2.2). **a.** Exemplar Gaussian prior (prior 4 in Figure 4.2a). **b.** Exemplar unimodal prior (platykurtic distribution: prior 4 in Figure 4.2b). **c.** Exemplar bimodal prior (prior 5 in Figure 4.2c). Note that in this case the mean response is not necessarily a good description of subjects' behaviour, since the marginal distribution of responses for central positions of the cue is bimodal.

tive coordinate system ($\mu_{prior} = 0$), the optimal target location takes the simple linear form:

$$s^*(x_{cue}) = w \cdot x_{cue} \qquad \text{with } w = \frac{\sigma^2_{prior}}{\sigma^2_{prior} + \sigma^2_{cue}} \qquad \text{(relative coordinates)}, \tag{4.24}$$

where w is the linear weight assigned to the cue.

We compared subjects' behaviour with the 'optimal' strategy predicted by Eq. 4.24 (see for instance Figure 4.4a; the dashed line corresponds to the optimal strategy). For each subject and each combination of σ_{prior} and cue type (either 'short' or 'long', corresponding respectively to low-noise and high-noise cues), we fit the responses r as a function of the cue position x_{cue} with a robust linear fit. The slopes of these fits for the training session are plotted in Figure 4.5; results were similar for the Gaussian test session. Statistical differences between different conditions were assessed using repeated-measures ANOVA (rm-ANOVA) with Greenhouse-Geisser correction (see Data analysis).

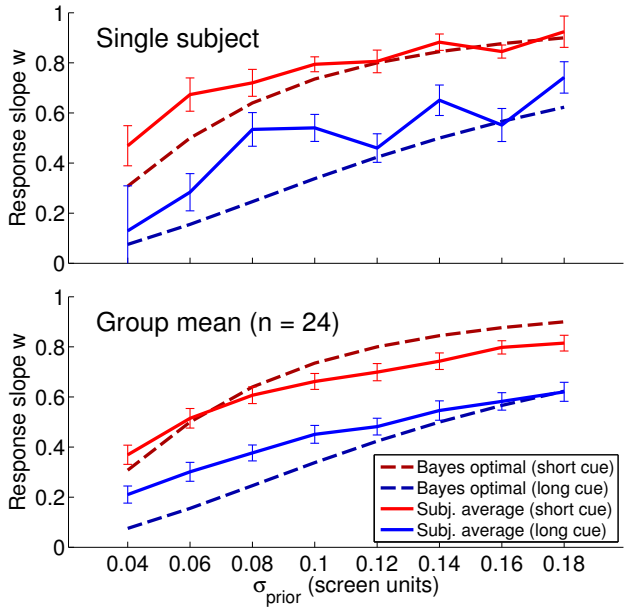

Figure 4.5: **Response slopes for the training session.** Response slope w as a function of the SD of the Gaussian prior distribution, σ_{prior}, plotted respectively for trials with low noise ('short' cues, red line) and high noise ('long' cues, blue line). The response slope is equivalent to the linear weight assigned to the position of the cue (Eq. 4.24). Dashed lines represent the Bayes optimal strategy given the generative model of the task in the two noise conditions. *Top:* Slopes for a representative subject in the training session (slope $\pm$ SE). *Bottom:* Average slopes across all subjects in the training session ($n = 24$, mean $\pm$ SE across subjects).

In general, subjects did not perform exactly as predicted by the optimal strategy (dashed lines), but they took into account the probabilistic nature of the task. Specifically, subjects tended to give more weight to low-noise cues than to high-noise ones (main effect: Low-noise cues, High-noise cues; $F_{(1,23)} = 145$, $p < 0.001$), and the weights were modulated by the width of the prior (main effect: prior width σ_{prior}; $F_{(3.45,79.2)} = 88$, $\epsilon = 0.492$, $p < 0.001$), with wider priors inducing higher weighting of the cue. Interestingly, cue type and width of the prior seemed to influence the weights independently, as no significant interaction was found (interaction: prior width $\times$ cue type; $F_{(4.86,112)} = 0.94$, $\epsilon = 0.692$, $p = 0.46$). Analogous patterns were found in the Gaussian test session.

Mean rightward bias

After analyzing the slope of linear fits of subjects' responses, we consider here the average bias (intercept). For a Bayes optimal observer we would expect the bias to be zero in relative coordinates (Eq. 4.24 has no constant term). Instead, we found that on average subjects exhibited a small but statistically significant positive (i.e. rightward)

bias in the training session, of the magnitude of 0.5–3 mm (Figure 4.6a). Interestingly, we found that the magnitude of this rightward bias was context-dependent, linearly related to the uncertainty (SD) of the posterior distribution in a trial ($R^2 = 0.93$, Figure 4.6b). Moreover, the rightward bias was not due to a systematic error that participants made in estimating the position of the cue, as separate measurements found that subjects' estimates were overall unbiased (see later, Section 4.3.2). These findings suggest that the bias emerged during the decision-making process or execution of the planned motor action (see Discussion).

We estimated the impact of the observed mean rightward bias on our subjects' performance by calculating how this bias would affect the performance of an optimal Bayesian observer. Specifically, for each subject and for all trials of the training session we computed the optimality index of a rightward-biased Bayesian observer, whose responses were shifted to the right according to the linear equation in Figure 4.6. We found a difference in efficiency of $\sim 2 \cdot 10^{-3}$, which is a tiny change in efficiency for an ideal observer. Given that, as we will see, the subjects were suboptimal in many ways, a similar change is empirically negligible among other sources of suboptimality. Therefore, at the level of detail afforded by our data, there is no need to explictly account for the rightward bias in order to explain subjects' performance.

Moreover, we found that the average bias was reduced in the Gaussian test session: $(3.2 \pm 1.6) \cdot 10^{-3}$ screen units (~ 1 mm) and only marginally different than zero (t-test $t_{(7)} = 2.06$, $p = 0.08$).

Optimality index

The optimality index is a general measure of performance that is applicable beyond the Gaussian case. Figure 4.7 shows the optimality index averaged across subjects for different conditions, in different sessions. Data are also summarized in Table 4.2. Priors in Figure 4.7 are listed in order of differential entropy (which corresponds to increasing variance for Gaussian priors), with the exception of 'unimodal test' priors which are in order of increasing width of the main peak in the prior, as computed through a Laplace approximation. We chose this ordering for priors in the unimodal test session as it highlights the pattern in subjects' performance (see below).

For a comparison, Figure 4.7 also shows the optimality index of two suboptimal models that represent two extremal response strategies. Dash-dotted lines correspond to the optimality index of a Bayesian observer that maximizes the probability of locating the correct target considering only the prior distribution. Conversely, dotted lines correspond to an observer that only uses the cue and ignores the prior: that is, the observer's response in a trial matches the current position of the cue. The shaded gray area specifies the *synergistic integration* zone, in which the subject is integrating

synergistic integration

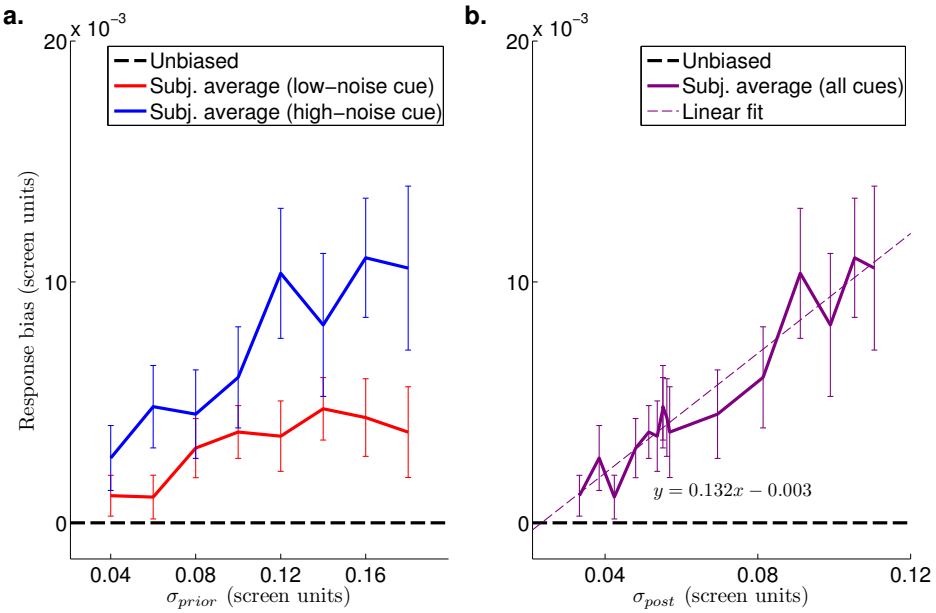

Figure 4.6: **Group mean response bias for the training session. a:** Group mean response bias as a function of the SD of the Gaussian prior distribution, σ_{prior}, plotted respectively for trials with low-noise cues (red line) and high-noise cues (blue line). Averages are taken across all subjects in the training session ($n = 24$, mean $\pm$ SE across subjects). A Bayes optimal observer should have overall zero bias ('unbiased' dashed line). Overall, the response biases for low-noise and high-noise cues are both statistically significantly different than zero (resp. $p < 10^{-7}$ and $p < 10^{-10}$, signed test on the pooled response biases), meaning that on average subjects exhibited a 'rightward bias'. **b:** Group mean response bias (same data as panel a) plotted as a function of the SD of the posterior distribution, σ_{post}. The purple dashed line is a linear fit of the group mean biases, showing that the average rightward bias is correlated with the width of the posterior ($R^2 = 0.93$).

Session	Low-noise cue	High-noise cue	All cues
Gaussian training	0.86 ± 0.02	0.87 ± 0.01	0.87 ± 0.01
Gaussian test	0.89 ± 0.02	0.88 ± 0.02	0.89 ± 0.01
Unimodal test	0.85 ± 0.03	0.80 ± 0.04	0.83 ± 0.02
Bimodal test	0.90 ± 0.02	0.89 ± 0.01	0.89 ± 0.01
All sessions	0.87 ± 0.01	0.87 ± 0.01	0.87 ± 0.01

Table 4.2: **Group mean optimality index.** Each entry reports mean $\pm$ SE of the group optimality index for a specific session and cue type, or averaged across all sessions/cues. See also Figure 4.7.

information from both prior and cue in a way that leads to better performance than by using either the prior or the cue alone. Qualitatively, the behaviour in the gray area can be regarded as 'close to optimal', whereas performance below the gray area

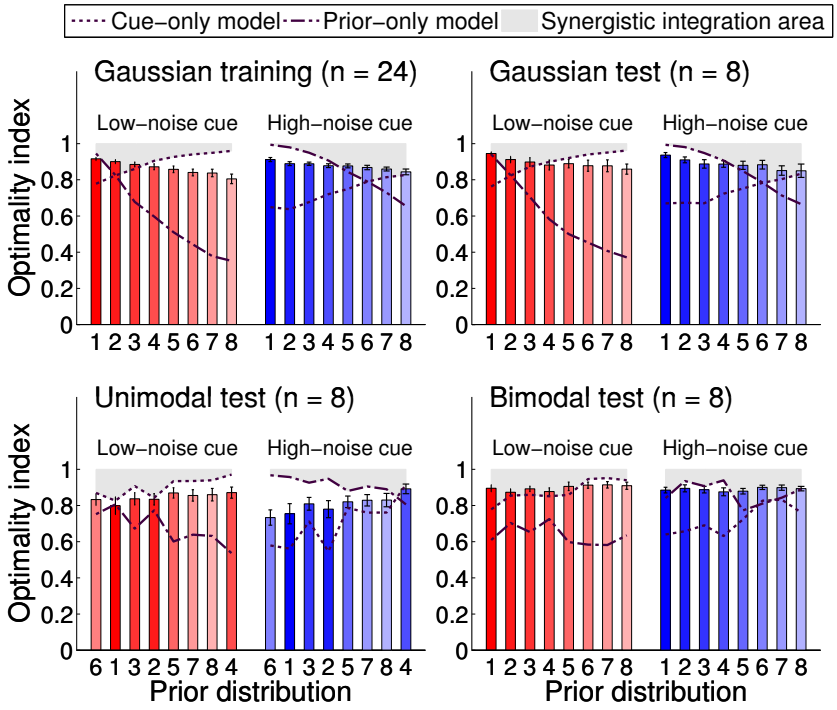

Figure 4.7: **Group mean optimality index.** Each bar represents the group-averaged optimality index for a specific session, for each prior (indexed from 1 to 8, see also Figure 4.2) and cue type, low-noise cues (red bars) or high-noise cues (blue bars). The optimality index in each trial is computed as the probability of locating the correct target based on the subjects' responses divided by the probability of locating the target for an optimal responder. The maximal optimality index is 1, for a Bayesian observer with correct internal model of the task and no sensorimotor noise. Error bars are SE across subjects. Priors are arranged in the order of differential entropy (i.e. increasing variance for Gaussian priors), except for 'unimodal test' priors which are listed in order of increasing width of the main peak in the prior (see text). The dotted line and dash-dotted line represent the optimality index of a suboptimal observer that takes into account respectively either only the cue or only the prior. The shaded area is the zone of synergistic integration, in which an observer performs better than using information from either the prior or the cue alone.

is suboptimal. As it is clear from Figure 4.7, in all sessions participants were sensitive to probabilistic information from both prior and cue – that is, performance is always above the minimum of the extremal models (dash-dotted and dotted lines) – in agreement with what we observed in Figure 4.5 for Gaussian sessions, although their integration was generally suboptimal.

We examined how the optimality index changed across different conditions. From the analysis of the training session, it seems that subjects were able to integrate low-noise and high-noise cues for priors of any width equally well, as we found no effect of cue type on performance (main effect: Low-noise cues, High-noise cues; $F_{(1,23)} =$

0.015, $p = 0.90$) and no significant interaction between cue types and prior width (interaction: prior width $\times$ cue type; $F_{(5.64,129.6)} = 1.56$, $\epsilon = 0.81$, $p = 0.17$). However, relative performance was significantly affected by the width of the prior per se (main effect: prior width σ_{prior}; $F_{(2.71,62.3)} = 17.94$, $\epsilon = 0.387$, $p < 0.001$); people tended to perform worse with wider priors, in a way that is not simply explained by the objective decrease in the probability of locating the correct target due to the less available information (see Discussion).

Results in the Gaussian test session (Figure 4.7 top right) replicated what we had obtained in the training session. Subjects' performance was not influenced by cue type (main effect: Low-noise cues, High-noise cues; $F_{(1,7)} = 0.026$, $p = 0.88$) nor by the interaction between cue types and prior width (interaction: prior width $\times$ cue type; $F_{(2.65,18.57)} = 0.67$, $\epsilon = 0.379$, $p = 0.56$). Conversely, as before, the width of the prior affected performance significantly (main effect: prior width σ_{prior}; $F_{(1.47,10.3)} = 5.21$, $\epsilon = 0.21$, $p < 0.05$); again, wider priors were associated with lower relative performance.

A similar pattern of results was found also for the bimodal test session (Figure 4.7 bottom right). Performance was affected significantly by the shape of the prior (main effect: prior shape; $F_{(4.01,28.1)} = 3.93$, $\epsilon = 0.573$, $p < 0.05$) but otherwise participants integrated cues of different type with equal skill (main effect: Low-noise cues, High-noise cues; $F_{(1,7)} = 1.42$, $p = 0.27$; interaction: prior shape $\times$ cue type; $F_{(2.84,19.9)} = 1.1$, $\epsilon = 0.406$, $p = 0.37$). However, in this case performance was not clearly correlated with a simple measure of the prior or of the average posterior (e. g., differential entropy).

Another scenario emerged in the unimodal test session (Figure 4.7 bottom left). Here, subjects' performance was affected not only by the shape of the prior (main effect: prior shape; $F_{(3.79,26.5)} = 20.7$, $\epsilon = 0.542$, $p < 0.001$) but also by the type of cue (main effect: Low-noise cues, High-noise cues; $F_{(1,7)} = 9.85$, $p < 0.05$) and the specific combination of cue and prior (interaction: prior shape $\times$ cue type; $F_{(3.53,24.7)} = 5.27$, $\epsilon = 0.504$, $p < 0.01$). Moreover, in this session performance improved for priors whose main peak was broader (see Discussion).

Notwithstanding this heterogeneity of results, an overall comparison of participants' relative performance in test sessions (averaging results over priors) did not show statistically significant differences between groups (main effect: group; $F_{(2,21)} = 2.13$, $p = 0.14$) nor between the two levels of reliability of the cue (main effect: Low-noise cues, High-noise cues; $F_{(1,21)} = 3.36$, $p = 0.08$); only performance in the unimodal session for high-noise cues was at most marginally worse. In particular, relative performance in the Gaussian test and the bimodal test sessions was surprisingly similar, unlike previous learning experiments (see Discussion). Note that this

near-constancy of efficiency is not visible when we look at the absolute performance, which does change considerably between different conditions due to the intrinsic variations in the amount of available probabilistic information (see Section B.2.2 in the Appendix).

Finally, we examined the average optimality index as a function of trial number in the training and test sessions (Figure 4.8). We found that group performance exhibited a small but statistically significant improvement between the first and last quarter of the training session (difference in optimality index: 0.023 ± 0.008, mean $\pm$ SE; paired t-test $t_{(23)} = 2.96$, $p < 0.01$), but no significant difference was found between the beginning and the end of the test sessions ($p > 0.30$ for each test session). This finding suggests that subjects were using the full performance feedback provided in the training session to (marginally) improve their performance, but there was no additional learning (or significant worsening) when only partial feedback was available, as per our initial assumption (see 'Experimental sessions' in Section 4.2.1).

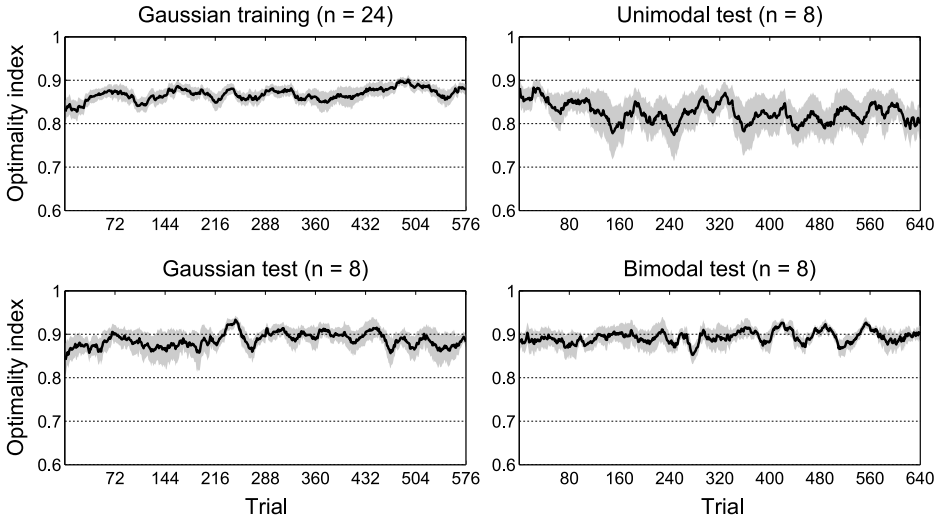

Figure 4.8: **Group mean performance per trial.** Mean optimality index per trial, averaged over all subjects for each session (shaded area ± 1 SE). Performance data are smoothed over a window of radius 10 trials, for visualization purposes.

Effects of uncertainty on reaction time

Lastly, we examined the effect of uncertainty on subjects' reaction time (time to start movement after the 'go' beep) in each trial. Uncertainty was quantified as the SD of the posterior distribution in the current trial, σ_{post}. We found that the average subjects' reaction time grew almost linearly with σ_{post} (Figure 4.9). The average change in reaction times (from lowest to highest uncertainty in the posterior) was substantial during

the training session ($\sim$ 50 ms, about 15% change), although less so in subsequent test sessions.

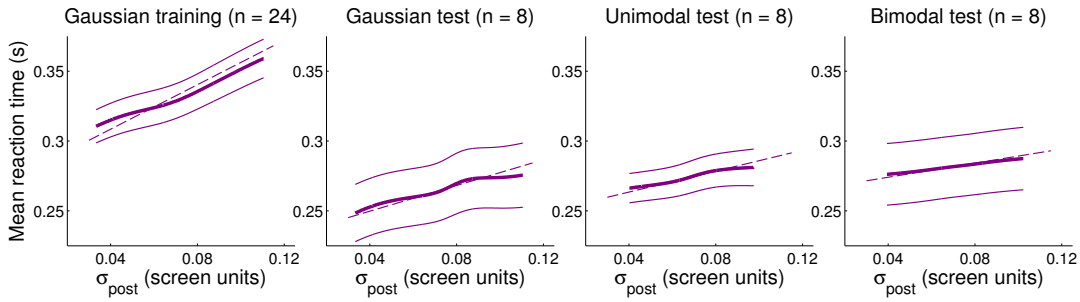

Figure 4.9: **Average reaction times as a function of the SD of the posterior distribution.** Each panel shows the average reaction times (mean $\pm$ SE across subjects) for a given session as a function of the SD of the posterior distribution, σ_{post} (individual data were smoothed with a kernel regression estimate, see Methods). Dashed lines are robust linear fits to the reaction times data. For all sessions the slope of the linear regression is significantly different than zero (t-test $p < 10^{-3}$ on pooled data, for all sessions).

4.3.2 *Sensorimotor measurement session*

A subset of observers ($n = 10$) performed in a sensorimotor measurement session to verify the impact of sensorimotor noise on their targeting performance (see 'Measuring sensorimotor noise' in Section 4.2.1). The root-mean-squared error (RMSE) of the response with respect to the true target position was on average $(9.3 \pm 0.8) \cdot 10^{-3}$ screen units for long-distance cues and $(5.2 \pm 0.3) \cdot 10^{-3}$ screen units for short-distance cues (mean $\pm$ SE across subjects). In general, the RMSE can be divided in a constant bias term and a variance term, but the bias term was overall small, on average $(0.6 \pm 0.5) \cdot 10^{-3}$ screen units, and not significantly different than zero (t-test $t_{(9)} = 1.18$, $p = 0.26$), which means that the error arose almost entirely from the subjects' response variability.

Since subjects knew that the cues were fully informative about the target position, all variability in their responses originated from two sources: sensory noise (error in projecting the cue position on the target line) and motor noise. We assumed that sensory and motor noise were independent and normally distributed, and that sensory variability was proportional to the distance of the cue from the target line (Weber's law). Under these assumptions, variance of subjects' responses was described by the following formula:

$$\sigma^2_{response} = \sigma^2_{motor} + w^2_{sensory} d^2_{cue}, \tag{4.25}$$

where $w_{sensory}$ is Weber's fraction and d_{cue} is the distance of the cue from the target line. Using Eq. 4.25 we were able to estimate participants' sensorimotor parameters; results are reported in Table 4.3.

Parameter	Description	Mean $\pm$ SD (screen units)	Mean $\pm$ SD (mm)
σ_{motor}	Motor noise	$(3.6 \pm 1.1) \cdot 10^{-3}$	1.1 ± 0.3
Σ_{low}	Sensory noise (short cues)	$(3.5 \pm 1.1) \cdot 10^{-3}$	1.1 ± 0.3
Σ_{high}	Sensory noise (long cues)	$(8.1 \pm 2.6) \cdot 10^{-3}$	2.4 ± 0.8

Table 4.3: **Average estimated sensorimotor parameters.** Group-average estimated motor and sensory noise parameters. Estimates were obtained from the data through Eq. 4.25.

The estimated parameters in Table 4.3 allowed us to assess the typical impact of realistic values of sensorimotor noise on subjects' performance. First, we computed the performance of the optimal ideal observer model with added realistic noise. In order to do so, we generated 1000 subjects by sampling from the distribution of estimated sensorimotor parameters and we then simulated their behaviour on our subjects' datasets according to the optimal observer model. We found an average optimality index of 0.997 ± 0.001, which is empirically indistinguishable from one. The difference in performance induced by the sensorimotor noise was analogously negligible for the simulations of other ideal observer models, such as the 'prior-only' or 'cue-only' models (see Figure 4.7). These results show that sensory noise in estimating the location of the cue and motor noise in executing the reaching movement had a very limited impact on subjects' performance.

The pooled estimated parameters summarized in Table 4.3 were used to construct the informative priors for the motor and sensory parameters that were applied in our model comparison (see next section). Bootstrapped parameters were fit with log-normal distributions with log-scale μ and shape parameter σ (which correspond to mean and SD in log space.The resulting parameters of the priors were $\mu = \log 3.4 \cdot 10^{-3}$ screen units, $\sigma = 0.38$ for σ_{motor}; and $\mu = \log 7.7 \cdot 10^{-3}$ screen units, $\sigma = 0.32$ for Σ_{high}. The prior on σ_{motor} was used in all observer models, whereas the prior on Σ_{high} was used only in the observer models with sensory noise (model factor S).

4.3.3 *Results of model comparisons*

We describe in this section the results of a first model comparison ('Main factorial model comparison') on the observer models described in Section 4.2.3. We subse-

quently present the findings of a second, more specific model comparison that looks at some aspects of the decision-making process ('Comparison of alternative models of decision making'). We conclude by analyzing in detail the features of the most supported observer model ('Analysis of best observer model').

Main factorial model comparison

Figure 4.10 shows the results of the Bayesian model selection (BMS) method applied to our basic model set (see Section 4.2.3). Figure 4.10a shows the model evidence for each individual model and subject. For each subject we computed the posterior probability of each observer model using DIC as an approximation of the marginal likelihood (see Section 4.2.4). We calculated model evidence as the Bayes factor (posterior probability ratio) between the subject's best model and a given model. In the graph we report model evidence in the same scale as DIC, that is as twice the log Bayes factor. A difference of more than 10 in this scale is considered very strong evidence (Kass and Raftery, 1995). Results for individual subjects show that model SPK-P-L (stochastic posterior with estimation noise on the prior and lapse) performed consistently better than other models for all conditions. A minority of subjects were also well represented by model SPK-P (same as above, but without the lapse component). All other models performed significantly worse. In particular, note that the richer SPK-S-P-L model was not supported, suggesting that that sensory noise on estimation of cue location was not needed to explain the data. Figure 4.10b confirms these results by showing the estimated probability of finding a given observer model in the population (assuming that multiple observer models could be present). Model SPK-P-L is significantly more represented ($P = 0.72$; exceedance probability $P^* > 0.999$), followed by model SPK-P ($P = 0.10$). For all other models the probability is essentially the same at $P < 0.01$. The probability of single model factors reproduced an analogous pattern (Figure 4.10c). The majority of subjects (more than 80% in each case) are likely to use a stochastic decision making (SPK), to have noise in the estimation of the priors (P), and lapse (L). Only a minority (10%) would be described by an observer model with sensory noise in estimation of the cue. The model comparison yielded similar results, although with a more graded difference between models, when looking directly at DIC scores (see Section B.3.1 in the Appendix; lower is better).

To assess in another way the relative importance of each model component in determining the performance of a model, we measured the average contribution to DIC of each model level within a factor across all tested models (Figure B.5 in the Appendix). In agreement with our previous findings, the lowest DIC (better score) in decision making is obtained by observer models containing the SPK factor. BDT increases (i.e.

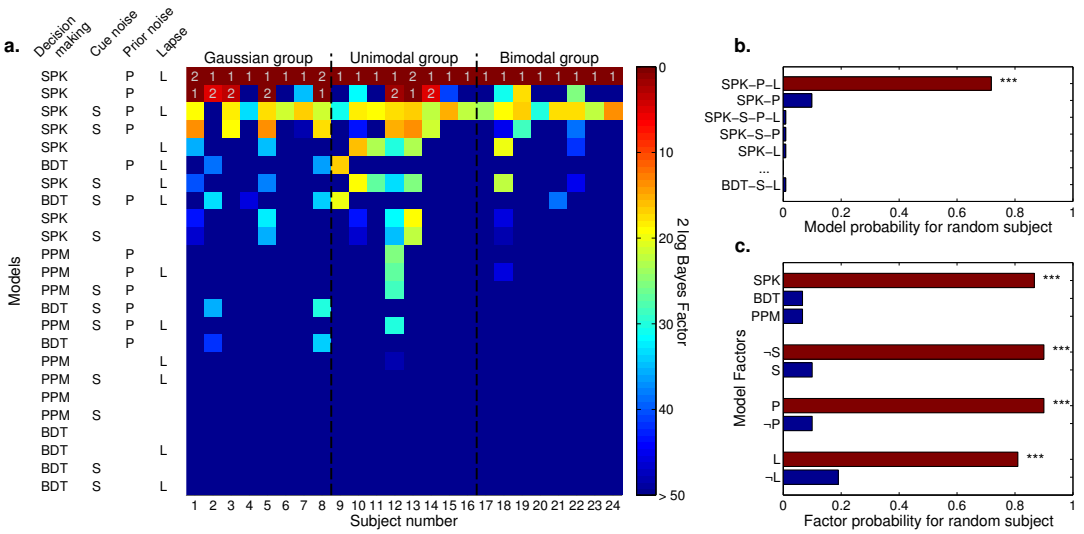

Figure 4.10: **Model comparison between individual models. a:** Each column represents a subject, divided by test group (all datasets include a Gaussian training session), each row an observer model identified by a model string (see Table 4.1). Cell colour indicates model's evidence, here displayed as the Bayes factor against the best model for that subject (a higher value means a worse performance of a given model with respect to the best model). Models are sorted by their posterior likelihood for a randomly selected subject (see panel b). Numbers above cells specify ranking for most supported models with comparable evidence (difference less than 10 in 2 log Bayes factor; Kass and Raftery, 1995). **b:** Probability that a given model generated the data of a randomly chosen subject. Here and in panel c, brown bars represent the most supported models (or model levels within a factor). Asterisks indicate a significant exceedance probability, that is the posterior probability that a given model (or model component) is more likely than any other model (or model component): $(^{***})P^* > 0.999$. **c:** Probability that a given model level within a factor generated the data of a randomly chosen subject.

worsens) average DIC scores substantially (difference in DIC, ΔDIC = 173 ± 14; mean $\pm$ SE across subjects) and PPM has devastating effects on model performance (ΔDIC = 422 ± 72), where 10 points of ΔDIC may already be considered a strong evidence towards the model with lower DIC (Spiegelhalter et al., 2002). Regarding the other factors (S, P, L), we found that in general the lack of a factor increases DIC (worse model performance; see Section B.3.1 in the Appendix for discussion about factor S). Overall, this analysis confirms the strong impact that an appropriate modelling of variability has on model performance (see Section B.3.1 in the Appendix for more details).

We performed a number of analyses on an additional set of observer models to validate the finding that model SPK-P-L provides the best explanation for the data in our model set.

First, in all the observer models described so far the subjects' parameters of the likelihood, $\tilde{\sigma}_{low}$ and $\tilde{\sigma}_{high}$, were allowed to vary. Preliminary analysis had suggested that observer models with mismatching likelihoods always outperformed models with true likelihood parameters, σ_{low} and σ_{high}. We tested whether this was the case also with our current best model, or if we could assume instead that at least some subjects were using the true parameters. Model SPK-P-L-true performed considerably worse than its counterpart with mismatching likelihood parameters ($P = 0.01$ with $P^* \approx 1$ for the other model; ΔDIC = 178 ± 33), suggesting that mismatching likelihoods are invariably necessary to explain our subjects' data.

We then checked whether the variability of subjects' estimates of the priors may have arisen instead due to the discrete representation of the prior distribution in the experiment (see Figure 4.1d). We, therefore, considered a model SPK-D-L in which priors were not noisy, but the model component 'D' replaces the continuous representations of the priors with their true discrete representation (a mixture of a hundred narrow Gaussians corresponding to the dots shown on screen). Model SPK-D-L performed worse than model SPK-P-L ($P = 0.01$ with $P^* \approx 1$ for the other model; ΔDIC = 145 ± 25) and, more interestingly, also worse than model SPK-L ($P = 0.09$ with $P^* \approx 1$ for the other model; ΔDIC = 59 ± 15). The discrete representation of the prior does not provide a better explanation for subjects' behaviour.

In summary, all analyses identify as the main sources of subjects' suboptimal behaviour the combined effect of both noise in estimating the shape of the 'prior' distributions and variability in the subsequent decision, plus some occasional lapses.

Comparison of alternative models of decision making

Our previous analyses suggest that subjects exhibit variability in decision making that conforms to some nontrivial transformation of the posterior distribution (such as a power function of the posterior, as expressed by model component SPK). We perform a second factorial model comparison that focusses on details of the decision-making process, by including additional model components that describe different transformations of the posterior.

We consider in this analysis the following factors (the additions are underlined):

1. *Decision making* (4 levels): Bayesian Decision Theory ('BDT'), stochastic posterior ('SPK'), posterior probability matching ('PPM'), posterior sampling-average ('PSA').

2. *Gaussian approximation of the posterior* (3 levels): no approximation, mean/variance approximation ('MV') or Laplace approximation ('LA').

3. *Lapse* (2 levels): absent or present ('L').

Our extended model set comprises 18 observer models since some combinations of model factors lead to equivalent observer models. In order to limit the combinatorial explosion of models, in this factorial analysis we do not include model factors S and P that were previously considered, since our main focus here is on decision making (but see below). All new model components are explained in Section 4.2.3 ('Additional observer models for non-Gaussian priors') and summarized in Table 4.1.

Figure 4.11 shows the results of the BMS method applied to this model set. As before, we consider first the model evidence for each individual model and subject (Figure 4.11a). Results are slighly different depending on the session (unimodal or bimodal), but in both cases model SPK-L (stochastic posterior with lapse) performs consistently better than other tested models for all conditions. Only a couple of subjects are better described by a different approximation of the posterior (either PSA or SPK-MV-L). These results are summarized in Figure 4.11b, which shows the estimated probability that a given model would be responsible of generating the data of a randomly chosen subject. We show here results for both groups; a separate analysis of each group did not show qualitative differences. Model SPK-L is significantly more represented ($P = 0.64$; exceedance probability $P^* > 0.99$), followed by model PSA ($P = 0.10$) and SPK-MV-L ($P = 0.08$). For all other models the probability is essentially the same at $P \approx 0.01$. The probability of single model factors reproduces the pattern seen before (Figure 4.11c). The majority of subjects (more than 75% in each case) are likely to use a stochastic decision making (SPK), to use the full posterior (no Gaussian approximations), and lapse (L).

The model comparison performed on group DIC scores (GDIC) obtained mostly similar results although with a more substantial difference between the unimodal group and the bimodal group (Figure B.4 in the Appendix). In particular, group DIC scores fail to find significant differences between distinct types of approximation of the posterior in the unimodal case. The reason is that for several subjects in the unimodal group differences between models are marginal, and GDIC does not have enough information to disambiguate between these models. Nonetheless, results in the bimodal case are non-ambigous, and overall the SPK-L model emerges again as the best description of subjects' behaviour (see Section B.3.1 in the Appendix for details).

As mentioned before, in order to limit model complexity we did not include model factors S and P in the current analysis. We can arguably ignore sensory noise in cue estimation, S, since it was already proven to have marginal effect on subjects' behaviour, but this is not the case for noisy estimation of the prior, P. We need, therefore, to verify that our main results about decision making in the case of non-Gaussian posteriors were not affected by the lack of this factor. We compared the four most represented

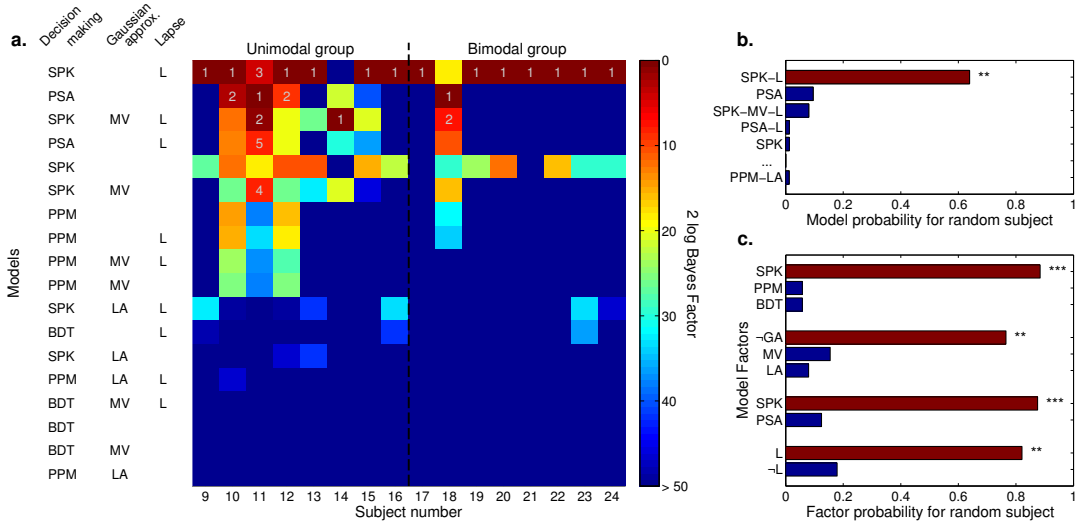

Figure 4.11: **Comparison between alternative models of decision making.** We tested a class of alternative models of decision making which differ with respect to predictions for non-Gaussian trials only. **a:** Each column represents a subject, divided by group (either unimodal or bimodal test session), each row an observer model identified by a model string (see Table 4.1). Cell colour indicates model's evidence, here displayed as the Bayes factor against the best model for that subject (a higher value means a worse performance of a given model with respect to the best model). Models are sorted by their posterior likelihood for a randomly selected subject (see panel b). Numbers above cells specify ranking for most supported models with comparable evidence (difference less than 10 in 2 log Bayes factor; Kass and Raftery, 1995). **b:** Probability that a given model generated the data of a randomly chosen subject. Here and in panel c, brown bars represent the most supported models (or model levels within a factor). Asterisks indicate a significant exceedance probability, that is the posterior probability that a given model (or model component) is more likely than any other model (or model component): $(^{**})P^* > 0.99$, $(^{***})P^* > 0.999$. **c:** Probability that a given model level within a factor generated the data of a randomly chosen subject. Label '¬GA' stands for no Gaussian approximation (full posterior).

models of the current analysis (Figure 4.11b) augmented with the P factor: SPK-P-L, PSA-P, SPK-MV-P-L and PSA-P-L. Model SPK-P-L was still the most representative model ($P = 0.80$, exceedance probability $P^* > 0.99$), showing that model factor P does not affect our conclusions on alternative models of decision making. We also found that model SPK-P-L obtained more evidence than any other model tested in this section ($P = 0.72$, exceedance probability $P^* > 0.99$), in agreement with the finding of our first factorial model comparison.

Finally, even though the majority of subjects' datasets is better described by the narrow loss function of the task, a few of them support also observer models that subtend a quadratic loss. To explore this diversity, we examined an extended BDT model in which the loss width σ_ℓ is a free parameter (see 'Observer model with free

loss width' in Section B.2.3 of the Appendix). This model performed slightly better than a BDT model with fixed σ_ℓ, but no better than the equivalent SPK model, so our findings are not affected.

In summary, subjects' variability in our task is compatible with them manipulating the full shape of the posterior corrupted by noise (SPK), and applying a close approximation of the loss function of the task. Our analysis marks as unlikely alternative models of decision making that use instead a quadratic loss or different low-order approximations of the posterior.

Analysis of best observer model

After establishing model SPK-P-L as the 'best' description of the data among the considered observer models, we examined its properties. First of all, we inspected the posterior distribution of the model parameters given the data for each subject. In almost all cases the marginalized posterior distributions were unimodal with a well-defined peak. We therefore summarized each posterior distribution with a point estimate (a robust mean) with minor loss of generality; group averages are listed in Table 4.4. For the analyses in this section we ignored outlier parameter values that fell more than 3 SDs away from the group mean (this rule excluded at most one value per parameter). In general, we found a reasonable statistical agreement between parameters of different sessions, with some discrepancies in the unimodal test session only. In this section, inferred values are reported as mean $\pm$ SD across subjects.

The motor noise parameter σ_{motor} took typical values of $(4.8 \pm 2.0) \cdot 10^{-3}$ screen units (~ 1.4 mm), somewhat larger on average than the values found in the sensorimotor estimation experiment, although still in a reasonable range (see Section 4.3.2). The inferred amount of motor noise is lower than estimates from previous studies in reaching and pointing (e. g., Tassinari et al., 2006), but in our task subjects had the possibility to adjust their end-point position.

The internal estimates of cue variability for low-noise and high-noise cues ($\tilde{\sigma}_{low}$ and $\tilde{\sigma}_{high}$) were broadly scattered around the true values ($\sigma_{low} = 0.06$ and $\sigma_{high} = 0.14$ screen units). In general, individual values were in qualitative agreement with the true parameters but showed quantitative discrepancies. Differences were manifest also at the group level, as we found statistically significant disagreement for both low and high-noise cues in the unimodal test session (t-test, $t_{(7)} > 3.73$, $p < 0.01$) and high-noise cues in the bimodal test session (t-test, $t_{(7)} = 2.51$, $p < 0.05$). The ratio between the two likelihood parameters, $\tilde{\sigma}_{high}/\tilde{\sigma}_{low} = 2.00 \pm 0.54$, differed significantly from the true ratio, $\sigma_{high}/\sigma_{low} = 2.33$ (t-test $t_{(22)} = 3.01$, $p < 0.01$).

Session	σ_{motor}	$\tilde{\sigma}_{low}$	$\tilde{\sigma}_{high}$	κ $(^*)$	η	λ
Gaussian training	$(4.8 \pm 2.0) \cdot 10^{-3}$	0.07 ± 0.02	0.13 ± 0.07	7.67 ± 4.33	0.48 ± 0.15	0.03 ± 0.02
Gaussian test	$(5.7 \pm 2.9) \cdot 10^{-3}$	0.07 ± 0.02	0.14 ± 0.07	7.31 ± 3.83	0.47 ± 0.20	0.02 ± 0.02
Unimodal test	$(6.3 \pm 4.8) \cdot 10^{-3}$	0.05 ± 0.01	0.08 ± 0.02	4.01 ± 2.77	0.48 ± 0.20	0.04 ± 0.02
Bimodal test	$(4.0 \pm 1.1) \cdot 10^{-3}$	0.06 ± 0.02	0.11 ± 0.03	6.38 ± 2.17	0.49 ± 0.28	0.04 ± 0.04
True values	–	$\sigma_{low} = 0.06$	$\sigma_{high} = 0.14$	–	–	–

Table 4.4: **Best observer model's estimated parameters.** Group-average estimated parameters for the 'best' observer model (SPK-P-L), grouped by session (mean $\pm$ SD across subjects). For each subject, the point estimates of the parameters were computed through a robust mean of the posterior distribution of the parameter given the data. For reference, we also report the true noise values of the cues, σ_{low} and σ_{high}. $(^*)$ We ignored values of $\kappa > 20$.

A few subjects ($n = 5$) were very precise in their decision-making process, with a power function exponent $\kappa > 20$. For the majority of subjects, however, κ took values between 1.8 and 14 (median 6.4), corresponding approximately to an amount of decision noise of $\sim$ 7–55% of the variance of the posterior distribution (median $\sim$ 15%). The range of exponents is compatible with values of κ ($\sim$ number of samples) previously reported in other experiments, such as a distance-estimation task (Battaglia et al., 2011) or 'intuitive physics' judgments (Battaglia et al., 2013). In agreement with the results of our previous model comparison, the inferred exponents suggest that subjects' stochastic decision making followed the shape of a considerably narrower version of the posterior distribution ($\kappa \gg 1$) which is not simply a form of posterior-matching ($\kappa = 1$).

The Weber's fraction of estimation of the parameters of the priors' density took typical values of $\eta_{prior} = 0.48 \pm 0.19$, with similar means across conditions. These values denote quite a large amount of noise in estimating (or manipulating) properties of the priors. Nonetheless, such values are in qualitative agreeement with a density/numerosity estimation experiment in which a change of $\sim$ 40% in density or numerosity of a field of random dots was necessary for subjects to note a difference in either property (Dakin et al., 2011). Although the two tasks are too different to allow a direct quantitative comparison, the thresholds measured by Dakin et al. (2011) suggest that density/numerosity estimation can indeed be as noisy as we found.

Finally, even though we did not set an informative prior over the parameter, the lapse rate took reasonably low values as expected from a probability of occasional mistakes (Wichmann and Hill, 2001; Kuss et al., 2005). We found $\lambda = 0.03 \pm 0.03$, and the inferred lapse rate averaged over training and test session was less than 0.06 for all but one subject.

We examined the best observer model's capability to reproduce our subjects' performance. For each subject and group, we generated 1000 datasets simulating the responses of the SPK-P-L observer model to the experimental trials experienced by the subject. For each simulated dataset, model parameters were sampled from the posterior distribution of the parameters given the data. For each condition (shape of prior and cue type) we then computed the optimality index and averaged it across simulated datasets. The model's 'postdictions' are plotted in Figure 4.12 as continuous lines (SE are omitted for clarity) and appear to be in good agreement with the data. Note that the postdiction is not exactly a fit since (a) the parameters are not optimized specifically to minimize performance error, and (b) the whole posterior distribution of the parameters is used and not just a 'best' point estimate. As a comparison, we also plotted in Figure 4.12 the postdiction for the best BDT ob-

server model, BDT-P-L (dashed line). As the model comparison suggested, standard Bayesian Decision Theory fails to capture subjects' performance.

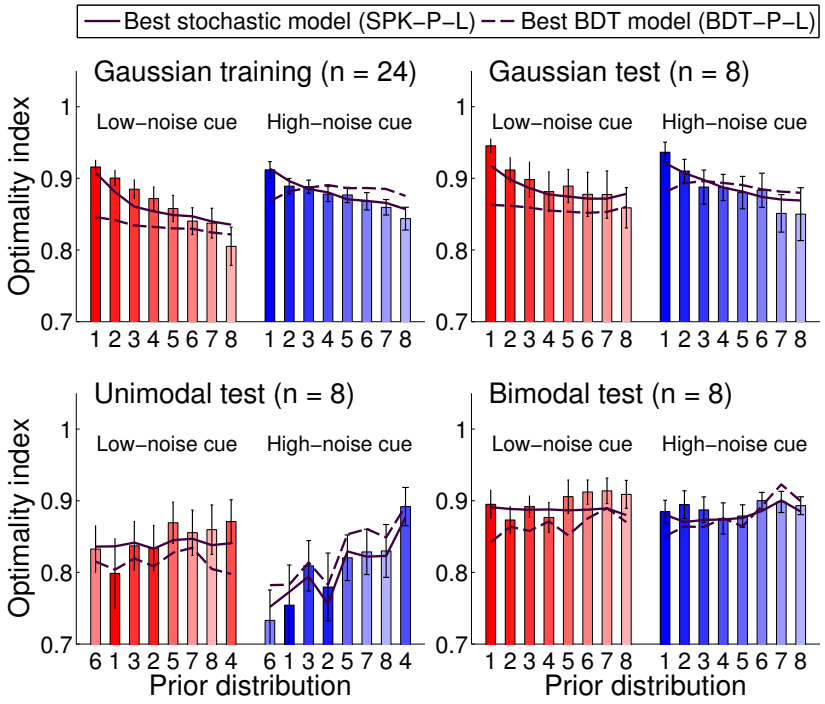

Figure 4.12: **Model 'postdiction' of the optimality index.** Each bar represents the group-averaged optimality index for a specific session, for each prior (indexed from 1 to 8, see also Figure 4.2) and cue type, either low-noise cues (red bars) or high-noise cues (blue bars); see also Figure 4.7. Error bars are SE across subjects. The continuous line represents the 'postdiction' of the best suboptimal Bayesian observer model, model SPK-P-L; see 'Analysis of best observer model' in the text). For comparison, the dashed line is the 'postdiction' of the best suboptimal observer model that follows Bayesian Decision Theory, BDT-P-L.

For each subject and group (training and test) we also plot the mean optimality index of the simulated sessions against the optimality index computed from the data, finding a good correlation ($R^2 = 0.98$; see Figure 4.13).

Lastly, to gain an insight on subjects' systematic response biases, we used our framework in order to non-parametrically reconstruct what the subjects' priors in the various conditions would look like (see Section 2.3.4). Due to limited data per condition and computational constraints, we recovered the subjects' priors at the group level and for model SPK-L, without additional noise on the priors (P). The reconstructed average priors for distinct test sessions are shown in Figure 4.14. Reconstructed priors display a very good match with the true priors for the Gaussian session and show minor deviations in the other sessions. The ability of the model to

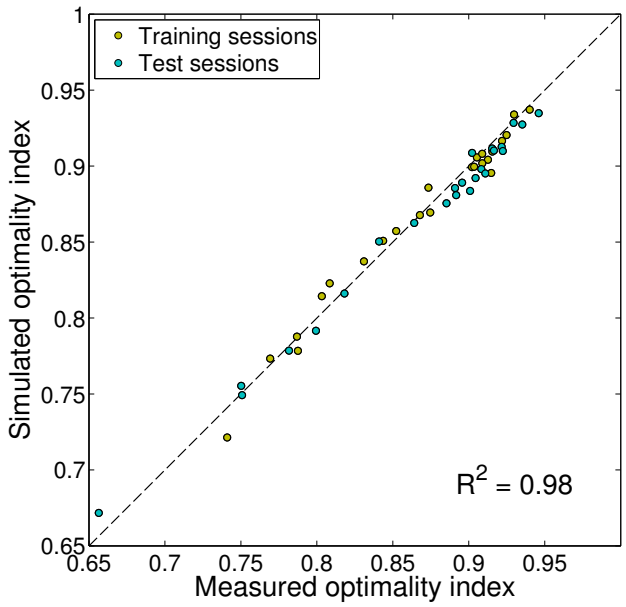

Figure 4.13: **Comparison of measured and simulated performance.** Comparison of the mean optimality index computed from the data and the simulated optimality index, according to the 'postdiction' of the best observer model (SPK-P-L). Each dot represents a single session for each subject (either training or test). The dashed line corresponds to equality between observed and simulated performance. Model-simulated performance is in good agreement with subjects' performance ($R^2 = 0.98$).

reconstruct the priors – modulo residual idiosyncrasies – is indicative of the goodness of the observer model in capturing subjects' sources of suboptimality.

4.4 DISCUSSION

We have explored human performance in probabilistic inference (a target estimation task) for different classes of prior distributions and different levels of reliability of the cues. Crucially, in our setup subjects were required to perform Bayesian computations with explicitly provided probabilistic information, thereby removing the need either for statistical learning or for memory and recall of a prior distribution. We found that subjects performed suboptimally in our paradigm but that their relative degree of suboptimality was similar across different priors and levels of cue noise. Based on a generative model of the task we built a set of suboptimal Bayesian observer models. Different methods of model comparison among this large class of models converged in identifying a most likely observer model that deviates from the optimal Bayesian observer in the following points: (a) a mismatching representation of the likelihood parameters, (b) a noisy estimation of the parameters of the prior, (c) a few occasional

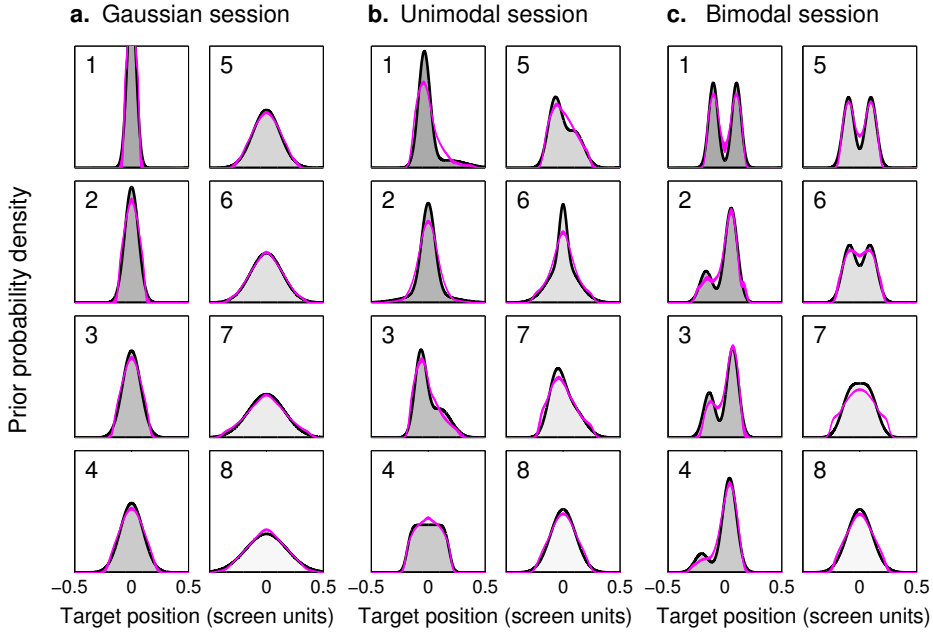

Figure 4.14: **Reconstructed prior distributions.** Each panel shows the (unnormalized) probability density for a 'prior' distribution of targets, grouped by test session, as per Figure 4.2. Purple lines are mean reconstructed priors (mean ± 1 SD) according to observer model SPK-L, smoothed with a small Gaussian kernel for visualization purposes. **a: Gaussian session.** Recovered priors in the Gaussian test session are very good approximations of the true priors (comparison between SD of the reconstructed priors and true SD: $R^2 = 0.94$). **b: Unimodal session.** Recovered priors in the unimodal test session approximate the true priors (recovered SD: 0.105 ± 0.007, true SD: 0.11 screen units) although with systematic deviations in higher-order moments (comparison between moments of the reconstructed priors and true moments: skewness $R^2 = 0.47$; kurtosis $R^2 < 0$). Reconstructed priors are systematically less kurtotic (less peaked, lighter-tailed) than the true priors. **c: Bimodal session.** Recovered priors in the bimodal test session approximate the true priors with only minor systematic deviations (recovered SD: 0.106 ± 0.004, true SD: 0.11 screen units; coefficient of determination between moments of the reconstructed priors and true moments: skewness $R^2 = 0.99$; kurtosis $R^2 = 0.80$).

lapses, and (d) a stochastic representation of the posterior, such that the target choice distribution is approximated by a power function of the posterior.

4.4.1 *Human performance in probabilistic inference*

Subjects integrated probabilistic information from both the prior and the cue in our task, but rarely exhibited the signature of full 'synergistic integration', i.e. a performance above that which could be obtained by using either the prior or the cue alone (see Figure 4.7). However, unlike most studies of Bayesian learning, on each trial in

our study subjects were presented with a new prior. Instances of suboptimality have been highlighted in several previous studies (see Chapter 2). In particular, previous work on movement planning with probabilistic information (but fewer conditions) had similarly found that subjects violated conditions of optimality (Hudson et al., 2007).

More interestingly, in our data the relative degree of suboptimality did not show significant differences across distinct classes of priors and noise levels of the cue (low-noise and high-noise). Due to the logic of null hypothesis testing, this does not mean that performance was truly identical across conditions – nor we are stating that, as we did observe some minor differences – but the data suggest that the effect of varying the experimental condition was not substantial. This finding suggests that human efficiency in probabilistic inference is only mildly affected by the complexity of the prior per se, at least for the distributions we have used. Conversely, the process of learning priors is considerably affected by the class of the distribution: for instance, learning a bimodal prior (when it is learnt at all) can require thousands of trials (Körding and Wolpert, 2004a), whereas the mean and variance of a single Gaussian can be acquired reliably within a few hundred trials (Berniker et al., 2010).

Within the same session, subjects' relative performance was influenced by the specific shape of the prior. In particular, for Gaussian priors we found a systematic effect of the variance; subjects performed worse with wider priors, more than what would be expected by taking into account the objective decrease in available information. Interestingly, neither noise in estimation of the prior width (factor P) nor occasional lapses that follow the shape of the prior itself (factor L) are sufficient to explain this effect. Model postdictions of model BDT-P-L show large systematic deviations from subjects' performance in the Gaussian sessions, whereas the best model with decision noise, SPK-P-L, is able to capture subjects' behaviour; see top left and top right panels in Figure 4.12. Moreover, the Gaussian priors recovered under model SPK-L match extremely well the true priors, furthering the role of the stochastic posterior in fully explaining subjects' performance with Gaussians. The crucial aspect of model SPK may be that decision noise is proportional to the width of the posterior, and not merely of the prior.

In the unimodal test session, subjects' performance was positively correlated with the width of the main peak of the distribution. That is, non-Gaussian, narrow-peaked priors (such as priors 1 and 6 in Figure 4.14b) induced worse performance than broad and smooth distributions (e.g. priors 4 and 8). Subjects tended to 'mistrust' the prior, especially in the high-noise condition, giving excess weight to the cue ($\tilde{\sigma}_{high}$ is significantly lower than it should be; see Table 4.4). This behaviour can be also interpreted as an overestimation of the width of the prior. In fact, the reconstructed priors in Fig-

ure 4.14b show a general tendency to overestimate the width of the narrower peaks, as we found in the previous chapter (see 'Exp. 4: High-Peaked distribution' in Section 3.3.4). This behaviour is locally compatible with a well-known human tendency of underestimating (or, alternatively, underweighting) the probability of occurrence of highly probable results and overestimating (overweighting) the frequency of rare events (see Kahneman and Tversky, 1979; Tversky and Kahneman, 1992; Zhang and Maloney, 2012); see Section 6.1.2 for further discussion. Similar biases in estimating and manipulating prior distributions may be explained with a hyperprior that favours more entropic and, therefore, smoother priors in order to avoid 'overfitting' to the environment (Feldman, 2013).

4.4.2 *Modelling suboptimality*

In building our observer models we made several assumptions. For all models we assumed that the prior adopted by observers in Eq. 4.5 corresponded to a continuous approximation of the probability density function displayed on screen, or a noisy estimate thereof. We verified that using the original discrete representation does not improve model performance. Clearly, subjects may have been affected by the discretization of the prior in other ways, but we assumed that such errors could be absorbed by other model components. We also assumed that subjects quickly acquired a correct internal model of the probabilistic structure of the task, through practice and feedback, although quantitative details (i.e. model parameters) could be mismatched with respect to the true parameters. Formally, our observer models were not 'actor' models in the sense that they did not take into account the motor error in the computation of the expected loss (see Section 2.1.2). However, this was with negligible loss of generality since the motor term has no influence on the inference of the optimal target for single Gaussians priors, and yields empirically negligible impact for other priors for small values of the motor error σ_{motor} (as those measured in our task; see Section 4.3.2).

Suboptimality was introduced into our observer models in three main ways: (a) miscalibration of the parameters of the likelihood; (b) models of approximate inference; and (c) additional stochasticity, either on the sensory inputs or in the decision-making process itself. Motor noise was another source of suboptimality, but its contribution was comparably low.

Miscalibration of the parameters of the likelihood means that the subjective estimates of the reliability of the cues ($\tilde{\sigma}_{low}$ and $\tilde{\sigma}_{high}$) could differ from the true values (σ_{low} and σ_{high}). In fact, we found slight to moderate discrepancies, which became substantial in some conditions. Previous studies have investigated whether subjects

have (or develop) a correct internal estimate of relevant noise parameters (i.e. the likelihood) such as their own sensory or motor variability, plus possibly some externally injected noise. In several cases, subjects were found to have a miscalibrated model of their own variability, which led to suboptimal behaviour (e. g., Mamassian, 2008; Zhang et al., 2010; Battaglia et al., 2011; Zhang et al., 2013a), although there are cases in which subjects were able to develop correct estimates of such parameters (e. g., Trommershäuser et al., 2005; Tassinari et al., 2006; Gepshtein et al., 2007); see Chapter 2 for more examples.

More generally, it could be that subjects were not only using incorrect parameters for the task, but built a wrong internal model or were employing approximations in the inference process. For our task, which has a relatively simple one-dimensional structure, we did not find evidence that subjects were using low-order approximations of the posterior distribution. Also, the capability of our models to recover the subjects' priors in good agreement with the true priors suggest that subjects' internal model of the task was not too discrepant from the true one.

A crucial element in all our models was the inclusion of extra sources of variability, in particular in decision making. Whereas most forms of added noise have a clear interpretation, such as sensory noise in the estimation of the cue location, or in estimating the parameters of the prior, the so-called 'stochastic posterior' deserves an extended explanation.

4.4.3 *Understanding the stochastic posterior*

We introduced the stochastic posterior model of decision making, SPK, with two intuitive interpretations, that is a noisy posterior or a sample-based approximation (see Figure 4.3 and Section B.1 in the Appendix), but clearly any process that produces a variability in the target choice distribution that approximates a power function of the posterior is a candidate explanation. The stochastic posterior captures the main trait of decision noise, that is a variability that depends on the shape of the posterior (Battaglia et al., 2011), as opposed to other forms of noise that do not depend on the decision process. Outstanding open questions are, therefore, which kind of process could be behind the observed noise in decision making, and during which stage it arises, e.g. whether it is due to inference or to action selection (Drugowitsch et al., 2014b).

A seemingly promising candidate for the source of noise in the inference is neuronal variability in the nervous system (Faisal et al., 2008). Although the noisy representation of the posterior distribution in Figure 4.3b through a population of units may be simplistic, the posterior could be encoded in subtler ways (see for instance

Ma et al., 2006). However, neuronal noise itself may not be enough to explain the amount of observed variability (see Section B.1 in the Appendix). An extension of this hypothesis is that the noise emerges because suboptimal computations magnify the underlying variability (Beck et al., 2012).

Conversely, another scenario is represented by the *sampling hypothesis*, an approximate algorithm for probabilistic inference which could be implemented at the neural level (Fiser et al., 2010). Our analysis ruled out an observer whose decision-making process consists in taking the average of κ samples from the posterior – operation that implicitly assumes a quadratic loss function – showing that averaging samples from the posterior is not a generally valid approach (although differences can be small for unimodal distributions). More generally, the sampling method should always take into account the loss function of the task, which in our case is closer to a delta function (a MAP solution) rather than to a quadratic loss. Our results are compatible with a proper sampling approach, whereby an empirical distribution is built out of a small number of samples from the posterior, and the expected loss is computed on the base of the sampled distribution (Fiser et al., 2010). A recent study has shown that sampling in bistable perception obeys the multiplicative rule of probability, consistent with the idea of sampling from the posterior and also from the posterior raised to a power (Moreno-Bote et al., 2011). *sampling hypothesis*

As a cognitive, non-mutually exclusive explanation, decision variability may have arisen because subjects adopted a probabilistic instead of deterministic strategy in action selection as a form of exploratory behaviour. In reinforcement learning this is analogous to the implementation of a probabilistic policy as opposed to a deterministic policy, with a 'temperature' parameter that governs the amount of variability (Sutton and Barto, 1998). Search strategies have been hypothesized to lie behind suboptimal behaviours that appear random, such as probability matching (Gaissmaier and Schooler, 2008). While generic exploratory behaviour is compatible with our findings, our analysis rejected a simple posterior-matching strategy (see Section 2.4.5).

All of these interpretations assume that there is some noise in the decision process itself. However, the noise could emerge from other sources, without the necessity of introducing deviations from standard BDT. For instance, variability in the experiment could arise from lack of stationarity: dependencies between trials, fluctuations of subjects' parameters, and time-varying strategies would appear as additional noise in a stationary model (Green et al., 2010; Raviv et al., 2012).

In summary, we showed that a decision strategy that implements a 'stochastic posterior' that introduces variability in the computation of the expected loss has several theoretical and empirical advantages when modelling subjects' performance, demonstrating improvement over previous models that implemented variability only

through a 'posterior-matching' approach or that implicitly assume a quadratic loss function (sampling-average methods).

5

EFFECTS OF UNCERTAINTY ON ERROR CORRECTION

> "*Hic manebimus optime*
> (Here we'll stay excellently)."
> — Marcus Furius Camillus,
> in Livy, *Ab Urbe Condita Libri*, V, 55

In this chapter, prompted by our previous findings, we examine how decision uncertainty alters the sensorimotor system control strategy for error correction, and whether this influence, possibly related to the cost of moving or replanning our actions, may constitute a relevant source of suboptimality. The results presented herein belong to a manuscript in preparation.

5.1 TARGET UNCERTAINTY MODULATES ERROR CORRECTION

Among several results, in Chapter 4 we have reported two apparently unrelated phenomena. The first finding is that observers' response variability was directly linked to the shape of the posterior distribution, which we interpreted as a stochastic form of decision making (such as a noisy representation of the posterior; see Section B.1 in the Appendix). A second, minor observation is that we noted a small but statistically significant average rightward bias in the responses during the training session (see 'Mean rightward bias' in Section 4.3.1). Systematic biases in sensorimotor tasks are often found and may arise due to asymmetries in the experimental layout (see e. g., Trommershäuser et al., 2003a; de Xivry, 2013). A curious aspect of our data, however, is that the bias was proportional to the width of the posterior distribution (Figure 4.6b). Assuming that there was some (possibly external) source of asymmetry, such as the kinematics of the arm and robotic manipulandum, it seems that subjects' capability or willingness to correct for the induced error reduced with increasing posterior uncertainty. This observation led us to ask whether part of the measured variability in sensorimotor decision making could arise due to a lack of correction of natural movement errors in the presence of target uncertainty.

A large body of work has investigated how subjects react to subliminal perturbation of visual feedback of hand position during movement in fast reaching tasks (Saunders and Knill, 2003, 2004). In general, it is clear that task-irrelevant deviations should be left uncorrected to maximize performance, according to the *minimal inter-*

minimal intervention principle

vention principle (Todorov and Jordan, 2002; Todorov, 2004). Indeed, Knill et al. (2011) found that subjects unconsciously adapted their corrective strategies depending on the shape of the target on a trial-to-trial basis, in agreement with previous studies that provided evidence that the central nervous system adapts its online control law to varying task demands (e. g., Liu and Todorov, 2007). Many experiments have also observed that human observers undershoot the target in the first movement (or undercompensate for perturbations), a phenomenon that has been explained via stochastic optimal control (Engelbrecht et al., 2003; Liu and Todorov, 2007). Namely, subjects undershoot as a trade-off between accuracy and precision, since the signal-dependent property of motor noise implies that longer reaches are more variable (Harris and Wolpert, 1998). Also, subjects may undershoot so as to minimize *effort*, an element of the subjective loss function that might play a major role in motor control (Lyons et al., 2006; O'Sullivan et al., 2009). These studies used extended targets with a well-defined shape and position, but according to stochastic optimal control we should expect similar results with point-like targets with uncertain position. For example, Izawa and Shadmehr (2008) showed evidence of continuous Bayesian integration of uncertain target information in a reaching task with a target that jumped to a new position and/or changed its reliability. Recent work on the interaction between uncertainty and motor control has also found that human sensorimotor behaviour exhibits risk-sensitivity, that is sensitivity to the uncertainty in the reward (Nagengast et al., 2010; Braun et al., 2011), which may stem from target variability (Grau-Moya et al., 2012). Finally, note that all these predictions were formulated for fast directed movement (duration under 1 second); we could expect subjects to behave differently when allowed full time to correct for their errors. Instead, a recent study found that it is not necessarily the case: human observers did not fully correct for their own endpoint errors in both fast and slow pointing reaches, even if they showed awareness of their mistakes (van Dam and Ernst, 2013; see also Discussion, Section 5.4).

effort

Together, these studies suggest that target uncertainty may affect error correction in sensorimotor estimation in a nontrivial way, in addition to considerations of task-dependent costs (Trommershäuser et al., 2003a). It is unclear the impact that such additional biases would have on task performance, especially in conditions of increased estimation uncertainty, as reflected by the shape of the posterior distribution. In particular, we wonder whether lack of error correction could be an important factor behind observed suboptimality in sensorimotor estimation tasks in the presence of complex distributions.

5.1.1 *Summary*

In this chapter we report results from a psychophysical experiment that assesses the effects of estimation uncertainty on error correction. Unbeknownst to participants, we randomly shifted visual feedback of their finger position during reaching in a centre of mass estimation task. In each trial, the *perturbation* (shift of visual feedback) was applied behind a large occluder and was zero, small (about ± 0.5 cm), or large (about ± 1.5 cm). Also, in each trial, the centre of mass (i. e., target) position was drawn from a trimodal distribution, intermixing trials with low and high uncertainty about target location.

perturbation

We reasoned that if subjects estimated the centre of mass position and then simply reported this with a reach, then we would expect that they should correct for the entire perturbation to be as accurate as possible – or at least they should correct just as much for the high and low uncertainty conditions. However, if subjects represented their uncertainty in the centre of mass location as reflected in their posterior distribution they may be less willing to correct in the high-uncertainty condition as the cost of correction (e. g., energy, movement time, computational) may outweigh the potential increases in accuracy that can be achieved through correction; if so, we could quantify the trade-off of effort and accuracy by examining the amount of correction as a function of uncertainty.

Even though participants were given enough time to compensate for the perturbation, they almost fully corrected for the induced error on trials with low uncertainty about target location and corrected only partially in conditions with more uncertainty. Surprisingly, correction gains were tuned so that overall task performance was not significantly affected. We show that the observed lack of correction can be explained by considering an additional cost of adjusting one's response in conditions of uncertainty. Our findings suggest that subjects' decision uncertainty, as reflected in the width of the posterior, is a factor in determining how their sensorimotor system responds to errors, but at the same time uncertainty-modulated error correction does not represent a significant source of suboptimality. These results support theoretical models which fully integrate the decision making and control processes.

5.2 METHODS

5.2.1 *Experimental procedures*

Participants

Sixteen naïve subjects (8 male and 8 female; age range 19–27 years) participated in the study. All participants were right-handed (Oldfield, 1971), with normal or corrected-to-normal vision and reported no neurological disorder. Participants were compensated for their time. The Cambridge Psychology Research Ethics Committee approved the experimental procedures and all subjects gave informed consent.

Behavioural task

Subjects performed a centre of mass estimation task. We used an OptoTrak 3020 (Northern Digital Inc, Ontario, Canada) to track the tip of a subject's right index finger at 500 Hz. The visual image from a LCD monitor (Apple Cinema HD, 64 cm $\times$ 40 cm, 60 Hz refresh rate) was projected into the plane of the hand via a mirror that prevented the subjects from seeing their arm. The workspace origin, coordinates $(0, 0)$, was $\sim$ 20 cm in front of the subject's torso in the mid-saggital plane, with positive axes towards the right ('horizontal' x axis) and away from the subject ('vertical' y axis). The workspace showed a home position (1.5 cm radius circle) at the origin and a cursor (0.25 cm radius circle) could be displayed that tracked the finger position.

On each trial a virtual object consisting of two filled circles (disks) and a thin horizontal line (*target line*) connecting the centres of the two disks (Friedenberg and Liby, 2002) was displayed on the screen (Figure 5.1a). The centres of the disks were $\ell = 24$ cm apart (length of the target line) and at vertical position $y = 20$ cm. In each trial, the object was horizontally displaced with a uniformly random jitter $\sim [-3, 3]$ cm from the centre of the screen. The radius of one of the disks was drawn from a log-normal distribution with mean log 1 cm and SD 0.1 in log space. The radius of the other disk was chosen so that on $1/3$ of the trials the disks were of equal size, making the task equivalent to a simple line bisection, and on $2/3$ of the trials the ratio of the disk radii was drawn from a log-normal distribution with mean log 1.5 and SD 0.1 in log space, leading to a trimodal distribution of centre of mass locations (Figure 5.1b). The position (left or right) of the larger disk in unequal-size trials was chosen randomly and counterbalanced across experimental blocks. We expected that the uncertainty in the centre of mass location would be low for the equal-disk trials ('Low-uncertainty'), when the task was equivalent to line bisection, but would be high for the unequal-disk trials ('High-uncertainty') due to both the spread of the

target line

experimental distribution and the nonlinear mapping between the disks' ratio and centre of mass, see below.

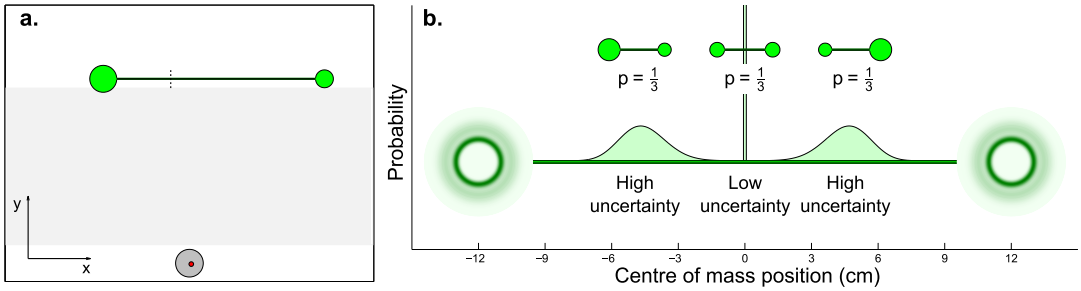

Figure 5.1: **Experimental setup. a: Screen setup at the start of a trial.** The screen showed a home position (grey circle), the cursor (red circle) and the object (green). The task consisted of locating the centre of mass of the object, here indicated by the small dashed line. The cursor disappeared in the region between the home position and the target line (here shaded for visualization purposes). **b: Centre of mass distribution.** The two disks were separated by 24 cm and, depending on the disks size ratio, the target (centre of mass) was either exactly halfway between the two disks ($p = 1/3$) or to the right ($p = 1/3$) or left ($p = 1/3$) of the midpoint.

target

After a 'go' tone, participants were required to reach from the home position to the centre of mass of the disks (the *target*) on the target line, thereby balancing the object on their finger. The horizontal location of the centre of mass s of two d-dimensional spheres with radii r_1 and r_2 is given by:

$$s = \frac{\ell}{2} \cdot \left(\frac{r_2^d - r_1^d}{r_1^d + r_2^d} \right), \tag{5.1}$$

with respect to the midpoint of the target line. In our case, $d = 2$ and subjects were explicitly told in the instructions that the circles were to be interpreted as disks in the estimation.

Importantly, during the reaching movement visual feedback of the cursor was extinguished in the region $y \in [2, 19]$ cm (shaded area in Figure 5.1a). Subjects were given 1.5 s to arrive in the proximity of the target line ($y > 19.5$ cm). After reaching the target line, subjects were allowed 3 seconds to adjust their endpoint position to correct for any errors that might have arisen during the movement when the cursor was hidden. The remaining time for adjustment was indicated by a pie-chart animation of the cursor, which gradually turned from red to yellow. The cursor's horizontal position at the end of the adjustment phase constituted the subject's response for that trial. If participants were still moving at the end of the adjustment phase (velocity of the finger greater than 0.5 cm/s), the trial was terminated with an error message. Such missed trials were presented again later during the session.

Experimental sessions

Participants performed a preliminary training session (120 trials) in which they received performance feedback at the end of each trial. That is both the correct location of the centre of mass was displayed on screen together with an integer score that depended on the (horizontal) distance from the centre of mass, Δs, according to a squared exponential formula:

$$\text{Score}(\Delta s) = \text{Round}\left(10 \cdot \exp\left\{-\frac{\Delta s^2}{2\sigma_{Score}^2}\right\}\right), \tag{5.2}$$

where σ_{Score} is the score length scale and Round(z) denotes the value of z rounded to the nearest integer. We chose the numerical constants in Eq. 5.2 ($\sigma_{Score} \approx 0.41$ cm) such that the score had a maximum of 10 and was nonzero up to 1 cm away from the centre of mass. If the score was zero an animation showed the object falling in the appropriate direction. A new trial started 500 ms after the subject had returned to the home position.

Subjects then performed a test session (576 trials) which included standard trials (192 trials) identical to the training session, and 'perturbation' trials in which, unbeknownst to the subjects, the visual feedback of the cursor was displaced horizontally from the finger when the cursor reappeared at the end of the movement ($y > 19$ cm), near the target line. Cursor displacement could either be small (drawn from a Gaussian distribution with mean ± 0.5 cm and SD 0.2 cm; 192 trials), or large (mean ± 1.5 cm and SD 0.2 cm; 192 trials). To avoid overlap between distinct perturbation levels, the Gaussian distributions were truncated at 2.5 SDs (0.5 cm away from the mean). All trials were presented in a pseudorandom order and left and right perturbations were counterbalanced within the session. To keep subjects motivated throughout the test session without giving away crucial information, participants received trial-to-trial performance feedback on unperturbed trials only (Körding and Wolpert, 2004a) and a summary screen communicated their block score, including all trials, every 36 trials (Whiteley and Sahani, 2008). All participants answered a debriefing questionnaire at the end of the session, the results of which showed that they were unaware of the perturbations or of any other difference between trials with feedback and trials without feedback.

5.2.2 *Data analysis*

For all analyses the criterion for statistical significance was $p < 0.05$. Unless specified otherwise, summary statistics are reported in the text as mean $\pm$ SE between subjects.

Trial response data

For each trial, we recorded the horizontal movement end position r of the visual cursor, the perturbation (difference between position of the visual cursor and position of the finger, which was 0 for unperturbed trials) and the horizontal position s of the centre of mass of the current stimulus. We also recorded the effective adjustment time (time before the subject stopped moving during the adjustment phase). We computed the response error Δs as the signed difference between movement end position of the visual cursor and position of the centre of mass of the current stimulus.

Variation of response bias and SD of the error

We analyzed how the bias (mean error) and SD of the error depended on the class of stimuli presented and on the perturbation level. Presented stimuli belonged to two classes: Low-uncertainty (centre of mass in the midpoint) and High-uncertainty, with centre of mass either to the Left or to the Right of the midpoint. First, we verified that we could pool Left and Right stimuli with High uncertainty. Limiting our analysis to High-uncertainty trials only, we examined how the bias and SD of the error varied with factors of side (Left, Right) and perturbation mean level (-1.5, -0.5, 0, 0.5, 1.5). Finding no significant effect of side nor interaction between side and perturbation, we pooled High-uncertainty trials from Left and Right. In the subsequent analysis, as reported in the paper, we examined how the mean bias and standard deviation of the responses varied with factors of trial uncertainty (Low, High) and perturbation mean level (-1.5, -0.5, 0, 0.5, 1.5). Statistical differences between conditions in these analyses were assessed using repeated-measures ANOVA (rm-ANOVA) with Greenhouse-Geisser correction of the degrees of freedom in order to account for deviations from sphericity (Greenhouse and Geisser, 1959). A logarithmic transformation was applied to the SDs before performing rm-ANOVA, in order to improve normality of the data (results were qualitatively similar for non-transformed data).

Slope of the mean bias

For each subject, we performed linear regression of the bias as a function of perturbation size (a continuous variable from -2 to 2 cm) for the Low and High uncertainty conditions. The slope of the regression fit is a measure of the fraction of the applied perturbation that was not corrected for. In the graphs, we remove the bias for the 0 perturbation condition from each subject's data to allow for a direct comparison between subjects; this has no effect on the estimation of the slope. The difference in slope between conditions was assessed with a paired Student's t-test on the individual slope coefficients.

5.2.3 *Observer model*

We built a standard Bayesian observer model to investigate whether our subjects' correction biases could be explained as probabilistic inference (see Chapter 2.1). In order to account for the biases (lack of correction) in the perturbation condition, we introduced a modification to the structure of the loss function that takes into account effort. As described below, subjects' datasets were fit individually and model fits were averaged to obtain the group prediction. To limit model complexity and avoid overfitting, some model parameters were either estimated from the individual training datasets or fixed to theoretically motivated values.

Perception stage

In our model, we assume that the observer estimates the log ratio of the radii of the two disks, whose true value is $\rho = \log(r_2/r_1)$, where r_i with $i = 1, 2$ is the radius of the i-th disk. Log coordinates are convenient as they naturally embed Weber's law and allow for a simple representation of (powers of) ratios (see Section 2.2.1). For instance, the log ratio of the *areas* of the disks can be easily expressed as $\log(r_2^2/r_1^2) = 2\rho$.

In the estimation process, the true ratio is corrupted by normally distributed noise with magnitude σ_ρ in log space, which yields a noisy measurement ρ_m. The parameter σ_ρ represents both log-normally distributed sensory noise in estimating the radii of the disks and additional independent sources of error in computing the ratio. The conditional measurement probability takes the form:

$$p_{meas}(\rho_m|\rho) = \mathcal{N}\left(\rho_m \,\middle|\, \rho, \sigma_\rho^2\right), \tag{5.3}$$

and we assume equivalence between the internal representation of sensory noise and its objective counterpart ($q_{meas} \equiv p_{meas}$, see Section 2.2.2). The experimental distribution of log ratios is a mixture of three components: two Gaussians centered at $\pm\log 1.5 \approx \pm 0.405$ with SD 0.1 and a delta function at $\rho = 0$ (Figure 5.1b). For simplicity, we assume the observer's prior, $q_{prior}(s)$, corresponds to the experimental distribution:

$$q_{prior}(\rho) = \frac{1}{3}\sum_{i=1}^{3} \mathcal{N}\left(\rho \,\middle|\, \mu_{prior}^{(i)}, {\sigma_{prior}^{(i)}}^2\right), \tag{5.4}$$

with $\boldsymbol{\mu}_{prior} = (-\log 1.5, 0, \log 1.5)$ and $\boldsymbol{\sigma}_{prior} = (0.1, 0, 0.1)$, using the formal definition $\mathcal{N}(x\,|\mu, 0) \equiv \delta(x - \mu)$.

Combining Eqs. 5.3, and 5.4, after some algebraic manipulations, the posterior can be expressed as a mixture of Gaussians:

$$q_{post}(\rho|\rho_m) = \frac{1}{\mathcal{Z}} \sum_{i=1}^{3} Z^{(i)} \mathcal{N}\left(\rho \,\middle|\, \mu_{post}^{(i)}, {\sigma_{post}^{(i)}}^2\right), \tag{5.5}$$

where we have defined the mixing weights, means and variances as:

$$\begin{aligned} Z^{(i)} &\equiv \mathcal{N}\left(\rho_m \,\middle|\, \mu_{prior}^{(i)}, {\sigma_{prior}^{(i)}}^2 + \sigma_\rho^2\right) \quad \text{and} \quad \mathcal{Z} \equiv \sum_{i=1}^{3} Z^{(i)}, \\ \mu_{post}^{(i)} &\equiv \frac{\rho_m {\sigma_{prior}^{(i)}}^2 + \mu_{prior}^{(i)} \sigma_\rho^2}{{\sigma_{prior}^{(i)}}^2 + \sigma_\rho^2}, \qquad \sigma_{post}^2 \equiv \frac{{\sigma_{prior}^{(i)}}^2 \sigma_\rho^2}{{\sigma_{prior}^{(i)}}^2 + \sigma_\rho^2}. \end{aligned} \tag{5.6}$$

The observer uses the inferred values of ρ to compute the location of the centre of mass of the two-disk object (here measured with respect to the midpoint between the two disks). From Eq. 5.1, the relationship between the log ratio of the radii of two spherical objects in a d-dimensional space and their centre of mass, s, can be represented by the mapping f_d:

$$f_d(\rho) = \frac{\ell}{2} \cdot \left[\frac{(-1)\cdot r_1^d + (+1)\cdot r_2^d}{r_1^d + r_2^d}\right] = \frac{\ell}{2} \cdot \left[\frac{\frac{r_2^d}{r_1^d} - 1}{\frac{r_2^d}{r_1^d} + 1}\right] = \frac{\ell}{2} \cdot \left[\frac{e^{d\rho} - 1}{e^{d\rho} + 1}\right], \tag{5.7}$$

whose inverse is $f_d^{-1}(s) = \frac{1}{d}\log\left[(\ell/2 + s)/(\ell/2 - s)\right]$.

We assume that the observer uses the mapping f_d from Eq. 5.7 with some fixed value of d, although not necessarily the correct value $d = 2$. Combining Eqs. 5.5 and 5.7, the posterior distribution of the location of the estimated centre of mass takes the form:

$$\begin{aligned} q_{post}(s|\rho_m) &= \int_{-\infty}^{\infty} \delta\left[f_d(\rho) - s\right] q_{post}(\rho|\rho_m) d\rho \\ &= \frac{1}{\mathcal{Z}} \sum_{i=1}^{3} Z^{(i)} \int_{-\infty}^{\infty} \delta\left(\rho' - s\right) \mathcal{N}\left(f_d^{-1}(\rho') \,\middle|\, \mu_{post}^{(i)}, {\sigma_{post}^{(i)}}^2\right) \frac{d\rho'}{\frac{df_d}{d\rho}\left(f^{-1}(\rho')\right)} \\ &= \frac{1}{\mathcal{Z}} \sum_{i=1}^{3} Z^{(i)} \mathcal{N}\left(\frac{1}{d}\log\left[\frac{\ell/2 + s}{\ell/2 - s}\right] \,\middle|\, \mu_{post}^{(i)}, {\sigma_{post}^{(i)}}^2\right) \frac{\ell}{d \cdot (\ell^2/4 - s^2)}, \end{aligned} \tag{5.8}$$

where we have used the composition rule $\delta[g(y)] = \sum_{j=1}^{n} \frac{1}{|g'(a_j)|}\delta(y - a_j)$ where $g(y)$ is a real function and a_j are its zeroes. The posterior in Eq. 5.8 is not a mixture of Gaussian distributions due to the nonlinear relationship in the argument of the Gaus-

sian function. However, by approximating each mixture component with a Gaussian, we can write:

$$q_{post}(s|\rho_m) \approx \frac{1}{\mathcal{Z}} \sum_{i=1}^{3} Z^{(i)} \mathcal{N}\left(s \left| m_{post}^{(i)}, {s_{post}^{(i)}}^2 \right.\right). \tag{5.9}$$

where $m_{post}^{(i)}$ and $s_{post}^{(i)}$ are respectively mean and SD of the mixture components in Eq. 5.8 (computed numerically, function `trapz` in MATLAB).

The 'Gaussianized' components in Eq. 5.9 are a very good approximation of their counterparts in Eq. 5.8 for the parameters in our task, as measured by an average Kullback-Leibler divergence of $(3.1 \pm 0.7) \cdot 10^{-3}$ nats (mean $\pm$ SD across all posteriors in the task). This amounts to roughly the KL divergence between two Gaussians with same variance and whose difference in means is one-twelfth of their SD. The approximation we chose works better than a Laplace approximation (MacKay, 2003), which yields worse values for the KL divergence of $(7.8 \pm 1.8) \cdot 10^{-3}$ nats.

Decision-making stage

According to Bayesian Decision Theory (BDT), the observer chooses the final cursor position that minimizes his or her expected loss. The typical loss functions used in perceptual and even sensorimotor tasks take into account only the error (distance between response and target); see Section 2.4. However, although the explicit goal of our task consists of minimizing endpoint error, subjects appeared to be influenced by other considerations.

We assume that the subjects' full loss function depends on an error-dependent cost term, $\mathcal{L}_{err}(r-s)$, which assesses the deviation of the response from the target, and a second adjustment cost, $\mathcal{L}_{adj}(r-\tilde{r})$, which expresses the cost of moving from the perturbed endpoint position $\tilde{r}$ (originally planned endpoint position plus perturbation b). The rationale is that there is an additional cost in moving from the initially planned endpoint position, possibly due to the effort involved in an additional unplanned movement (e. g., for replanning the action).

In a preliminary motor planning stage, the endpoint s_{pre}^* is chosen by minimizing the error loss:

$$\begin{aligned} s_{pre}^*(\rho_m) &= \arg\min_{\hat{s}} \left[\int_{-\ell/2}^{\ell/2} q_{post}(s|\rho_m) \mathcal{L}_{err}\left(\hat{s}-s\right) ds \right] \\ &= \arg\min_{\hat{s}} \left[-\sum_{i=1}^{3} Z^{(i)} \mathcal{N}\left(\hat{s} \left| m_{post}^{(i)}, {s_{post}^{(i)}}^2 + \sigma_{err}^2 \right.\right) \right], \end{aligned} \tag{5.10}$$

where for the loss function we assumed the shape of a (rescaled) inverted Gaussian, $\mathcal{L}_{err}(\hat{s}-s) = -\exp\left\{-(\hat{s}-s)^2/2\sigma_{err}^2\right\}$. In addition to the modelling advantages that

we already discussed (see e. g. Körding and Wolpert, 2004b and Section 1.2.2), the Gaussian loss is a continuous approximation of the scoring system of the task (Eq. 5.2). To limit model complexity, we assumed subjects conformed to the error length scale of the performance feedback, that is $\sigma_{err} = \sigma_{score}$ (Eq. 5.2).

After the initial movement, subjects are allowed plenty of time to adjust their endpoint position. Due to the applied perturbation b, the (average) endpoint position after movement will be $\tilde{r} \equiv s^*_{pre}(\rho_m) + b$. We introduce, therefore, the adjustment cost in the final loss function:

$$\mathcal{L}\,(r, s, \tilde{r}) = \mathcal{L}_{err}(r - s) + \alpha \mathcal{L}_{adj}(r - \tilde{r}), \tag{5.11}$$

where $\alpha \geq 0$ specifies the relative weight of the adjustment loss with respect to the error term. The 'optimal' final position s^* that minimizes the expected loss in Eq. 5.11 is:

$$s^*(\rho_m, \tilde{r}) = \arg\min_{\hat{s}} \left[\alpha \mathcal{L}_{adj}(\hat{s} - \tilde{r}) + \int_{-\ell/2}^{\ell/2} q_{post}(s|\rho_m) \mathcal{L}_{err}\,(\hat{s} - s)\, ds \right]. \tag{5.12}$$

For simplicity, for $\mathcal{L}_{adj}(\hat{s} - \tilde{r})$ we also assume the shape of an inverted Gaussian loss with length scale σ_{adj}, a free parameter of the model representing the scale of the cost of moving away from the originally planned target. In Section 5.3.2, 'Alternative observer models', we will see how the solution of Eq. 5.12 changes depending on the shape of the loss functions.

The final expression for the 'optimal' target after adjustment becomes:

$$s^*(\rho_m, \tilde{r}) = \arg\min_{\hat{s}} \left[-\widetilde{\alpha} \mathcal{N}\left(\hat{s} \,\middle|\, \tilde{r}, \sigma^2_{adj}\right) - \sum_{i=1}^{3} Z^{(i)} \mathcal{N}\left(\hat{s} \,\middle|\, m^{(i)}_{post}, {s^{(i)}_{post}}^2 + \sigma^2_{err}\right) \right], \tag{5.13}$$

with $\widetilde{\alpha} \equiv \alpha \mathcal{Z} \sigma_{adj} / \sigma_{err}$.

In order to find s^*_{pre} (Eq. 5.10) and subsequently the 'optimal' final position s^* (Eq. 5.13), we implemented a fast numerical algorithm (Carreira-Perpiñán, 2000), as both equations have no known analytical solution.

Full observer model

In each trial, the decision-making process is simulated in two stages. First, the observer computes the preliminary endpoint position $s^*_{pre}(\rho_m)$ for a given internal measurement ρ_m (Eq. 5.10). For simplicity, we assume that the endpoint position is systematically altered only by the external perturbation b, so that (on average) the arrival position is $\tilde{r} = s^*_{pre}(\rho_m) + b$. In the second step, the observer adjusts his or her endpoint position, moving to the optimal target as per Eq. 5.13. Gaussian noise with

variance σ^2_{motor} is added to the final choice to simulate any residual noise in the response.

According to this model, the response probability of observing response r in a trial with perturbation b and disks' ratio ρ is:

$$\Pr(r|\rho, b; \boldsymbol{\theta}) = \int_{-\infty}^{\infty} \mathcal{N}\left(\rho_m \middle| \rho, \sigma_\rho^2\right) \mathcal{N}\left(r \middle| s^*(\rho_m, x^*_{pre}(\rho_m) + b), \sigma^2_{motor}\right) d\rho_m, \quad (5.14)$$

where we integrated over the internal measurement ρ_m which is not directly accessible in our experiment, and $\boldsymbol{\theta} = \{\sigma_\rho, d, \alpha, \sigma_{adj}, \sigma_{motor}\}$ is the vector of model parameters.

Model fitting

We estimated the model parameters for each subject by maximizing the (log) likelihood of the data:

$$\log \mathcal{L}(\boldsymbol{\theta}) = \sum_{i=1}^{N} \log \left[\Pr^*\left(r^{(i)}|\rho^{(i)}, b^{(i)}; \boldsymbol{\theta}\right)\right], \quad (5.15)$$

where $N = 576$ is the total number of trials and we have assumed independence between trials. We modified Eq. 5.14 with a very small probability ϵ to improve robustness of the inference:

$$\Pr^*(r|\rho, b; \boldsymbol{\theta}) = (1 - \epsilon)\Pr(r|\rho, b; \boldsymbol{\theta}) + \epsilon, \quad (5.16)$$

where $\epsilon = 1.5 \cdot 10^{-5}$ is the value of the pdf of a normal distribution five SDs away from the mean. Eq. 5.16 allows for a minute lapse rate that prevents a few outliers in a subject's dataset from having an unlimited effect on the log likelihood of the data in Eq. 5.15.

To limit the possibility of overfitting, the sensory variability parameter of each subject, σ_ρ, was estimated from a separate model fit of the training datasets. The observer model fit to the individual test datasets had, therefore, effectively 3 free parameters: d, α and σ_{adj} (σ^2_{motor} represents the mean square of the residuals and is not typically counted as a free parameter).

5.3 RESULTS

5.3.1 *Human performance*

Subjects found the task straightforward to perform and the debriefing questionnaire at the end of the session showed that they were unaware of the perturbations on the

trials. On unperturbed Low-uncertainty trials they received on average 7.36 ± 0.43 points and balanced the object on 97.4% of trials. In contrast on High-uncertainty trials they received on average 3.35 ± 0.15 points and balanced the object on 60.2% of trails.

Mean bias and variability

We analyzed the participants' response (visual location of cursor) as a function of trial uncertainty (Low, High) and mean perturbation level (-1.5, -0.5, 0, 0.5, 1.5). To confirm that the trials with equal-sized and unequal-sized disks correspond to low and high-uncertainty we examined the variability (SD) of subjects' response. As expected, we found that the variability was significantly affected only by trial uncertainty (main effect: Low, High; $F_{(1,15)} = 297$, $p < 0.001$) with average SD of 0.40 ± 0.06 cm and 1.02 ± 0.05 cm for the Low and High-uncertainty trials, respectively. We found no significant effect of perturbation and no interaction ($p > 0.40$ for both). This confirms that subjects were more variable in their judgments of the center of mass in 'High-uncertainty' trials.

We also examined the subjects' bias (mean difference between cursor endpoint and center of mass). The bias was not significantly affected by trial uncertainty (main effect: Low, High; $F_{(1,15)} = 0.69$, $p > 0.40$) but was significantly affected by the perturbation level (main effect: perturbation level; $F_{(3.88,58.1)} = 25.7$, $\epsilon = 0.969$, $p < 0.001$) and in particular by the interaction between the two (interaction: perturbation $\times$ uncertainty; $F_{(3.64,54.7)} = 15.1$, $\epsilon = 0.91$, $p < 0.001$). This suggests that uncertainty modulates the effect of the perturbation on subjects' biases.

To assess the proportion of the perturbation which subjects corrected for, we performed a linear regression of their bias as a function of the perturbation size for Low and High uncertainty trials (after subtracting the baseline bias from unperturbed trials, Figure 5.2). A slope of zero would correspond to no residual error and hence a full correction, whereas a positive slope correspond to a smaller fraction of the perturbation that subjects correct for, with a slope of 1 corresponding to no correction at all. The regression slopes were small (0.03 ± 0.01) for Low uncertainty trials but large (0.16 ± 0.02) for High uncertainty trials, both significantly different than zero (t-test Low: $t_{(15)} = 3.61$, $p < 0.01$; High: $t_{(15)} = 8.15$, $p < 0.001$) and significantly different from each other (paired t-test $t_{(15)} = 6.80$, $p < 0.001$). These results show that subjects corrected almost entirely for the perturbation in the Low-uncertainty condition and left sizeable errors in the High-uncertainty trials by only correcting on average for 84% of the perturbation.

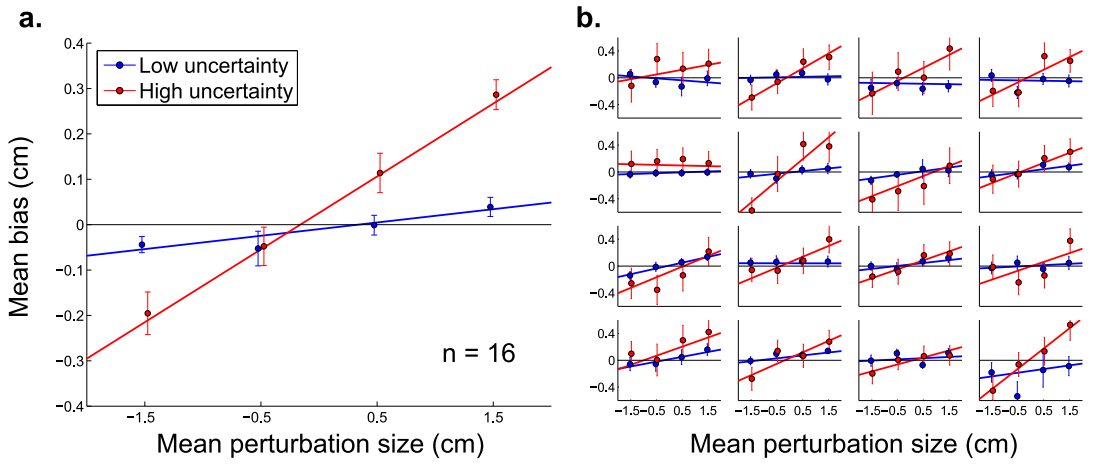

Figure 5.2: **Mean response bias.** Mean response bias (i.e., residual error) against mean perturbation size, for Low-uncertainty (blue) and High-uncertainty (red) trials. The bias for the 0 perturbation condition has been removed from each subject's data. **a: Group mean bias.** Mean response bias against mean perturbation size. Error bars are SEM between subjects. Fits are are linear regressions to the mean data. **b: Individual mean bias.** Each panel reports the mean response bias against mean perturbation size for a single subject, for Low-uncertainty (blue) and High-uncertainty (red) trials. Error bars are SEM between trials. Fits are linear regressions to the individual data.

Exit position

In each trial we also recorded the hidden cursor horizontal position when it crossed the end of the no-feedback zone ($y = 19$ cm), before applying visual perturbations, as exit position x_{exit}. The variability (SD) of x_{exit} was respectively 1.30 ± 0.04 cm (Low uncertainty trials) and 1.96 ± 0.06 cm (High uncertainty). We found a statistically significant but weak correlation between the target position and the exit position in the High uncertainty trials (considering Left and Right separately), with an average correlation coefficient of $r = 0.31 \pm 0.02$ (t-test $t_{(15)} = 14.4$, $p < 10^{-3}$). Accordingly, the variability of exit position when considered with respect to target position was statistically significantly lower than the variability of x_{exit} itself, but nevertheless essentially the same (1.91 ± 0.07 cm; paired t-test $t_{(15)} = 3.3$, $p < 0.01$). Also, note that the variability of exit position in Low and High uncertainty trials was substantially higher than the corresponding endpoint variability ($p < 0.001$ for both). Together, these findings suggest that the subjects' strategy consisted in aiming at a general area depending on stimulus broad category type (e.g., towards the right of the target line when $r_2 > r_1$, towards the left for $r_1 < r_2$, and to the middle otherwise) and then refined their endpoint position in the adjustment phase. This strategy, encouraged by our experimental layout, is reminiscent of the two-component model of goal-directed

movement, which is divided in a ballistic phase aimed at the target followed by a 'homing' (adjustment) phase (Elliott et al., 2001, 2010).

Effective adjustment time

We assessed the time subjects spent in the adjustment phase before they stopped making corrections as a function of trial uncertainty (Low, High) and absolute perturbation size (0, 0.5, 1.5).[1] The mean effective adjustment time (1.60 ± 0.06 s) was not affected by trial uncertainty per se (main effect: Low, High; $F_{(1,15)} = 0.2$, $p = 0.66$), but was significantly influenced by perturbation size (main effect: perturbation size; $F_{(1.93,28.9)} = 20.9$, $\epsilon = 0.96$, $p < 0.001$) with no interaction (interaction: uncertainty $\times$ perturbation size; $F_{(2,30)} = 0.74$, $\epsilon \approx 1$, $p > 0.40$). On average, there was no difference in adjustment time between baseline and small (0.5) perturbation trials (time difference 1 ± 16 ms, $p > 0.95$). However, subjects spent significantly more time adjusting their endpoint position in large (1.5) perturbation trials than baseline trials (time difference 93 ± 14 ms, paired t-test $t_{(15)} = 6.89$, $p < 0.001$). Effective adjustment times were broadly scattered in the range 0–3 s and approximately symmetric around the mean (skewness 0.03 ± 0.08), with no sign of an accumulation near 3 s. Together, these results suggest that subjects had ample time to make the needed corrections in both Low and High uncertainty trials.

Analysis of performance

Overall subjects' showed significant biases (Figure 5.3a) that depended on the uncertainty level (Low, High) and perturbation size (0, 0.5, 1.5). To determine how these biases affected performance, we analyzed their mean score per trial as a function of trial uncertainty and perturbation size (Figure 5.3b). Interestingly, the mean score was significantly influenced only by trial uncertainty (Low: 7.36 ± 0.38, High: 3.32 ± 0.14; main effect: $F_{(1,15)} = 177$, $p < 0.001$), with no significant effect of perturbation size nor interaction ($p > 0.60$ for both). Analogous results hold if we split the High-uncertainty trials in left and right, depending on their location (having, thus, three levels of trial uncertainty: High-Left, Low-Middle, High-Right), and five levels of perturbations (-1.5, -0.5, 0, 0.5, 1.5), suggesting that difference are not hidden by the pooling procedure. These findings suggest that subjects' partial lack of correction did not significantly affect their performance.

We compared subjects' average score with that of optimal Bayesian observers (see Methods) which shared the same disks' ratio estimation noise σ_ρ as the subjects but correctly computed the location of the center of mass ($d = 2$) and fully compensated

1 We found qualitatively similar results by defining as 'effective ajustment time' the fraction of time that subjects spent moving in the adjustment phase, instead of the time elapsed before they stopped moving.

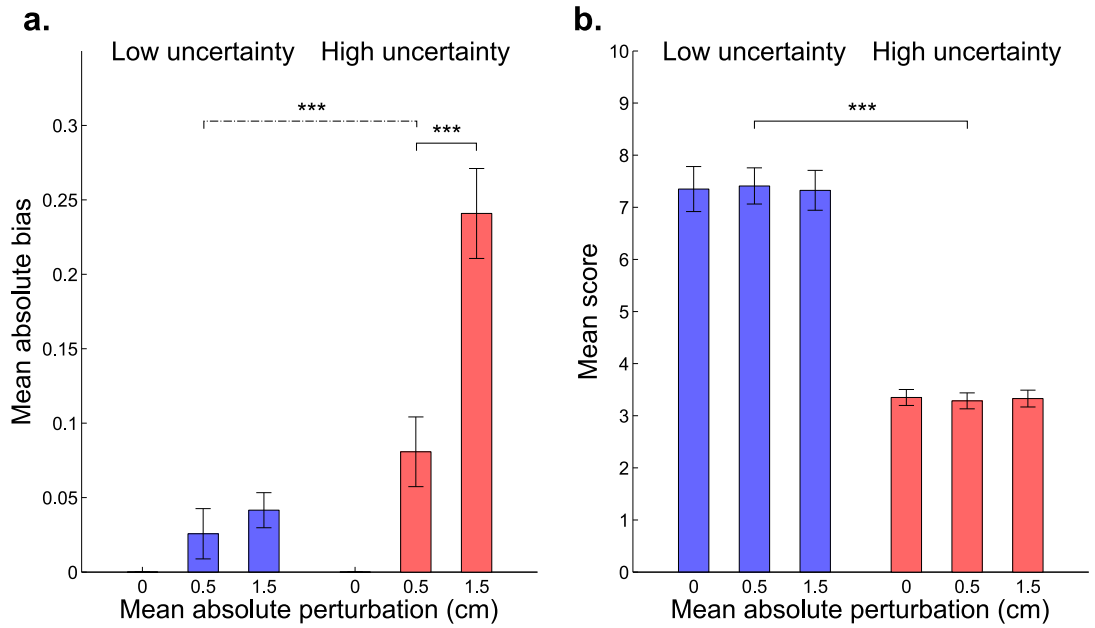

Figure 5.3: **Participants' absolute biases and mean scores. a:** Mean absolute bias (mean $\pm$ SE across subjects; biases are computed after removing the bias for the 0 perturbation condition) by perturbation size (0, $\pm$0.5, $\pm$1.5 cm) and trial uncertainty (Low, High). These data are the same as in Figure 5.2a, here shown in absolute value and aggregated by perturbation size. **b:** Participants' mean scores (mean $\pm$ SE between subjects) by perturbation size and trial uncertainty. Even though the biases (panel a) are significantly different from zero and significantly modulated by perturbation size ($p < 0.001$) and the interaction between the uncertainty and perturbation size ($p < 0.001$), the scores (panel b) are significantly affected only by the trial uncertainty ($p < 0.001$).

for any movement error in the adjustment phase ($\alpha = 0$). The mean score expected from the ideal observer was 9.88 ± 0.12 for Low uncertainty trials and 6.03 ± 0.26 for High uncertainty ones (mean $\pm$ SD computed via bootstrap). Overall, subjects' average score was significantly lower (paired t-test $p < 0.001$ for both conditions), with a relative efficiency of about ~ 0.75 and ~ 0.55 for respectively Low and High uncertainty trials. [2]

Our previous analysis ('Mean bias and variability') showed that subjects' corrective strategy differed between the two levels of uncertainty, with an 'almost-full' correction for Low uncertainty trial ($\sim$ 3% uncorrected perturbation) and a 'partial' correction for High uncertainty trials ($\sim$ 16% uncorrected perturbation). We estimated what would have been the score in the perturbed Low uncertainty conditions, had the

2 This difference in relative efficiency between Low and High uncertainty trials does not constrast our conclusions of Chapter 4, which found instead a comparable relative performance across a variety of conditions in a target estimation task, when the distributions were explicitly provided. In the current task, subjects had to learn both the experimental distribution of stimuli and the nonlinear mapping from disks' ratio to centre of mass, which affected performance differently in the two conditions.

participants adopted the partial amount of correction as in the High uncertainty trials. To estimate subjects' score in this hypothetical case we considered their baseline, unperturbed responses and added the mean response bias from baseline, which we had previously estimated from both Low and High uncertainty trials (corresponding respectively to almost-full and partial correction). We simulated also the almost-full correction strategy as a control, expecting to observe no difference with baseline. The score in each trial was recomputed through Eq. 5.2. The original mean score in the Low uncertainty condition, without perturbation, was 7.36 ± 0.43 (see Figure 5.3b). As expected, hypothetical mean scores under the almost-full correction strategy were not significantly different from baseline (7.52 ± 0.35 and 7.40 ± 0.39, respectively for small, ± 0.5, and large, ± 1.5, perturbations; main effect: perturbation size, $F_{(1.96,29.4)} = 0.87$, $\epsilon = 0.98$, $p > 0.40$). On the contrary, hypothetical mean scores under the partial correction strategy were significantly different from baseline (6.59 ± 0.49 and 6.41 ± 0.41; main effect: perturbation size, $F_{(1.99,29.9)} = 16.1$, $\epsilon \approx 1$, $p < 0.001$). These numbers mean that had the participants been equally sloppy in their correction strategy in the Low uncertainty trials as they were in the High uncertainty trials, the drop in score would have been statistically significant and notable (ΔScore -0.97 ± 0.18; paired t-test $t_{(15)} = -6.31$, $p < 0.001$). This suggests that participants' adjustment strategy took into account task demands, even in the absence of performance feedback in perturbation trials.

5.3.2 *Bayesian model fit*

We examined subjects' response bias as a function of the actual center of mass location relative to the midpoint of the bar and mean perturbation level (Figure 5.4). Even though individual participants' datasets are variable, their mean response bias exhibited a clear nonlinear pattern as a function of center of mass location, partly driven by the prior over center of mass locations (Figure 5.1b). We fit the Bayesian observer model to the individual datasets and obtained a good qualitative agreement with the group data (Figure 5.4) and quantitative agreement for the slope of bias for individual subjects ($R^2 = 0.87$; see Figure 5.5). A crucial element of the model is a loss function that takes into account both a final targeting error cost and an additional cost of moving in the adjustment phase. Due to the width of the posterior distribution in the High-uncertainty condition, the expected gain for an adjustment is smaller than in the Low-uncertainty condition and therefore subjects may be less willing to adjust. Our model qualitatively predicts that the lack of correction to external perturbations should correlate with the trial uncertainty (as measured by the spread of

the posterior distribution). For example, we observed this signature in the 'rightward bias' that emerged in the experimental setup of the previous chapter (Figure 4.6b).

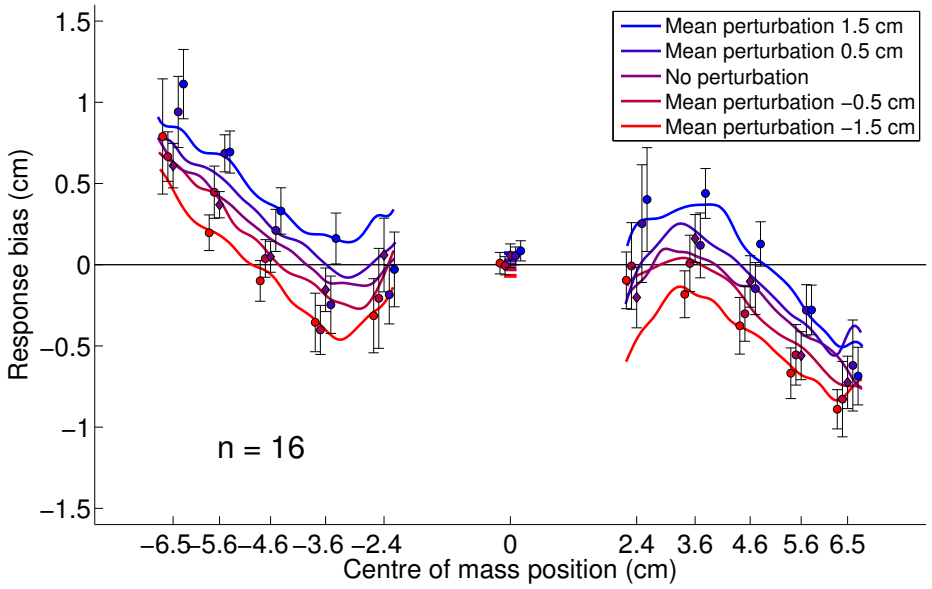

Figure 5.4: **Response bias (data and model).** Mean response bias as a function of the location of the centre of mass. Circles and error bars are mean data ± SE across subjects in the test session. Colours correspond to different mean perturbation levels (displayed with a slight offset on the x axis for visualization purposes). Continuous lines are the fits of the Bayesian model.

The best fit model parameters to the data were: $\sigma_p = 0.063 \pm 0.004$ (estimated from the training session), $d = 1.94 \pm 0.04$ (not significantly different from the true value $d = 2$; t-test $t_{(15)} = 1.51$, $p = 0.15$), $\sigma_{motor} = 0.76 \pm 0.06$ cm.[3] Regarding the loss-related parameters, for 3 subjects the adjustment loss was almost constant ($\sigma_{adj} \to \infty$). For the other 13 subjects we found: $\alpha = 3.1 \pm 0.9$, $\sigma_{adj} = 2.8 \pm 0.5$ cm, suggesting that the cost would change slowly, with a relatively large length scale (at least as big as the largest perturbations of $\approx \pm 2$ cm), and in general these subjects were giving a sizeable weight to the adjustment term ($\alpha > 1$; t-test $t_{(12)} = 2.19$, $p < 0.05$). Interpreting the adjustment cost as effort, this result is in qualitative agreement with a previous study that found that effort had a considerably greater relative weight in the loss function than the error term (relative weight ~ 7 for the force production task described in the study; see O'Sullivan et al., 2009).

3 For a comparison, the residual motor noise in this experiment is about two-thirds of the motor noise estimated in the Gaussian training session described in the previous chapter ($\sigma_{motor} = 1.20 \pm 0.12$ cm, converted in cm from Table 4.4). The significantly lower value in the current setup ($p < 0.01$) is likely due to the adjustment phase and possibly to the adoption of an optical tracking system (the robotic manipulandum may have small mechanical biases that reduce precision).

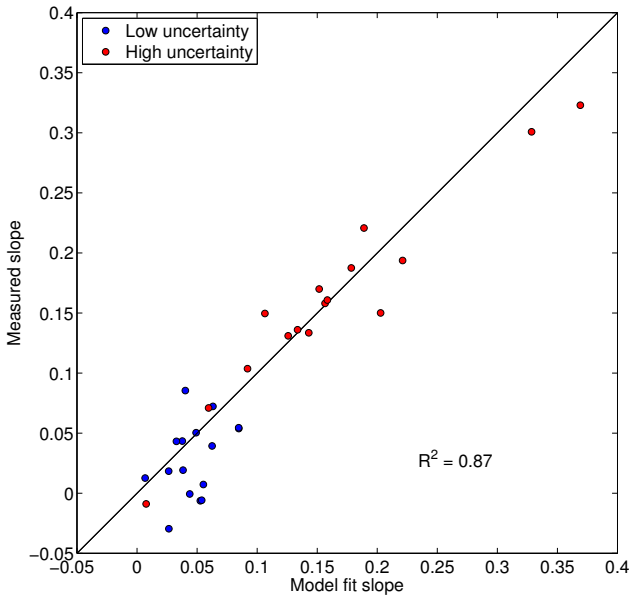

Figure 5.5: **Slope of bias, comparison between data and model.** Each circle represents the slope of the mean bias (Figure 5.2b) for a single subject for Low-uncertainty trials (blue circles) and High-uncertainty trials (red circles).The x axis indicates the slope predicted by the Bayesian observer model, while the y axis reports the slope measured from the data (slope of linear regressions in Figure 5.2b). The model correctly predicts the substantial difference between Low-uncertainty and High-uncertainty trials and is in good quantitative agreement with individual datasets.

Alternative observer models

We analyze here the predictions of a number of alternative observer models, such as different models of loss for Eq. 5.11, showing that in many cases alternative models are unable to account for the principal effect that we observed, that is a modulation of the amount of correction that depends on target uncertainty. These results further validate our modelling choices.

First, as an alternative model of loss for the error term in Eq. 5.11, let us consider the typical quadratic loss function: $\mathcal{L}_{quad}(r-s) = (r-s)^2$. In this case, the 'optimal' target (Eq. 5.12) takes the form:

$$\begin{aligned} s^*(\rho_m, x_0) &= \arg\min_{\hat{s}} \left[\alpha \mathcal{L}_{adj}(\hat{s}-\tilde{r}) + \int_{-\ell/2}^{\ell/2} q_{post}(s|\rho_m)\,(\hat{s}-s)^2\, ds \right] \\ &= \arg\min_{\hat{s}} \left[\alpha \mathcal{L}_{adj}(\hat{s}-\tilde{r}) + \hat{s}^2 - 2\hat{s}\cdot m_{post} \right], \end{aligned} \tag{5.17}$$

where m_{post} is the mean of the full posterior in Eqs. 5.8 and 5.9. For example, for a quadratic adjustment loss, Eq. 5.17 reduces to a simple analytical solution: $s^*(\rho_m, \tilde{r}) = (m_{post} + \alpha\tilde{r})/(1+\alpha)$. However, for *any* shape of the adjustment loss, Eq. 5.17 predicts that the optimal target, and therefore the amount of correction to a perturbation, does

not depend on the variance of the posterior distribution (i. e., on the uncertainty). This prediction is at odds with the patterns observed in the experiment, so the quadratic loss model of the error is unable to account for some important features of our data.

To explore alternative models of adjustment cost in Eq. 5.11, we assume an inverted Gaussian for the error combined with a power function for the adjustment loss. A power function with power $\nu > 0$ includes several common models of loss as specific cases (absolute, sub-quadratic, quadratic) and therefore represents a valid alternative to the inverted Gaussian (Körding and Wolpert, 2004b). The 'optimal' target is:

$$s^*(\rho_m, x_0) = \arg\min_{\hat{s}} \left[\frac{\alpha \mathcal{Z}}{\sigma_{err}} |\hat{s} - \tilde{r}|^\nu - \sum_{i=1}^{3} Z^{(i)} \mathcal{N}\left(\hat{s} \left| m_{post}^{(i)}, {s_{post}^{(i)}}^2 + \sigma_{err}^2 \right. \right) \right]. \quad (5.18)$$

We compared the performances of the observer models with power loss and inverted Gaussian loss in terms of (log) maximum likelihood.[4] The performance of the two models was largely similar, with a nonsignificant advantage of the inverted Gaussian model (0.7 ± 1.6 difference in log likelihood; t-test $t_{(15)} = 0.44$, $p > 0.60$). An analogous lack of empirical difference between the inverted Gaussian loss and the power loss was reported in a previous study (Körding and Wolpert, 2004b). The choice between the two functions must therefore be driven by other considerations, such as mathematical tractability (e. g., in our case the inverted Gaussian loss allows to write the expected loss as a mixture of non-normalized Gaussians, see Eq. 5.13).

Finally, we examined the predictions for an observer model built from a different set of assumptions. For this model, we hypothesized that the source of the lack of correction is not effort, but a miscalibration of the perceived position of the cursor. Even though in our task the visual feedback of the cursor location during the adjustment phase is unambiguous, subject's perception may be systematically altered by proprioceptive feedback according to the relative reliability of vision and proprioception (see van Beers et al., 1996, 1999). In particular, the posterior distribution of cursor position r for visual cue x_{vis} and proprioceptive cue position x_{prop} is given by (Ernst and Banks, 2002):

$$\begin{aligned} q_{cursor}\left(r \left| x_{vis}, x_{prop} \right.\right) &= \mathcal{N}\left(r \left| x_{vis}, \sigma_{vis}^2 \right.\right) \mathcal{N}\left(r \left| x_{prop}, \sigma_{prop}^2 \right.\right) \\ &\propto \mathcal{N}\left(r \left| \frac{x_{vis}\sigma_{prop}^2 + x_{prop}\sigma_{vis}^2}{\sigma_{vis}^2 + \sigma_{prop}^2}, \frac{\sigma_{vis}^2 \sigma_{prop}^2}{\sigma_{vis}^2 + \sigma_{prop}^2} \right. \right), \end{aligned} \quad (5.19)$$

4 Since the models have the same number of parameters, several common metrics of model comparison such as AIC and BIC would yield the same penalty for complexity.

where σ^2_{vis} and σ^2_{prop} are the (subjective) variances of visual and proprioceptive noise. Noting that in our setup $x_{prop} \approx x_{vis} - b$, where b is the visual perturbation applied in the trial, we can rewrite Eq. 5.19 as:

$$\begin{aligned} q_{cursor}\left(r \,|x_{vis}, x_{prop}\right) &\propto \mathcal{N}\left(r \,\middle|\, x_{vis} - b\frac{\sigma^2_{vis}}{\sigma^2_{vis}+\sigma^2_{prop}}, \frac{\sigma^2_{vis}\sigma^2_{prop}}{\sigma^2_{vis}+\sigma^2_{prop}}\right) \\ &\equiv \mathcal{N}\left(r \,|x_{vis} - \mu_{cursor}, \sigma^2_{cursor}\right), \end{aligned} \tag{5.20}$$

where we have defined μ_{cursor} and σ_{cursor} for notational convenience. We assume now that, according to BDT, the observer places the visual cursor so as to match the 'optimal' visual cursor location x^*_{vis} that minimizes the expected loss of the task:

$$\begin{aligned} x^*_{vis}(\rho_m) &= \arg\min_{\hat{x}_{vis}} \left[-\int_{-\ell/2}^{\ell/2} q_{post}(s|\rho_m)\mathcal{N}\left(r \,|\hat{x}_{vis} - \mu_{cursor}, \sigma^2_{cursor}\right)\mathcal{N}\left(r \,|s, \sigma^2_{score}\right) ds dr\right] \\ &= \arg\min_{\hat{x}_{vis}} \left[-\int_{-\ell/2}^{\ell/2} q_{post}(s|\rho_m)\mathcal{N}\left(s \,|\hat{x}_{vis} - \mu_{cursor}, \sigma^2_{cursor} + \sigma^2_{score}\right) ds\right], \end{aligned} \tag{5.21}$$

where the subjective error in the loss function is computed with respect to the unknown exact cursor position r, whose distribution is inferred via cue combination (Eq. 5.20). The posterior over target locations, $q_{post}\left(s\,|\rho_m\right)$, is defined by the mixture of Gaussians of Eq. 5.9. For the sake of argument, let us consider the case in which the posterior is mainly represented by a single Gaussian component with mean m_{post} and variance s^2_{post} (both depend on ρ_m). This is a reasonable approximation in most of the trials as our observers' sensory noise on the estimation of the disks' (log) ratio, σ_ρ, is much smaller than the separation between components of the prior over (log) ratios ($0.063 \ll 0.405$, see previous section). Using a single Gaussian in Eq. 5.21 we obtain:

$$\begin{aligned} x^*_{vis}(\rho_m) &= \arg\min_{\hat{x}_{vis}} \left[-\int_{-\ell/2}^{\ell/2} \mathcal{N}\left(s \,\middle|\, m_{post}, s^2_{post}\right)\mathcal{N}\left(s \,|\hat{x}_{vis} - \mu_{cursor}, \sigma^2_{cursor} + \sigma^2_{score}\right) ds\right] \\ &= \arg\min_{\hat{x}_{vis}} \left[-\mathcal{N}\left(\hat{x}_{vis} \,\middle|\, m_{post} + \mu_{cursor}, \sigma^2_{cursor} + \sigma^2_{score} + s^2_{post}\right)\right] \\ &= m_{post} + b\frac{\sigma^2_{vis}}{\sigma^2_{vis}+\sigma^2_{prop}}, \end{aligned} \tag{5.22}$$

where we used the definition of μ_{cursor} from Eq. 5.20. Crucially, as for previous alternative models, the solution in Eq. 5.22 does *not* depend on the variance of the posterior s^2_{post}, meaning that for the majority of trials the observer model does not present the features that we observe in our data. Still, for trials with multimodal posteriors, the

solution of Eq. 5.21 *might* depend on the uncertainty in the trial. If so, albeit unlikely, these trials alone might be enough to produce the effect that we observe in our data. We, therefore, analyzed the behaviour that this observer model would predict for our observers for a range of reasonable values of the parameters σ_{vis} and σ_{prop} from 0.1 cm to 2.5 cm (van Beers et al., 1996). For all combinations of parameters and for all subjects we did not find any sign of interaction between trial uncertainty and residual error (data not shown), confirming the results of our first approximation (Eq. 5.22). In conclusion, subjects' perception of the perturbed cursor position may be altered by proprioceptive feedback, but this effect alone cannot account for the uncertainty-dependent modulation of the bias.

5.4 DISCUSSION

We found that target uncertainty significantly affected subjects' error correction strategy for perturbations of the visual feedback on a trial-by-trial basis, but in such a way that did not hinder overall performance.

Our study differs from previous work that examines how uncertainty affects sensorimotor behaviour. Studies which show that subjects can integrate priors with sensory evidence to produce optimal, yet biased, estimates are consistent with a point estimate being used by the motor system when enacting a movement (see Chapter 2). The bias we show here is a bias arising from error correction which acts in addition to any biases from Bayesian integration, and would not be predicted if the motor system only had a point estimate of the target location. Moreover, the partial corrections we see relate to the posterior width within a trial. This contrasts with studies which show that the distribution of perturbations can affect the corrections seen from one trial to the next (Wei and Körding, 2010).

Qualitatively similar trial-to-trial, context-dependent responses to perturbations were observed in a study that asked people to reach to spatially extended target (Knill et al., 2011). In that case, corrections happened during fast reaching movements and were compatible with external task demands: errors along the larger dimension of the targets required smaller compensations to still successfully hit the targets (according to the principle of minimal intervention). In our experiment, however, subjects were sensitive to the implicit posterior width, as opposed to explicit visual target width. Optimal feedback control predicts that, under time constraints, humans often fail to fully correct for errors that arise late in a movement even though there is no target uncertainty (Todorov and Jordan, 2002; Todorov, 2004). However, our bias is hardly driven by time constraints as a 3 seconds adjustment time ensures that sensory delays cannot prevent corrections (Izawa and Shadmehr, 2008), and our data support

that subjects had all the time to correct for mistakes up to the desired precision. Also, note that the long, fixed adjustment time window prevented decision strategies that become available when subjects can choose freely when to end the adjustment period, such as 'skipping' the more difficult trials (Drugowitsch et al., 2012). Finally, an interaction between target uncertainty and response bias has been previously reported in motor planning (Grau-Moya et al., 2012). In their task subjects were required to hit a visual target whose horizontal location uncertainty was manipulated. A robotic interface was used to generate a resistive force that opposed motion in the outward direction with the force linearly related to the horizontal location of the hand. They found that on higher uncertainty trials subjects chose to err on the side of the target with the lower resistive force. There are several key differences of this previous study to ours. In their study, the 'effort' cost is explicit and externally imposed, hit/miss performance feedback is provided on all trials, and explicit manipulations of the cost are blocked by session. By contrast, here we showed an implicit, unconscious trade-off between accuracy and effort in online error correction during a naturalistic task. Moreover, in our study task-relevant perturbations (i.e., implicit manipulations of the cost) were unbeknownst to the subjects and intermixed on a trial-by-trial basis, and we did not provide performance feedback on perturbed trials. Critically, their work does not address correction to ongoing motor commands and shows that subjects can pre-plan a trade-off whereas we show that the online error correction is affected by target uncertainty. Our work provides, therefore, a stronger test of the interaction between uncertainty in the estimate and feedback control.

A somewhat surprising finding is that subjects did not fully correct for the perturbations, but in a way that did not significantly affect performance. Clearly, a null effect on score differences might simply due to lack of statistical power in our analysis, but we demonstrated that had subjects used the same partial correction strategy in all trials, their performance would have dropped by almost one point on average. This means that subjects' correction strategy for Low and High uncertainty trials was well adapted to task demands.

A similar finding of limited but 'optimal' correction was reported in a recent study that looked at subjects' awareness of their own pointing errors (van Dam and Ernst, 2013). Participants performed a reaching movement to a one-dimensional target, and visual feedback of both hand and target position was withheld after the commencement of the movement. After movement termination, subjects responded in a 2AFC task whether they had landed to the left or to the right of the target. In the condition that is most related to our work, subjects were also allowed to correct for their natural pointing mistakes, with no time limit. Also, at this point subjects would receive a brief visual feedback (with small or large blur) about their current endpoint position.

The study reports that subjects hardly corrected for their mistakes, but the applied correction gains turned out to be sensible (if not 'optimal') when taking into account information subjects had about their own pointing errors and their current endpoint position.

Our study differs from the work by van Dam and Ernst (2013) in several fundamental aspects. Most importantly, their work probes a form of Bayesian integration between (a) the current knowledge of endpoint position or, equivalently, estimated distance from the target (due to proprioception and provided noisy visual feedback) and (b) the prior knowledge of the error distribution (and target position). One of their main findings is that it seems that subjects acquire more detailed information of the endpoint position only after the end of the movement, even for slow reaches (van Dam and Ernst, 2013). We showed instead that in our task the lack of correction cannot be explained by a simple form of Bayesian integration. Even if subjects integrated visual feedback of the cursor with (conflicting) proprioceptive information, the expected biases would not yield the observed pattern of uncertainty-dependent corrections.

Our data are consistent with an additional term in the loss function that can be interpreted as 'effort' (whether energy, time or computational; see Todorov and Jordan, 2002; Trommershäuser et al., 2003a; O'Sullivan et al., 2009). The exact nature of this cost is left open, as our experiment does not allow us to pinpoint a specific interpretation. Our model provides good fits to the subjects' data, and, moreover, we showed that other common models of loss used in Bayesian estimation and motor planning, which either ignore the cost of adjustment or use a quadratic error loss term, fail to account for the key features of our datasets. These results are consistent with an interpetation of subjects' behaviour as a form of risk-sensitivity (Nagengast et al., 2010; Grau-Moya et al., 2012). An interesting alternative hypothesis inspired by van Dam and Ernst (2013) is that subjects built an internal expectation of their average error during the trials with performance feedback, and therefore were less willing to correct for large perturbations that were reputed to be unlikely. This interpretation predicts, among other things, that σ_{adj} should correlate with the spread of the errors made by the subject, but we did not find any evidence for this pattern in the data.

In conclusion, our results show that even for simple, naturalistic tasks such as centre of mass estimation, the effect of this additional correction cost can be noticeable and is significantly modulated by trial uncertainty. At the same time, somewhat paradoxically, the effects on performance of this cost are statistically insignificant, suggesting that subjects' may have been 'optimally lazy' in correcting for their mistakes, according to the minimal intervention principle (Todorov and Jordan, 2002; Todorov, 2004), even in the absence of performance feedback. Our findings suggest that there

is no clear-cut separation between the decision making and motor component of a task, since perceptual or cognitive uncertainty affects subsequent motor behaviour beyond action initiation, as the posterior distribution is used even in the adjustment period.

6

DISCUSSION

> "I began by removing the deeply curved plate that formed the back and top of my head; then the two, more shallowly curved plates that formed the sides. [...] I then turned my microscope to the cognition engine. Here too I observed a latticework of wires, but they did not bear leaves suspended in position; instead the leaves flipped back and forth almost too rapidly to see. [...] For many hours I scrutinized the leaves, until I realized that they themselves were playing the role of capillaries; the leaves formed temporary conduits and valves that existed just long enough to redirect air at other leaves in turn, and then disappeared as a result. This was an engine undergoing continuous transformation, indeed modifying itself as part of its operation. The lattice was not so much a machine as it was a page on which the machine was written, and on which the machine itself ceaselessly wrote."
>
> — Ted Chiang, *Exhalation*

In this final chapter we summarize the results of our investigations on the nature of complex internal representations and manipulation of probabilistic information in the brain. We put our findings into perspective, discuss the limitations of our approach, and point to avenues for future work.

6.1 SENSORIMOTOR DECISION MAKING WITH COMPLEX DISTRIBUTIONS

The driving question in our thesis has been whether the standard Bayesian model is a good description of human performance in sensorimotor decision making. Our work probes the Bayesian brain hypothesis (BBH) at the behavioural level (equivalent to Marr's computational; see Section 1.1). Since it has been largely established that the BBH indeed applies to a large variety of relatively simple cases (Chapter 2), mostly with Gaussian statistics and involving linear computations between a few variables, we explored the limits of the BBH in more complex scenarios. There are several directions in which a task (and its analysis) could be made more complex, such as:

- *Dimensionality and causal structure:* Complexity may be increased by augmenting the number of task-relevant and task-irrelevant variables the observer needs to take into account (corresponding to a larger graphical model). Optimal inference in these cases may require the observer to marginalize over a number of

unobserved variables such as in visual search (Ma et al., 2011), categorization (van den Berg et al., 2012; Qamar et al., 2013), and perceptual *explaining away* (Battaglia et al., 2011). *explaining away*

- *Temporal correlations and non-stationarity:* Most psychophysical studies in the field assume a stationary, i.i.d. distribution of stimuli in the task and a (mostly) stationary observer. A promising direction of generalization consists of looking at how the observer reacts to details, such as real or spurious correlations, of the trial-to-trial statistics, the so-called *sequential effects* (DeCarlo and Cross, 1990; Raviv et al., 2012; Kwon and Knill, 2013). Understanding these effects is crucial for a theory of Bayesian update and learning (Berniker et al., 2010; Nassar et al., 2010; Petzschner and Glasauer, 2011). *sequential effects*

- *Statistical complexity:* Complexity of the inference may be increased with statistical distributions that deviate from Gaussian. Crucially, non-Gaussian distributions entail nonlinear solutions, probing aspects of BDT that are indistinguishable for Gaussian variables (see e. g., Körding and Wolpert, 2004b and Chapter 2).

In this thesis, we chose to focus on the complexity of the statistical features of a univariate distribution that needs to be learnt and/or manipulated by the observer. We identified three qualitative aspects of the shape of a distribution: symmetry, behaviour of the tails, and multimodality. These features are linked to three quantitative summary statistics, respectively: skewness, excess kurtosis, and number of modes. For the purpose of this thesis, a statistic becomes 'complex' when Bayesian integration predicts a behaviour that deviates from linear, and the degree of complexity is loosely related to the amount of nonlinearity; we did not formalize the concept further, but rather explored it experimentally with different classes of distributions. We examined human behaviour in the presence of Gaussian, skewed, platykurtic, leptokurtic, bimodal, and trimodal distributions (Chapters 3–5).

In particular, we analyzed human performance both while learning and computing with complex distributions, arguing that any observed suboptimality can be broadly imputed to two sources: mismatched internal representations, and erroneous or approximate Bayesian computations (Ma and Jazayeri, 2014). Generally, the distinction between these two classes of explanations is blurred, but, by devising tasks that rely more on one aspect (e. g., inference or learning) at a time, we may explore their relative contributions to behaviour. We found evidence that both processes are involved in observed deviations from ideal performance, but in qualitatively different ways. Incidentally, our results suggest that it is unlikely that there is a simple generic measure of statistical complexity that correlates with human performance in perceptual and

sensorimotor decision making.[1] Any realistic measure of performance would likely need to take into account a full process model of human learning and inference in the task under consideration (see e. g., Griffiths et al., 2009 for a study of function learning).

6.1.1 *Learning complex internal representations*

One of the questions that we addressed in this thesis is what is the complexity of the internal representations that can be acquired in the course of an experiment. This issue was thoroughly explored in the temporal domain (Chapter 3). We did not focus on the dynamics of learning; instead, we trained subjects for several sessions until their performance plateaued (Jazayeri and Shadlen, 2010), and only then we examined their acquired distributions. Before us, other studies had applied non-parametric techniques to infer subjects' beliefs, but most only to reconstruct pre-existing priors (e. g., Stocker and Simoncelli, 2006b; Stone et al., 2009; Girshick et al., 2011; see Section 2.3). Previous studies had reconstructed priors as a means to qualitatively validate findings (Körding and Wolpert, 2004a) or fit the model to the data (Chalk et al., 2010), but did not perform a quantitative comparison between empirical and reconstructed distributions beyond the Gaussian case. Our results suggest that subjects not only had a good internal representation of the mean and variance of the experimental distributions, as found by previous studies (e. g., Berniker et al., 2010), but also showed qualitative learning of higher-order moments.

Our observers accurately learnt the mean and variance of the experimental distributions in the time interval reproduction task, in agreement with previous studies (Berniker et al., 2010; Cicchini et al., 2012). Results were also compatible with a good learning of the skewness of the distributions. We found, instead, major deviations in the representation of kurtosis and multimodality. Note that our reconstruction of the priors is based on the specific assumptions of the observer model. Higher-order statistical features are very sensitive to outliers, so any process that increases subjects' variability will also affect the shape of the inferred prior. We mentioned non-Gaussian noise distributions and a non-quadratic loss function as possible sources for these deviations. Moreover, results from Chapter 4 suggest that there is also an element of stochasticity in decision making itself that introduces additional variability in subjects' behaviour. Our findings with bimodal distributions are not inconsistent with previous studies, which typically found that subjects had more difficulty learning multimodal distributions, ultimately achieving various degrees of success (Körding

1 An example would be algorithmic complexity, which has been applied with some success to explain the human perception of randomness (Griffiths and Tenenbaum, 2004).

and Wolpert, 2004c,a). Even though our subjects practiced for 1500–2000 trials before the test session (duration of training was comparable to those in the previous studies), it is still possible that our participants simply needed more trials to accurately learn the distributions.

Somewhat surprisingly, in some tasks observers display a rapid emergence of Bayesian biases in the presence of a multimodal distribution (e. g., Chalk et al., 2010). Indeed, in our centre of mass estimation task, in Chapter 5, we found evidence that subjects developed nonlinear biases consistent with Bayesian integration within a few hundred trials (although they become apparent only with pooled data; see Figure 5.4). We hypothesize that a fundamental feature for rapidly acquiring complex statistics of the stimuli is the presence of a stable reference frame, so that individual stimuli (and responses) can be reliably encoded in memory. For example, in our centre of mass experiment, the object to be balanced provides such reference frame for both memorizing and recalling the empirical distribution of centres of mass (Figure 5.1b). Conversely, time perception is notoriously shifty and lacks a fixed external frame (Eagleman, 2008), so it could be that this imposes major constraints on the learning of complex distributions (in addition to the limitations due to sensorimotor noise). It would be interesting to verify how expert musicians, who are likely to have a better internal framework for representing durations, fare with learning multimodal distributions of intervals, as Cicchini et al. (2012) did with uniform distributions.

Our findings about learning have two major caveats. First, we consistently provided trial-by-trial performance feedback to facilitate acquisition and retention of the experimental distribution (as e. g., Körding and Wolpert, 2004a in the bimodal learning experiment). This means that, strictly speaking, we cannot rule out the possibility that our subjects and Jazayeri and Shadlen's (2010) directly learnt a nonlinear, block-dependent 'optimal mapping' between a perceived interval and a reproduced duration, instead of the distribution of intervals. Humans have been shown to change their learning strategy depending on the type of training they receive (Fulvio et al., 2014). On the other hand, Cicchini et al. (2012) showed that subjects behave in a Bayes-optimal fashion in a time interval reproduction task even without trial-to-trial knowledge of results, suggesting that people are able to collect, and compute with, the statistics of durations. These arguments suggest that the conditions of our study set an approximate higher bound on the learning of temporal statistics for average human subjects (i. e., without specific timing skills). That is, we can generally expect people's internal representations of novel temporal distributions to be less accurate with less training, and without performance feedback. It remains an open question whether observers would still learn complex temporal statistical features, such as skewness, in the absence of feedback.

A second important proviso of our modelling work is the assumption of stationarity, as per the majority of studies in the field. Recent work, however, has highlighted that non-stationary and recency effects – that is, the statistics of recent stimuli, recent responses and recent feedback – play an important role in shaping perceptual and sensorimotor biases (Petzschner and Glasauer, 2011; Verstynen and Sabes, 2011; Cicchini et al., 2012; Raviv et al., 2012; Kwon and Knill, 2013; Wiener et al., 2014). An ideal experiment for the in-depth study of non-stationary effects in sensorimotor estimation should exclude performance feedback, so as to reduce confounds in the analysis, and wisely counterbalance the order of the stimuli across the session (Wiener et al., 2014). For example, a strategy for examining the role of non-stationarity consists of observing how subjects react to alterations in the trial-to-trial correlations. Kwon and Knill (2013) found that subjects, in an interception task, adapted their internal representations to the statistics of target speed, but systematically overestimated the correlation between subsequent trials. In their case, the experimental distributions of target speed were uniform with varying width; future work could investigate how skewed or bimodal distributions affect behaviour within a non-stationary modelling framework.

In summary, our work provides evidence for the existence of rapidly acquired complex internal representations in time perception (beyond low-order statistics), in agreeement with recent work (e. g., in motion perception; Chalk et al., 2010; Gekas et al., 2013). More in general, considering also results from Chapter 4, we show that internal representations of experimental distributions are likely to be (highly) approximate. The degree of approximation depends on the details of the experimental setup and of the distribution, but systematic deviations are found even for seemingly simple distributions such as uniform. This means that claims that follow from assumptions of near-perfect learning of the statistics of the task ought to be assessed accordingly (e. g., Jazayeri and Shadlen, 2010). For example, it should be checked whether such claims are robust to minor-to-moderate deviations in the internal representations. Motivated by these considerations, we proposed a simple generic formula to simulate approximate learning (Eq. 3.13) that could be used as a coarse tool in the absence of more specific information about subjects' priors. Results and techniques presented in this thesis pave the way for further quantitative investigation on the nature of internal representations and their approximations in sensorimotor decision making.

6.1.2 *Computing with complex distributions*

In Chapter 4 we proposed a novel experimental layout to study how humans perform probabilistic inference 'on the fly', with distributions that change on a trial-to-trial basis, which is an important test of Bayesian inference (Ma, 2012). We side-stepped the problem of the acquisition of complex priors by providing subjects with explicit visual representations of the distributions they had to compute with. In this setup, therefore, suboptimal performance is mostly due to inaccuracies and approximations in probabilistic inference (although there is also the contribution of a mismatching internal model of the task). We performed an analysis of the possible sources of suboptimality in our task (see e. g., Tjan et al., 1995; Tassinari et al., 2006), finding that variability had a considerable role in decision making. Results from Chapter 4 and 5 provide evidence that other considerations than maximizing task score, such as effort, may have affected subjects' behaviour, but the effects on measured performance were likely negligible.

We proposed a simple power-function formula to model decision variability (Eq. 4.10; see also Moreno-Bote et al., 2011) and showed that such model is equally consistent with two conceptually distinct interpretations: internal noise in the representation and approximate inference via sampling (see Figure 4.3 and Section B.1 in the Appendix). Nondescript neuronal noise is the classical explanation for observed behavioural variability (e. g., Shadlen et al., 1996; Denève et al., 2001; Faisal et al., 2008), but a recent study has pointed out that the cause could, instead, be deterministic or stochastic approximate inference (Beck et al., 2012). Stochastic sampling is one of the major hypotheses of how the brain could implement Bayesian inference, both in perception (Sundareswara and Schrater, 2008; Fiser et al., 2010; Moreno-Bote et al., 2011; Battaglia et al., 2011) and cognition (e. g., Vul et al., 2009, 2014; Battaglia et al., 2013). The fact that the power-function formula of decision variability is agnostic about the level of implementation is both an advantage and a limitation of our model, but it is not surprising as it is quite common for distinct low-level models to give empirically indistinguishable predictions at the behavioural level (e. g., Grabska-Barwinska et al., 2013). Another limitation of the proposed formula is that it is justified only for decision rules that are close to MAP.[2] This may not be a major issue for a large number of perceptual studies, since MAP is a common assumption. Finding a more general approximate expression for noisy decision making in the presence of an arbitrary

2 For example, the response patterns of a noisy decision maker under a quadratic loss function is spread around the mean the posterior. This behaviour generally differs from a noisy MAP, that instead produces clusters around the peaks of the posterior (in approximate agreement with a power function).

loss function (or at least for a larger class) remains an issue of great theoretical and practical interest.[3]

Our experimental setup to investigate suboptimalities in probabilistic inference can be extended in several ways, in addition to obvious manipulations, such as by varying the distributions and the scoring system (i. e., the loss function). First, an improved familiarization stage and multiple training sessions may be used to ensure that participants' internal model of the task is as close to the true one as possible. Second, during both training and test, we could prompt participants to produce samples from the short and long-distance cue distributions at regular intervals (Acerbi et al., 2013). This information would allow us to assess the subjects' internal model of cue noise, to see whether and how it changes in the course of the experiment, and it could further constrain the analysis. Also, we designed the experiment as a sensorimotor task motivated by previous work in motor planning (Trommershäuser et al., 2003a; Hudson et al., 2007), but it would be interesting to perform an analogous study as pure estimation. The task could be easily implemented as a 2AFC in which observers are asked whether the target is to the right or to the left of a given vertical line, which would be placed in each trial to probe interesting decision boundaries. Additionally, this setup would easily allow other experimental manipulations, such as varying stimulus presentation time, or the sequential presentation of multiple cues, as per a currently ongoing study of suboptimal inference in perceptual categorization (Drugowitsch et al., 2014b).

Interestingly, the pattern of systematic deviations that we found in the reconstructed priors in Chapter 4 ('priors-from-description') is very different from those apparent in the recovered priors of Chapter 3 ('priors-from-experience'). We assume that, due to the experimental layout, the former priors are mostly influenced by errors in the inference process, while the latter are predominantly affected by errors in learning and recalling the statistics of the experiment. First, we note that the reconstruction of both Gaussian and bimodal priors-from-description is generally very accurate, with an excellent match of higher-order moments (Figure 4.14). Conversely, unimodal priors-from-description present more substantial deviations from the true priors. This finding may be partly because subjects were trained on Gaussian distributions, and, therefore, may have found it easy to generalize from linear solutions (Gaussian) to mostly piecewise-linear solutions (bimodal), but were less prepared to switch to fully nonlinear solutions (unimodal). On the contrary, unimodal priors-from-experience were generally more accurate than bimodal ones. Moreover, priors-from-experience tended to have a *higher* kurtosis than the experimental distributions,

3 See, e.g., Ortega and Braun (2013) for a promising theoretical framework that, by drawing an analogy between decision making and thermodynamical concepts, formalizes the maximal information gain (and, thus, the uncertainty) in the computations of an observer with bounded resources.

whereas priors-from-description were, if anything, *less* kurtotic than the true priors. Curiously, our findings seem to go in the opposite direction of the usual description-experience gap (see Hertwig and Erev, 2009 for a review). The description-experience gap holds that the probability of rare events is overestimated when learnt by description, and underestimated when acquired by experience (and vice versa for the probability of common events). However, these results pertain to the domain of discrete (often binomial) distributions (Hertwig and Erev, 2009), so it is not completely clear how they would generalize to continuous distributions as in our tasks. Also, a recent study has challenged the existence of a description-experience gap altogether, when all task parameters are equated (Jarvstad et al., 2013). Our current understanding is that the systematic difference that we observe between priors-from-description and priors-from-experience stems from distinct suboptimalities in the separate processes of learning and inference.

6.2 UNCOVERING INTERNAL REPRESENTATIONS

The main objects of interest in this thesis are the internal representations built and manipulated by human observers while engaged in a variety of sensorimotor tasks. Unlike the protagonist of Ted Chiang's short story in our opening quotation, our instruments for revealing the inner workings of the mind are still extremely coarse. For example, one study applied fMRI to pinpoint a differential representation of priors and likelihoods in the brain (Vilares et al., 2012), but several other factors may have affected the results (Ma and Jazayeri, 2014). Still, a fuller understanding of approximate representations and inference at the behavioural level, beyond statements of optimality or lack thereof, may be crucial to guide the research at lower levels, since neural coding will likely reflect such approximations and not the optimal solution (Grabska-Barwinska et al., 2013; Ma and Jazayeri, 2014).

Given the inaccessible nature, for the moment, of our objects of study, our analyses of the psychophysical data and modelling techniques were an integral part of our approach. In the following, after critically reviewing our methods, we tackle two fundamental questions. The first one is whether we have enough information from behavioural data, with our 'black box' approach, to *really* uncover such hidden mental representations and processes – a problem related to the issue of non-identifiability. The second, more fundamental question is whether internal representations and processes of a Bayesian kind are there in the first place, and what we are recovering otherwise.

6.2.1 *Bayesian methods for Bayesian brains*

doubly Bayesian

The approach of this thesis has been *doubly Bayesian* (Huszár et al., 2010), whereby we analyzed the behaviour of (alleged) Bayesian observers with a variety of Bayesian techniques. Two classes of analyses were key to our investigations in Chapters 3 and 4: (a) a *sensitivity* and identifiability analysis of the parameters within each dataset and model, and (b) a factorial comparison of a large set of plausible observer models. Neither analysis *required* us to be Bayesian, but the Bayesian framework provides natural tools to deal with both problems. We performed analysis (a) through the computation of the full posterior over parameters for each dataset and model (either via explicit calculation or via sampling), and analysis (b) through a factorial Bayesian model comparison (via computation of the posterior probability of each model, or an approximation thereof). When computing the 'postdictions' of our model class, after fitting the data, we generally did not commit to a single model and parameter set but considered the full posterior (see Section A.2 in the Appendix). Such detailed analyses were needed because in Chapters 3 and 4 we wanted to infer the *hidden causes* – respectively, the internal representations and potential sources of suboptimality – for the observed behaviour. Due to the potential non-identifiability of Bayesian models in general, our approach allowed us to perform a sweep search over both parameters and models, and verify whether multiple equally-good explanations for the data would arise. This crucial information could be lost if we had computed, instead, only a point estimate, or had performed a comparison within a small set of ad-hoc models.

sensitivity analysis

hidden causes

We remark that a full analysis over parameters and factorially-combined models is conceptually simple, but can become extremely time-consuming for the modeller for a long list of practical reasons, from the obvious computational costs to the overhead of coding, optimizing, and separately testing dozens of different models. Therefore, although we generally recommend being 'as Bayesian as possible', the modelling and analysis efforts need to match the complexity of the problem. For example, in Chapter 5 we were interested in examining the existence and size of a specific experimental effect, rather than the detailed inner workings of the observer. We put forth an observer model that could account for some relevant features of the data, and showed that a number of alternative models could not explain the same features. Our analysis essentially consisted of a 'proof of existence', for which we did not need the full Bayesian toolbox. As another example, in Chapter 3, due to the low dimensionality of the parameter space ($k = 2$ or 3), we could directly compute the marginal likelihood and, therefore, the posterior probability of each model. Conversely, in Chapter 4 we could only compute an approximation of the model evidence, the DIC score (see Section A.3.3 in the Appendix). For this reason, and due to the increased complexity of

the model space, we performed a slightly more sophisticated analysis via a hierarchical Bayesian model comparison (see Section A.4 in the Appendix), although in the end we found that differences with a usual group comparison were minor (Chapter 4 and Section B.3.1 in the Appendix).

6.2.2 *Identifiability of Bayesian models*

The problem of non-identifiability in the modelling of mental representations and processes from psychophysical data has been acknowledged early in cognitive science and psychology (e. g., Anderson, 1978) and has prompted the development of several techniques (Pitt et al., 2002; Navarro et al., 2004; Wagenmakers et al., 2004; van den Berg et al., 2014). As a recent example, van den Berg and Ma (2014) showed with extensive simulations that the usage of certain summary statistics in the study of working memory is catastrophically unsuitable for the recovery of the true observer model, due to severe indistinguishability. On the other hand, aside from a few studies that raised a number of objections to the Bayesian approach, including the issue of non-identifiability (Jones and Love, 2011; Bowers and Davis, 2012; Marcus and Davis, 2013), relatively meagre attention has been given to the problem on the perceptual and sensorimotor side, with only occasional reminders (Mamassian and Landy, 2010).

Clearly, the issue of identifiability is particularly important for studies whose primary goal is to recover internal representations from the data (e. g., Stocker and Simoncelli, 2006b; Stone et al., 2009; Girshick et al., 2011; see Section 2.3), and it is not a minor technical detail as the whole feasibility of the enterprise is questionable a priori due to the degeneracy at the heart of BDT (see Section 1.2.3). The fact that multiple – in fact, infinite – combinations of priors, likelihoods and loss functions yield identical behaviour is a pure mathematical equivalence that holds even before adding to the model empirical sources of confusion such as limited data, motor noise, and lapses in the observer responses. This line of reasoning seems to condemn the Bayesian models of perception to a fatal form of non-identifiability that prevents the reliable recovery of model parameters and components, and, in particular, the sought-after internal representations, from the data. On the other hand, the aforementioned studies obtained independent validations, such as agreement with statistics of the natural environment (Girshick et al., 2011) or with findings from other independent studies (Stocker and Simoncelli, 2006b; Hedges et al., 2011; Sotiropoulos et al., 2014), suggesting that, perhaps, the problem of identifiability is not so pressing in practice.

We hypothesize that the common set of conditions that applies in perception, such as the shape of the sensory noise (Section 2.2.1), or reasonable assumptions over a natural loss function (Section 2.4.3), provide strong restrictions on the shapes that the

internal models are allowed to take. These constraints on the space of solutions may lead to an explicit symmetry breaking, whereby the degeneracy of BDT is substantially reduced or even eliminated. To our knowledge, no previous study has explicitly analyzed this scenario, possibly due to a series of technical difficulties. Although in the body of this thesis we did not directly tackle the problem of identifiability from a general standpoint, we did develop several techniques and computational tools that have been instrumental in building a framework for the study of the identifiability of Bayesian modelling of perception (Acerbi et al., 2014a). In addition to its foundational relevance for clarifying a number of open issues in the field, a general understanding of identifiability in the Bayesian modelling of perception would be useful for improving the design of psychophysical experiments; for example for maximizing information gain on model parameters of interest.

Finally, we remark that the majority of Bayesian models of perception only focusses on modelling response biases or variability – or, more generally, the distribution of responses for a given stimulus (see Chapter 2). However, response data is not the only information we can obtain from a psychophysical experiment. Reaction times and confidence judgments, just to mention two common measures used in psychological studies, could be explicitly included in Bayesian models to augment the available information on subjects' decision-making process (Drugowitsch et al., 2014a). These additional sources of information may further help abate the degeneracy of Bayesian models.

6.2.3 *The real nature of internal models*

We began our investigation with the working hypothesis of BDT as a process model of perceptual and sensorimotor decision making (Maloney and Mamassian, 2009). We assumed that human observers build internal representations of the statistics of the task (i.e., priors, likelihoods, and loss functions) and combine them according to the rules of decision theory. Our results are consistent with a 'realistic' or sub-ideal form of BDT, according to which subjects' internal representation are approximate (Chapter 3) and the decision making process itself is approximate or noisy (Chapter 4). When taking into account these elements, we did not find other major systematic deviations from BDT. However, this does not mean that there are not any, as some discrepancies may be mistakenly classified as 'approximate priors' or 'decision noise' by our current models. Specific studies need to be designed to look into nontrivial deviations from BDT. For example, we investigated a potentially spurious influence of trial uncertainty on error correction. We found that the phenomenon, albeit present, did not significantly affect subjects' performance (Chapter 5). In summary, we did

not find evidence that we should reject BDT as a process model for decision making – although we generally found that human observers are Bayes-sensible ('probabilistic') but quite suboptimal (Ma, 2012). On the other hand, more work is needed to provide positive evidence that substantiates the BBH beyond the computational level.

In fact, a major limitation of our work – as in all psychophysical studies – is that we cannot provide direct proof that our models of internal representations and inference are (approximately) correct. Aside from a good fit to the data (which, as we know, has little to do with being correct, see e. g. Gelman et al., 2013), evidence is only indirect, such as agreement between parameters of the models and independently measured ones (Chapter 3), or the capacity of the model to reconstruct the true priors used in the task (Chapter 4). As it has been repeatedly pointed out (Maloney and Mamassian, 2009; Ma, 2012; Ma and Jazayeri, 2014), proving that an observer is actually performing (approximate) Bayesian inference, as opposed to some heuristic that mimics Bayesian inference, is quite difficult. Although some requirements have been spelled out, such as the capacity to compute with changing levels of uncertainty on a trial-by-trial basis, without performance feedback (Ma, 2012), and the ability to instantly transfer probabilistic information from one context to the other (Maloney and Mamassian, 2009), we note that the logic for testing that an observer is 'Bayesian' is not dissimilar to that of a Turing test of human intelligence, i. e., presenting a series of tasks that an observer can perform only if he or she has a working (Bayesian) brain – with all the drawbacks and methodological issues of such definition. Nonetheless, as more and more studies show successes and failures of human observers at Bayesian tasks, we can focus our understanding of the inner workings of the probabilistic mind and direct future research.

6.3 CONCLUSIONS

In this thesis we challenged the human limitations in building complex statistical representations of the sensorimotor task at hand, and in performing probabilistic inference with them. At the same time, we used human data to put to the test our models of human behaviour. This symmetry is also reflected in the fact that we used the same machinery of Bayesian inference to estimate hidden properties of systems, ideal observers, that are supposed to be performing Bayesian computations as well.

In every era, the functioning of the brain, or of the mind, has been assimilated to the most advanced technology of the period – hydraulics in the ancient times, clockworks in the Renaissance, electrical wirings in the Nineteenth century, and computers in recent times (Daugman, 2001). Nowadays, machine learning and Bayesian analysis techniques represent the state of the art of our technical knowledge for extracting

meaningful information from large amounts of data. So, maybe the BBH is just another step of this historical trend. However, it seems that this sequence of metaphors is not merely an empty byproduct of the times. While fluid-based or mechanical analogies fail to capture relevant properties of the brain, cable equations originally developed for telegraphs do describe action potential transmission between neurons (Hodgkin and Huxley, 1952), and the view of the brain as an information-processing system has proven extremely fruitful in subfields, such as vision (Marr, 1982). The fact that today we are studying brain processes with the same probabilistic tools that we hypothesize the brain is using may be taken as a signal that this sequence of conceptual paradigms is actually, slowly, recursively converging by successive iterations to a peak of real understanding – and a promise for the years to come.

APPENDIX

A

MODEL ANALYSIS AND COMPARISON

In this thesis we build several mathematical models of the systems of interest, which are idealized human observers engaged in a psychophysical task. Our models serve two purposes: (a) to present a compact description of the data at hand; and (b) to capture real properties of the modelled systems, the human observers. Namely, we want to *infer* hidden features of the observers from the experimental measurements, a task for which we borrow the machinery of Bayesian inference described in Section 1.2. In this Appendix, we briefly revise a number of useful techniques for analyzing and comparing models that we extensively use in the thesis.

A.1 INFERENCE OF MODEL PARAMETERS

parameter vector

Each model M is characterized by a *parameter vector* $\boldsymbol{\theta}^M$ of parameters $\theta_1^M, \ldots, \theta_{k_M}^M$, where k_M is the number of parameters of the model. Different models may have different parametrizations so the specific form of $\boldsymbol{\theta}^M$ depends on the model under consideration – however, to avoid clutter, we remove the superscript M from the notation, leaving it to the context.

Given a dataset $\mathcal{D}$, we typically want to find the set of model parameters that best captures the data under model M. In our case, a dataset is represented by a series of trial data $(\boldsymbol{\pi}_1, \boldsymbol{\tau}_1) \ldots (\boldsymbol{\pi}_N, \boldsymbol{\tau}_N)$, where N is the total number of trials for the dataset, $\boldsymbol{\pi}_i$ represents a vector of trial parameters for the i-th trial (for example, the trial number and data regarding the stimulus showed), and $\boldsymbol{\tau}_i$ represents a vector of observed data in the i-th trial (e. g., the observer's response). The $\boldsymbol{\pi}_i$ are assumed to be fixed (they may be random but their generative process is fully under the control of the

data likelihood

experimenter), whereas the $\boldsymbol{\tau}_i$ are considered as random variables. The *data likelihood* under model M and parameter vector $\boldsymbol{\theta}$ can be written as:

$$\Pr(\mathcal{D}\,|\boldsymbol{\theta}, M) \;=\; \Pr(\boldsymbol{\tau}_1, \ldots, \boldsymbol{\tau}_N\,|\boldsymbol{\pi}_1, \ldots, \boldsymbol{\pi}_N, \boldsymbol{\theta}, M) \;=\; \prod_{i=1}^{N} \Pr(\boldsymbol{\tau}_i\,|\boldsymbol{\pi}_i, \boldsymbol{\theta}, M)\,, \quad \text{(A.1)}$$

statistical independence

where the last passage holds if we take the common assumption of *statistical independence* of measurements between trials. This assumption is an approximation, since the observer's behaviour in a trial is usually influenced by the events in the previous trials, but Eq. A.1 does not represent a restriction because, if needed, we could add

correlations between trials through the model parameters.[1] The key quantity that a model has to specify is the probability of observing the trial data, $\Pr(\boldsymbol{\tau} \,|\, \boldsymbol{\pi}, \boldsymbol{\theta}, M)$.

A common approach to finding the 'best' model parameters consists of maximizing the probability of the data under the model, a method known as *maximum-likelihood estimation* (MLE). Due to the limits of computational precision, it is preferred to equivalently maximize the log likelihood: *maximum likelihood*

$$\boldsymbol{\theta}^{ML} = \arg\max_{\boldsymbol{\theta}} \left[\log \Pr(\mathcal{D} \,|\, \boldsymbol{\theta}, M) \right] = \arg\max_{\boldsymbol{\theta}} \left[\sum_{i=1}^{N} \log \Pr(\boldsymbol{\tau}_i \,|\, \boldsymbol{\pi}_i, \boldsymbol{\theta}, M) \right]. \quad \text{(A.2)}$$

The advantage of MLE is that it is typically easy to obtain through numerical optimization methods and it has several appealing asymptotic properties. On the other hand, the ML estimate may overfit the data and does not provide any information about uncertainty on the estimate.

The Bayesian approach aims instead at finding the full posterior distribution of the parameters given the data, $\Pr(\boldsymbol{\theta} \,|\, \mathcal{D}, M)$, for a specific model. Applying Bayes' theorem, Eq. 1.1, we find:

$$\Pr(\boldsymbol{\theta} \,|\, \mathcal{D}, M) = \frac{\Pr(\mathcal{D} \,|\, \boldsymbol{\theta}, M) \Pr(\boldsymbol{\theta} \,|\, M)}{\int \Pr(\mathcal{D} \,|\, \tilde{\boldsymbol{\theta}}, M) \Pr(\tilde{\boldsymbol{\theta}} \,|\, M) \, d\tilde{\boldsymbol{\theta}}}, \quad \text{(A.3)}$$

where $\Pr(\boldsymbol{\theta} \,|\, M)$ is the prior probability density of the parameters (which in general depends on the model). In our work we typically assume statistical independence between model parameters and use *non-informative* or *weakly-informative* priors, for example uniform over a large interval that includes all plausible values, or with a mild preference towards parameter values estimated from previous studies, when available. However, this is not always the case: to prevent degeneracies, in Chapter 4 we performed an independent experiment to build strong priors of the sensorimotor parameters of the subjects. As a health-and-safety rule, we avoid improper priors (non-normalizable priors) when performing a model comparison among models with different sets of parameters, since this may constitute a problem (see Section A.3). *non-informative* *weakly-informative*

The denominator of Eq. A.3 is the marginal likelihood of the model, the likelihood averaged over all possible parameter values, and it is typically hard to compute (see Section A.3), except for very low-dimensional parameter spaces ($k = 1$ or 2). For this reason, we generally compute the posterior probability of the parameters via *sampling* from the unnormalized posterior, $\Pr(\boldsymbol{\theta} \,|\, \mathcal{D}, M) \propto \Pr(\mathcal{D} \,|\, \boldsymbol{\theta}, M) \Pr(\boldsymbol{\theta} \,|\, M)$, using a MCMC method such as slice sampling (Neal, 2003). We refer the reader to MacKay *sampling*

1 Technically, Eq. A.1 states that the observed trial data are conditionally independent *given the trial and model parameters*.

(2003); Gelman et al. (2013) for an introduction to Monte Carlo methods applied to inference problems.

The posterior distribution of the parameters automatically encodes the uncertainty on the parameter estimates through its breadth in the various dimensions. Inspection of this posterior distribution may highlight non-trivial interactions between parameters and issues of *identifiability*. In fact, in a complex model several distinct combinations of parameters may be able to explain the data equally well – especially since we are dealing with a class of systems, ideal Bayesian observers, whose inner features may be inherently non-identifiable (see Section 1.2.3). Lack of identifiability in the form of a near-flat[2] marginalized posterior for a specific parameter may also indicate that a parameter has little or no effect on the model predictions. Note that we could not become aware of such problems had we only calculated a ML estimate.

identifiability

If analysis reveals that the marginalized posterior distribution of a parameter is unimodal and reasonably peaked, it is meaningful to summarize the parameter with a point estimate such as the mode (MAP) or mean of the posterior, or with a robust estimator such as a trimmed mean. Nevertheless, for most computations we still want to keep the full posterior distribution.

A.2 MODEL PREDICTIONS

The inferred values of $\boldsymbol{\theta}$ from dataset $\mathcal{D}$ represent our 'best' estimates for the model parameters under a specific model M. However, there is no guarantee that model M allows for a good description of the data. Therefore, we perform a series of *model checks* to validate our findings and to understand which features of the data are and which are not captured by the model (Gelman et al., 2013). The most natural validation is to compare predictions of the model against actual data or summary statistics thereof. Let $\mathcal{O}(\mathcal{D}) : \{\mathcal{D}\} \longrightarrow \mathbb{R}$ be an *observable* of the data, a function that summarizes aspects of interest of the data in a single real number, such as the mean response of the observer in a subset of trials (corresponding to a certain experimental condition).

model checks

observable

If we have a point estimate for the best model parameters, $\boldsymbol{\theta}^*$, such as the ML estimate or the mean of the posterior, we define the *predictive distribution* of observable $\mathcal{O}$ as follows:

predictive distribution

$$\Pr\left(\mathcal{O}\,|\boldsymbol{\theta}^*, M\right) = \int \delta\left[\mathcal{O}\left(\widetilde{\mathcal{D}}\right) - \mathcal{O}\right] \Pr\left(\widetilde{\mathcal{D}}\,|\boldsymbol{\theta}^*, M\right) \delta\widetilde{\mathcal{D}}, \tag{A.4}$$

2 Or, more in general, equal to the prior of the parameter.

where the formal integration is performed on all datasets that can be generated by model M. In practice, we generate a number S of simulated datasets $\widetilde{\mathcal{D}}_1, \ldots, \widetilde{\mathcal{D}}_S$ according to the generative model $\Pr(\mathcal{D}|\boldsymbol{\theta}^*, M)$ and approximate the predictive distribution with a set of samples $\left\{\mathcal{O}\left(\widetilde{\mathcal{D}}_1\right), \ldots, \mathcal{O}\left(\widetilde{\mathcal{D}}_S\right)\right\}$. We can, then, compare the agreement of the predictive distribution with the real observable $\mathcal{O}(\mathcal{D})$ by visual inspection or with classical statistical methods.

In case the posterior distribution of the parameters is available, we can compute the full Bayesian solution to the problem, the *posterior predictive distribution*:

posterior predictive distribution

$$\Pr(\mathcal{O}|\mathcal{D}, M) = \int \delta\left[\mathcal{O}\left(\widetilde{\mathcal{D}}\right) - \mathcal{O}\right] \Pr\left(\widetilde{\mathcal{D}}|\boldsymbol{\theta}, M\right) \Pr(\boldsymbol{\theta}|\mathcal{D}, M)\, d\boldsymbol{\theta}\delta\widetilde{\mathcal{D}}, \tag{A.5}$$

which again can be easily approximated by sampling – we first take a sample $\boldsymbol{\theta}$ from the posterior distribution and then generate a random dataset $\widetilde{\mathcal{D}}$ according to $\Pr\left(\widetilde{\mathcal{D}}|\boldsymbol{\theta}, M\right)$.

As a conclusive remark, note that the in the extreme case the observables under consideration may be the data themselves. However, sometimes we are not interested for a model to capture all details of the data, but only a subset. Gelman et al. (2013) contains a detailed chapter with additional techniques for model checking.

A.3 INDIVIDUAL MODEL COMPARISON

So far we have only considered the case of a single model M, but we often face the situation of having a whole set of alternative models $\{M_i\}$, for $1 \leq i \leq N_{\text{models}}$, and we want to determine which one is the 'best' model for a single subject dataset $\mathcal{D}$. The difficulty of *model comparison* is that we do not simply want the model that best fits the data, but ideally we would like to find the 'true' model that characterizes some real, independently verifiable aspects of the observer. Intuitively, this suggests that we need to trade-off goodness of fit with some metric of model complexity, so to take into account the fact that more flexible models tend to fit the data better (Pitt et al., 2002). There are several approaches to model comparison, supported by different schools of thought. In this thesis we use the following methods, chosen depending on the circumstance.

model comparison

A.3.1 *Marginal likelihood*

The first approach to model comparison consists of proceeding along the Bayesian road. For each model M_i, we compute the posterior probability of the model given the data:

$$\Pr(M_i|\mathcal{D}) = \frac{\Pr(\mathcal{D}|M_i)\Pr(M_i)}{\sum_{j=1}^{N_{\text{models}}}\Pr(\mathcal{D}|M_j)\Pr(M_j)}, \tag{A.6}$$

where $\Pr(M_i)$ is the prior probability of model M_i and we recognize $\Pr(\mathcal{D}|M_i) = \int \Pr(\mathcal{D}|\boldsymbol{\theta}, M_i)\Pr(\boldsymbol{\theta}|M_i)\,d\boldsymbol{\theta}$ as the marginal likelihood of model M_i. Since the prior probability is usually assumed to be equal across models and the denominator of Eq. A.6 is equal for all models, we compare models directly according to their marginal likelihood. The ratio of the marginal likelihood of two models is the *Bayes factor*, which is a common metric of comparison (Kass and Raftery, 1995). In some occasions we may quantify evidence in the same scale as the *deviance*, as other metrics described later, which leads to the formula $-2\log\Pr(\mathcal{D}|M_i)$ (where a higher score means less support for the model). We usually report differences in evidence since only relative evidence scores are meaningful.

Bayes factor

deviance

A very appealing point of the marginal likelihood as a metric for model comparison is that it automatically includes a penality for model complexity due to *Bayesian Occam's razor* (MacKay, 2003). Namely, since the marginal likelihood is a probability distribution over datasets, it needs to integrate to one. This simple requirement implies that a complex, flexible model that can describe well a large number of datasets has to give lower values for the likelihood of each 'good' dataset, compared to a simpler model that is able to describe only a small number of 'good' datasets.

Bayesian Occam's razor

A.3.2 *Laplace's approximation of the marginal likelihood*

Computation of the marginal likelihood requires a marginalization over all model parameters. As mentioned before, this calculation usually cannot be done analytically and it is also hard to obtain numerically, unless the model has very few parameters (2 or 3). A common approximation of the marginal likelihood is obtained through *Laplace approximation* (see e. g., MacKay, 2003). Laplace's method approximates the unnormalized posterior distribution of the parameters with an unnormalized multivariate normal distribution centered on the mode of the posterior, the MAP solution

Laplace approximation

$\boldsymbol{\theta}^*$. The marginal likelihood is computed as the normalization factor of the posterior distribution of the parameters:

$$\begin{aligned}\log \Pr(\mathcal{D}|M) &= \log \int \Pr(\mathcal{D}|\boldsymbol{\theta}, M) \Pr(\boldsymbol{\theta}|M)\, d\boldsymbol{\theta} \\ &\approx \log \left[\Pr(\mathcal{D}|\boldsymbol{\theta}^*, M) \sqrt{\frac{(2\pi)^k}{\det[\boldsymbol{A}(\boldsymbol{\theta}^*)]}} \int \mathcal{N}\left(\boldsymbol{\theta} \middle| \boldsymbol{\theta}^*, \boldsymbol{A}^{-1}\right) d\boldsymbol{\theta} \right] \\ &\approx \log \Pr(\mathcal{D}|\boldsymbol{\theta}^*, M) + \frac{k}{2} \log 2\pi - \frac{1}{2} \log \det[\boldsymbol{A}(\boldsymbol{\theta}^*)],\end{aligned} \tag{A.7}$$

where k is the number of parameters and $\boldsymbol{A}(\boldsymbol{\theta}^*)$, obtained through a Taylor expansion of the (minus) log posterior at the peak, is the matrix of second derivatives (Hessian):

$$A_{ij}(\boldsymbol{\theta}^*) = -\frac{\partial^2}{\partial\theta_i \partial\theta_j} \log \Pr(\mathcal{D}|\boldsymbol{\theta}, M) \Big|_{\boldsymbol{\theta}=\boldsymbol{\theta}^*}. \tag{A.8}$$

Both the MAP solution and the determinant of the Hessian are relatively easy to compute numerically. Note, however, that the marginal likelihood obtained through Laplace's approximation considers only the main peak of the posterior and clearly works well only with posteriors that are close to Gaussian (which depends on the choice of basis; see MacKay, 1998). Convergence to a normal posterior is verified for large datasets and independent parameters but it may fail to hold for small datasets or when there are complex interactions between parameters.

A.3.3 *Information criteria and DIC*

There are several other metrics for model comparison that explicitly include a term of goodness of fit and a penalty for model complexity. In theory, these metrics instantiate different assumptions and possess different asymptotic properties. In practice, it is often found that the differences are subtle and no single metric is better than the others in all cases. Akaike's Information Criterion (AIC; Akaike, 1973) and the Bayesian Information Criterion (BIC; Schwarz, 1978) are two well-known examples of such metrics. In this thesis, we adopt the Deviance Information Criterion (DIC) by Spiegelhalter et al. (2002). The advantage of DIC over other metrics is that it takes into account an estimate of the effective number of parameters of the model and it is particularly easy to compute given the output of a MCMC algorithm. The DIC score of model M is calculated as:

$$\mathrm{DIC} = 2\left[\frac{1}{N_{\mathrm{smpl}}} \sum_{i=1}^{N_{\mathrm{smpl}}} D\left(\boldsymbol{\theta}^{(i)}\right)\right] - D(\boldsymbol{\theta}^*), \qquad D(\boldsymbol{\theta}) \equiv -2 \log \Pr(\mathcal{D}|\boldsymbol{\theta}, M), \tag{A.9}$$

where $D(\boldsymbol{\theta})$ is the deviance given parameter vector $\boldsymbol{\theta}$, the $\boldsymbol{\theta}^{(i)}$ are MCMC parameter samples (out of N_{smpl} samples from the posterior), and $\boldsymbol{\theta}^*$ is a 'good' parameter estimate for the model (e. g., the mean, median, or another measure of central tendency of the sampled parameters). As a robust estimate of $\boldsymbol{\theta}^*$ we usually compute a trimmed mean (discarding 10% from each side, which eliminates outlier parameter values). Like other approximate methods, DIC is only valid when the posterior distribution is approximately multivariate normal.

A.3.4 *Complete continuous model*

model selection

All previous methods assume that our main goal is *model selection*, that is the identification of the best model among a discrete set of alternatives. However, there are theoretical reasons for being wary of the Bayesian approach to model selection through the marginal likelihood (or approximations thereof). The main problem is that the marginal likelihood is sensitive to the choice of prior over parameters and this influence does not disappear with the acquisition of more data. For this reason, improper priors over parameters are to be avoided in a model comparison, and some authors eschew the marginal likelihood and Bayes factors altogether unless for very specific cases (Gelman et al., 2013). An alternative Bayesian approach that avoids model selection consists of having a single continuous model that includes all models of interest as special cases. Such a *complete model* can be analyzed in the usual Bayesian way through the posterior distribution of the parameters. However, this solution is not always feasible, sometimes because very different models cannot be resonably described with the same parameter set, and in other occasions the scientific questions of interest may call for a discrete answer (e. g., whether a given assumption is needed or not to explain the data).

A.4 GROUP MODEL COMPARISON

Another goal of model comparison can be to learn the model (or models) that overall best capture the group behaviour of the observers. The methods in Section A.3 allow us to compute a measure of evidence, η_{ij}, such as the log marginal likelihood or the DIC score, for each indivual dataset $\mathcal{D}_i$ and model M_j. A simple measure for group model evidence is the mean model evidence across subjects. Differences between models can be assessed through classical statistical methods such as t-tests or ANOVAs (or non-parametric versions of the same tests). This method assumes that all datasets have been generated by the same observer model, and all subjects contribute independently to the evidence of each model.

A more sophisticated approach treats both subjects and models as random factors, that is, multiple observer models may be present in the population, and the posterior probability over individual subjects' models is inferred by taking into account information from the whole group. These assumptions are at the core of the hierarchical Bayesian model selection (BMS) method developed by Stephan et al. (2009). BMS uses an iterative algorithm based on variational inference to compute model evidence from individual subjects' log marginal likelihoods (or analogous measures such as $-\frac{1}{2}$ DIC). BMS is particularly appealing because it naturally deals with group heterogeneity and outliers. Moreover, the output of the algorithm has an immediate interpretation as the probability that a given model is responsible for generating the data of a randomly chosen subject.

At times, we are not interested in evaluating a single model but we want to know the performance of a whole subset of models (for an individual or for the group). This is a natural question for a modelling technique recently called *factorial model comparison* (van den Berg et al., 2014), in which models are built factorially by mixing and matching several independent components (factors) that may take different shapes (levels). We may then ask what is the support from the data for a specific model component, independently of all the others. If the posterior probability of each model is available (either through a standard Bayesian computation or via BMS), the posterior probability for a set of models is simply obtained by summing the posterior probability of each model in the set.

factorial model comparison

B

ADDENDA TO TARGET ESTIMATION WITH COMPLEX PROBABILISTIC INFORMATION

In this appendix we describe a number of supplementary analyses and results for Chapter 4. In Section B.1 we describe how two different models of noisy Bayesian computations give rise to a target choice probability that is approximated by a power of the posterior distribution (observer model SPK). In Section B.2 we report additional analyses and data that support our results in Section 4.3.1. Finally, in Section B.3 we describe results of an alternative way of performing model comparison based on group DIC scores (GDIC), instead of the hierarchical method (BMS) used in the main body of the thesis; we also report the results of a preliminary model comparison to establish the parameters shared across sessions.

B.1 NOISY PROBABILISTIC INFERENCE

In this section we introduce two alternative models of stochastic computations in Bayesian inference (Section B.1.1). The first one (noisy posterior) comprises a representation of the posterior corrupted by noise; in the second one (sample-based posterior), a discrete, approximate representation of the posterior distribution is built out of a number of samples drawn from the posterior. We show that, for the loss function of our task, for both models the predicted distribution of chosen targets is quantitatively very close to a power function of the posterior distribution in the trial (Section B.1.2). The generality of this result motivates the power function approximation used for decision-making model level SPK (stochastic posterior), Eq. 4.10 in the main text. Lastly, we show that, under specific assumptions, the stochasticity in the posterior can also represent a certain type of noise in the prior (Section B.1.3).

B.1.1 *Stochastic posterior models*

According to Bayesian Decision Theory (BDT), the computation of the optimal target s^* for a given loss function $\mathcal{L}$ requires three steps:

1. Computation of the posterior probability $p_{post}(s)$.
2. Computation of the expected loss, $\mathcal{E}(\hat{s}) = \int p_{post}(s)\mathcal{L}(\hat{s}, s)ds$.

3. Computation of the target s^* that minimizes the expected loss, $s^* = \arg\min_{\hat{s}} \mathcal{E}(\hat{s})$.

Step 1 corresponds to the *inference* step and is described by Eq. 4.5 in the main text. Steps 2 and 3 correspond to *action selection* (Eq. 4.7 in the main text). *inference* *action selection*

In principle, noise in decision making could be added to any of the above steps. For parsimony, here we consider models that add stochasticity to the computation (or representation) of the posterior distribution (step 1), and we analyze how this noise propagates to the inferred optimal target s^*. However, our results are compatible also with noise injected at later stages (e. g., in action selection).

Noisy posterior

For ease of calculation, we convert the continuous posterior distribution $p_{post}(s)$ to a discrete probability distribution $p_i = p_{post}(s_i)$, for a discrete set of target values $\{s_i\}_{1 \le i \le N}$, where we assume that the s_i cover uniformly the target space with dense spacing Δs.[1]

We model the computation of a 'noisy posterior' (step 1) by adding normally distributed noise to the posterior (see Figure 4.3b):

$$\widetilde{p}_{post}(s) = \sum_{i=1}^{N} y_i \delta(s - s_i) \qquad \text{with} \quad y_i = p_i + \sigma(p_i)\eta_i, \tag{B.1}$$

where the η_i are i.i.d. normal random variables and $\sigma(p_i)$ is the SD of the 'decision noise', that in general depends on the value p_i.[2] For simplicity, the η_i are assumed to be statistically independent but it is easy to extend the model to take into account correlations in the noise.

For the form of $\sigma(p)$ we consider two common alternative rules:

- ▷ A Poisson-like law: $\sigma_{Poisson}(p) = \sqrt{p/g}$, where we have defined $g > 0$ as a 'neuronal gain' parameter; higher gain corresponds to less noise. The rationale for this rule is that the y_i can be thought of as a population of N independent units or channels ('neurons'), each one noisily encoding the posterior probability at a given target value s_i (see Figure 4.3b). The activation of each unit ('firing rate'), with a global rescaling factor g, takes the form $y_i = gp_i + \sqrt{gp_i}\eta_i$, which approximates the response of a Poisson neuron with mean activation gp_i.

1 The discretization step could be skipped by modelling continuous noise with a Gaussian process (Rasmussen and Williams, 2006). However, the discrete representation makes the model simpler and easier to interpret. The lattice spacing Δs is related to the correlation length of a Gaussian process and affects the amount of noise and discretization error.

2 Formally, $\widetilde{p}_{post}(s)$ as defined in Eq. B.1 is not a probability distribution since, aside of normalization, it is not always non-negative (the p_i's may take negative values for large amounts of noise in the inference). In this case the 'noisy posterior' could be interpreted simply as an intermediate step in a noisy computation of the expected loss.

▷ Weber's law (multiplicative noise), in which the noise is proportional to the probability itself, a form of variability which is typical to many sensory magnitudes: $\sigma_{Weber}(p) = w \cdot p$, with $w > 0$ the *Weber's fraction*.

For a fixed lattice spacing Δs, this model of noise in decision making has only one free parameter, g (or w), that sets the amount of variability in the inference. Note that the 'neural population' description allows for an intuitive understanding of Eq. B.1, but the noisy posterior model does not require to commit to this intepretation.

Sample-based posterior

This model assumes that a discrete, approximate representation of the posterior is constructed by drawing K samples from the posterior (see Section 2.4.5 and Figure 4.3c):

$$\widetilde{p}_{post}(s) = \frac{1}{K}\sum_{i=1}^{K}\delta\left(s - s^{(i)}\right) \qquad \text{with} \quad s^{(i)} \sim p_{post}, \tag{B.2}$$

where the $s^{(i)}$ are i.i.d. samples from the posterior. The parameter K is inversely proportional to the noise in the representation.

Target choice distribution

For a given posterior distribution $p_{post}(s)$, Eqs. B.1 and B.2 allow us to compute several instances of a stochastic posterior $\widetilde{p}_{post}(s)$ which, after minimization of the expected loss, entail different chosen targets s^*. By repeating this procedure and binning the results, we can obtain the shape of the distribution of target choices $p_{target}(\hat{s})$ for a given model of stochasticity (see Figure 4.3e & 4.3f). However, this method is computationally very expensive.

A simple expression for $p_{target}(\hat{s})$ is needed in order to make efficient use of a stochastic posterior model in data analysis, e.g. to compute the marginal likelihood of a dataset. Our goal is to show that the target choice probability of these noisy decision-making models is well approximated by a power function of the posterior distribution:

$$p_{target}(\hat{s}) \sim \left[p_{post}(\hat{s})\right]^{\kappa}, \tag{B.3}$$

where $\kappa \geq 0$ is an appropriate exponent that is the direct equivalent of the noise parameter g, w or K; higher values of κ correspond to less decision noise. In general, we would like the exponent in Eq. B.3 to be a function of the noise parameter, that is for example $\kappa = \kappa(g)$, where the mapping does not depend on the posterior

distribution itself but only on the decision noise level (note that the mapping will depend on other fixed details of the model such as the loss function, and the chosen discretization spacing Δs for the 'noisy posterior' model).

B.1.2 *Results*

We computed the target choice probability predicted by the stochastic posterior models in our task (noisy posterior with either Poisson-like or Weber's law noise, and sample-based posterior). We chose as loss function the inverted Gaussian approximation used by the observer models in the main text (see Section 4.2.3; results did not qualitatively change with the square well loss). We took as posterior distributions a representative set of all posterior distributions of the task, built out of several combinations of prior, cue position and cue type (low-noise and high-noise cues), for a total of about 1000 posterior distributions. We took several levels of decision noise (values of g, w or K, depending on the model), ranging from an approximately correct inference to an extremely noisy inference. For each posterior distribution and decision noise level we calculated the shape of the target choice distribution via Monte Carlo sampling (10^5 samples per distribution).

Figure B.1 shows the target choice distributions and related posterior-power fit distributions (Eq. B.3) for three illustrative posteriors and five levels of decision noise for the noisy posterior model with Poisson-like noise. For high levels of decision noise, the target choice distribution resembles the posterior distribution (i.e. a posterior-matching strategy), whereas for low levels of decision noise it becomes a narrow distribution peaked on the mode of the posterior (the model tends to a MAP strategy for $g \to \infty$). This may intuitively explain why a power function of the posterior would be a good approximation of the target choice distribution.

We quantified how well a power function of the posterior can approximate the target choice distributions in terms of Kullback-Leibler (KL) divergence. For each noise level, we computed the exponent κ that minimizes the KL divergence between posterior-power distributions and target choice distributions in the set (crucially, the same exponent κ fit simultaneously all ~ 1000 distributions). To assess the goodness of fit in our experiment, we computed mean and SD of the KL divergence according to a log-normal approximation of the posterior distribution of the values of κ found in the test sessions for our subjects (see 'Analysis of best observer model', Section 4.3.3).

In general, we found that the posterior-power fit approximates quite well the target choice distribution of all stochastic posterior models. The KL divergence between the true distribution and its approximation was $\sim 0.02 \pm 0.02$ nats (mean $\pm$ SD across

the distribution of values of κ) for all distinct models of noisy inference. These values are equivalent to the KL divergence between two Gaussian distributions with same SD and whose means differ by about one-fourth of their SD.

This analysis shows that a power function of the posterior represents a good approximation of the distribution of target choices of a Bayesian oberver that takes action according to a noisy or sample-based representation of the posterior. This result provides a sound basis for the analytical form chosen for model level SPK (stochastic posterior), Eq. 4.10 in the main text.

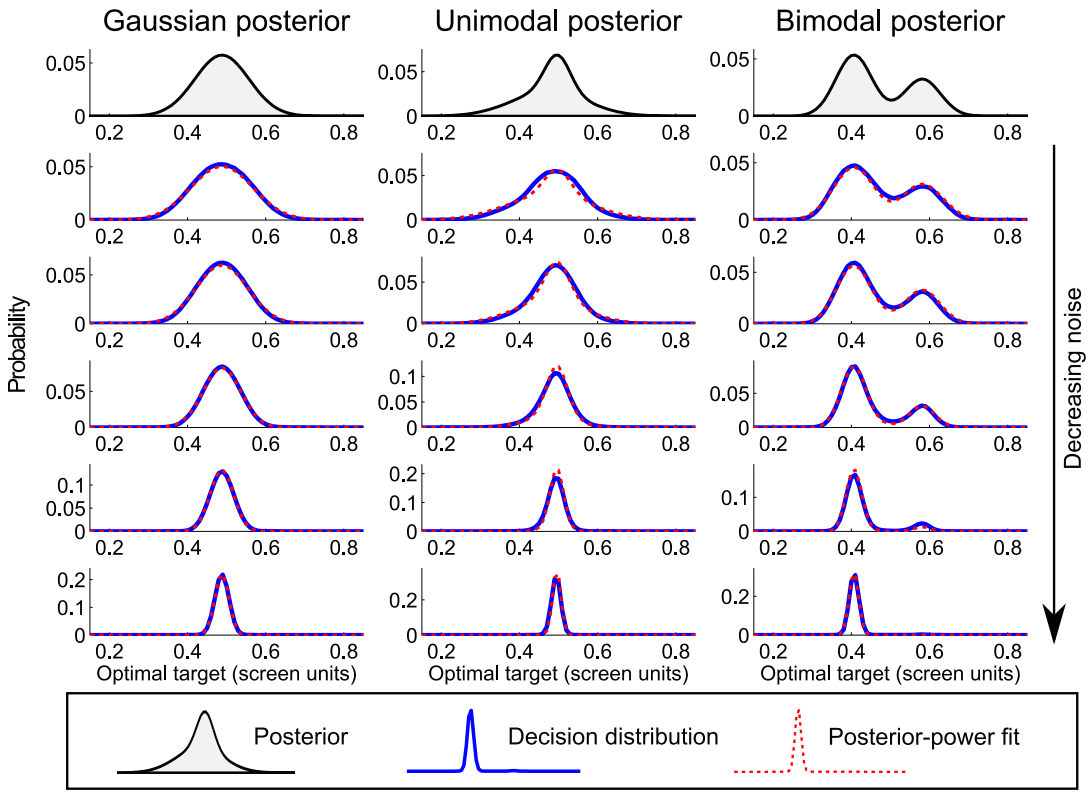

Figure B.1: **Posterior-power approximation of the noisy posterior model.** Comparison between the target choice distributions computed according to the true noisy posterior model (here with Poisson-like noise) and their posterior-power approximations. The various panels show the target choice distributions $p_{target}(\hat{s})$ (blue lines) and the associated posterior-power fits (red dashed lines) for different posterior distribution and noise level g in the computation. Each column corresponds to a different illustrative posterior distribution, shown on top, divided by class (Gaussian, unimodal and bimodal). Each row, excluding the first, corresponds to a different level of decision noise, with noise decreasing from top to bottom. Analogous fits were found for the sample-based approximation of the posterior.

B.1.3 *Stochastic posterior from unstructured noise in the prior*

We show here that the posterior noise model SPK may also subsume the unstructured components of noise in the prior.

If we assume that the internal measurement of the prior is corrupted by multiplicative sensory noise (according to the approximate Weber's law for density or numerosity esimation; Ross, 2003) and that it changes smoothly in the target position, the estimated prior can be written as:

$$\tilde{p}_{prior}(s) = p_{prior}(s) \cdot (1 + \epsilon(s)), \tag{B.4}$$

where $\epsilon(s)$ is a Gaussian process with zero mean and some appropriately chosen SD and covariance function (Rasmussen and Williams, 2006). Crucially, if the observer uses Eq. B.4 to build a posterior distribution, we obtain:

$$\tilde{p}_{post}(s) = p_{post}(s)\,(1 + \epsilon(s)), \tag{B.5}$$

where $p_{post}(s)$ is the usual, non-noisy posterior (Eq. 4.5 in the main text). Eq. B.5, once appropriately discretized, is formally equivalent to the equation we used to describe a noisy posterior with multiplicative noise (Eq. B.1; see also Figure 4.3b). Therefore, under these assumptions, the random, unstructured components of noise in the prior can be absorbed within the noisy posterior model.

Note that the estimation noise on the prior that we considered in Section 4.2.3, model factor P, is a structured form of noise that varies along task-relevant dimensions (such as the width of the prior or the relative weights of bimodal priors). Whereas structured noise can be identified at least in principle, teasing out which stage or component unstructured noise belongs to represents a greater challenge. For example, an experiment that involves a variable number of inference step may be able to distinguish whether noise stems from the computation of the posterior, which is repeated at every step, or from noise in the encoding of the original prior, which happens only once. A paradigm of this kind has been recently used to explore similar issues in a perceptual categorization task (Drugowitsch et al., 2014b). However, this method is still unable to distinguish whether noise appears in the first step (in the encoding or recall of the prior) or at the very last stage, during action selection. Another way to identify noise in the prior could consist in imposing a strong hyperprior on the subjects via extensive training. The level of attraction to such hyperpriors, once learned, may be indicative of the amount of uncertainty in the subjects' measurement of the prior.

B.2 SUPPLEMENTARY DATA ANALYSIS

B.2.1 *Translational invariance of subjects' targeting behaviour*

In Chapter 4 we assumed that all variables (e. g., cue position x_{cue}, subjects' response r, target position s) can be expressed relative to the current location of the prior (μ_{prior}); a shift of μ_{prior} simply produces an equal shift in all other position variables. That is, subjects' behaviour is independent of screen coordinates (translational invariance). The alternative hypothesis is that subjects' responses instead show some form of bias that is screen-coordinate dependent, for example a central tendency towards the middle of the screen.

In order to test whether subjects' relative responses depend on the absolute location of the prior, for each subject we fit a linear regression line to the relation between the relative response $\tilde{r} = r - \mu_{prior}$ and the prior mean μ_{prior} across all trials of the training session. Given the generative model of our task, we expected the average relative response to be zero irrespective of prior mean, $\langle \tilde{r} \rangle = 0$ and therefore tested whether the slope or intercept are different than zero. For almost all subjects, the slope and intercept were not significantly different than zero ($p > 0.05$). For two subjects we found that slope or intercept may have been significantly different from zero ($p = 0.002$ and $p = 0.04$). However, even in these cases a correction for multiple comparisons ($n = 24$) suggests that the these differences are not statistically significant or at most marginally so. This analysis confirms that subjects' responses in general do not show statistically significant departures from the assumption of translational invariance.

B.2.2 *Success probability*

Figure B.2 shows the success probability averaged across subjects, divided by sessions (see 'Optimality index and success probability' in Section 4.2.2). Note how the success probability depends substantially on the prior and on the magnitude of noise of the cue, that is on the amount of available probabilistic information, as opposed to the near-constancy of the optimality index (Figure 4.7).

B.2.3 *Inverted Gaussian loss function*

We show here that the inverted Gaussian loss function described by Eq. 4.17 is a very good approximation of the true loss model of the task, the (inverted) boxcar loss

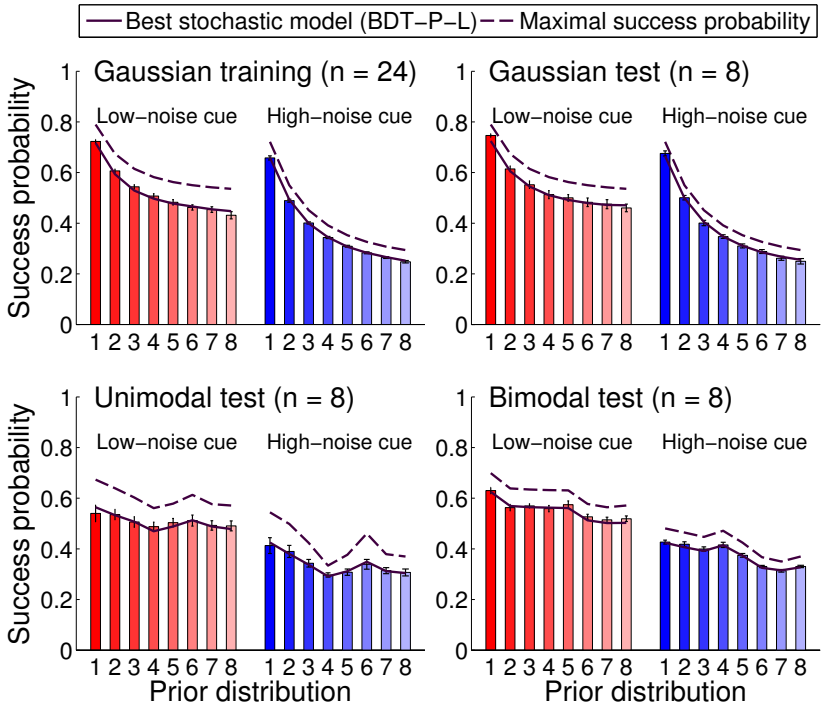

Figure B.2: **Group mean success probability for all sessions.** Each bar represents the group-averaged success probability for a specific session, for each prior (indexed from 1 to 8) and cue type, low-noise cues (red bars) or high-noise cues (blue bars). Error bars are SE across subjects. Priors are arranged in the order of differential entropy (i.e. increasing variance for Gaussian priors), except for 'unimodal test' priors which are listed in order of increasing width of the main peak in the prior. The dashed line represents the maximal success probability for an ideal observer. The continuous line represents the 'postdiction' of the best Bayesian model, BDT-P-L (see 'Analysis of best observer model' in Section 4.3.3). Compare this figure with Figure 4.7 in the main text, which shows the optimality index.

(Eq. 4.16). In order to compare the Gaussian loss with the boxcar loss, we computed the expected RMSE of the predicted target location between the true loss function (boxcar with $\ell^* = 0.083$ screen units, the cursor diameter) and its approximation (inverted Gaussian), averaged over the distributions of targets and cues in our task. We excluded from the analysis single-Gaussian priors, since in that case the predicted optimal target is identical for both loss models. We repeated the calculation for a range of values of the scale of the inverted Gaussian, σ_ℓ, finding the value for which the inverted Gaussian loss best approximates the true loss function of the task in terms of observable behaviour (minimum RMSE). We found an optimal value of $\sigma_\ell^* \approx 0.027$ screen units, close to the SD of a boxcar distribution (i.e. continuous uniform) of range ℓ^*, which is 0.024 screen units. For σ_ℓ^*, the total RMSE is $1.2 \cdot 10^{-4} \pm 1.5 \cdot 10^{-4}$ screen units (mean $\pm$ SD across different conditions), which is on average less than

a tenth of a mm. In terms of performance, the optimality index of an ideal Bayesian observer that uses the inverted Gaussian loss in place of the boxcar loss is 0.9999 ± 0.0001 (mean $\pm$ SE across conditions), which is empirically indistinguishable from 1. This analysis shows that the inverted Gaussian loss approximates the behaviour of the boxcar loss far below empirical error for our set of distributions. Hence, we can use the inverted Gaussian loss function for our Bayesian observer models without loss of generality.

The inverted Gaussian loss has several advantages over the boxcar loss (see Section 1.2.2). Primarily for us, it allows us to derive an analytic expression of the expected loss that involves only sums of Gaussian distributions (Eq. 4.7). In addition to theoretical appeal, experimentally the inverted Gaussian loss has been proven to account very well for people's behaviour in a spatial targeting task (Körding and Wolpert, 2004b).

Observer model with free loss width

In the main analysis we either fixed σ_ℓ to the value that best approximates the square well loss or we considered models that explictly or implicitly assume a quadratic loss ($\sigma_\ell \to \infty$). Here we examine the performance of an extended BDT-P-L model (the best model that follows BDT) in which the loss width σ_ℓ is allowed to vary freely. Since the parameter σ_ℓ is irrelevant for Gaussian posteriors, we perform this analysis only for non-Gaussian posteriors. Given the typical scale of the posteriors in the task, a value of $\sigma_\ell \gtrsim 0.2$ screen units should be considered near-quadratic for all practical purposes.

We find that subjects fall in two classes with respect to the posterior distribution of parameter σ_ℓ. For the majority of subjects (10 out of 16), mostly in the bimodal session, the posterior is peaked around $\sigma_\ell = 0.11 \pm 0.02$ screen units (mean $\pm$ SE across subjects), which is significantly higher than the 'true' value ($\sigma_\ell^* = 0.027$ screen units; signed rank test, $p < 0.01$) but still qualitatively different from a near-quadratic loss. For the other six subjects the posterior is much broader and flat in the range of σ_ℓ from 0.2 to 1 screen units, compatibly with a near-quadratic loss. In fact, according to the comparison between alternative models of decision making, these subjects show some preference for a quadratic loss or, similarly, a low-order approximation of the posterior (see Figure 4.11a in the main text and Figure B.4a here, subjects 10–14 and 18). However, note that most of these subjects belong to the unimodal group, where posteriors are still very close to Gaussians and therefore the exact value of the loss width may not be necessarily meaningful. The reason why we find a relatively large loss width in the case of a BDT observer is that it needs to account for large, posterior-dependent targeting errors that are explained instead by stochasticity in

decision making by the SPK observer (in neither case posterior-dependent errors can be adequately explained by constant motor noise σ_{motor}).

Performance of model BDT-P-L with variable loss is better than its corresponding version with fixed σ_ℓ ($\Delta\text{DIC} = -11.5 \pm 4.0$, $p < 0.05$), but still slightly worse than a model with variability in decision making with the same number of parameters, SPK-L ($\Delta\text{DIC} = 22.5 \pm 8.9$, $p < 0.05$). In conclusion, allowing a degree of freedom to the loss function at most slightly improves model performance for BDT but does not seem to provide a better explanation for the data than models with variability in decision making.

B.3 SUPPLEMENTARY MODEL COMPARISONS

In this section we describe the results of a slightly different method for model comparisons (Section B.3.1) and a preliminary comparison that we performed to establish which model parameters are shared between training and test session (Section B.3.2).

B.3.1 *Model comparison with group DIC*

We report here the DIC scores of invidual models for all subjects, and results of the group DIC (GDIC) model comparison. DIC scores are used in the main text to approximate the marginal likelihood of each dataset and model within a hierarchical Bayesian model selection (BMS) framework (Stephan et al., 2009). Here we also use DIC scores to compute the average impact of each model factor.

Basic model comparison

Figure B.3a shows the model evidence for each individual model and subject. We calculated model evidence as the difference in DIC between a given model and the subject's best model (lower values are better). A difference of more than 10 in this scale should be considered strong evidence for the model with lower DIC. Individual results show that model SPK-P-L performed better than other models for almost all datasets, with the exception of a minority that favoured model SPK-P instead. Unlike our BMS analysis, here we see a considerable similarity of performance between model SPK-P-L and SPK-S-P-L, although the latter performs slightly worse than the former in almost all cases. Figure B.3b shows the group average DIC (GDIC), relative to the model with lowest average DIC (lower scores are better). SPK-P-L is confirmed as the best model. Model SPK-S-K-L comes second in terms of average score, but note that the difference with SPK-P-L is significant (pairwise signed-rank test with

Bonferroni correction for multiple comparisons, $p < 0.001$). This suggests that the extra model factor S is not improving model performance, and therefore that SPK-S-P-L is not a 'good' model, in agreement with the small support it obtained in the BMS analysis (see Section 4.3.3).

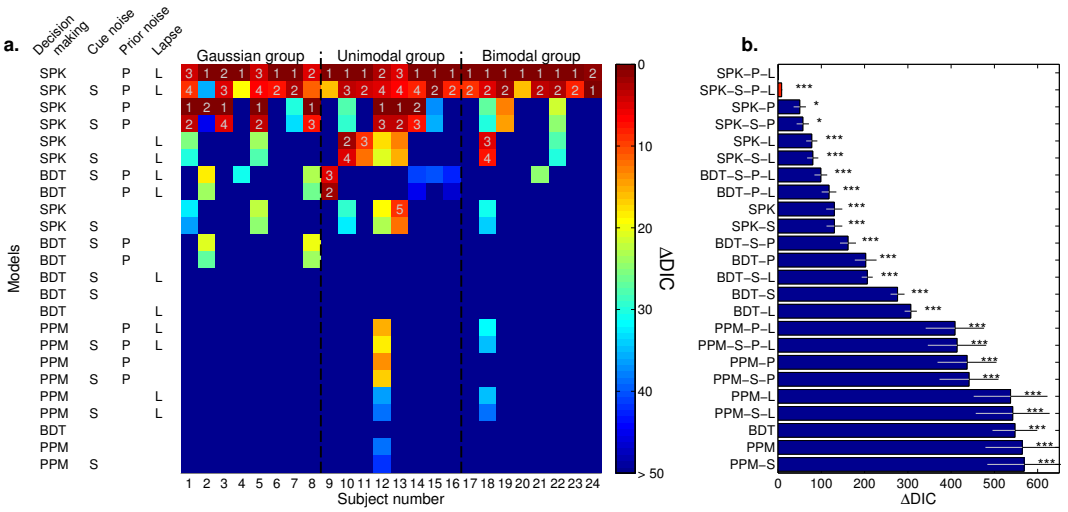

Figure B.3: **Comparison between individual models (DIC scores). a:** Each column represents a subject, divided by test group (all datasets include a Gaussian training session), each row an observer model identified by a model string (see Table 4.1). Cell colour indicates model's evidence, here displayed as the DIC difference (ΔDIC) with the best model for that subject (a higher value means a worse performance of a model with respect to the best model). Models are sorted by their group average DIC score (see panel b). Numbers above cells specify ranking for most supported models with comparable evidence (ΔDIC less than 10). **b:** Group average ΔDIC score, relative to the best model (mean ± SE). Higher scores indicate worse performance. Asterisks denote significant difference in DIC between a given model and the best model, after correction for multiple comparisons: (*) $p < 0.05$, (***) $p < 0.001$.

Comparison of alternative models of decision making

We consider first the model evidence for each individual model and subject (Figure B.4a). Results differ depending on the session (unimodal or bimodal). In both sessions model SPK-L performs consistently well, closely followed by model SPK. However, in the unimodal session there are quite a few subjects whose behaviour is well described by several other models. These results are summarized in Figure B.4b, which shows the group DIC relative to the model with lowest average DIC (lower scores are better). Due to the difference between sessions we separately computed the group averages for the unimodal and bimodal group. GDIC analysis in the unimodal session alone fails to find significant differences between SPK-L and several other observer models.

Conversely, GDIC shows significant results in the bimodal session, finding that all models but SPK perform worse than SPK-L.

These results agree with the BMS analysis in the main text in indicating SPK-L as the best model, but otherwise present quite a different pattern. Discrepancies between the two model comparison methods emerge for the following reasons. Firstly, as mentioned in the main text, BMS is not affected by outliers and by construction takes into account group heterogeneity, contrarily to DIC. Secondly, posteriors in the unimodal session may still be very close to Gaussian and therefore distinct models share very similar predictions, which DIC scores alone cannot disambiguate. The hierarchical probabilistic structure of BMS, instead, allows information to flow between global model evidence and individual model evidence for each subject (respectively α and u_{nk} in Stephan et al., 2009), at each iteration of the model comparison algorithm. This propagation of belief led BMS to discard less likely models in the main text.

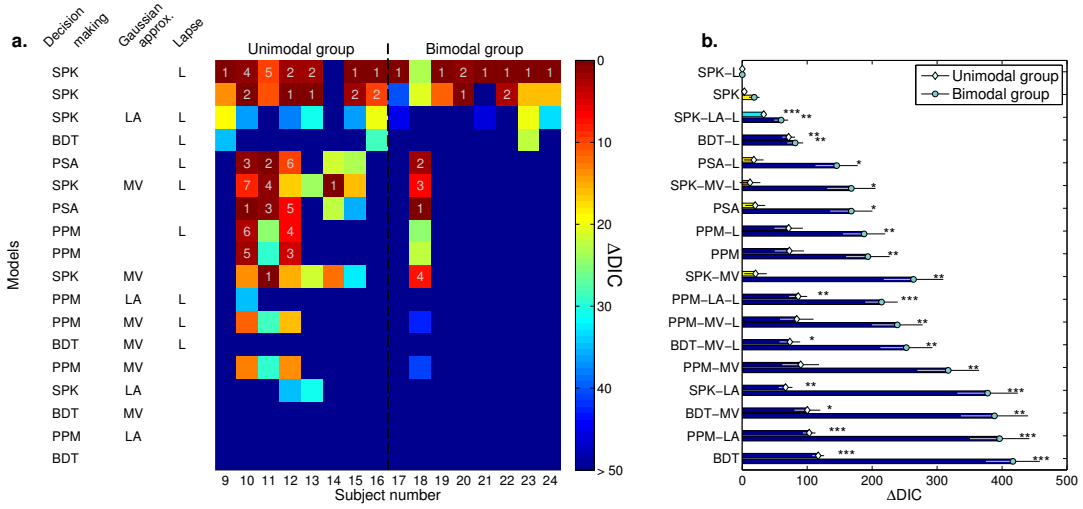

Figure B.4: **Comparison between alternative models of decision making (DIC scores).** We tested a class of alternative models of decision making which differ with respect to predictions for non-Gaussian trials only. **a:** Each column represents a subject, divided by group (either unimodal or bimodal test session), each row an observer model identified by a model string (see Table 4.1). Cell colour indicates model's evidence, here displayed as the DIC difference (ΔDIC) with the best model for that subject (a higher value means a worse performance of a model with respect to the best model). Models are sorted by their group average DIC score across both sessions (see panel b). Numbers above cells specify ranking for most supported models with comparable evidence (ΔDIC less than 10). **b:** Group average ΔDIC, divided by test group (unimodal or bimodal session), relative to the best model (mean ± SE). Higher scores indicate worse performance. Asterisks denote significant difference in DIC between a given model and the best model, after correction for multiple comparisons: (*) $p < 0.05$, (**) $p < 0.01$, (***) $p < 0.001$.

Comparison of distinct model components

We assess the relevance of each model level within a factor by measuring the average contribution to DIC of each level across all tested observer models, relative to the best level (Figure B.5). This is the GDIC counterpart of the BMS computation of the posterior likelihood of each model component (Figures 4.10c and 4.11c in the main text). Results of the GDIC analysis are qualitatively similar to BMS for all factors, with the sole exception of factor S (sensory noise in estimation of the cue position). BMS rejects factor S, whereas from GDIC we can see that, on average, it seems that *not* having factor S decreases model performance (ΔDIC: 33.0 ± 5.6, mean $\pm$ SE across subjects). This is not a contradiction: for many simple observer models the addition of any reasonable form of noise, including cue-estimation noise, will improve model performance. However, model factor S becomes redundant when other more fitting forms of noise are present. Since GDIC weights equally all model contributions, model S appears to have a useful influence on model performance due to the average contribution of 'simpler' models. On the contrary, BMS weights evidence differentially and component S appears to be irrelevant for the most likely models (see Section 4.3.3).

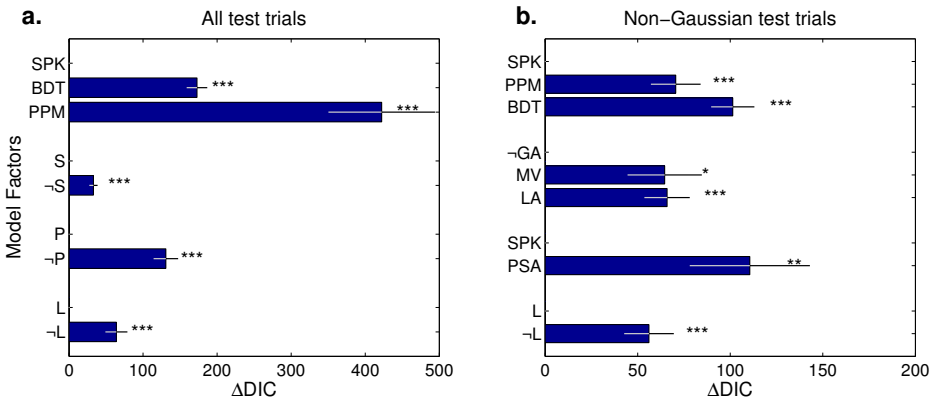

Figure B.5: **Influence of different model factors on DIC.** Difference in DIC between different levels within factors, relative to the best level (lowest DIC); highest scores denote worse performance. Each group of bars represent a factor, each bar a level within the factor, identified by a model label (see Table 4.1 in the main text). Error bars are SE across subjects. Asterisks denote significant difference in DIC between a given level and the best level, after correction for multiple comparisons: (*) $p < 0.05$, (**) $p < 0.01$, (***) $p < 0.001$. **a:** Factors in the basic model comparison. **b:** Factors in the comparison of alternative models of decision making. Label '¬GA' stands for no Gaussian approximation (full posterior).

B.3.2 *Model comparison for different shared parameters between sessions*

In the analyses in the main text we assumed that each subject shared two parameters between the training session and the test session (the motor noise σ_{motor} and the ratio between the cue noise, $\tilde{\sigma}_{high}/\tilde{\sigma}_{low}$), whereas all the other parameters were specified separately for the two sessions (see Section 4.2.4). Here we motivate our modelling choice by showing that it is optimal, at least on a subset of observer models. By 'optimal' we mean that models that share more parameters between sessions perform substantially worse, whereas models that share less parameters (and therefore have more free parameters to specify) do not provide a significant advantage.

For the current analysis we consider a set of variants of observer model SPK (stochastic posterior). We focus on this model since it is the simplest model with the 'best' decision-making component, as found in the main text. These variants differ from the standard SPK model only with respect to the number of parameters shared between training and test sessions. For a single session, model SPK can be characterized by four parameters ($\sigma_{motor}, \tilde{\sigma}_{low}, \tilde{\sigma}_{high}, \kappa$; see Section 4.2.3). Table B.1 lists the considered variants, labelled by number of parameters shared across sessions (model SPK#2 corresponds to the variant adopted in the main text).[3]

Model	Total number of parameters	Free parameters ($\boldsymbol{\theta}$)
SPK#4	4	$\sigma_{motor}, \tilde{\sigma}_{low}, \tilde{\sigma}_{high}, \kappa$
SPK#3	5	$\sigma_{motor}, \tilde{\sigma}_{low}, \tilde{\sigma}_{high}, \kappa \times 2$
SPK#2	6	$\sigma_{motor}, \tilde{\sigma}_{low}, (\tilde{\sigma}_{high}, \kappa) \times 2$
SPK#1	7	$\sigma_{motor}, (\tilde{\sigma}_{low}, \tilde{\sigma}_{high}, \kappa) \times 2$
SPK#0	8	$(\sigma_{motor}, \tilde{\sigma}_{low}, \tilde{\sigma}_{high}, \kappa) \times 2$

Table B.1: **Observer model SPK with different shared parameters.** Table of observer models based on SPK (stochastic posterior) but with different number of shared parameters (model SPK#2 corresponds to the version in the main text). The number after the '#' symbol represents the number of parameters the model shares between training and test session. For each model it is also specified the total number of free parameters used to characterize both sessions. A '$\times 2$' means that a parameter is specified independently for training and test sessions; otherwise parameters are shared across sessions. See main text for the meaning of the various parameters.

Here we use GDIC instead of BMS since we want to find the modelling choice that works best on average for all subjects. Figure B.6 shows the relative DIC scores of the model for different number of shared parameters. Unsurprisingly, the model

3 Although there are in total 16 variants of model SPK that share different combinations of parameters between sessions, the five models in Table B.1 represent the most natural combinations, in order of increasing model complexity.

with lowest group DIC is the model with the highest number of parameters (SPK#0). However, models SPK#1 and SPK#2 closely match the performance of model SPK#0. In particular, the difference between SPK#2 and SPK#0 is nonsignificant (ΔDIC = 3.5 ± 2.1; $p = 0.55$). Conversely, observer models with 3 or more shared parameters perform significantly worse (e. g.., for SPK#3: ΔDIC = 32.4 ± 7.3; $p < 0.001$).

These results show that a model that shares the motor noise parameter and the ratio between the estimated cues' SDs between sessions achieves the optimal balance between model fit and simplicity, supporting our choice in the main text.

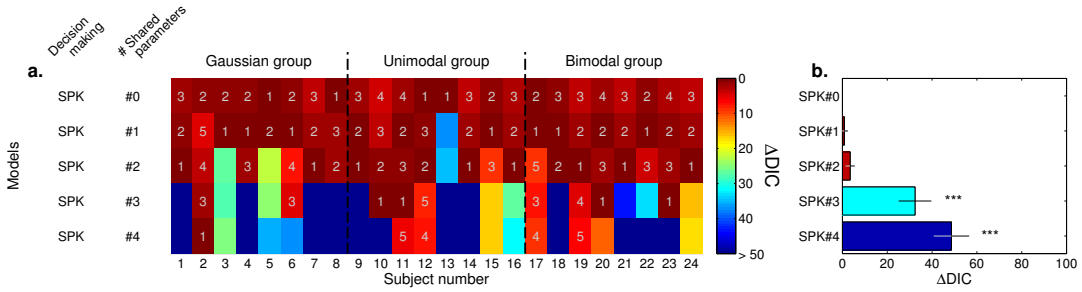

Figure B.6: **Comparison of models with different number of shared parameters.** Model comparison between observer models based on model SPK but with different number of shared parameters between sessions. **a:** Each column represents a subject, divided by test group (all datasets include a Gaussian training session), each row an observer model identified by a model string (see Table 4.1). Cell colour indicates model's evidence, here displayed as the DIC difference (ΔDIC) with the best model for that subject (a higher value means a worse performance of a model with respect to the best model). Models are sorted by their group average DIC score (see panel b). Numbers above cells specify ranking for most supported models with comparable evidence (ΔDIC less than 10). **b:** Group average ΔDIC score, relative to the best model (mean $\pm$ SE). Higher scores indicate worse performance. Asterisks denote significant difference in DIC between a given model and the best model, after correction for multiple comparisons: (***) $p < 0.001$.

BIBLIOGRAPHY

Acerbi, L., Ma, W. J., and Vijayakumar, S. (2014a). A framework for testing identifiability of bayesian models of perception. In *Advances in Neural Information Processing Systems 27*, pages 1026–1034. Curran Associates, Inc. (Cited on pages viii, 6, 26, and 193.)

Acerbi, L., Marius't Hart, B., Behbahani, F. M., and Peters, M. A. (2013). Optimality under fire: Dissociating learning from Bayesian integration. Presented at Translational and Computational Motor Control (TCMC) satellite meeting at the Society for Neuroscience Annual Meeting, San Diego, CA. (Cited on page 189.)

Acerbi, L. and Vijayakumar, S. (2011). Bayesian causal inference drives temporal sensorimotor recalibration. Cosyne Abstracts 2012, Salt Lake City USA. (Cited on page 98.)

Acerbi, L., Vijayakumar, S., and Wolpert, D. M. (2014b). On the origins of suboptimality in human probabilistic inference. *PLoS Computational Biology*, 10(6):e1003661. (Cited on pages viii and 103.)

Acerbi, L., Wolpert, D. M., and Vijayakumar, S. (2012). Internal representations of temporal statistics and feedback calibrate motor-sensory interval timing. *PLoS Computational Biology*, 8(11):e1002771. (Cited on pages viii and 57.)

Adams, W. J. (2007). A common light-prior for visual search, shape, and reflectance judgments. *Journal of Vision*, 7(11):1–7. (Cited on page 42.)

Adams, W. J., Graf, E. W., and Ernst, M. O. (2004). Experience can change the 'light-from-above' prior. *Nature Neuroscience*, 7(10):1057–1058. (Cited on pages 35 and 42.)

Ahrens, M. B. and Sahani, M. (2011). Observers exploit stochastic models of sensory change to help judge the passage of time. *Current Biology*, 21(3):200–206. (Cited on pages 58 and 101.)

Akaike, H. (1973). Information theory and an extension of the maximum likelihood principle. In Petrov, B. N. and Csáki, F., editors, *Information Theory: Proceedings of the 2nd International Symposium*, pages 267–281. Akadémiai Kiadó. (Cited on page 204.)

Alais, D. and Burr, D. (2004). The ventriloquist effect results from near-optimal bimodal integration. *Current Biology*, 14(3):257–262. (Cited on pages 31 and 101.)

Anderson, J. R. (1978). Arguments concerning representations for mental imagery. *Psychological Review*, 85(4):249–277. (Cited on page 192.)

Bach, D. R. and Dolan, R. J. (2012). Knowing how much you don't know: A neural organization of uncertainty estimates. *Nature Reviews Neuroscience*, 13(8):572–586. (Cited on page 29.)

Barlow, H. B. (1961). Possible principles underlying the transformation of sensory messages. In Ronsenblith, W. A., editor, *Sensory communication*, pages 217–234. MIT Press. (Cited on page 4.)

Barthelmé, S. and Mamassian, P. (2009). Evaluation of objective uncertainty in the visual system. *PLoS Computational Biology*, 5(9):e1000504. (Cited on page 29.)

Barthelmé, S. and Mamassian, P. (2010). Flexible mechanisms underlie the evaluation of visual confidence. *Proceedings of the National Academy of Sciences*, 107(48):20834–20839. (Cited on pages 29 and 31.)

Battaglia, P. W., Hamrick, J. B., and Tenenbaum, J. B. (2013). Simulation as an engine of physical scene understanding. *Proceedings of the National Academy of Sciences*, 110(45):18327–18332. (Cited on pages 147 and 188.)

Battaglia, P. W., Jacobs, R. A., and Aslin, R. N. (2003). Bayesian integration of visual and auditory signals for spatial localization. *The Journal of the Optical Society of America A*, 20(7):1391–1397. (Cited on page 31.)

Battaglia, P. W., Kersten, D., and Schrater, P. R. (2011). How haptic size sensations improve distance perception. *PLoS Computational Biology*, 7(6):e1002080. (Cited on pages 26, 56, 94, 120, 122, 128, 147, 153, 184, and 188.)

Battaglia, P. W. and Schrater, P. R. (2007). Humans trade off viewing time and movement duration to improve visuomotor accuracy in a fast reaching task. *The Journal of Neuroscience*, 27(26):6984–6994. (Cited on page 54.)

Bays, P. M. and Wolpert, D. M. (2007). Computational principles of sensorimotor control that minimize uncertainty and variability. *The Journal of Physiology*, 578(2):387–396. (Cited on page 18.)

Beck, J. M., Ma, W. J., Pitkow, X., Latham, P. E., and Pouget, A. (2012). Not noisy, just wrong: The role of suboptimal inference in behavioral variability. *Neuron*, 74:30–39. (Cited on pages 3, 4, 154, and 188.)

Beierholm, U. R., Quartz, S. R., and Shams, L. (2009). Bayesian priors are encoded independently from likelihoods in human multisensory perception. *Journal of Vision*, 9(5):1–9. (Cited on page 101.)

Berger, J. O. (1985). *Statistical decision theory and Bayesian analysis*. Springer. (Cited on pages 5, 7, and 13.)

Berniker, M. and Kording, K. (2011). Bayesian approaches to sensory integration for motor control. In Seth, A. K., Prescott, T. J., and Bryson, J. J., editors, *Modelling natural action selection*, pages 419–428. Cambridge University Press. (Cited on page 18.)

Berniker, M., Voss, M., and Kording, K. (2010). Learning priors for Bayesian computations in the nervous system. *PloS One*, 5(9):e12686. (Cited on pages 38, 43, 151, 184, and 185.)

Blackwell, J. R. and Newell, K. M. (1996). The informational role of knowledge of results in motor learning. *Acta Psychologica*, 92(2):119–129. (Cited on pages 63 and 100.)

Bowers, J. S. and Davis, C. J. (2012). Bayesian just-so stories in psychology and neuroscience. *Psychological Bulletin*, 138(3):389–414. (Cited on pages 19, 40, 96, and 192.)

Brainard, D. (1997). The psychophysics toolbox. *Spatial Vision*, 10(4):433–436. (Cited on page 62.)

Braun, D. A., Nagengast, A. J., and Wolpert, D. (2011). Risk-sensitivity in sensorimotor control. *Frontiers in Human Neuroscience*, 5:1. (Cited on page 158.)

Brouwer, A.-M. and Knill, D. C. (2007). The role of memory in visually guided reaching. *Journal of Vision*, 7(5):1–12. (Cited on page 37.)

Brouwer, A.-M. and Knill, D. C. (2009). Humans use visual and remembered information about object location to plan pointing movements. *Journal of Vision*, 9(1):1–19. (Cited on page 37.)

Buhusi, C. V. and Meck, W. H. (2005). What makes us tick? Functional and neural mechanisms of interval timing. *Nature Reviews Neuroscience*, 6(10):755–765. (Cited on page 58.)

Bülthoff, H. H. and Yuille, A. L. (1991). Bayesian models for seeing shapes and depth. *Comments on Theoretical Biology*, 2(4):283–314. (Cited on page 28.)

Buonomano, D. V. and Laje, R. (2010). Population clocks: Motor timing with neural dynamics. *Trends in Cognitive Sciences*, 14(12):520–527. (Cited on page 102.)

Burge, J., Ernst, M. O., and Banks, M. S. (2008). The statistical determinants of adaptation rate in human reaching. *Journal of Vision*, 8(4):1–19. (Cited on page 98.)

Burr, D., Banks, M. S., and Morrone, M. C. (2009). Auditory dominance over vision in the perception of interval duration. *Experimental Brain Research*, 198(1):49–57. (Cited on page 59.)

Cai, M., Stetson, C., and Eagleman, D. M. (2012). A neural model for temporal order judgments and their active recalibration: A common mechanism for space and time? *Frontiers in Psychology*, 3. (Cited on page 102.)

Campbell, L. L. (1966). Exponential entropy as a measure of extent of a distribution. *Journal of Probability Theory and Related Fields*, 5(3):217–225. (Cited on page 113.)

Cantlon, J. F., Cordes, S., Libertus, M. E., and Brannon, E. M. (2009). Comment on "Log or linear? Distinct intuitions of the number scale in Western and Amazonian indigene cultures". *Science*, 323(5910):38b–38b. (Cited on page 27.)

Carreira-Perpiñán, M. Á. (2000). Mode-finding for mixtures of Gaussian distributions. *IEEE Transactions on Pattern Analysis and Machine Intelligence*, 22(11):1318–1323. (Cited on pages 124, 125, and 167.)

Chalk, M., Seitz, A. R., and Seriès, P. (2010). Rapidly learned stimulus expectations alter perception of motion. *Journal of Vision*, 10(8):1–18. (Cited on pages 39, 43, 59, 90, 104, 185, 186, and 187.)

Churchland, M. M., Afshar, A., and Shenoy, K. V. (2006). A central source of movement variability. *Neuron*, 52(6):1085–1096. (Cited on page 51.)

Cicchini, G. M., Arrighi, R., Cecchetti, L., Giusti, M., and Burr, D. C. (2012). Optimal encoding of interval timing in expert percussionists. *The Journal of Neuroscience*, 32(3):1056–1060. (Cited on pages 38, 43, 58, 74, 94, 101, 185, 186, and 187.)

Colombo, M. and Hartmann, S. (2014). Bayesian cognitive science, unification, and explanation. http://philsci-archive.pitt.edu/10787/. Unpublished. (Cited on page 41.)

Colombo, M. and Seriès, P. (2012). Bayes in the brain—on Bayesian modelling in neuroscience. *The British Journal for the Philosophy of Science*, 63(3):697–723. (Cited on pages 2 and 18.)

Cox, R. T. (1946). Probability, frequency, and reasonable expectation. *American Journal of Physics*, 14(1):1–13. (Cited on page 3.)

Cox, R. T. (1961). *The algebra of probable inference*. Johns Hopkins University Press. (Cited on page 3.)

Cunningham, D. W., Billock, V. A., and Tsou, B. H. (2001a). Sensorimotor adaptation to violations of temporal contiguity. *Psychological Science*, 12(6):532–535. (Cited on page 100.)

Cunningham, D. W., Chatziastros, A., Von der Heyde, M., and Bülthoff, H. H. (2001b). Driving in the future: Temporal visuomotor adaptation and generalization. *Journal of vision*, 1(2):88–98. (Cited on page 100.)

Dakin, S. C., Tibber, M. S., Greenwood, J. A., Morgan, M. J., et al. (2011). A common visual metric for approximate number and density. *Proceedings of the National Academy of Sciences of the United States of America*, 108(49):19552–19557. (Cited on page 147.)

Daugman, J. G. (2001). Brain metaphor and brain theory. In Bechtel, W., Mandik, P., Mundale, J., and Stufflebeam, R. S., editors, *Philosophy and the neurosciences: A reader*, pages 23–36. Blackwell Publishing. (Cited on page 194.)

De Finetti, B. (1937). Foresight: Its logical laws, its subjective sources. In Kyburg, H. E. and Smokler, H. E., editors, *Studies in subjective probability*. Robert E. Kreiger Publishing Co. (Cited on page 3.)

de Xivry, J.-J. O. (2013). Trial-to-trial reoptimization of motor behavior due to changes in task demands is limited. *PloS One*, 8(6):e66013. (Cited on page 157.)

DeCarlo, L. T. and Cross, D. V. (1990). Sequential effects in magnitude scaling: Models and theory. *Journal of Experimental Psychology: General*, 119(4):375. (Cited on page 184.)

Dehaene, S. (2001). Subtracting pigeons: Logarithmic or linear? *Psychological Science*, 12(3):244–246. (Cited on page 27.)

Dehaene, S., Izard, V., Spelke, E., and Pica, P. (2008). Log or linear? Distinct intuitions of the number scale in Western and Amazonian indigene cultures. *Science*, 320(5880):1217–1220. (Cited on page 27.)

Denève, S., Latham, P. E., and Pouget, A. (2001). Efficient computation and cue integration with noisy population codes. *Nature Neuroscience*, 4(8):826–831. (Cited on page 188.)

Di Luca, M., Machulla, T.-K., and Ernst, M. O. (2009). Recalibration of multisensory simultaneity: Cross-modal transfer coincides with a change in perceptual latency. *Journal of Vision*, 9(12):1–16. (Cited on page 98.)

Doya, K., Ishii, S., Pouget, A., and Rao, R. P. N. (2007). *Bayesian brain: Probabilistic approaches to neural coding*. MIT Press. (Cited on pages 1, 2, and 18.)

Drewing, K. and Ernst, M. O. (2006). Integration of force and position cues for shape perception through active touch. *Brain Research*, 1078(1):92–100. (Cited on page 32.)

Drugowitsch, J., Moreno-Bote, R., Churchland, A. K., Shadlen, M. N., and Pouget, A. (2012). The cost of accumulating evidence in perceptual decision making. *The Journal of Neuroscience*, 32(11):3612–3628. (Cited on pages 51 and 179.)

Drugowitsch, J., Moreno-Bote, R., and Pouget, A. (2014a). Relation between belief and performance in perceptual decision making. *PloS One*, 9(5):e96511. (Cited on page 193.)

Drugowitsch, J., Wyarta, V., and Koechlin, E. (2014b). The origin and structure of behavioral variability in perceptual decision-making. Cosyne Abstracts 2014, Salt Lake City USA. (Cited on pages 153, 189, and 212.)

Eagleman, D. M. (2008). Human time perception and its illusions. *Current Opinion in Neurobiology*, 18(2):131–136. (Cited on pages 57 and 186.)

Eagleman, D. M. and Pariyadath, V. (2009). Is subjective duration a signature of coding efficiency? *Philosophical Transactions of the Royal Society B: Biological Sciences*, 364(1525):1841–1851. (Cited on page 57.)

Elliott, D., Hansen, S., Grierson, L. E., Lyons, J., Bennett, S. J., and Hayes, S. J. (2010). Goal-directed aiming: Two components but multiple processes. *Psychological Bulletin*, 136(6):1023–1044. (Cited on page 171.)

Elliott, D., Helsen, W. F., and Chua, R. (2001). A century later: Woodworth's (1899) two-component model of goal-directed aiming. *Psychological Bulletin*, 127(3):342–357. (Cited on page 171.)

Engelbrecht, S. E., Berthier, N. E., and O'Sullivan, L. P. (2003). The undershoot bias: Learning to act optimally under uncertainty. *Psychological Science*, 14(3):257–261. (Cited on page 158.)

Ernst, M. O. (2006). A Bayesian view on multimodal cue integration. In Knoblich, G., Thornton, I., Grosjean, M., and Shiffrar, M., editors, *Human body perception from the inside out*, pages 105–131. Oxford University Press. (Cited on page 18.)

Ernst, M. O. (2007). Learning to integrate arbitrary signals from vision and touch. *Journal of Vision*, 7(5):1–14. (Cited on page 40.)

Ernst, M. O. and Banks, M. S. (2002). Humans integrate visual and haptic information in a statistically optimal fashion. *Nature*, 415(6870):429–433. (Cited on pages 30, 31, 101, and 176.)

Ernst, M. O. and Bülthoff, H. H. (2004). Merging the senses into a robust percept. *Trends in Cognitive Sciences*, 8(4):162–169. (Cited on pages 18, 29, and 31.)

Faisal, A. A., Selen, L. P., and Wolpert, D. M. (2008). Noise in the nervous system. *Nature Reviews Neuroscience*, 9(4):292–303. (Cited on pages 25, 153, and 188.)

Faisal, A. A. and Wolpert, D. M. (2009). Near optimal combination of sensory and motor uncertainty in time during a naturalistic perception-action task. *Journal of Neurophysiology*, 101(4):1901–1912. (Cited on page 54.)

Feldman, J. (2013). Tuning your priors to the world. *Topics in Cognitive Science*, 5(1):13–34. (Cited on pages 4, 22, 35, 36, 40, 81, and 152.)

Feldman, J. (2014). Bayesian models of perceptual organization. In Wagemans, J., editor, *Handbook of perceptual organization*. Oxford University Press. (Cited on page 18.)

Fetsch, C. R., DeAngelis, G. C., and Angelaki, D. E. (2013). Bridging the gap between theories of sensory cue integration and the physiology of multisensory neurons. *Nature Reviews Neuroscience*, 14(6):429–442. (Cited on page 29.)

Fiser, J., Berkes, P., Orbán, G., and Lengyel, M. (2010). Statistically optimal perception and learning: From behavior to neural representations. *Trends in Cognitive Sciences*, 14(3):119–130. (Cited on pages 55, 154, and 188.)

Fleming, S. M., Maloney, L. T., and Daw, N. D. (2013). The irrationality of categorical perception. *The Journal of Neuroscience*, 33(49):19060–19070. (Cited on page 50.)

Fraisse, P. (1984). Perception and estimation of time. *Annual Review of Psychology*, 35(1):1–36. (Cited on page 57.)

Franssen, V. and Vandierendonck, A. (2002). Time estimation: Does the reference memory mediate the effect of knowledge of results? *Acta Psychologica*, 109(3):239–267. (Cited on page 100.)

Friedenberg, J. and Liby, B. (2002). Perception of two-body center of mass. *Perception & Psychophysics*, 64(4):531–539. (Cited on page 160.)

Friston, K. (2012). The history of the future of the Bayesian brain. *NeuroImage*, 62(2):1230–1233. (Cited on pages 1 and 18.)

Fründ, I., Haenel, N. V., and Wichmann, F. A. (2011). Inference for psychometric functions in the presence of nonstationary behavior. *Journal of Vision*, 11(6):1–19. (Cited on page 29.)

Fujisaki, W., Shimojo, S., Kashino, M., and Nishida, S. (2004). Recalibration of audiovisual simultaneity. *Nature Neuroscience*, 7(7):773–778. (Cited on pages 57, 59, and 98.)

Fulvio, J. M., Green, C. S., and Schrater, P. R. (2014). Task-specific response strategy selection on the basis of recent training experience. *PLoS Computational Biology*, 10(1):e1003425. (Cited on page 186.)

Gaissmaier, W. and Schooler, L. J. (2008). The smart potential behind probability matching. *Cognition*, 109(3):416–422. (Cited on pages 55 and 154.)

Geisler, W. S. (2003). Ideal observer analysis. In Chalupa, L. M. and Werner, J. S., editors, *The visual neurosciences*, pages 825–837. MIT Press. (Cited on page 18.)

Geisler, W. S. (2011). Contributions of ideal observer theory to vision research. *Vision Research*, 51(7):771–781. (Cited on page 2.)

Geisler, W. S. and Diehl, R. L. (2002). Bayesian natural selection and the evolution of perceptual systems. *Philosophical Transactions of the Royal Society of London. Series B: Biological Sciences*, 357(1420):419–448. (Cited on page 3.)

Geisler, W. S. and Diehl, R. L. (2003). A Bayesian approach to the evolution of perceptual and cognitive systems. *Cognitive Science*, 27(3):379–402. (Cited on page 3.)

Geisler, W. S. and Kersten, D. (2002). Illusions, perception and Bayes. *Nature Neuroscience*, 5(6):508–510. (Cited on pages 18, 40, and 41.)

Gekas, N., Chalk, M., Seitz, A. R., and Seriès, P. (2013). Complexity and specificity of experimentally induced expectations in motion perception. *Journal of Vision*, 13(4):1–20. (Cited on pages 39, 40, 43, 104, and 187.)

Gelman, A., Carlin, J. B., Stern, H. S., Dunson, D. B., Vehtari, A., and Rubin, D. B. (2013). *Bayesian data analysis (3rd edition)*. CRC Press. (Cited on pages 43, 54, 127, 194, 201, 202, and 205.)

Gelman, A. and Rubin, D. B. (1992). Inference from iterative simulation using multiple sequences. *Statistical Science*, 7(4):457–472. (Cited on page 127.)

Gepshtein, S. and Banks, M. S. (2003). Viewing geometry determines how vision and haptics combine in size perception. *Current Biology*, 13(6):483–488. (Cited on page 31.)

Gepshtein, S., Seydell, A., and Trommershäuser, J. (2007). Optimality of human movement under natural variations of visual–motor uncertainty. *Journal of Vision*, 7(5):1–

18. (Cited on pages 52 and 153.)

Gershman, S. J. and Blei, D. M. (2012). A tutorial on Bayesian nonparametric models. *Journal of Mathematical Psychology*, 56(1):1–12. (Cited on page 43.)

Getty, D. J. (1975). Discrimination of short temporal intervals: A comparison of two models. *Perception & Psychophysics*, 18(1):1–8. (Cited on page 26.)

Ghahramani, Z., Wolpert, D. M., and Jordan, M. I. (1997). Computational models of sensorimotor integration. In Morasso, P. G. and Sanguineti, V., editors, *Self-organization, computational maps, and motor control*, pages 117–147. Elsevier. (Cited on pages 30 and 31.)

Gibbon, J. (1977). Scalar expectancy theory and Weber's law in animal timing. *Psychological Review*, 84(3):279–325. (Cited on pages 26, 52, and 73.)

Gibbon, J. (1981). On the form and location of the psychometric bisection function for time. *Journal of Mathematical Psychology*, 24(1):58–87. (Cited on page 71.)

Gifford, A. M., Cohen, Y. E., and Stocker, A. A. (2014). Characterizing the impact of category uncertainty on human auditory categorization behavior. *PLoS Computational Biology*, 10(7):e1003715. (Cited on page 55.)

Girshick, A. R. and Banks, M. S. (2009). Probabilistic combination of slant information: Weighted averaging and robustness as optimal percepts. *Journal of Vision*, 9(9):1–20. (Cited on page 33.)

Girshick, A. R., Landy, M. S., and Simoncelli, E. P. (2011). Cardinal rules: Visual orientation perception reflects knowledge of environmental statistics. *Nature Neuroscience*, 14(7):926–932. (Cited on pages 41, 44, 96, 185, and 192.)

Goldreich, D. (2007). A Bayesian perceptual model replicates the cutaneous rabbit and other tactile spatiotemporal illusions. *PLoS One*, 2(3):e333. (Cited on page 41.)

Goldreich, D. and Tong, J. (2013). Prediction, postdiction, and perceptual length contraction: A Bayesian low-speed prior captures the cutaneous rabbit and related illusions. *Frontiers in Psychology*, 4(221). (Cited on page 41.)

Gorea, A. and Sagi, D. (2000). Failure to handle more than one internal representation in visual detection tasks. *Proceedings of the National Academy of Sciences*, 97(22):12380–12384. (Cited on page 40.)

Grabska-Barwinska, A., Beck, J., Pouget, A., and Latham, P. (2013). Demixing odors – fast inference in olfaction. In Burges, C., Bottou, L., Welling, M., Ghahramani, Z., and Weinberger, K., editors, *Advances in Neural Information Processing Systems 26*, pages 1968–1976. Curran Associates, Inc. (Cited on pages 188 and 190.)

Grau-Moya, J., Ortega, P. A., and Braun, D. A. (2012). Risk-sensitivity in Bayesian sensorimotor integration. *PLoS Computational Biology*, 8(9):e1002698. (Cited on pages 158, 179, and 180.)

Green, C. S., Benson, C., Kersten, D., and Schrater, P. (2010). Alterations in choice behavior by manipulations of world model. *Proceedings of the National Academy of Sciences*, 107(37):16401–16406. (Cited on pages 55 and 154.)

Green, D. M. and Swets, J. A. (1988). *Signal detection theory and psychophysics*. Peninsula Publishing. (Cited on pages 19, 26, and 28.)

Greenhouse, S. W. and Geisser, S. (1959). On methods in the analysis of profile data. *Psychometrika*, 24(2):95–112. (Cited on pages 114 and 163.)

Griffiths, T. L., Chater, N., Kemp, C., Perfors, A., and Tenenbaum, J. B. (2010). Probabilistic models of cognition: Exploring representations and inductive biases. *Trends in Cognitive Sciences*, 14(8):357–364. (Cited on page 3.)

Griffiths, T. L., Kemp, C., and Tenenbaum, J. B. (2008). Bayesian models of cognition. In Sun, R., editor, *Cambridge handbook of computational cognitive modeling*, pages 59–100. Cambridge University Press. (Cited on page 3.)

Griffiths, T. L., Lucas, C., Williams, J., and Kalish, M. L. (2009). Modeling human function learning with Gaussian processes. In Koller, D., Schuurmans, D., Bengio, Y., and Bottou, L., editors, *Advances in Neural Information Processing Systems 21*, pages 553–660. Curran Associates, Inc. (Cited on page 185.)

Griffiths, T. L. and Tenenbaum, J. B. (2004). From algorithmic to subjective randomness. In Thrun, S., Saul, L., and Schölkopf, B., editors, *Advances in Neural Information Processing Systems 16*, pages 953–960. MIT Press. (Cited on page 185.)

Grondin, S. (2010). Timing and time perception: A review of recent behavioral and neuroscience findings and theoretical directions. *Attention, Perception, & Psychophysics*, 72(3):561–582. (Cited on page 101.)

Gross, C. G. (1995). Aristotle on the brain. *The Neuroscientist*, 1(4):245–250. (Cited on page 1.)

Haggard, P., Clark, S., and Kalogeras, J. (2002). Voluntary action and conscious awareness. *Nature Neuroscience*, 5(4):382–385. (Cited on page 77.)

Härdle, W., Müller, M., Sperlich, S., and Werwatz, A. (2004). *Nonparametric and semiparametric models: An introduction*. Springer. (Cited on page 114.)

Harris, C. M. and Wolpert, D. M. (1998). Signal-dependent noise determines motor planning. *Nature*, 394(6695):780–784. (Cited on pages 50, 51, 52, and 158.)

Hartcher-O'Brien, J. and Alais, D. (2011). Temporal ventriloquism in a purely temporal context. *Journal of Experimental Psychology: Human Perception and Performance*, 37(5):1383. (Cited on page 59.)

Hartcher-O'Brien, J., Di Luca, M., and Ernst, M. O. (2014). The duration of uncertain times: Audiovisual information about intervals is integrated in a statistically optimal fashion. *PloS One*, 9(3):e89339. (Cited on pages 32 and 58.)

Hass, J. and Herrmann, J. M. (2012). The neural representation of time: An information-theoretic perspective. *Neural Computation*, 24(6):1519–1552. (Cited on page 101.)

Hedges, J. H., Stocker, A. A., and Simoncelli, E. P. (2011). Optimal inference explains the perceptual coherence of visual motion stimuli. *Journal of Vision*, 11(6):14. (Cited on pages 42, 44, and 192.)

Helbig, H. B. and Ernst, M. O. (2007). Optimal integration of shape information from vision and touch. *Experimental Brain Research*, 179(4):595–606. (Cited on page 31.)

Helmholtz, H. L. F. (1925). *Treatise on physiological optics. Vol. III: The perceptions of vision.* The Optical Society of America. Original work published 1867. (Cited on page 2.)

Heron, J., Aaen-Stockdale, C., Hotchkiss, J., Roach, N. W., McGraw, P. V., and Whitaker, D. (2012). Duration channels mediate human time perception. *Proceedings of the Royal Society B: Biological Sciences*, 279(1729):690–698. (Cited on pages 88 and 102.)

Heron, J., Hanson, J. V. M., and Whitaker, D. (2009). Effect before cause: Supramodal recalibration of sensorimotor timing. *PLoS One*, 4(11):e7681. (Cited on pages 77, 88, and 98.)

Hershberger, W. (1970). Attached-shadow orientation perceived as depth by chickens reared in an environment illuminated from below. *Journal of Comparative and Physiological Psychology*, 73(3):407–411. (Cited on pages 35 and 42.)

Hertwig, R. and Erev, I. (2009). The description–experience gap in risky choice. *Trends in Cognitive Sciences*, 13(12):517–523. (Cited on page 190.)

Hillis, J. M., Watt, S. J., Landy, M. S., and Banks, M. S. (2004). Slant from texture and disparity cues: Optimal cue combination. *Journal of Vision*, 4(12):967–992. (Cited on pages 32 and 54.)

Hodgkin, A. L. and Huxley, A. F. (1952). A quantitative description of membrane current and its application to conduction and excitation in nerve. *The Journal of Physiology*, 117(4):500–544. (Cited on page 195.)

Hogan, N. (1984). An organizing principle for a class of voluntary movements. *The Journal of Neuroscience*, 4(11):2745–2754. (Cited on page 50.)

Hollingworth, H. L. (1910). The central tendency of judgment. *The Journal of Philosophy, Psychology and Scientific Methods*, 7(17):461–469. (Cited on pages 57 and 94.)

Hospedales, T. M., Cartwright, J., , and Vijayakumar, S. (2007). Structure inference for Bayesian multisensory perception and tracking. In *Proceedings of the International Joint Conference on Artificial Intelligence (IJCAI '07)*, pages 2122–2128. (Cited on page 33.)

Houlsby, N. M., Huszár, F., Ghassemi, M. M., Orbán, G., Wolpert, D. M., and Lengyel, M. (2013). Cognitive tomography reveals complex, task-independent mental representations. *Current Biology*, 23(21):2169–2175. (Cited on pages 1 and 43.)

Howard, I. S., Ingram, J. N., Körding, K. P., and Wolpert, D. M. (2009a). Statistics of natural movements are reflected in motor errors. *Journal of Neurophysiology*, 102(3):1902–1910. (Cited on page 52.)

Howard, I. S., Ingram, J. N., and Wolpert, D. M. (2009b). A modular planar robotic manipulandum with end-point torque control. *Journal of Neuroscience Methods*, 181(2):199–211. (Cited on page 107.)

Howard, I. S., Wolpert, D. M., and Franklin, D. W. (2013). The effect of contextual cues on the encoding of motor memories. *Journal of Neurophysiology*, 109(10):2632–2644. (Cited on page 40.)

Hudson, T. E., Maloney, L. T., and Landy, M. S. (2007). Movement planning with probabilistic target information. *Journal of Neurophysiology*, 98(5):3034–3046. (Cited on pages 105, 151, and 189.)

Hudson, T. E., Maloney, L. T., and Landy, M. S. (2008). Optimal compensation for temporal uncertainty in movement planning. *PLoS Computational Biology*, 4(7):e1000130. (Cited on pages 53, 54, 58, 78, 87, 100, and 101.)

Hudson, T. E., Tassinari, H., and Landy, M. S. (2010). Compensation for changing motor uncertainty. *PLoS Computational Biology*, 6(11):e1000982. (Cited on page 53.)

Hürlimann, F., Kiper, D. C., and Carandini, M. (2002). Testing the Bayesian model of perceived speed. *Vision Research*, 42(19):2253–2257. (Cited on page 41.)

Huszár, F., Noppeney, U., and Lengyel, M. (2010). Mind reading by machine learning: A doubly Bayesian method for inferring mental representations. In *Proceedings of the Thirty-Second Annual Conference of the Cognitive Science Society*, pages 2810–2815. (Cited on pages 43 and 191.)

Izawa, J. and Shadmehr, R. (2008). On-line processing of uncertain information in visuomotor control. *The Journal of Neuroscience*, 28(44):11360–11368. (Cited on pages 158 and 178.)

Jacobs, R. A. (1999). Optimal integration of texture and motion cues to depth. *Vision Research*, 39(21):3621–3629. (Cited on page 31.)

Jacobs, R. A. (2002). What determines visual cue reliability? *Trends in Cognitive Sciences*, 6(8):345–350. (Cited on page 31.)

Jarvstad, A., Hahn, U., Rushton, S. K., and Warren, P. A. (2013). Perceptuo-motor, cognitive, and description-based decision-making seem equally good. *Proceedings of the National Academy of Sciences*, 110(40):16271–16276. (Cited on pages 104 and 190.)

Jarvstad, A., Hahn, U., Warren, P. A., and Rushton, S. K. (2014). Are perceptuo-motor decisions really more optimal than cognitive decisions? *Cognition*, 130(3):397–416. (Cited on pages 47, 49, 55, and 104.)

Jaynes, E. T. (2003). *Probability theory: The logic of science*. Cambridge University Press. (Cited on pages 4, 5, 13, 25, and 46.)

Jazayeri, M. and Shadlen, M. N. (2010). Temporal context calibrates interval timing. *Nature Neuroscience*, 13(8):1020–1026. (Cited on pages 17, 38, 58, 74, 75, 76, 78, 94, 95, 101, 185, 186, and 187.)

Jogan, M. and Stocker, A. A. (2014). A new two-alternative forced choice method for the unbiased characterization of perceptual bias and discriminability. *Journal of Vision*, 14(3):1–18. (Cited on page 29.)

Jones, M. and Love, B. (2011). Bayesian Fundamentalism or Enlightenment? On the explanatory status and theoretical contributions of Bayesian models of cognition. *Behavioral and Brain Sciences*, 34(4):169–188. (Cited on pages 19, 96, and 192.)

Jones, M. R. and Mcauley, J. D. (2005). Time judgments in global temporal contexts. *Perception & Psychophysics*, 67(3):398–417. (Cited on pages 58, 74, 94, and 101.)

Jürgens, R. and Becker, W. (2006). Perception of angular displacement without landmarks: Evidence for Bayesian fusion of vestibular, optokinetic, podokinesthetic, and cognitive information. *Experimental Brain Research*, 174(3):528–543. (Cited on page 26.)

Kahneman, D. and Tversky, A. (1979). Prospect theory: An analysis of decision under risk. *Econometrica: Journal of the Econometric Society*, pages 263–291. (Cited on pages 47, 48, and 152.)

Kanai, R., Paffen, C. L., Hogendoorn, H., and Verstraten, F. A. (2006). Time dilation in dynamic visual display. *Journal of Vision*, 6(12):8. (Cited on page 57.)

Karmarkar, U. R. and Buonomano, D. V. (2007). Timing in the absence of clocks: Encoding time in neural network states. *Neuron*, 53(3):427–438. (Cited on page 102.)

Kass, R. E. and Raftery, A. E. (1995). Bayes factors. *Journal of the American Statistical Association*, 90(430):773–795. (Cited on pages 140, 141, 144, and 203.)

Kerrigan, I. S. and Adams, W. J. (2013). Learning different light prior distributions for different contexts. *Cognition*, 127(1):99–104. (Cited on pages 40 and 42.)

Kersten, D., Mamassian, P., and Yuille, A. (2004). Object perception as Bayesian inference. *Annual Review of Psychology*, 55:271–304. (Cited on pages 2 and 18.)

Kleiner, M., Brainard, D., Pelli, D., Ingling, A., Murray, R., and Broussard, C. (2007). What's new in Psychtoolbox-3. *Perception*, 36:ECVP Abstract Supplement. (Cited on page 62.)

Knill, D. C. (1998a). Discrimination of planar surface slant from texture: Human and ideal observers compared. *Vision Research*, 38(11):1683–1711. (Cited on pages 26, 28, and 31.)

Knill, D. C. (1998b). Surface orientation from texture: Ideal observers, generic observers and the information content of texture cues. *Vision Research*, 38(11):1655–1682. (Cited on page 31.)

Knill, D. C. (2003). Mixture models and the probabilistic structure of depth cues. *Vision Research*, 43(7):831–854. (Cited on page 32.)

Knill, D. C. (2007). Robust cue integration: A Bayesian model and evidence from cue-conflict studies with stereoscopic and figure cues to slant. *Journal of Vision*, 7(7):1–24. (Cited on page 32.)

Knill, D. C., Bondada, A., and Chhabra, M. (2011). Flexible, task-dependent use of sensory feedback to control hand movements. *The Journal of Neuroscience*, 31(4):1219–1237. (Cited on pages 158 and 178.)

Knill, D. C. and Pouget, A. (2004). The Bayesian brain: The role of uncertainty in neural coding and computation. *Trends in Neurosciences*, 27(12):712–719. (Cited on pages 1 and 2.)

Knill, D. C. and Richards, W. (1996). *Perception as Bayesian inference*. Cambridge University Press. (Cited on pages 1, 2, and 18.)

Knill, D. C. and Saunders, J. A. (2003). Do humans optimally integrate stereo and texture information for judgments of surface slant? *Vision Research*, 43(24):2539–2558. (Cited on pages 31, 32, and 54.)

Kontsevich, L. L. and Tyler, C. W. (1999). Bayesian adaptive estimation of psychometric slope and threshold. *Vision Research*, 39(16):2729–2737. (Cited on page 66.)

Körding, K. P., Beierholm, U., Ma, W. J., Quartz, S., Tenenbaum, J. B., and Shams, L. (2007). Causal inference in multisensory perception. *PLoS One*, 2(9):e943. (Cited on page 33.)

Körding, K. P., Fukunaga, I., Howard, I. S., Ingram, J. N., and Wolpert, D. M. (2004a). A neuroeconomics approach to inferring utility functions in sensorimotor control. *PLoS Biology*, 2(10):e330. (Cited on page 51.)

Körding, K. P., Ku, S.-P., and Wolpert, D. M. (2004b). Bayesian integration in force estimation. *Journal of Neurophysiology*, 92(5):3161–3165. (Cited on page 38.)

Körding, K. P. and Tenenbaum, J. B. (2007). Causal inference in sensorimotor integration. In Schölkopf, B., Platt, J. C., and T, H., editors, *Advances in Neural Information Processing Systems 19*, pages 737–744. MIT Press. (Cited on page 33.)

Körding, K. P. and Wolpert, D. M. (2004a). Bayesian integration in sensorimotor learning. *Nature*, 427(6971):244–247. (Cited on pages 37, 39, 44, 90, 94, 101, 104, 151,

162, 185, and 186.)

Körding, K. P. and Wolpert, D. M. (2004b). The loss function of sensorimotor learning. *Proceedings of the National Academy of Sciences of the United States of America*, 101(26):9839–9842. (Cited on pages 6, 12, 51, 83, 84, 97, 110, 167, 176, 184, and 215.)

Körding, K. P. and Wolpert, D. M. (2004c). Probabilistic inference in human sensorimotor processing. In Thrun, S., Saul, L., and Schölkopf, B., editors, *Advances in Neural Information Processing Systems 16*, pages 1327–1334. MIT Press. (Cited on pages 39 and 185.)

Körding, K. P. and Wolpert, D. M. (2006). Bayesian decision theory in sensorimotor control. *Trends in Cognitive Sciences*, 10(7):319–326. (Cited on pages 5, 6, 7, and 18.)

Kuss, M., Jäkel, F., and Wichmann, F. A. (2005). Bayesian inference for psychometric functions. *Journal of Vision*, 5(5):478–492. (Cited on pages 28, 82, and 147.)

Kwon, O.-S. and Knill, D. C. (2013). The brain uses adaptive internal models of scene statistics for sensorimotor estimation and planning. *Proceedings of the National Academy of Sciences*, 110(11):E1064–E1073. (Cited on pages 36, 184, and 187.)

Laje, R., Cheng, K., and Buonomano, D. V. (2011). Learning of temporal motor patterns: An analysis of continuous versus reset timing. *Frontiers in Integrative Neuroscience*, 5(61). (Cited on page 102.)

Landy, M. S., Goutcher, R., Trommershäuser, J., and Mamassian, P. (2007). Visual estimation under risk. *Journal of Vision*, 7(6):1–15. (Cited on page 49.)

Landy, M. S. and Kojima, H. (2001). Ideal cue combination for localizing texture-defined edges. *The Journal of the Optical Society of America A*, 18(9):2307–2320. (Cited on pages 30 and 31.)

Landy, M. S., Maloney, L. T., Johnston, E. B., and Young, M. (1995). Measurement and modeling of depth cue combination: In defense of weak fusion. *Vision Research*, 35(3):389–412. (Cited on page 31.)

Lee, T. S. and Mumford, D. (2003). Hierarchical Bayesian inference in the visual cortex. *The Journal of the Optical Society of America A*, 20(7):1434–1448. (Cited on pages 2 and 3.)

Leopold, D. A. and Logothetis, N. K. (1999). Multistable phenomena: Changing views in perception. *Trends in Cognitive Sciences*, 3(7):254–264. (Cited on page 5.)

Lewis, P. A. and Miall, R. C. (2009). The precision of temporal judgement: Milliseconds, many minutes, and beyond. *Philosophical Transactions of the Royal Society B: Biological Sciences*, 364(1525):1897–1905. (Cited on pages 26, 58, 71, 94, and 102.)

Liu, D. and Todorov, E. (2007). Evidence for the flexible sensorimotor strategies predicted by optimal feedback control. *The Journal of Neuroscience*, 27(35):9354–9368. (Cited on page 158.)

Lloyd, K. and Leslie, D. S. (2013). Context-dependent decision-making: A simple Bayesian model. *Journal of The Royal Society Interface*, 10(82):20130069. (Cited on page 43.)

Lyons, J., Hansen, S., Hurding, S., and Elliott, D. (2006). Optimizing rapid aiming behaviour: Movement kinematics depend on the cost of corrective modifications. *Experimental Brain Research*, 174(1):95–100. (Cited on page 158.)

Ma, W. J. (2010). Signal detection theory, uncertainty, and Poisson-like population codes. *Vision Research*, 50(22):2308–2319. (Cited on pages 18 and 19.)

Ma, W. J. (2012). Organizing probabilistic models of perception. *Trends in Cognitive Sciences*, 16(10):511–518. (Cited on pages 4, 18, 101, 105, 188, and 194.)

Ma, W. J., Beck, J. M., Latham, P. E., and Pouget, A. (2006). Bayesian inference with probabilistic population codes. *Nature Neuroscience*, 9(11):1432–1438. (Cited on pages 30 and 154.)

Ma, W. J. and Jazayeri, M. (2014). Neural coding of uncertainty and probability. *Annual Review of Neuroscience*, 37:205–220. (Cited on pages 18, 184, 190, and 194.)

Ma, W. J., Körding, K. P., and Goldreich, D. (2014). *Bayesian modeling of perception*. Unpublished. (Cited on pages 2 and 18.)

Ma, W. J., Navalpakkam, V., Beck, J. M., Van Den Berg, R., and Pouget, A. (2011). Behavior and neural basis of near-optimal visual search. *Nature Neuroscience*, 14(6):783–790. (Cited on page 184.)

MacKay, D. J. (1998). Choice of basis for Laplace approximation. *Machine Learning*, 33(1):77–86. (Cited on page 204.)

MacKay, D. J. (2003). *Information theory, inference and learning algorithms*. Cambridge University Press. (Cited on pages 166, 200, and 203.)

Maloney, L. T. (2002). Statistical decision theory and biological vision. In Heyer, D. and Mausfeld, R., editors, *Perception and the physical world: Psychological and philosophical issues in perception*, pages 145–189. Wiley. (Cited on pages 5, 7, and 18.)

Maloney, L. T. and Mamassian, P. (2009). Bayesian decision theory as a model of human visual perception: Testing Bayesian transfer. *Visual Neuroscience*, 26(1):147–155. (Cited on pages 2, 3, 14, 101, 110, 193, and 194.)

Maloney, L. T., Trommershäuser, J., and Landy, M. S. (2007). Questions without words: A comparison between decision making under risk and movement planning under risk. In Gray, W., editor, *Integrated models of cognitive systems*, pages 297–315. Oxford University Press. (Cited on pages 48 and 104.)

Maloney, L. T. and Zhang, H. (2010). Decision-theoretic models of visual perception and action. *Vision Research*, 50(23):2362–2374. (Cited on pages 18 and 35.)

Mamassian, P. (2008). Overconfidence in an objective anticipatory motor task. *Psychological Science*, 19(6):601–606. (Cited on pages 53, 100, and 153.)

Mamassian, P. and Goutcher, R. (2001). Prior knowledge on the illumination position. *Cognition*, 81(1):B1–B9. (Cited on page 42.)

Mamassian, P. and Landy, M. S. (1998). Observer biases in the 3D interpretation of line drawings. *Vision Research*, 38(18):2817–2832. (Cited on page 55.)

Mamassian, P. and Landy, M. S. (2001). Interaction of visual prior constraints. *Vision Research*, 41(20):2653–2668. (Cited on pages 42, 43, and 55.)

Mamassian, P. and Landy, M. S. (2010). It's that time again. *Nature Neuroscience*, 13(8):914–916. (Cited on pages 6, 59, 95, and 192.)

Mamassian, P., Landy, M. S., and Maloney, L. T. (2002). Bayesian modelling of visual perception. In Rao, R. P. N., Olshausen, B. A., and Lewicki, M. S., editors, *Probabilistic models of the brain: Perception and neural function*, pages 13–36. MIT Press. (Cited on page 18.)

Marcus, G. F. and Davis, E. (2013). How robust are probabilistic models of higher-level cognition? *Psychological Science*, 24(12):2351–2360. (Cited on pages 19, 40, and 192.)

Marr, D. (1982). *Vision: A computational investigation into the human representation and processing of visual information*. W. H. Freeman and Company. (Cited on pages 2 and 195.)

Mates, J. (1994). A model of synchronization of motor acts to a stimulus sequence. *Biological Cybernetics*, 70(5):463–473. (Cited on page 78.)

Mauk, M. D. and Buonomano, D. V. (2004). The neural basis of temporal processing. *Annual Review of Neuroscience*, 27:307–340. (Cited on page 58.)

Miyazaki, M., Nozaki, D., and Nakajima, Y. (2005). Testing Bayesian models of human coincidence timing. *Journal of Neurophysiology*, 94(1):395–399. (Cited on pages 38, 58, and 101.)

Miyazaki, M., Yamamoto, S., Uchida, S., and Kitazawa, S. (2006). Bayesian calibration of simultaneity in tactile temporal order judgment. *Nature Neuroscience*, 9(7):875–877. (Cited on pages 38, 57, 58, 98, and 101.)

Moreno-Bote, R., Knill, D. C., and Pouget, A. (2011). Bayesian sampling in visual perception. *Proceedings of the National Academy of Sciences*, 108(30):12491–12496. (Cited on pages 56, 120, 154, and 188.)

Morgenstern, Y., Murray, R. F., and Harris, L. R. (2011). The human visual system's assumption that light comes from above is weak. *Proceedings of the National Academy of Sciences*, 108(30):12551–12553. (Cited on pages 42 and 43.)

Morrone, M. C., Ross, J., and Burr, D. (2005). Saccadic eye movements cause compression of time as well as space. *Nature Neuroscience*, 8(7):950–954. (Cited on page 57.)

Nagengast, A. J., Braun, D. A., and Wolpert, D. M. (2010). Risk-sensitive optimal feedback control accounts for sensorimotor behavior under uncertainty. *PLoS Computational Biology*, 6(7):e1000857. (Cited on pages 158 and 180.)

Nassar, M. R., Wilson, R. C., Heasly, B., and Gold, J. I. (2010). An approximately Bayesian delta-rule model explains the dynamics of belief updating in a changing environment. *The Journal of Neuroscience*, 30(37):12366–12378. (Cited on page 184.)

Natarajan, R., Murray, I., Shams, L., and Zemel, R. (2009). Characterizing response behavior in multisensory perception with conflicting cues. In Koller, D., Schuurmans, D., Bengio, Y., and Bottou, L., editors, *Advances in Neural Information Processing Systems 21*, pages 1153–1160. Curran Associates, Inc. (Cited on pages 33 and 97.)

Navarro, D. J., Pitt, M. A., and Myung, I. J. (2004). Assessing the distinguishability of models and the informativeness of data. *Cognitive Psychology*, 49(1):47–84. (Cited on page 192.)

Neal, R. M. (2003). Slice sampling. *Annals of Statistics*, 31(3):705–741. (Cited on pages 72, 127, and 200.)

Oldfield, R. C. (1971). The assessment and analysis of handedness: The Edinburgh inventory. *Neuropsychologia*, 9(1):97–113. (Cited on pages 106 and 160.)

Olshausen, B. A. and Field, D. J. (1997). Sparse coding with an overcomplete basis set: A strategy employed by V1? *Vision Research*, 37(23):3311–3325. (Cited on page 4.)

Orbán, G. and Wolpert, D. M. (2011). Representations of uncertainty in sensorimotor control. *Current Opinion in Neurobiology*, 21(4):629–635. (Cited on pages 18 and 29.)

O'Reilly, J. X., Jbabdi, S., and Behrens, T. E. (2012). How can a Bayesian approach inform neuroscience? *European Journal of Neuroscience*, 35(7):1169–1179. (Cited on page 2.)

Ortega, P. A. and Braun, D. A. (2013). Thermodynamics as a theory of decision-making with information-processing costs. *Proceedings of the Royal Society A: Mathematical, Physical and Engineering Science*, 469(2153):20120683. (Cited on page 189.)

Oruç, I., Maloney, L. T., and Landy, M. S. (2003). Weighted linear cue combination with possibly correlated error. *Vision Research*, 43(23):2451–2468. (Cited on page 33.)

Osborne, L. C., Lisberger, S. G., and Bialek, W. (2005). A sensory source for motor variation. *Nature*, 437(7057):412–416. (Cited on page 51.)

O'Sullivan, I., Burdet, E., and Diedrichsen, J. (2009). Dissociating variability and effort as determinants of coordination. *PLoS Computational Biology*, 5(4):e1000345. (Cited on pages 51, 158, 174, and 180.)

Paninski, L. (2006). Nonparametric inference of prior probabilities from Bayes-optimal behavior. In Weiss, Y., Schölkopf, B., and Platt, J., editors, *Advances in Neural Information Processing Systems 18*, pages 1067–1074. MIT Press. (Cited on pages 44 and 54.)

Pariyadath, V. and Eagleman, D. (2007). The effect of predictability on subjective duration. *PloS One*, 2(11):e1264. (Cited on page 57.)

Pelli, D. (1997). The videotoolbox software for visual psychophysics: Transforming numbers into movies. *Spatial Vision*, 10(4):437–442. (Cited on page 62.)

Petzschner, F. H. (2013). *Magnitude estimation in humans: A Bayesian approach to characteristic behavior in path integration*. PhD thesis, Ludwig-Maximilians-Universität München. (Cited on page 38.)

Petzschner, F. H. and Glasauer, S. (2011). Iterative Bayesian estimation as an explanation for range and regression effects: A study on human path integration. *The Journal of Neuroscience*, 31(47):17220–17229. (Cited on pages 26, 38, 43, 102, 184, and 187.)

Petzschner, F. H., Maier, P., and Glasauer, S. (2012). Combining symbolic cues with sensory input and prior experience in an iterative Bayesian framework. *Frontiers in Integrative Neuroscience*, 6:1–18. (Cited on page 40.)

Pitt, M. A., Myung, I. J., and Zhang, S. (2002). Toward a method of selecting among computational models of cognition. *Psychological Review*, 109(3):472–491. (Cited on pages 192 and 202.)

Poggio, T., Torre, V., and Koch, C. (1985). Computational vision and regularization theory. *Nature*, 317:314–319. (Cited on pages 25 and 28.)

Pouget, A., Beck, J. M., Ma, W. J., and Latham, P. E. (2013). Probabilistic brains: Knowns and unknowns. *Nature Neuroscience*, 16(9):1170–1178. (Cited on page 18.)

Press, W. H., Flannery, B. P., Teukolsky, S. A., and Vetterling, W. T. (2007). *Numerical recipes 3rd edition: The art of scientific computing*. Cambridge University Press. (Cited on page 124.)

Prins, N. (2012). The psychometric function: The lapse rate revisited. *Journal of Vision*, 12(6):1–16. (Cited on page 29.)

Qamar, A. T., Cotton, R. J., George, R. G., Beck, J. M., Prezhdo, E., Laudano, A., Tolias, A. S., and Ma, W. J. (2013). Trial-to-trial, uncertainty-based adjustment of decision boundaries in visual categorization. *Proceedings of the National Academy of Sciences*, 110(50):20332–20337. (Cited on page 184.)

Rakitin, B., Gibbon, J., Penney, T., Malapani, C., Hinton, S., and Meck, W. (1998). Scalar expectancy theory and peak-interval timing in humans. *Journal of Experimental Psychology: Animal Behavior Processes*, 24(1):15–33. (Cited on pages 73 and 78.)

Rasmussen, C. and Williams, C. K. I. (2006). *Gaussian processes for machine learning*. MIT Press. (Cited on pages 72, 208, and 212.)

Raviv, O., Ahissar, M., and Loewenstein, Y. (2012). How recent history affects perception: The normative approach and its heuristic approximation. *PLoS Computational Biology*, 8(10):e1002731. (Cited on pages 29, 36, 102, 154, 184, and 187.)

Roach, N. W., Heron, J., Whitaker, D., and McGraw, P. V. (2011). Asynchrony adaptation reveals neural population code for audio-visual timing. *Proceedings of the Royal Society B: Biological Sciences*, 278(1710):1314–1322. (Cited on page 98.)

Rohde, M., Greiner, L., and Ernst, M. O. (2014a). Asymmetries in visuomotor recalibration of time perception: Does causal binding distort the window of integration? *Acta Psychologica*, 147:127–135. (Cited on page 98.)

Rohde, M., van Dam, L. C., and Ernst, M. O. (2014b). Predictability is necessary for closed-loop visual feedback delay adaptation. *Journal of Vision*, 14(3):1–23. (Cited on pages 98 and 100.)

Rosas, P., Wagemans, J., Ernst, M. O., and Wichmann, F. A. (2005). Texture and haptic cues in slant discrimination: Reliability-based cue weighting without statistically optimal cue combination. *The Journal of the Optical Society of America A*, 22(5):801–809. (Cited on page 33.)

Rosas, P. and Wichmann, F. A. (2011). Cue combination: Beyond optimality. In Trommershauser, J., Körding, K., and Landy, M. S., editors, *Sensory cue integration*, pages 144–152. Oxford University Press. (Cited on page 33.)

Rosas, P., Wichmann, F. A., and Wagemans, J. (2007). Texture and object motion in slant discrimination: Failure of reliability-based weighting of cues may be evidence for strong fusion. *Journal of Vision*, 7(6):1–21. (Cited on page 33.)

Ross, J. (2003). Visual discrimination of number without counting. *Perception*, 32(7):867–870. (Cited on page 212.)

Ryan, L. J. (2011). Temporal context affects duration reproduction. *Journal of Cognitive Psychology*, 23(1):157–170. (Cited on pages 59, 75, 77, 90, 94, and 101.)

Ryan, L. J. and Fritz, M. S. (2007). Erroneous knowledge of results affects decision and memory processes on timing tasks. *Journal of Experimental Psychology: Human Perception and Performance*, 33(6):1468–1482. (Cited on page 100.)

Ryan, L. J., Henry, K., Robey, T., and Edwards, J. A. (2004). Resolution of conflicts between internal and external information sources on a time reproduction task: The role of perceived information reliability and attributional style. *Acta Psychologica*, 117(2):205–229. (Cited on page 100.)

Ryan, L. J. and Robey, T. B. (2002). Learning and performance effects of accurate and erroneous knowledge of results on time perception. *Acta Psychologica*, 111(1):83–100. (Cited on page 100.)

Salmoni, A. W., Schmidt, R. A., and Walter, C. B. (1984). Knowledge of results and motor learning: A review and critical reappraisal. *Psychological Bulletin*, 95(3):355–386. (Cited on page 63.)

Sato, Y. and Aihara, K. (2009). Integrative Bayesian model on two opposite types of sensory adaptation. *Artificial Life and Robotics*, 14(2):289–292. (Cited on page 98.)

Sato, Y., Toyoizumi, T., and Aihara, K. (2007). Bayesian inference explains perception of unity and ventriloquism aftereffect: Identification of common sources of audio-visual stimuli. *Neural Computation*, 19(12):3335–3355. (Cited on pages 33 and 98.)

Saunders, I. and Vijayakumar, S. (2012). Continuous evolution of statistical estimators for optimal decision-making. *PloS One*, 7(6):e37547. (Cited on page 102.)

Saunders, J. A. and Knill, D. C. (2001). Perception of 3D surface orientation from skew symmetry. *Vision Research*, 41(24):3163–3183. (Cited on page 31.)

Saunders, J. A. and Knill, D. C. (2003). Humans use continuous visual feedback from the hand to control fast reaching movements. *Experimental Brain Research*, 152(3):341–352. (Cited on page 157.)

Saunders, J. A. and Knill, D. C. (2004). Visual feedback control of hand movements. *The Journal of Neuroscience*, 24(13):3223–3234. (Cited on page 157.)

Schrater, P. R. and Kersten, D. (2000). How optimal depth cue integration depends on the task. *International Journal of Computer Vision*, 40(1):71–89. (Cited on page 28.)

Schwarz, G. (1978). Estimating the dimension of a model. *The Annals of Statistics*, 6(2):461–464. (Cited on page 204.)

Seriès, P. and Seitz, A. R. (2013). Learning what to expect (in visual perception). *Frontiers in Human Neuroscience*, 7:668. (Cited on pages 4, 18, 22, 35, 41, and 42.)

Serwe, S., Drewing, K., and Trommershäuser, J. (2009). Combination of noisy directional visual and proprioceptive information. *Journal of Vision*, 9(5):1–14. (Cited on page 33.)

Serwe, S., Körding, K. P., and Trommershäuser, J. (2011). Visual-haptic cue integration with spatial and temporal disparity during pointing movements. *Experimental Brain Research*, 210(1):67–80. (Cited on page 33.)

Seydell, A., Knill, D. C., and Trommershäuser, J. (2010). Adapting internal statistical models for interpreting visual cues to depth. *Journal of Vision*, 10(4):1–27. (Cited on page 40.)

Seydell, A., McCann, B. C., Trommershäuser, J., and Knill, D. C. (2008). Learning stochastic reward distributions in a speeded pointing task. *The Journal of Neuroscience*, 28(17):4356–4367. (Cited on pages 48 and 105.)

Shadlen, M. N., Britten, K. H., Newsome, W. T., and Movshon, J. A. (1996). A computational analysis of the relationship between neuronal and behavioral responses to visual motion. *The Journal of Neuroscience*, 16(4):1486–1510. (Cited on page 188.)

Shi, Z., Chen, L., and Müller, H. J. (2010). Auditory temporal modulation of the visual Ternus effect: The influence of time interval. *Experimental Brain Research*, 203(4):723–735. (Cited on page 59.)

Shi, Z., Church, R. M., and Meck, W. H. (2013a). Bayesian optimization of time perception. *Trends in Cognitive Sciences*, 17(11):556–564. (Cited on pages 58 and 101.)

Shi, Z., Ganzenmüller, S., and Müller, H. J. (2013b). Reducing bias in auditory duration reproduction by integrating the reproduced signal. *PloS One*, 8(4):e62065. (Cited on page 58.)

Simoncelli, E. P. (2009). Optimal estimation in sensory systems. In Gazzaniga, M. S., editor, *The cognitive neurosciences, IV edition*, pages 525–535. MIT Press. (Cited on page 18.)

Sotiropoulos, G., Seitz, A. R., and Seriès, P. (2011). Changing expectations about speed alters perceived motion direction. *Current Biology*, 21(21):R883–R884. (Cited on pages 35 and 43.)

Sotiropoulos, G., Seitz, A. R., and Seriès, P. (2014). Contrast dependency and prior expectations in human speed perception. *Vision Research*, 97:16–23. (Cited on pages 42, 44, and 192.)

Spiegelhalter, D. J., Best, N. G., Carlin, B. P., and Van Der Linde, A. (2002). Bayesian measures of model complexity and fit. *Journal of the Royal Statistical Society: Series B (Statistical Methodology)*, 64(4):583–639. (Cited on pages 127, 128, 141, and 204.)

Stephan, K. E., Penny, W. D., Daunizeau, J., Moran, R. J., and Friston, K. J. (2009). Bayesian model selection for group studies. *Neuroimage*, 46(4):1004–1017. (Cited on pages 128, 129, 206, 216, and 218.)

Stetson, C., Cui, X., Montague, P. R., and Eagleman, D. M. (2006). Motor-sensory recalibration leads to an illusory reversal of action and sensation. *Neuron*, 51(5):651–659. (Cited on pages 57, 59, 77, and 98.)

Stewart, N., Brown, G. D., and Chater, N. (2005). Absolute identification by relative judgment. *Psychological Review*, 112(4):881–911. (Cited on page 102.)

Stocker, A. and Simoncelli, E. P. (2005). Constraining a Bayesian model of human visual speed perception. In Saul, L., Weiss, Y., and Bottou, L., editors, *Advances in Neural Information Processing Systems 17*, pages 1361–1368. MIT Press. (Cited on page 42.)

Stocker, A. and Simoncelli, E. P. (2006a). Sensory adaptation within a Bayesian framework for perception. In Weiss, Y., Schölkopf, B., and Platt, J., editors, *Advances in Neural Information Processing Systems 18*, pages 1289–1296. MIT Press. (Cited on page 98.)

Stocker, A. A. and Simoncelli, E. P. (2006b). Noise characteristics and prior expectations in human visual speed perception. *Nature Neuroscience*, 9(4):578–585. (Cited on pages 26, 41, 42, 44, 96, 185, and 192.)

Stocker, A. A. and Simoncelli, E. P. (2008). A Bayesian model of conditioned perception. In Platt, J., Koller, D., Singer, Y., and Roweis, S., editors, *Advances in Neural Information Processing Systems 20*, pages 1409–1416. MIT Press. (Cited on page 50.)

Stone, J., Kerrigan, I., and Porrill, J. (2009). Where is the light? Bayesian perceptual priors for lighting direction. *Proceedings of the Royal Society B: Biological Sciences*, 276(1663):1797–1804. (Cited on pages 42, 44, 55, 185, and 192.)

Sundareswara, R. and Schrater, P. R. (2008). Perceptual multistability predicted by search model for Bayesian decisions. *Journal of Vision*, 8(5):1–19. (Cited on pages 56 and 188.)

Sutton, R. S. and Barto, A. G. (1998). *Reinforcement learning: An introduction*. MIT press. (Cited on page 154.)

Tassinari, H., Hudson, T. E., and Landy, M. S. (2006). Combining priors and noisy visual cues in a rapid pointing task. *The Journal of Neuroscience*, 26(40):10154–10163. (Cited on pages 38, 52, 95, 104, 105, 114, 145, 153, and 188.)

Tenenbaum, J. B., Kemp, C., Griffiths, T. L., and Goodman, N. D. (2011). How to grow a mind: Statistics, structure, and abstraction. *Science*, 331(6022):1279–1285. (Cited on page 3.)

Teuscher, F. and Guiard, V. (1995). Sharp inequalities between skewness and kurtosis for unimodal distributions. *Statistics & Probability Letters*, 22(3):257–260. (Cited on page 111.)

Thurstone, L. L. (1927). Psychophysical analysis. *The American Journal of Psychology*, 38(3):368–389. (Cited on pages 19 and 28.)

Tjan, B. S., Braje, W. L., Legge, G. E., and Kersten, D. (1995). Human efficiency for recognizing 3-D objects in luminance noise. *Vision Research*, 35(21):3053–3069. (Cited on page 188.)

Todorov, E. (2004). Optimality principles in sensorimotor control. *Nature Neuroscience*, 7(9):907–915. (Cited on pages 52, 158, 178, and 180.)

Todorov, E. and Jordan, M. I. (2002). Optimal feedback control as a theory of motor coordination. *Nature Neuroscience*, 5(11):1226–1235. (Cited on pages 51, 158, 178, and 180.)

Trommershäuser, J. (2009a). Acquisition of knowledge about uncertainty in the outcome of sensory motor decision tasks. In *IEEE 8th International Conference on Development and Learning, 2009 (ICDL 2009).*, pages 1–6. IEEE. (Cited on page 48.)

Trommershäuser, J. (2009b). Biases and optimality of sensory-motor and cognitive decisions. *Progress in Brain Research*, 174:267–278. (Cited on page 18.)

Trommershäuser, J., Gepshtein, S., Maloney, L. T., Landy, M. S., and Banks, M. S. (2005). Optimal compensation for changes in task-relevant movement variability. *The Journal of Neuroscience*, 25(31):7169–7178. (Cited on pages 48, 52, 53, and 153.)

Trommershauser, J., Körding, K., and Landy, M. S. (2011). *Sensory cue integration*. Oxford University Press. (Cited on page 29.)

Trommershäuser, J., Landy, M. S., and Maloney, L. T. (2006a). Humans rapidly estimate expected gain in movement planning. *Psychological Science*, 17(11):981–988. (Cited on pages 49 and 55.)

Trommershäuser, J., Maloney, L., and Landy, M. (2008a). Decision making, movement planning and statistical decision theory. *Trends in Cognitive Sciences*, 12(8):291–297. (Cited on pages 18, 47, and 104.)

Trommershäuser, J., Maloney, L. T., and Landy, M. S. (2003a). Statistical decision theory and the selection of rapid, goal-directed movements. *The Journal of the Optical Society of America A*, 20(7):1419–1433. (Cited on pages 17, 47, 48, 52, 157, 158, 180, and 189.)

Trommershäuser, J., Maloney, L. T., and Landy, M. S. (2003b). Statistical decision theory and trade-offs in the control of motor response. *Spatial Vision*, 16(3):255–275. (Cited on pages 48 and 52.)

Trommershäuser, J., Maloney, L. T., and Landy, M. S. (2008b). The expected utility of movement. In Glimcher, P. W., Fehr, E., Camerer, C. F., and Poldrack, R. A., editors, *Neuroeconomics: Decision making and the brain*, pages 95–111. Academic Press. (Cited on pages 18, 47, and 50.)

Trommershäuser, J., Mattis, J., Maloney, L. T., and Landy, M. S. (2006b). Limits to human movement planning with delayed and unpredictable onset of needed information. *Experimental Brain Research*, 175(2):276–284. (Cited on page 49.)

Tsotsos, J. K. (2001). Complexity, vision, and attention. In Harris, L. R. and Jenkin, M., editors, *Vision and attention*, pages 105–128. Springer. (Cited on page 3.)

Tversky, A. and Kahneman, D. (1992). Advances in prospect theory: Cumulative representation of uncertainty. *Journal of Risk and Uncertainty*, 5(4):297–323. (Cited on page 152.)

Uno, Y., Kawato, M., and Suzuki, R. (1989). Formation and control of optimal trajectory in human multijoint arm movement. *Biological Cybernetics*, 61(2):89–101. (Cited on page 50.)

van Beers, R. J., Haggard, P., and Wolpert, D. M. (2004). The role of execution noise in movement variability. *Journal of Neurophysiology*, 91(2):1050–1063. (Cited on pages 51 and 52.)

van Beers, R. J., Sittig, A. C., and van der Gon, J. J. D. (1996). How humans combine simultaneous proprioceptive and visual position information. *Experimental Brain Research*, 111(2):253–261. (Cited on pages 31, 176, and 178.)

van Beers, R. J., Sittig, A. C., and van der Gon, J. J. D. (1999). Integration of proprioceptive and visual position-information: An experimentally supported model. *Journal of Neurophysiology*, 81(3):1355–1364. (Cited on page 176.)

van Dam, L. C. and Ernst, M. O. (2013). Knowing each random error of our ways, but hardly correcting for it: An instance of optimal performance. *PloS One*, 8(10):e78757. (Cited on pages 158, 179, and 180.)

van den Berg, R., Awh, E., and Ma, W. J. (2014). Factorial comparison of working memory models. *Psychological Review*, 121(1):124–149. (Cited on pages 7, 68, 95, 106, 115, 192, and 206.)

van den Berg, R. and Ma, W. J. (2014). "Plateau"-related summary statistics are uninformative for comparing working memory models. *Attention, Perception, & Psychophysics*, pages 1–19. (Cited on page 192.)

van den Berg, R., Vogel, M., Josić, K., and Ma, W. J. (2012). Optimal inference of sameness. *Proceedings of the National Academy of Sciences*, 109(8):3178–3183. (Cited on page 184.)

van Ee, R., Adams, W. J., and Mamassian, P. (2003). Bayesian modeling of cue interaction: Bistability in stereoscopic slant perception. *The Journal of the Optical Society of America A*, 20(7):1398–1406. (Cited on page 50.)

Verstynen, T. and Sabes, P. N. (2011). How each movement changes the next: An experimental and theoretical study of fast adaptive priors in reaching. *The Journal of Neuroscience*, 31(27):10050–10059. (Cited on page 187.)

Vilares, I., Howard, J., Fernandes, H., Gottfried, J., and Kording, K. (2012). Differential representations of prior and likelihood uncertainty in the human brain. *Current Biology*, 22(18):1641–1648. (Cited on page 190.)

Vilares, I. and Kording, K. (2011). Bayesian models: The structure of the world, uncertainty, behavior, and the brain. *Annals of the New York Academy of Sciences*, 1224(1):22–39. (Cited on page 18.)

Vroomen, J. and Keetels, M. (2010). Perception of intersensory synchrony: A tutorial review. *Attention, Perception, & Psychophysics*, 72(4):871–884. (Cited on page 98.)

Vul, E., Goodman, N., Griffiths, T. L., and Tenenbaum, J. B. (2014). One and done? Optimal decisions from very few samples. *Cognitive Science*, 38(4):599–637. (Cited on page 188.)

Vul, E., Goodman, N. D., Griffiths, T. L., and Tenenbaum, J. B. (2009). One and done? Optimal decisions from very few samples. In *Proceedings of the 31st annual conference of the cognitive science society*, volume 1, pages 66–72. (Cited on page 188.)

Vulkan, N. (2000). An economist's perspective on probability matching. *Journal of Economic Surveys*, 14(1):101–118. (Cited on pages 5 and 55.)

Wagenmakers, E.-J., Ratcliff, R., Gomez, P., and Iverson, G. J. (2004). Assessing model mimicry using the parametric bootstrap. *Journal of Mathematical Psychology*, 48(1):28–50. (Cited on page 192.)

Walsh, V. (2003). A theory of magnitude: Common cortical metrics of time, space and quantity. *Trends in Cognitive Sciences*, 7(11):483–488. (Cited on page 57.)

Wei, K. and Körding, K. (2010). Uncertainty of feedback and state estimation determines the speed of motor adaptation. *Frontiers in Computational Neuroscience*, 4. (Cited on page 178.)

Weiss, Y., Simoncelli, E. P., and Adelson, E. H. (2002). Motion illusions as optimal percepts. *Nature Neuroscience*, 5(6):598–604. (Cited on pages 41 and 54.)

Whiteley, L. (2008). *Uncertainty, reward, and attention in the Bayesian brain*. PhD thesis, Gatsby Computational Neuroscience Unit, University College London. (Cited on page 1.)

Whiteley, L. and Sahani, M. (2008). Implicit knowledge of visual uncertainty guides decisions with asymmetric outcomes. *Journal of Vision*, 8(3):1–15. (Cited on pages 49, 101, and 162.)

Wichmann, F. A. and Hill, N. J. (2001). The psychometric function: I. Fitting, sampling, and goodness of fit. *Perception & Psychophysics*, 63(8):1293–1313. (Cited on pages 28, 29, 82, 121, and 147.)

Wiener, M., Thompson, J. C., and Coslett, H. B. (2014). Continuous carryover of temporal context dissociates response bias from perceptual influence for duration. *PloS One*, 9(6):e100803. (Cited on page 187.)

Wolpert, D. M. (2007). Probabilistic models in human sensorimotor control. *Human Movement Science*, 26(4):511–524. (Cited on page 18.)

Wolpert, D. M. and Landy, M. S. (2012). Motor control is decision-making. *Current Opinion in Neurobiology*, 22:1–8. (Cited on page 18.)

Wozny, D. R., Beierholm, U. R., and Shams, L. (2010). Probability matching as a computational strategy used in perception. *PLoS Computational Biology*, 6(8):e1000871. (Cited on pages 5 and 55.)

Wu, S.-W., Delgado, M. R., and Maloney, L. T. (2009). Economic decision-making compared with an equivalent motor task. *Proceedings of the National Academy of*

Sciences, 106(15):6088–6093. (Cited on pages 48 and 104.)

Wu, S.-W., Trommershäuser, J., Maloney, L. T., and Landy, M. S. (2006). Limits to human movement planning in tasks with asymmetric gain landscapes. *Journal of Vision*, 6(1):53–63. (Cited on page 49.)

Xuan, B., Zhang, D., He, S., and Chen, X. (2007). Larger stimuli are judged to last longer. *Journal of Vision*, 7(10):1–5. (Cited on page 57.)

Young, M. J., Landy, M. S., and Maloney, L. T. (1993). A perturbation analysis of depth perception from combinations of texture and motion cues. *Vision Research*, 33(18):2685–2696. (Cited on page 30.)

Yuille, A. and Kersten, D. (2006). Vision as Bayesian inference: Analysis by synthesis? *Trends in Cognitive Sciences*, 10(7):301–308. (Cited on page 18.)

Yuille, A. L. and Bülthoff, H. H. (1996). Bayesian decision theory and psychophysics. In Knill, D. C. and Richards, W., editors, *Perception as Bayesian inference*, pages 123–162. Cambridge University Press. (Cited on pages 6, 31, 43, and 50.)

Zarco, W., Merchant, H., Prado, L., and Mendez, J. C. (2009). Subsecond timing in primates: Comparison of interval production between human subjects and rhesus monkeys. *Journal of neurophysiology*, 102(6):3191–3202. (Cited on page 102.)

Zednik, C. and Jäkel, F. (2014). How does Bayesian reverse-engineering work? In Bello, P., Guarini, M., McShane, M., and Scassellati, B., editors, *Proceedings of the 36th Annual Conference of the Cognitive Science Society*, pages 666–671. (Cited on page 3.)

Zhang, H., Daw, N. D., and Maloney, L. T. (2013a). Testing whether humans have an accurate model of their own motor uncertainty in a speeded reaching task. *PLoS Computational Biology*, 9(5):e1003080. (Cited on pages 53 and 153.)

Zhang, H. and Maloney, L. T. (2012). Ubiquitous log odds: A common representation of probability and frequency distortion in perception, action, and cognition. *Frontiers in Neuroscience*, 6:1–14. (Cited on pages 96, 121, and 152.)

Zhang, H., Morvan, C., and Maloney, L. T. (2010). Gambling in the visual periphery: A conjoint-measurement analysis of human ability to judge visual uncertainty. *PLoS Computational Biology*, 6(12):e1001023. (Cited on page 153.)

Zhang, R., Kwon, O.-S., and Tadin, D. (2013b). Illusory movement of stationary stimuli in the visual periphery: Evidence for a strong centrifugal prior in motion processing. *The Journal of Neuroscience*, 33(10):4415–4423. (Cited on pages 42, 44, 72, and 96.)

COLOPHON

This document was typeset using the typographical look-and-feel `classicthesis` developed by André Miede. The style was inspired by Robert Bringhurst's seminal book on typography "*The Elements of Typographic Style*". `classicthesis` is available for both LaTeX and LyX:

http://code.google.com/p/classicthesis/

Happy users of `classicthesis` usually send a real postcard to the author, a collection of postcards received so far is featured here:

http://postcards.miede.de/

Final Version as of December 1, 2014 (`classicthesis` version 4.0).